LIQUEFACTION OF LIGNOCELLULOSIC BIOMASS TO HIGH-VALUE CHEMICAL PRODUCTS

The University Of Sheffield.

Cynthia Kakie Kartey
(150106122)

Supervisor: Dr. James McGregor

Department of Chemical and Biological Engineering
The University of Sheffield

Thesis submitted for the degree of

Doctor of Philosophy

December 2019

ABSTRACT

The utilisation of edible resources as alternative and renewable sources of energy and chemicals in the battle against climate change is unsustainable and poses a potential threat to food security. As such, the use of waste-derived resources (whether plastics, biomass, or metals) is at the forefront of sustainable technology research today, owing to the abundance of waste and the need to reduce reliance on fossil resources.

This research, therefore, exploited the potential to convert (via liquefaction) lignocellulosic biomass to valuable products that could serve as precursors to the chemical and fuel industries. Specifically, pine needles (exemplar forest waste) and sugarcane bagasse (an agricultural waste) were employed as feedstock in this work. The influence of various low-cost solvents (glycerol, ethylene glycol, and water) used as liquefaction solvents and reaction conditions (temperature, pressure, and catalyst) on both biomass conversion and product yields were investigated.

In this study, sugarcane bagasse was found to be predominantly cellulosic in nature whereas that of pine needles was more ligninic. The application of water as liquefaction solvent facilitated better degradation of cellulose and hemicellulose whereas glycerol and ethylene glycol were found to facilitate better degradation of the most recalcitrant biomass component, lignin. As such, the highest biomass conversion was achieved in the presence of glycerol (94 wt.%) followed by ethylene glycol (86 wt.%), and water (76 wt.%) at 250 °C, 1 h reaction time, 30 bar initial helium pressure, and biomass:solvent ratio of 1:10 (wt:wt). Acetic acid, glucose, levulinic acid, phenol, and various esters were the most prominent biomass-based products identified in the liquid fraction, all of which are important platform chemicals for industry.

It was also observed that the use of water enhanced the selectivity of the targeted biomass derivatives; particularly, acetic acid, phenol, and levulinic acid. Meanwhile, glycerol and ethylene glycol were found to generate additional valuable chemicals through various side reactions. Hence, a novel one-pot process was designed for the simultaneous valorisation of biomass and glycerol using acetone as a cosolvent and reagent. This process produced mainly acetic acid and phenol as biomass-based chemicals while solketal and mesityl oxide were synthesised from the excess glycerol and acetone. The one-pot valorisation of biomass and low-value solvents such as glycerol would potentially significantly reduce the number of steps needed to achieve the same results in separate processes, making future biorefineries more economical.

Finally, it was discovered in this research that bio-char formed *in situ* during biomass liquefaction is catalytically active towards the conversion of liquefaction solvents to value-added chemicals. The activity of the bio-char was largely attributed to its ash content. This catalytic activity was particularly observed in the conversion of acetone to mesityl oxide. Consequently, the potential role of biomass and its components; bio-char and ash as a heterogeneous catalyst for mesityl oxide synthesis was demonstrated in this thesis for the first time. The application of catalysts from renewable and environmentally friendly sources in place of fossil-derived catalyst or expensive precious metals is crucial for future research in light of the development of a sustainable industry.

Proudly dedicated

to

*my **mother**, Lydia Apeku*
who invested all her resources into my undergraduate education,

and

*my **grandparents**, Felicia and Ebenezer Apeku*
who since childhood believed in me and always urged me on!

ACKNOWLEDGMENTS

My heartfelt gratitude to my supervisor, Dr. James McGregor, for his incredible supervision and relentless support in diverse ways all throughout this research.

I am profoundly thankful to the “Schlumberger Foundation Faculty for the Future” for funding this work. Special appreciation to Dr. James McGregor, Dr. Paul Kwasi Blay, Prof. Lima Rose Miranda, and Dr. Lawrence Darkwah who always assisted me with recommendation letters to renew this scholarship every year.

Sincere thanks to colleagues and members of the Sheffield catalysis group for various expertise and ideas: Dr. Laura Quintana-Gomez (GCMS training) Dr. Nur Atiqah Nasir and Dr. Nurul Razali (autoclave reactor set up training), Dr. Catherine H. Collett (FTIR training and provision of the bio-chars), María Andérez-Fernández (HPLC analysis), Dr. Ali Al-Shathr, Justin Driver, Gareth Davies, Ali Hameed, Ming Liu, Eleanor L O'Doherty and the entire Sheffield catalysis group for various technical and non-technical contributions.

Special appreciation to Duncan Schofield, James Grinham, Adrian Lumby, Dave Wengraf, Julie Swales, Keith Penny, Usman Younis, Richard Stacey and all staff of the technical and safety department of the Chemical and Biological Engineering Department for the consistent, valuable and diverse technical support all throughout this work. Thanks to Wil Ward, who helped me gather momentum to start the write up of this thesis.

Special thanks to my family and friends for all the prayers and encouragement.

Finally, to Philip Stratford, Kirsty Bowen, Dr. James McGregor, and the University of Sheffield media team for the exceptional guidance and support before and during the national and international media coverage of this research. I am forever grateful for this great opportunity and experience.

TABLE OF CONTENTS

ABSTRACT ..... **ii**
ACKNOWLEDGMENTS ..... **iv**
TABLE OF CONTENTS ..... **v**
LIST OF FIGURES ..... **viiviii**
LIST OF TABLES ..... **xii**
LIST OF SCHEMES ..... **xv**
NOMENCLATURE ..... **xvi**
CHAPTER 1: INTRODUCTION **1**
1.1 Background 2
1.2 Aims and objectives 5
CHAPTER 2: LITERATURE REVIEW **7**
2.1 Introduction 8
2.2 Lignocellulosic biomass and its constituents 8
2.2.1 Lignin 11
2.2.2 Cellulose 12
2.2.3 Hemicellulose 12
2.2.4 Inorganic and organic extractives 13
2.3 Biomass utilisation 14
2.4 Biomass conversion techniques 15
2.4.1 Biochemical processes 15
2.4.2 Thermochemical processes 17
2.5 Potential applications of sugarcane bagasse and pine needles 42
2.5.1 Sugarcane bagasse 42
2.5.2 Pine needles 45
2.6 Conclusion 47
CHAPTER 3: EXPERIMENTAL AND ANALYTICAL PROCEDURES **49**
3.1 Introduction 49
3.2 Materials 49
3.3 Preparation of biomass materials 51
3.4 Characterisation of biomass feedstocks 51
3.4.1 Thermogravimetric analysis (TGA) 51
3.4.2 Proximate analysis (conventional manual method) 53
3.4.3 Fourier transform infrared spectroscopy (FTIR) 56

3.4.4 Elemental composition (ultimate) analysis 57
3.4.5 Determination of extractives and bio-polymer constituents 58
3.5 Reaction studies: Liquefaction procedures and reactors set-up 61
3.5.1 Atmospheric pressure liquefaction 61
3.5.2 Moderate pressure liquefaction 62
3.5.3 Product (liquid-solid) separation 64
3.5.4 Analysis of liquid product (bio-oil) 65
3.5.5 Analyte quantification 69
3.5.6 Analysis of solid residue (bio-char) 71
3.5.7 Conversion calculations 71
3.6 X-ray fluorescence (XRF) spectrometry 72
3.7 Reproducibility check 73
CHAPTER 4: COMPREHENSIVE BIOMASS FEEDSTOCK CHARACTERISATION 76
4.1 Introduction 76
4.2 Methods 77
4.3 Results and discussion 78
4.3.1 Thermochemical characteristics 78
4.3.2 Structural chemistry and elemental composition 90
4.3.3 Extractives and bio-polymer composition 94
4.4 Conclusion 101
CHAPTER 5: NON-CATALYTIC LIQUEFACTION 104
5.1 Introduction 104
5.2 Methods 105
5.3 Results and discussion 107
5.3.1 Effect of glycerol on biomass conversion 107
5.3.2 Composition of liquid product 110
5.3.3 Effect of water and acetone 114
5.3.4 Effect of glycerol-cosolvent mixtures 117
5.3.5 Quantification of targeted products 123
5.4 Conclusion 129
CHAPTER 6: CATALYTIC LIQUEFACTION AND INFLUENCE OF REACTION PARAMETERS 132
6.1 Introduction 132
6.2 Methods 132
6.3 Results and discussion 134

6.3.1 Effect of catalyst 134
6.3.2 Effect of temperature 138
6.3.3 Effect of liquefaction solvent (water versus ethylene glycol) 144
6.3.4 Effect of pressure 152
6.3.5 Role of different biomass 154
6.4 Conclusion 156
CHAPTER 7: POTENTIAL ROLE OF BIOMASS AS A HETEROGENEOUS CATALYST 159
7.1 Introduction 159
7.2 Methods 160
7.3 Results and discussion 162
7.3.1 Catalytic effect of pine needles (PN) 162
7.3.2 Catalytic effect of bio-chars and ash 165
7.4 Conclusion 169
CHAPTER 8: CONCLUSIONS AND SUGGESTIONS FOR FUTURE WORK 170
8.1 Introduction 170
8.2 Conclusion 171
8.3 Suggestions for future work 172
REFERENCES 174
APPENDIX A 194
A.1 Mass balances of preliminary liquefaction experiments 194
A.2 Suitability of solvent and method for product (liquid-solid) separation 196
APPENDIX B 200
B.1 Supplementary information on proximate composition of pine needles and sugarcane bagasse (Chapter 4) 200
APPENDIX C 201
C.1 Supplementary information for Chapter 6 201
APPENDIX D 203
D.1 Supplementary information for Chapter 7 203
APPENDIX E 204
E.1 Selected media publications 204
E.1.1 Your Christmas tree could help save the planet (BBC News) 204
E.1.2 New recycling process could help your Christmas tree lead a surprising second life (The Conversation) 207

LIST OF FIGURES

Figure 1.1: Global temperature change and projections relative to the period between 1850 and 1900 [1]. 2
Figure 1.2: Evolution of global ethanol production (in billion litres) by feedstocks used [7]. 3
Figure 2.1: Structure of plant cell wall and microfibril cross-section (strands of cellulose molecules embedded in a matrix of hemicellulose and lignin) [11]. 9
Figure 2.2: Chemical structure of lignin (p-coumaryl alcohol – green background, coniferyl alcohol – orange background, and sinapyl alcohol – blue background) [11]. . 11
Figure 2.3: Chemical structure of cellulose chains [11]. 12
Figure 2.4: Chemical structure of hemicellulose compounds (xylan and glucomannan are the most existing biopolymer) [11]. 13
Figure 2.5: Simplified process diagram for the production of ethanol from lignocellulose and carbohydrates. Adapted from Mergner et al. [7]. 16
Figure 2.6: Thermochemical biomass processing and products [19]. Dashed arrows are to distinguish criss-cross paths only. 17
Figure 2.7: Key chemicals obtained from the decomposition of lignocellulose polymers during liquefaction [99]. 5-HMF is 5-hydroxymethylfurfural. 26
Figure 2.8: The temperature-pressure phase diagram of water showing typical regions employed for biomass liquefaction and gasification. Adapted from Al-Muntaser [121]. 32
Figure 2.9: Yield of liquefaction products from eucalyptus as a function of temperature Sugano et al. [143]. Where d.a.f means dry ash-free. Note that the liquid product in this research has been divided into oil, water-soluble product (WS), and water. Reaction conditions: 3 g eucalyptus, 30 g solvent (paper regeneration wastewater), 2 MPa N2 initial pressure, 7 °C /min heating rate, and 0 min hold time at set the temperature 39
Figure 2.10: World's top 10 sugarcane producing countries. Data obtained from Atlas Big [147]. 42
Figure 2.11: Photographs of (a) sugarcane trash [152] and (b) sugarcane bagasse[153]. 43
Figure 2.12: Quantity of sugarcane bagasse available (SCB-A), used for power generation (SCB-PG), and for steam production (SCB-SP) in Brazil from 1999/2000 to 2010/2011 [151]. 44
Figure 2.13: Wood waste generated, recovered, combusted or not usable, and available for recovery in the United States, 2002 [167]. 46
Figure 3.1: Photographs of biomass feedstocks used in this work. 49
Figure 3.2: Schematic diagram of a typical reflux set up [203]. 61
Figure 3.3: Schematic diagram of the autoclave reactor used for biomass liquefaction. Adapted from Gómez 2017 [204]. 62
Figure 3.4: Photographs of the autoclave reactor used for biomass liquefaction highlighting the key components. 63
Figure 3.5: Schematic representation of a gas chromatography-mass spectrometry system [206]. 66
Figure 3.6: Components of an HPLC system [210]. 68
Figure 3.7: Sample GCMS chromatogram for phenol calibration showing various concentrations of phenol with a fixed amount of propylene glycol (1 µL per 1500 µL of analyte solution) as an internal standard. Injection volume = 0.5 µL. 70
Figure 3.8: A sample calibration curve (for phenol) via GCMS analysis. 71

Figure 4.1: TG (a) and DTG (b) curves at 20 °C/min heating rate for dried pine needles (PN) and sugarcane bagasse (SCB), compared with commercial lignin, commercial cellulose, and a 1:1 (wt:wt) mixture of commercial cellulose and lignin. ..79
Figure 4.2: Proximate analysis results for dried (a) pine needles and (b) sugarcane bagasse obtained via non-instrumental (manual) versus TGA methods. 83
Figure 4.3: Proximate composition in wt.% (TGA method) of dried pine needles and sugarcane bagasse compared with commercial cellulose, lignin and a 1:1 weight mixture of cellulose and lignin (i.e. C-L mix). 87
Figure 4.4: FTIR spectra of dried pine needles and sugarcane bagasse compared with commercial cellulose and lignin. Annotations designate key characteristic bands of hemicellulose, lignin, and cellulose. 90
Figure 4.5: Elemental composition of dried pine needles and bagasse compared with commercial cellulose and lignin. Note: commercial lignin was received with 4 wt.% sulphur content from the supplier. 93
Figure 4.6: FTIR spectra of extractive-free biomass compared with non-extracted biomass samples. PN = pine needles and SCB = sugarcane bagasse. 97
Figure 4.7: Figures (a) to (d) compares the TG and DTG results of extractive-free versus non-extracted dried biomass samples. PN = pine needles and SCB = sugarcane bagasse. 98
Figure 4.8: FTIR spectra of extracted lignin compared with extractive-free biomass and commercial lignin. PN = pine needles and SCB = sugarcane bagasse. 99
Figure 5.1: Flow chart for biomass liquefaction studies. 106
Figure 5.2: Pine needles conversion in concentrated glycerol. Conditions: 2 g pine needles, 20 g concentrated glycerol, 250 °C, 30 bar He initial pressure, 300 rpm, 1 h.107
Figure 5.3: FTIR spectra of bio-char compared with pine needles. Conditions: 2 g pine needles, 20 g concentrated glycerol at 250 °C, 30 bar He initial pressure, 300 rpm, 1 h. 108
Figure 5.4: Effect of pine needles on selected compounds in the liquid product obtained from glycerol. Conditions: 2 g pine needles, 20 g solvent, 250 °C, 30 bar He intial pressure, 300 rpm, 1 h. Both samples were diluted to the same concentration and analysed by the same method. 112
Figure 5.5: Pine needles conversion in various solvent systems. Conditions: 2 g pine needles, 20 g solvent, 250 °C, 30 bar He initial pressure, 300 rpm, 1 h. 114
Figure 5.6: FTIR spectra of bio-chars obtained from pine needles liquefaction using concentrated glycerol (G) and water (W) compared with dried pine needles. Conditions: 2 g pine needles, 20 g solvent at 250 °C, 30 bar He initial pressure, 300 rpm, 1 h. 115
Figure 5.7: Impact of glycerol-cosolvent mixtures on pine needles (solid lines) and glycerol (dashed lines) conversion. Conditions: 2 g pine needles, 20 g solvent, 250 °C, 30 bar He initial pressure, 300 rpm, 1 h. Shown fits are to guide the eye only. 117
Figure 5.8: Sample GCMS chromatograms of liquid products obtained from the liquefaction of pine needles using glycerol only versus glycerol-cosolvent mixtures..118
Conditions: 2 g pine needles, 20 g solvent, 250 °C, 30 bar He initial pressure, ...118
300 rpm, 1 h. Glycerol:cosolvent = 1:3(mol:mol). 118
Figure 5.9: Concentration of acetic acid and phenol in liquid products obtained from the liquefaction of pine needles using various glycerol-water (G:W) concentrations. .124
Conditions: 2 g pine needles (PN), 20 g solvent, 250 °C, 30 bar He initial pressure, 300 rpm, 1 h. Shown fits are to guide the eye only. 124
Figure 5.10: Concentration of acetic acid and phenol in liquid products obtained from the liquefaction of pine needles using various glycerol-acetone (G:A) concentrations. Conditions: 2 g pine needles (PN), 20 g solvent, 250 °C, 30 bar He initial pressure, 300 rpm, 1 h. Shown fits are to guide the eye only. 125

Figure 5.11: Concentration of monoacetin obtained under various glycerol-water (G:W) concentrations. Conditions: 2 g pine needles (PN), 20 g solvent, 250 °C, 30 bar He initial pressure, 300 rpm, 1 h. Shown fits are to guide the eye only. 126
Figure 5.12: Concentration of solketal and mesityl oxide obtained under various glycerol-acetone (G:A) concentrations. Conditions: 2 g pine needles (PN), 20 g solvent, 250 °C, 30 bar He initial pressure, 300 rpm, 1 h. Shown fits are to guide the eye only. 127
Figure 6.1: Flow chart for biomass liquefaction studies. *HPLC analysis was conducted on liquid products obtained from the water system only. 133
Figure 6.2: Sample GCMS chromatogram of the liquid product obtained from the catalytic hydrothermal liquefaction of pine needles. Conditions:2 g pine needles, 20 g water, 1 wt.% catalyst, 160 °C, 30 bar He initial pressure, 300 rpm, 1 h. 134
Figure 6.3: Effect of catalyst on biomass (pine needles) conversion and key compounds identified (GCMS cum HPLC) in the liquid product. 20 g water 1 wt.% catalyst (where applicable) at 250 °C, 30 bar He initial pressure, 300 rpm, 1 h. 135
Figure 6.4: FTIR spectra of bio-chars obtained from pine needles via catalytic (W-cat) vs non-catalytic (W) hydrothermal liquefaction. Conditions: 2 g pine needles, 20 g water, 1 wt.% catalyst (where applicable) at 250 ^{o}C, 30 bar He initial pressure, 300 rpm, 1 h. 137
Figure 6.5: Effect of temperature on pine needles conversion during catalytic hydrothermal liquefaction. Conditions: 2 g pine needles, 20 g water,1 wt.% catalyst, 30 bar He initial pressure, 300 rpm, 1 h. Shown fits are to guide the eye only. 138
Figure 6.6: Effect of temperature on biomass conversion and concentration of key GCMS identified compounds in the liquid product obtained via catalytic hydrothermal liquefaction of pine needles. Conditions: 2 g pine needles, 20g water, 1 wt.% catalyst, 30 bar He initial pressure, 300 rpm, 1 h. 142
Figure 6.7: Effect of liquefaction solvent on pine needles conversion. Conditions: 2 g pine needles, 20 g solvent, 1 wt.% catalyst (cat), 30 bar He initial pressure, 300 rpm, 1 h. Shown fits are to guide the eye only. 144
Figure 6.8: FTIR spectra of bio-chars obtained via catalytic liquefaction of pine needles with water (W-cat) and ethylene glycol (EG-cat). Conditions: 2 g pine needles, 20 g solvent, 1 wt.% catalyst, 250 °C, 30 bar He initial pressure, 300 rpm, 1 h. 145
Figure 6.9: Effect of liquefaction solvent; water (W) and ethylene glycol (EG) on the concentration of acetic acid, acetone, levulinic acid, and phenol at various temperatures. Conditions: 2 g pine needles, 20 g solvent, 1 wt.% catalyst, 30 bar He initial pressure, 300 rpm, 1 h. Shown fits are to guide the eye only. 151
Figure 6.10: Effect of pressure on pine needles (BM) and ethylene glycol (EG) conversion. Conditions: 2 g pine needles, 20 g ethylene glycol, 1 wt.% catalyst, 160 °C, 300 rpm, 1 h. Shown fits are to guide the eye only. 153
Figure 6.11: Sample GCMS chromatogram of liquid product obtained via atmospheric liquefaction of biomass. Conditions: 2 g sugarcane bagasse, 20 g ethylene glycol, 0.6 wt.% catalyst, 160 °C, 300 rpm, 1 h. Note: ethylene glycol represents the left-over reactant. 154
Figure 6.12: Sugarcane bagasse (SCB) versus pine needles (PN) conversion. Conditions:2 g biomass, 20 g ethylene glycol, 1wt.% catalyst, 300 rpm, atmospheric pressure, 1 h. 155
Figure 6.13: Comparison of biomass derived products from the atmospheric liquefaction of sugarcane bagasse (SCB), and pine needles (PN). Conditions:2 g biomass, 20 g ethylene glycol, 160 °C, 300 rpm, 1 h. 0.6 wt.% and 1 wt.% catalyst were used for SCB, and PN respectively. 155
Figure 7.1: Flow chart for studies on the potential application of biomass, bio-char, and ash as heterogeneous catalysts. 161

Figure 7.2: Effect of pine needles as catalyst on the concentration of key products obtained from the liquefaction of pine needles with various mixtures of glycerol (G) and acetone (A). Conditions: 2 g pine needles, 20 g solvent, 250 °C, 30 bar He initial pressure, 300 rpm, 1 h. 162
Figure 7.3: Effect of pine needles (PN) and glycerol (G) on mesityl oxide concentration. Conditions: 2 g PN*, 20 g solvent, 250 °C, 30 bar He He initial pressure, 300 rpm, 1h. *Where applicable. PN is whole pine needles, PN-m is milled pine needles, < 200 µm). 163
Figure 7.4: Pictures of dried pine needles compared with residues obtained from the liquefaction of pine needles with various solvents. Conditions: 2 g pine needles (PN), 20 g solvent, 250 °C, 30 bar He initial pressure, 300 rpm, 1 h. 164
Figure 7.5: Effect of various bio-chars and ash as catalyst on mesityl oxide concentration (g/L). Conditions: 20 g acetone, 1 g catalyst, 250 °C, ... 167
30 bar He initial pressure, 300 rpm, 1 h. 167
Figure 7.6: Effect of pine needles, bio-chars, and ash as catalyst on mesityl oxide selectivity and acetone conversion. Conditions: 20 g acetone, 1 g catalyst, 250 °C, 30 bar He initial pressure, 300 rpm, 1 h. 168
Figure A1: Effect of solvent used for product separation on biomass and ethylene glycol conversion for different batches of reaction. Conditions:2 g BM (sugarcane bagasse), 20 g EG, and 0.12 g H_2SO_4 as catalyst at 160 °C, 30 bar He, 300 rpm, 1 h. 198
Figure A2: GCMS chromatogram for control experiment "II" using two separate solvents; acetone, and ethanol for product dilution. Note the peak heights of ethylene glycol and propylene glycol in both cases, as well as the appearance of dioxolane derivatives when acetone was used. 198
Figure C1: Photographs of biomass feedstocks and samples of liquid products from pine needles liquefaction using (A) ethylene glycol and (B) water as liquefaction solvent. Picture C is a sample bio-char obtained from the liquefaction process..... 202

LIST OF TABLES

Table 2.1: Proximate composition of various types of biomass in weight percent [42]. 10
Table 2.2: Typical product yields(dry weight basis) obtained from wood via different modes of pyrolysis [67,69].....19
Table 2.3: Properties of sawdust derived biofuels compared with commercial/military jet fuels. Biofuel-I: aromatics biofuel, produced by the catalytic cracking of sawdust over the HZSM-5 catalyst at 500 °C along with the alkylation of the sawdust-derived monomers using the [bmim]Cl–2$AlCl_3$ ionic liquid at 60 °C for 1 hour. Biofuel-II: cyclic alkanes biofuel, produced by the hydrogenation of aromatics over the Pd/AC catalyst at 200 °C for 6 hours. AC = Activated Carbon, u.d. = undetected [85]. 21
Table 2.4: Typical product yields (based on biomass dry weight) obtained from the liquefaction of various biomasses under different conditions.....24
Table 2.5: Continuous hydrothermal liquefaction (HTL) plants and setups documented in the literature [109].....28
Table 2.6: Typical properties of wood pyrolysis bio-oil, liquefaction (HTL) bio-oil, and heavy fuel oil [91]. 30
Table 2.7: Main chemical compounds identified (via GC-MS) in liquid products obtained from the liquefaction of brewer's spent grain using water and various alcohol-water mixtures as solvents. MeOH = methanol:water, EtOH = ethanol:water, and 2-PrOH = 2-propanol:water, all at alcohol:water ratio of 70:30 (wt:wt). Conditions: 250 °C, 30 bar initial He pressure, 30 min reaction time and biomass:solvent ratio of 1:10 (wt:wt) [14].....35
Table 2.8: Average molecular weights of liquid products (bio-crude) obtained from the liquefaction of red pine sawdust using water and ethanol at various temperatures. Conditions: 50 bar initial N_2 pressure, 30 min reaction time, and biomass:solvent ratio of 6:100 (wt:wt) [26].....36
Table 3.1: List of chemicals used in this work with their specifications and suppliers. 50
Table 3.2: Thermal program used for TGA and DTG analyses of biomass samples. ...53
Table 3.3: GCMS method employed for liquid product analysis. 67
Table 4.1: Degradation profile of cellulose, lignin, sugarcane bagasse, and pine needles. 80
Table 4.2: Shoulder peaks from the DTG curves of pine needles and sugarcane bagasse along with assigned components.....81
Table 4.3a: Summary of the manual method (ASTM E870 – 82) used for proximate analysis of the biomass materials.....86
Table 4.3b: Summary of the TGA method used for proximate analysis of the biomass materials. 86
Table 4.4a: Proximate composition of pine needles compared with others investigated in the literature. 88
Table 4.4b: Proximate composition of sugarcane bagasse compared with others investigated in the literature.....88
Table 4.5: Functional groups and equivalent wave numbers from FTIR spectra (Figure 4.4) of pine needles and sugarcane bagasse. 91
Table 4.6a: Elemental constituents of dried pine needles compared to others studied in the literature. 94
Table 4.6b: Elemental constituents of dried sugarcane bagasse compared to others studied in the literature.....94
Table 4.7: Percentage of extractives in dried pine needles (Picea abies) and sugarcane bagasse. db = dry biomass.....95

Table 4.8a: Chemical composition of extractives from dried pine needles (Picea abies). 96
Table 4.8b: Chemical composition of extractives from dried sugarcane bagasse. 96
Table 4.9: Bio-polymer constituents of extractive-free pine needles and sugarcane bagasse compared with others researched in literature. 101
Table 4.10: Summary of the composition of pine needles (Picea abies) and sugarcane bagasse on a dry weight basis. 102
Table 5.1: Chemical compounds identified (via GCMS) in the liquid product obtained from the liquefaction of pine needles with concentrated glycerol (G+PN) compared with those obtained from glycerol without pine needles (G). Conditions: 2 g pine needles, 20 g concentrated glycerol, 250 °C, 30 bar He initial pressure, 300 rpm, 1 h. 111
Table 5.2: Chemical compounds identified (GCMS) in the liquid product obtained from the liquefaction of pine needles with acetone (A) and water (W). Conditions: 2 g pine needles, 20 g solvent, 250 °C, 30 bar He initial pressure, 300 rpm, 1 h. 116
Table 5.3: Chemical compounds identified (GCMS) in the liquid product obtained from the liquefaction of pine needles with various glycerol-acetone mixtures. Conditions: 2 g pine needles, 20 g solvent, 250 °C, 30 bar He initial pressure, 300 rpm, 1 h. Glycerol:acetone (mol:mol). 119
Table 5.4: Chemical compounds identified (GCMS) in the liquid product obtained from the liquefaction of pine needles with various glycerol-water mixtures. Conditions: 2 g pine needles, 20 g solvent, 250 °C, 30 bar He initial pressure, 300 rpm, 1 h. Glycerol:water (mol:mol).....120
Table 6.1: GCMS identified chemicals in the liquid product obtained from the catalytic hydrothermal liquefaction of pine needles at various temperatures. Conditions: 2 g pine needles, 20 g water, 1 wt.% catalyst, 30 bar He initial pressure, 300 rpm, 1 h. 141
Table 6.2: Effect of liquefaction solvent on the distribution of compounds identified in the liquid product obtained from the catalytic liquefaction of pine needles. 2 g pine needles, 20 g solvent, 1 wt.% catalyst, 200 °C, 30 bar He initial pressure, 300 rpm, 1 h. 148
Table 7.1: Ash content and mineral composition of bio-chars and ash used as catalyst in mesityl oxide synthesis studies. Softwood bio-char (SWB), rice husk bio-char (RHB), pine needles bio-char (PNB), and pine needles ash (PNA). 166
Table A1: Mass balances of preliminary liquefaction experiments of sugarcane bagasse and pine needles. Liquefaction solvent: ethylene glycol, catalyst:H_2SO_4. 195
Table A2: Process input and methods of product separation for various batches of liquefied biomass (sugarcane bagasse). Conditions:2 g BM, 20 g EG, 0.12 g H_2SO_4 as catalyst at 160 °C, atmospheric pressure, 300 rpm, 1 h. 196
Table A3: Amount of solvent used versus amount recovered during product separation. 199
Table B1-a: Proximate composition of pine needles obtained via manual versus TGA methods with the corresponding standard deviations and experimental errors. Values reported as the mean ± standard deviation in weight %.....200
Table B1-b: Proximate composition of sugarcane bagasse obtained via manual versus TGA methods with the corresponding standard deviations and experimental errors. Values reported as the mean ± standard deviation in weight %. 200
Table C1: GCMS identified compounds in liquid products obtained from the liquefaction of pine needles using ethylene glycol as solvent. Reaction conditions: 2 g pine needles, 20 g ethylene glycol, 0.12 g H_2SO_4 as catalyst (1 wt.% catalyst), 30 bar He initial pressure, 300 rpm and 1 h. Control is a blank experiment without pine needles (only ethylene glycol and 1 wt.% catalyst at 250 ^oC.....201
Table D1: Key products identified (GCMS) in the liquid product obtained from the self-condensation of acetone (A) using various catalysts. Softwood bio-char (SWB),

rice husk bio-char (RHB), pine needles bio-char (PNB), and pine needles ash (PNA). 203

LIST OF SCHEMES

Scheme 2.1: Simplified reactions that occur during hydrothermal gasification of cellulose and glucose [97]. 22
Scheme 2.2: Transesterification of triglyceride to mono-alkyl esters and glycerol. 33
Scheme 2.3: Esterification of fatty acid to mono-alkyl ester. 33
Scheme 5.1: Ketalisation of glycerol with acetone. 105
Scheme 5.2: Proposed pathways for liquid phase glycerol conversion to useful chemicals adapted from Tran & Kannangara [262]. 110
Scheme 5.3: Exemplar proposed reaction scheme for the formation of valuable chemicals during the liquefaction of lignocellulosic biomass, ... 121
adapted from Pedersen & Rosendahl [266]. 121
Scheme 5.4: Simplified reaction scheme for aldol condensation of acetone to mesityl oxide. 123
Scheme 5.5: Reaction for the synthesis of glycerol carbonate from glycerol and carbon dioxide [263]. 127
Scheme 5.6: Proposed pathway to the production of monoacetin from glycerol and acetonitrile [263]. 128
Scheme 6.1: Proposed reaction pathway to the formation of levulinic acid and other products. Adapted from Liu et al. [269]. Detected products in bold. 136
Scheme 6.2: Plausible routes for the conversion of ethylene glycol to useful chemicals. Conditions: 20 g ethylene glycol, 0.12 g H_2SO_4 as catalyst (1 wt.% catalyst), 30 bar He initial pressure, 300 rpm and 1 h. 147
Scheme 6.3: Proposed reaction pathways for the formation of various esters and ketals via acid catalysed liquefaction of biomass with ethylene glycol, adapted from Amarasekara and Wiredu 149
Scheme A1: Reaction of ethylene glycol with acetone to form 1,2dioxolane,2,2-dimethyl-, and water. 199
Scheme A2: Reaction of propylene glycol with acetone to form 1,3dioxolane,2,2,4-trimethyl- and water. 199

NOMENCLATURE

Abbreviations

ASTM	American standard for testing materials
BM	biomass
DTG	derivative thermogravimetric analysis
FTIR	Fourier transform and infrared spectroscopy
GCMS	gas chromatography mass spectrometry
HPLC	high performance liquid chromatography
m/z	mass to charge ratio
Mtoe	million tonnes of oil equivalent
NREL	national renewable energy laboratory
PN	pine needles
rpm	revolutions per minute
SCB	sugarcane bagasse
TGA	thermogravimetric analysis
wt.%	weight percent
XRF	X-ray fluorescence

Other names/abbreviations for chemical compounds

These are a list of other names or terms used interchangeably in various sections of this thesis. For instance, the tables of GCMS data largely display the scientific names of compounds. However, in few cases where the scientific names are too long, these names were replaced with equivalent shorter common names or abbreviations in the discussion to ease reading.

5-HMF	5-Hydroxymethylfurfural
BBOT	2,5-bis (5-tert-butyl-benzoxazol-2-yl) thiophene
diacetone alcohol	4-hydroxy-4-methyl-2-pentanone
DPME	ethyl 3-(2-methyl-1,3-dioxolan-2-yl)propanoate
HLEK	2-hydroxyethyl levulinate ethylene ketal
isomesityl oxide	4-methyl-4-penten-2-one
levulinic acid	4-oxo-pentanoic acid
mesityl oxide	4-methyl-3-penten-2-one
monoacetin	2,3-dihydroxypropyl acetate
solketal	2,2-dimethyl-1,3-dioxolane-4-methanol

Chapter 1

Introduction

CHAPTER 1: INTRODUCTION

1.1 Background

The 2018 IPCC's Special Report on Global Warming of 1.5 °C (SR15) warned that global temperature rise could reach 1.5 °C above pre-industrial levels by 2040, causing major crises if steps are not taken to reduce the current rate of warming (Figure 1.1) [1]. This calls for the fast development of solutions to mitigate the excessive greenhouse gas emissions [2].

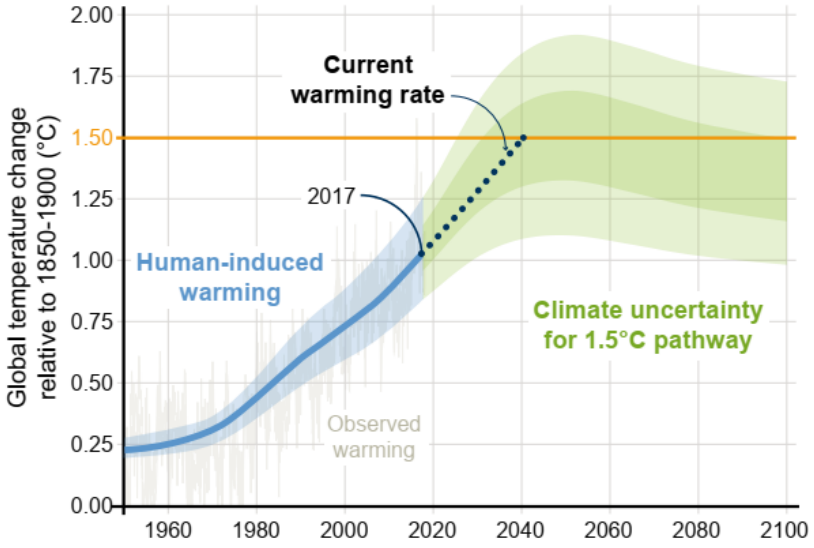

Figure 1.1: *Global temperature change and projections relative to the period between 1850 and 1900* [1].

Current commercial-scale interventions in the battle against climate change are mostly based on the utilisation of food resources (first-generation biomass) as alternative and renewable sources of energy and chemicals; e.g. the conversion of vegetable oils to biodiesel, grains to bioethanol [3,4] and recently, cassava to carrier bags [5,6]. It is clear from Figure 1.2 that food resources play a significant role as feedstocks for the production of ethanol, which is popularly used for fuel and other non-food applications. By 2020, 80 % of the global ethanol production is expected to originate from coarse grains and sugarcane; whereas non-agricultural sources are projected to contribute only 5 % [7].

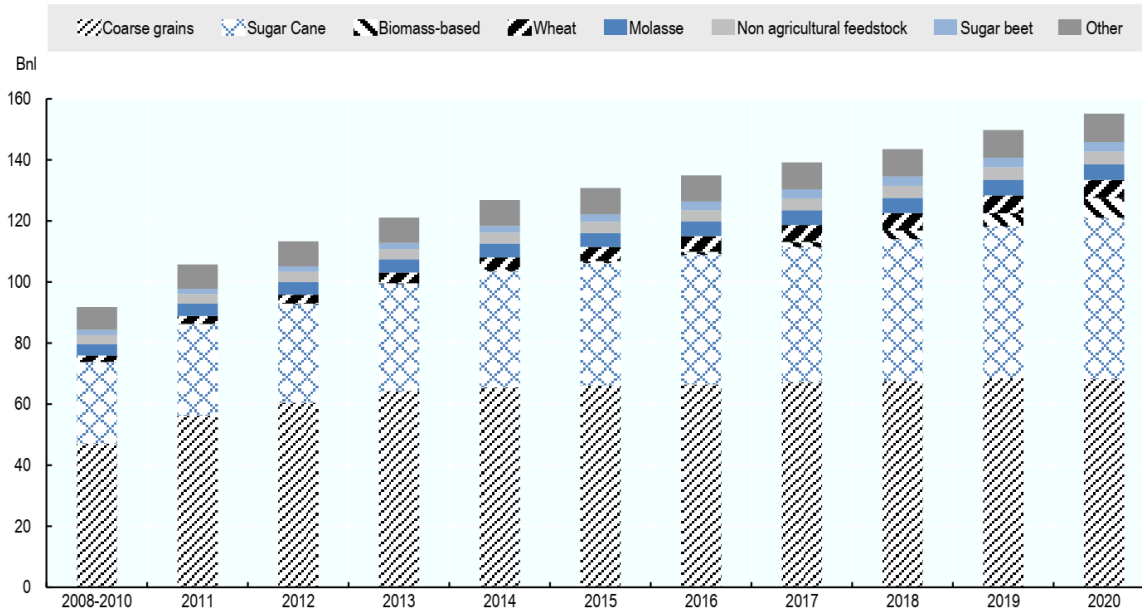

Figure 1.2: *Evolution of global ethanol production (in billion litres) by feedstocks used* [7].

Edible biomass, however, constitutes a minor percentage of the entire biomass mix. For example, the amount of residue (*i.e.* stalk/straw, leaves, cobs, and chaff) generated during the harvest of corn and wheat is estimated to be 30 – 75 wt.% (fresh weight basis), depending on crop yield [8]. In other words, the edible proportion of corn and wheat obtained during harvest range from 25 to 70 wt.%, depending on crop yield. Hence, the use of food-based biomass for energy and chemicals supply is unsustainable and poses a potential threat to food security. A prospective sustainable solution to this threat is the utilisation of waste resources like agricultural and forest residues. This will not only guarantee food security, but also ease the waste management challenges, and save land space needed for landfills for more important purposes like agriculture, and infrastructure developments.

Biomass waste (be it agricultural or forest-based) is an indispensable resource due to the fact that it is renewable, relatively environmentally friendly, and widely available. It is estimated that 63 % of global municipal solid waste is made up of biomass [9]. Non-edible biomasses are predominantly lignocellulosic in nature. Lignocellulosic biomass, an inevitable and dominant proportion of the primary food supply chain waste is a complex heterogeneous mixture of organic matter, and to a lesser extent, inorganic matter [10,11]. The organic fraction is made up of three main structural polymers: cellulose,

hemicellulose, and lignin. These polymers are composed of various C_5 and C_6 compounds which could be harnessed for chemicals synthesis, aside from energy and fuel applications. Consequently, recent research has been focused on the exploitation of lignocellulosic biomass and other forms of non-edible biomass (second and third-generation biomass) for energy and chemicals production. For example, the conversion of wheat straws [12], sugarcane bagasse [13], brewers spent grain [14], and algae [15,16] to bioethanol, other platform chemicals, and bio-oil (which is an oily liquid product made via thermochemical processing of biomass); the exploitation of fats and oils from waste resources is also on the rise [17,18]. Amidst the wide range of available agricultural and forest waste, pine needles and sugarcane bagasse remain under-explored, particularly as feedstock for the chemical industry.

Various thermochemical technologies (i.e. pyrolysis, combustion, gasification, and liquefaction) and biochemical technologies (i.e. anaerobic digestion and fermentation) [19,20] have been employed for the conversion of biomass wastes to value-added products. Among these, liquefaction is one of the developing techniques with great potentials in terms of sustainability. Liquefaction offers a uniquely flexible approach to process wet or dry feedstocks and can be virtually used with all types of organic materials. Besides, it is able to effectively convert all three major complex components of the lignocellulose (i.e. lignin, cellulose and hemicellulose) without the need for extensive pretreatment [14]. The application of heat (typically, 150 - 420 °C at 1 - 240 bar [21]) and solvents are the core components of this process. The solvent introduced to the process must possess the ability to breakdown the complex structure of lignocellulose under the chosen reaction conditions as well as aid in the conversion of the resultant fragments to useful chemicals.

Though several solvents including water and alcohols were applied in biomass liquefaction in literature, they are not directly comparable as these studies were conducted in different systems and sometimes under different conditions. Water (under subcritical, near-critical or supercritical conditions) [14,22] is the most widely used solvent owing to its low cost, abundance, and more importantly, acts as a source of hydrogen through the water-gas shift reaction [23]. Biomass conversion and bio-oil yields are, however, largely reported to be relatively low in this process, due to the repolymerisation of biomass fragments, which sometimes lead to solids formation at the expense of liquid yield [24–

27]. As such, solvents including, alcohols [14,26,28], ionic liquids, and 1,4-dioxane have been exploited [29] in attempts to improve biomass conversion. The use of simple alcohols (C_1-C_4) or alcohol-water mixtures have been reported to achieve relatively higher biomass conversions and higher bio-oil yields over water [14,26,28]. These alcohols nonetheless due to their low volatilities evaporate very quickly demanding high solvent/feed ratios up to 16:1 [26], making the process less economical. Similarly, solvents such as ionic liquids and 1,4-dioxane are very expensive [30] and potentially less practical for a cost-effective large-scale process.

This necessitates the search for alternative and cheaper sources of solvent. Ethylene glycol, a potential cheaper option has lately been demonstrated to be effective at converting different types of biomass under milder conditions; ≤ 190 °C and 1 atm. [31]. The application of glycerol [32,33] an undesired by-product from biodiesel production is also gaining recognition these days, but severely understudied. Glycerol is a simple polyol, colourless, odourless, viscous, and non-toxic liquid. It is widely produced as an undesired by-product from the biodiesel production industry; as such, its use in biomass liquefaction would be greatly beneficial in terms of cost and waste minimisation and sustainability. Glycerol has lately been reported to enhance biomass conversion and bio-oil yield [30,34]. Nonetheless, this area is still novel with lots of opportunities for further research into the chemistry behind the process. In other researches, the potential to transform glycerol to value-added chemicals such as glycerol carbonate [35] acrolein [36] and acrylic acid [37,38] has been demonstrated. Thus, a plausible sustainable route worth considering is the possibility to co-valorise biomass waste and glycerol in one pot, which might be particularly beneficial for the upgrading of crude glycerol from the biodiesel industry.

1.2 Aims and objectives

This research seeks to utilise waste from biomass-derived sources to produce high-value products that could serve as feedstock to the chemical and fuel industries, thereby contributing to the circular economy. Sugarcane bagasse (a common food supply chain waste) and pine needles (a readily available forest waste) will be used as feedstocks in this study. The choice of pine needles and sugarcane bagasse is to gain insight into the behaviour of biomass wastes of differing physical and chemical characteristics in

chemical synthesis. Specifically, the impact of three selected low-cost solvents; glycerol, water, and ethylene glycol on biomass degradation and resultant products will be investigated. The following objectives were therefore established to accomplish the set goal:

1. To understand the chemical composition, as well as the physical, chemical and thermal characteristics of sugarcane bagasse and pine needles via various characterisation techniques.
2. To explore the range of chemicals that could be synthesised from the liquefaction of lignocellulosic biomass in various solvent systems (water, glycerol and ethylene glycol) using pine needles as an exemplary feedstock.
3. To advance our understanding of the role of various solvents (water, glycerol and ethylene glycol) in biomass liquefaction processes under similar reaction conditions.
4. To design a novel route to the one-pot simultaneous valorisation of biomass and glycerol.
5. To investigate the effect of sulphuric acid as a homogeneous catalyst and the effect of process parameters (temperature, and pressure) on biomass conversion and product yield.
6. To evaluate the effect of biomass type (pine needles versus sugarcane bagasse) on biomass conversion and the chemical composition of the resultant liquid product.
7. To investigate the potential role of biomass and bio-char formed *in situ* as a heterogeneous catalyst during liquefaction.

Chapter 2

Literature review

CHAPTER 2: LITERATURE REVIEW

2.1 Introduction

Biomass is the term used to describe all biologically produced matter. The elementary sources of biomass include agricultural crops, standing forests, woods, and their waste by-products, animal wastes, waste from food processing, aquatic plants, and algae [20]. Approximately 63 % of global municipal solid waste is made up of biomass [9]. Biomass wastes from plants (be it agricultural- or forest-based) are predominantly lignocellulosic in nature, e.g. sugarcane bagasse and pine needles [39,40]. Therefore, the literature survey first provided a general overview of lignocellulosic biomass and its composition. This was then followed by a consideration of prevailing technologies for the conversion of such lignocellulosic biomasses into value-added products. The last section of the literature survey was focused on the liquefaction technique which was considered in this work as the most suitable technique to adapt for the conversion of pine needles and sugarcane bagasse to platform chemicals due to its versatility in terms of feedstock choice; liquefaction can be effectively applied to a wide variety of biomass, whether wet or dry.

2.2 Lignocellulosic biomass and its constituents

Biomass is a complex heterogeneous mixture of organic matter and, to a lesser extent, inorganic matter, containing various solid and fluid phases with different contents [10]. The main structural organic components in lignocellulosic biomass are cellulose, hemicellulose, and lignin. Lignocellulose is the primary building block of plant cell walls. Figure 2.1 depicts the characteristic structure of a plant cell wall and different bio-compositions. Cellulose fibrils are generally coated with hemicellulose to form an open network, whose empty spaces are gradually filled up with lignin [11]. The complex hierarchy structure of lignocellulosic biomass is a major obstacle in the separation of cellulose, hemicellulose, and lignin for different applications.

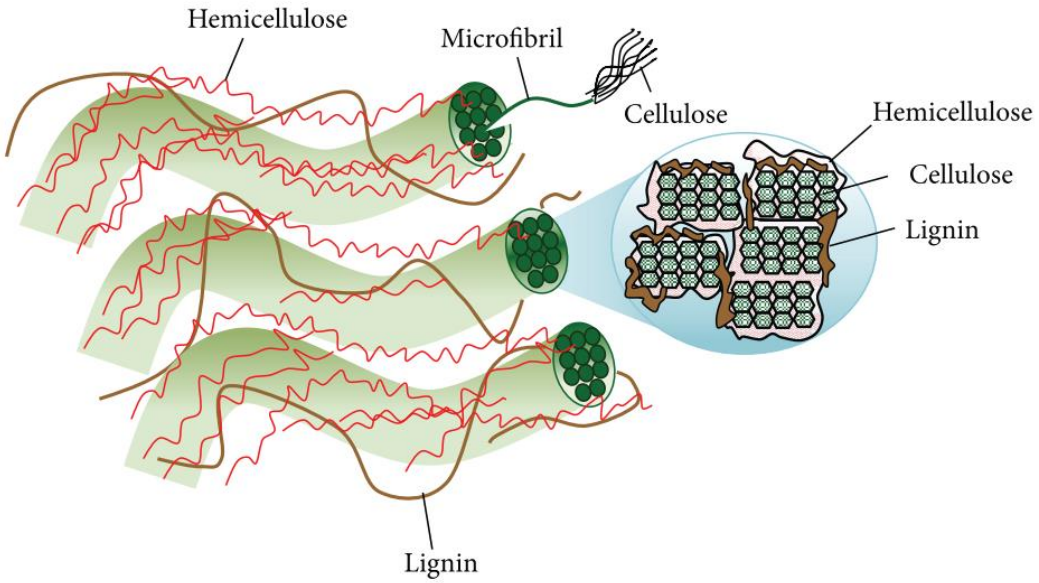

Figure 2.1: *Structure of plant cell wall and microfibril cross-section (strands of cellulose molecules embedded in a matrix of hemicellulose and lignin)* [11].

Lignin, cellulose, and hemicellulose usually exist in variable percentages in various forms of biomass. A study conducted by Vassilev and co-workers [10] on the structural composition of 93 varieties of biomass confirms these variations; the different types of virgin and contaminated feedstock studied disclosed 12 - 93 wt.% cellulose, 0 - 67 wt.% hemicellulose, and 0 - 54 wt.% lignin. It is, therefore, important that biomass feedstocks are properly characterised before their application in conversion processes to facilitate a better understanding of the influence of the biomass constituent on the process and products. For instance, feedstocks rich in lignin are likely to yield products rich in phenolics whereas feedstocks rich in cellulose and hemicellulose are likely to yield products containing significant amounts of sugars (e.g. glucose or xylose) or sugar derivatives (e.g. organic acids, alcohols, and furans).

Determining the proximate composition (amount of moisture, volatile matter, fixed carbon, and ash) of biomass feedstocks could also help determine the appropriate technique suitable for their valorisation. For example, biomasses with > 50 wt.% moisture are typically less efficient when applied as feedstocks for processes such as combustion and pyrolysis [41]. Such feedstocks require an energy-intensive pre-drying process which makes the entire biomass conversion route less economical. A typical example of differences in the proximate composition of various biomasses is summarised in

Table 2.1. A more comprehensive documentation of such variances in biomass constituents could be found in works done by Garcia *et al.* [42] and Vassilev *et al.* [10].

Table 2.1: *Proximate composition of various types of biomass in weight percent* [42].

	Moist. (%)	Ash (%)	VM (%)	FC (%)
Commercial fuels				
Almond shell	8.68 ± 0.08	2.2 ± 0.3	82 ± 2	15.80
Beet root pellets	12.5 ± 0.2	9 ± 2	76 ± 1	15.00
Briquette	5.84 ± 0.06	0.8 ± 0.1	85 ± 1	14.20
Holm oak branch chips	11.1 ± 0.3	7.4 ± 0.2	74.9 ± 0.5	17.70
Olive stone	11 ± 1	1.4 ± 0.3	78.3 ± 0.6	20.35
Pine and pine apple leaf pellets	8.2 ± 0.1	3.2 ± 0.3	75 ± 1	21.80
Pine chips	10.25 ± 0.05	0.6 ± 0.02	81.6 ± 0.4	17.80
Pine cone heart	23.1 ± 0.5	3.5 ± 0.6	66 ± 7	23.1
Pine cone leaf	9.14 ± 0.08	1.3 ± 0.1	80 ± 0.9	18.70
Pine kernel shell	8.33 ± 0.09	2.7 ± 0.1	77.6 ± 0.8	19.70
Pine pellets	6.75 ± 0.04	1.3 ± 0.2	83.5 ± 0.1	15.20
Sawdust	11.3 ± 0.2	1.6 ± 0.2	81 ± 1	17.4
Straw pellets	7.3 ± 0.1	9.8 ± 0.2	79 ± 2	11.20
Vegetal coal	5.29 ± 0.09	5.9 ± 0.1	26 ± 1	68.10
Vine shoot chips	22 ± 1	9.7 ± 0.9	66 ± 2	24.30
Wood chips	25.6 ± 0.6	1.5 ± 0.7	68.6 ± 0.2	29.90
Wood pellets	7.7 ± 0.8	1.3 ± 0.9	82 ± 2	17.08
Energy crops				
Gorse	43 ± 5	5 ± 4	45.2 ± 0.9	50.17
Miscanthus	7.53 ± 0.05	9.6 ± 0.2	79 ± 1	11.40
Oats and vetch	7.8 ± 0.1	7.33 ± 0.08	72 ± 2	20.67
Pine cone leaf	9.3 ± 0.2	1.9 ± 0.2	75.9 ± 0.4	22.20
Sainfoin	9.6 ± 0.2	9.2 ± 0.2	73 ± 2	17.80
Sorghum	6.1 ± 0.1	17 ± 2	62 ± 4	21.00
Straw	6.8 ± 0.2	6.1 ± 0.4	82 ± 1	11.90
Thistle	11.6 ± 0.1	0 ± 2	80.67 ± 0.04	21.65
Triticale	9.8 ± 0.1	6.2 ± 0.1	75 ± 2	18.80
Cereals				
Barley	9.9 ± 0.2	3 ± 0.6	76.9 ± 0.6	20.10
Maize	11.1 ± 0.2	2.1 ± 0.2	78.9 ± 0.4	19.05
Oats bran	9.9 ± 0.3	4.15 ± 0.09	77 ± 1	18.85
Rye	10.76 ± 0.06	1.8 ± 0.04	78.9 ± 0.5	19.30
Soya	10.9 ± 0.1	4.8 ± 0.2	77 ± 0.8	18.20
Wheat	10.3 ± 0.2	2.8 ± 1.2	80 ± 1	17.20
Wheat bran	9 ± 0.1	3.5 ± 0.4	78 ± 1	18.50
Industry wastes				
Apple	10.1 ± 0.4	2.6 ± 0.7	79 ± 1	18.40
Apple rind	12.3 ± 0.1	2.2 ± 0.2	76.9 ± 0.4	20.90
Apricot stone	7.8 ± 0.2	0.7 ± 0.1	N/D	N/D
Avocado pear peel	9.87 ± 0.07	3.1 ± 0.6	82 ± 1	14.90
Avocado pear stone	16.7 ± 0.6	2.0 ± 0.1	72 ± 1	26.00
Bagasse	3.9 ± 0.3	33 ± 4	N/D	N/D
Barley straw	9.8 ± 0.2	6.1 ± 0.4	77.9 ± 0.4	16.00

2.2.1 Lignin

Lignin is a complex molecular structure made up of cross-linked polymers of phenolic monomers mainly *p*-coumaryl alcohol, coniferyl alcohol, and sinapyl alcohol (Figure 2.2) [3,11]. The presence of lignin in biomass is the main cause of biomass recalcitrance during separation processes. Lignin acts as a protective barrier for plant cell permeability and resistance against microbial attacks and thus prevents plant cell destruction. Chemical and physical pretreatments are, therefore, necessary to de-polymerise lignin seal in order to access the carbohydrate portions of the biomass [3]. Woody biomasses generally contain slightly higher amounts of lignin compared to non-woody (herbaceous and agricultural) biomasses. According to Vassilev *et al*. [10], woody biomasses contained 10 - 45 wt.% lignin, an average of 26 wt.% whereas non-woody biomasses had 0 - 54 wt.% lignin, an average of 24 wt. %. The higher lignin content of woody biomasses makes them more recalcitrant during pretreatment or cellulose separation processes [11].

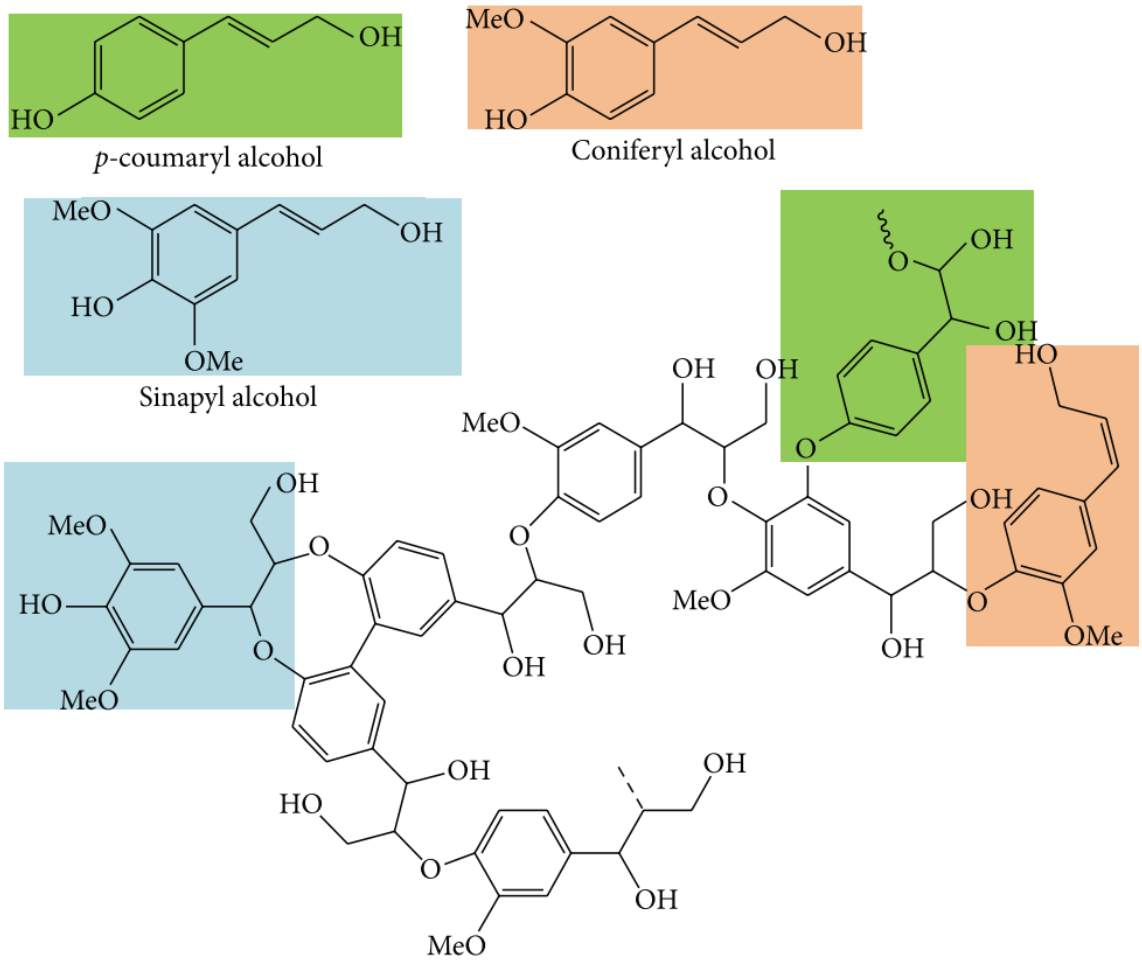

Figure 2.2: *Chemical structure of lignin (p-coumaryl alcohol – green background, coniferyl alcohol – orange background, and sinapyl alcohol – blue background)* [11].

2.2.2 Cellulose

Cellulose appears in both crystalline (organised) or amorphous forms [43]. It is a linear homo-polysaccharide that consists of glucose (D-glucopyranose) units linked together by β-(1-4) glycosidic bonds (β-D-glucan) [44]. These form long chains (called microfibrils) linked together by hydrogen bonds and van der Waals forces (Figure 2.3) [43]. Hence, cellulose is insoluble in water as the hydroxyl groups in the sugar chains are bonded to each other - making a hydrophobic scenario. For this reason, the crystalline domain of microfibrils cellulose, with the presence of extensive intermolecular hydrogen bonds and van der Waals interactions makes it another challenge for hydrolysis accessibility to chemical synthesis [3,11]. Overall, woody biomasses possess lower percentages of cellulose (12 - 66 wt.%, an average of 40 wt.%) compared to non-woody biomasses (24 wt.% - 88 wt.%, an average of 46 wt.%) [10].

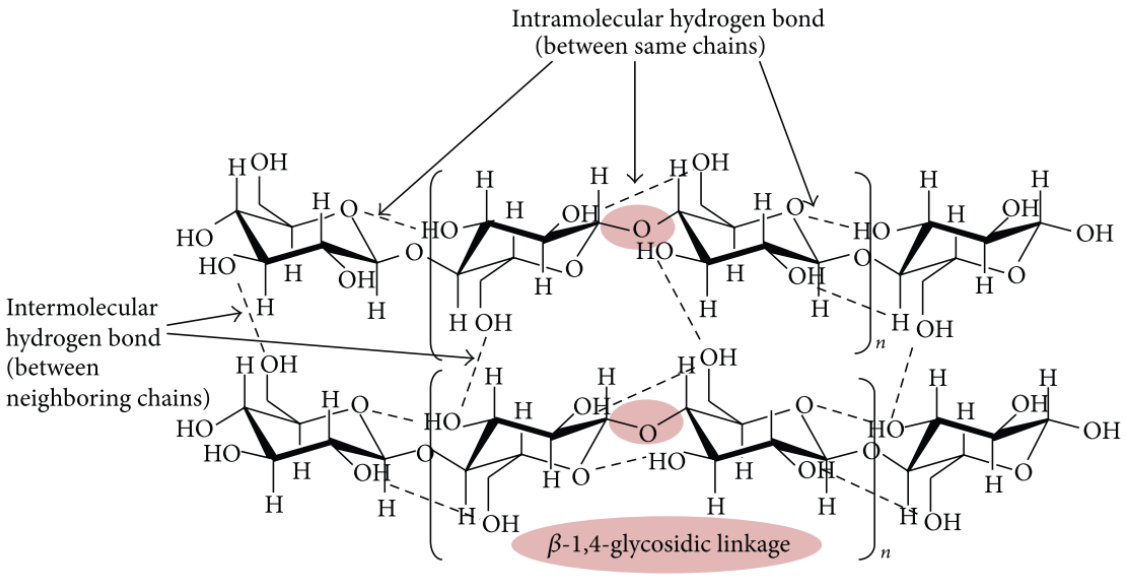

Figure 2.3: *Chemical structure of cellulose chains* [11].

2.2.3 Hemicellulose

Cellulose fibrils are generally "coated" with hemicellulose branches with short lateral chains consisting of different sugars (pentoses, hexoses, and acetylated sugars) (Figure 2.4) with xylan and glucomannan being the most existing polymers [3,11]. Similar to lignin, hemicellulose fractions of biomass are usually isolated via pretreatment

methods, such that subsequent hydrolysis steps to recover glucose from cellulose are more effective [3]. Percentage of hemicellulose in dry woody biomasses is normally within the range of 7 - 66 wt.% (an average of 35 wt.%) whereas non-woody biomasses contain 12 - 55 wt.% (an average of 30 wt.%) [10].

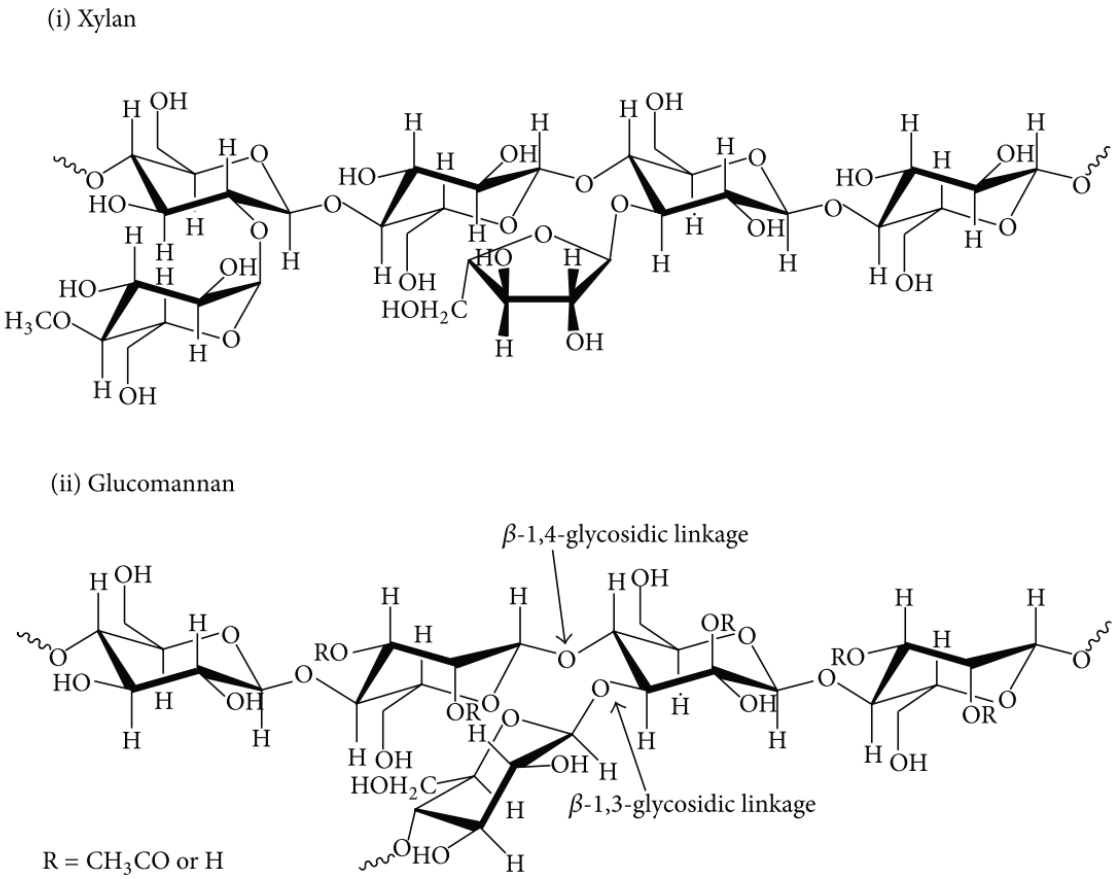

Figure 2.4: *Chemical structure of hemicellulose compounds (xylan and glucomannan are the most existing biopolymer)* [11].

2.2.4 Inorganic and organic extractives

Biomass also contains a small mineral content that ends up in combustion ash. These minerals typically include K, Ca, Na, P, and Mg. Extractives such as fats, waxes, alkaloids, proteins, aromatics, simple sugars, pectins, mucilages, gums, resins, terpenes, starches, glycosides, saponins, and essential oils [45] could be obtained from various forms of biomass using polar solvents (e.g. water, and alcohol) or nonpolar solvents (e.g. toluene, and hexane). In plants, extractives function as intermediates in metabolism, as energy reserves, and as fortifications against microbial and insect attack [10].

2.3 Biomass utilisation

Biomass is the oldest energy source known to man; it has been burned directly for cooking and space heating - contributing about 12% of today's world energy supply, while in many developing countries its contribution ranges from 40 to 50 % [20,32]. Though replaced by fossil fuel as a main source of energy during the industrial revolution, biomass remain an indispensable resource since it is renewable and relatively environmentally friendly. Various forms of biomass materials are exploited today to produce energy (including electricity; heat; solid, liquid, and gaseous fuels), and other valuable chemicals through many developed and developing processes.

Technologies for the conversion of edible biomass (mainly starch, sugar, and vegetable oils) to conventional fuels (*i.e.* bioethanol and biodiesel) have far advanced. Bioethanol and biodiesel are known to be the world's leading forms of biofuel [3] with global annual productions of 132 billion litres [46] and > 40 billion litres [47] respectively in 2019. The industrial-scale production of bioethanol for fuel applications is principally achieved via the hydrolysis and fermentation of sugarcane and grains (commonly corn) [3,48]. Biodiesel, on the other hand is largely produced via the transesterification of edible oils (e.g. sunflower oil, rapeseed oil, soybean oil, and corn oil) using simple alcohols in the presence of an alkaline or acidic catalyst [49–51].

However, the edible portion of many biomass materials generally constitutes a minor percentage of the entire biomass mix; for instance, 25 – 75 wt.% for crops like corn and wheat [8]. Hence, the net energy outcome from utilising only the edible portions for fuels and chemicals production is low and food security is as well threatened [52]. There is, therefore, the need to exploit the non-edible portions of biomass (mainly lignocellulosic in nature) for energy and chemicals production. Extensive research is currently underway into the production of energy and chemicals from waste biomass resources, such as the conversion of bagasse, rice, and wheat straws to bioethanol [12,13,53,54], production of biodiesel from used/waste oils and fats [18,55] and the conversion of algae to bio-crude oil [16]. The following sections, therefore, highlight some developed and developing techniques using various forms of biomass waste as feedstock for the synthesis of chemicals and other value-added products.

2.4 Biomass conversion techniques

Biomass conversion methods could be broadly classified into thermochemical and biochemical processes. Thermochemical techniques involve the application of heat and chemical processes to convert biomass feedstock into chemicals or other forms of energy. These include; combustion, pyrolysis, gasification, and liquefaction. Biochemical processes such as anaerobic digestion and fermentation, on the other hand, utilise the activity of micro-organisms to transform biomass into useful products, such as ethanol and biogas. The conversion technologies are largely the same for both chemical and energy production. However, where necessary the process may be tweaked to optimise the yield of the product of interest.

2.4.1 Biochemical processes

Two main processes; fermentation and anaerobic digestion are employed in biochemical/biological conversion of biomass to value-added products. Anaerobic digestion is a commercially established technology for converting wet organic waste into biogas; made up of nearly 60 % methane and 40 % carbon dioxide [56]. Like syngas, the biogas can be combusted directly for domestic and other purposes. It can also be used in secondary conversion devices to produce electricity or shaft work. Small-scale biogas digesters have been used in many developing countries, including China, India, etc. [56]. Biogas energy production in Europe was put at 13.5 million tonnes of oil equivalent (Mtoe) in 2013, reflecting 11.9% growth up in 2012 [57]. With an improvement in digester designs, many biogas plants process a wide range of biomass feedstocks including animal and human wastes, sewage sludge, crop residues, industrial by-products, and landfill materials. Strong lignified organic substances such as wood are, however, less suitable due to their slow decomposition rates [58].

Fermentation is popularly used to produce bioethanol from various types of biomass including starches and lignocellulose. Four main stages (Figure 2.5) are classically employed for a successful conversion of biomass to ethanol via fermentation. The process commences with the pretreatment (crushing and hydrolysis) of biomass into sugars followed by fermentation using micro-organisms (e.g., yeast, bacteria, and mold) to produce ethanol. The ethanol product is then refined by distillation, after which it is suitable for direct use as a fuel or additive [3,48,59].

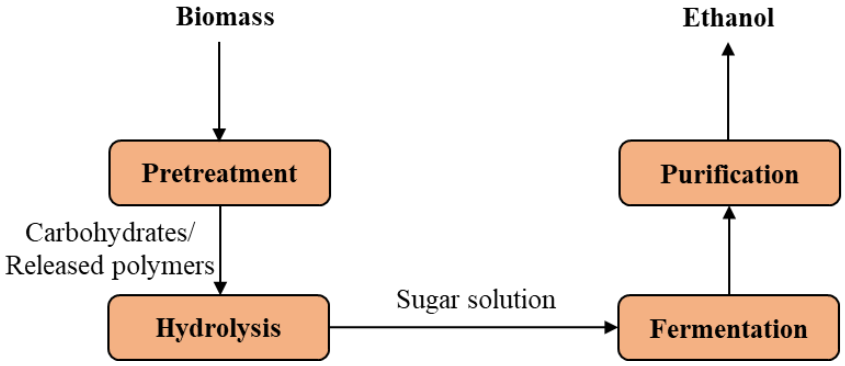

Figure 2.5: *Simplified process diagram for the production of ethanol from lignocellulose and carbohydrates. Adapted from Mergner et al.* [7].

While the biological conversion of starches and carbohydrates to ethanol is commercially well established, the lignocellulosic ethanol industry is currently faced with a crucial economic challenge due to high production cost [2,60]. In a technical report published by the National Renewable Energy Laboratory in the year 2000 [61], the production cost of lignocellulosic (corn stover) derived ethanol was estimated to be $1.5/gallon, 70 % more than corn starch derived ethanol, which was $0.88/gallon; both estimates were based on an annual production capacity of 25 million gallons of ethanol. A recent (2019) techno-economic evaluation of ethanol production from corn stover by Hossain *et al.* [62] reported slightly higher production costs. The estimated costs were $2.67/gallon and $2.0/gallon to produce ethanol via non-heat and heat integrated biochemical routes respectively, both based on a production capacity of 58.8 million gallons per annum.

Though the cost of lignocellulose is lower than that of the starch and sugar crops, the conversion process is complex and expensive, making the price of the resultant ethanol less competitive to fossil fuels [60]. The main bottleneck to achieving cost-effective production of lignocellulosic ethanol is the conversion of lignocellulose to sugars. As highlighted in Section 2.2, the complex hierarchical structure of lignocellulosic biomass creates a major obstacle to efficient enzymatic hydrolysis of the polysaccharides. Lignin sometimes adsorbs and inhibits cellulases, the enzymes in charge of depolymerizing polysaccharides to glucose [60]. As such, cost and energy-intensive pretreatment procedures are usually employed to first breakdown the lignin barrier and polysaccharides into fermentable sugars. Furthermore, this process is unable to degrade lignin, neither do the monomers of lignin contribute to ethanol formation. Thus, the process becomes much less economical as the quantity of lignin in the biomass feedstock increases. This indicates

the need for a technology that can effectively valorise all three components of such biomass materials.

2.4.2 Thermochemical processes

Figure 2.6 illustrates a summary of the prevalent thermochemical routes to biomass conversion and the products obtained. Compared to biochemical techniques, the application of heat in thermochemical processes makes them more suitable for the conversion of strong lignified materials.

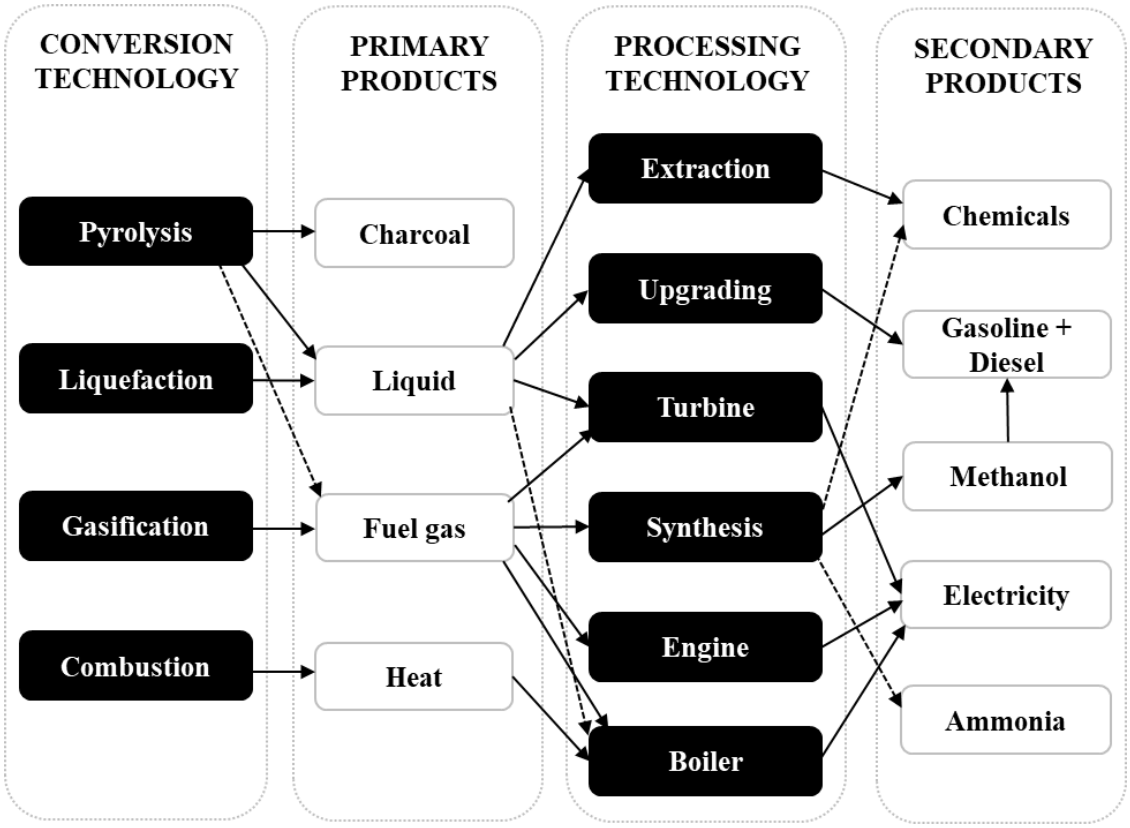

Figure 2.6: *Thermochemical biomass processing and products* [19]. *Dashed arrows are to distinguish criss-cross paths only.*

2.4.2.1 Combustion

The most common and simplest way to retrieve the energy stored in biomass is through direct burning. Combustion systems are widely available in various sizes and shapes for the burning of virtually any kind of biomass, from chicken manure and straw bales to tree trunks, and municipal refuse. Some of the ways in which heat from burning wastes is currently used include space and water heating, industrial processing, and electricity generation in boilers [20].

Combustion systems are, however, accompanied by problems of low efficiency as most of the heat (30% - 90%) is wasted; especially with open fire systems [20]. Secondly, it emits substantial amounts of pollutants such as CO_2, NOx, particles of ash, CO, and various organic compounds originating from incomplete combustion processes [63]. Some of these pollutants contribute to global warming, hence, recent research has been looking at the integration of heterogeneous catalyst in combustion systems to reduce the amount of pollutants emitted. For example, Biding and co-workers [64] integrated an alumina-supported mixed metal oxide (MMO/α-Al_2O_3) catalyst in the combustion chamber of a small-scale wood log stove and discovered the emissions of CO and Volatile Organic Compounds (VOCs) were reduced by 21 % and 42 % respectively (in comparison to the reference test, where no catalyst was used). The dust emissions were also abated by 55 %.

Another challenge with combustion is its inability to effectively handle feedstocks with high moisture content. For fuel applications, dry biomasses with 5-20 % are typically utilised [65], whereas feedstocks with > 50 % moisture content are recommended to be taken through a pre-drying process [41]. Depending on the moisture content of the feedstock, pre-drying could reduce the overall energy outcome or economic potential of the process.

2.4.2.2 Pyrolysis

Pyrolysis converts biomass into liquid (referred to as bio-oil or pyrolysis oil), char (charcoal), and non-condensable gases (fuel gas) by heating the feedstock at a temperature range of 250 to 1000 °C, in the absence of air [66–68]. Based on the heating rate and residence time of the biomass, pyrolysis may be broadly classified as slow, fast/flash, and intermediate. Table 2.2 illustrates the three main modes of pyrolysis along with typical

reaction conditions and products distribution. Slow (conventional) pyrolysis is ideal for char production and often carried out at a very low heating rate (< 1 °C/s), long residence time (hours to days), and temperatures between 300 – 700 °C [66,69,70]. Fast pyrolysis on the other hand, is usually employed for bio-oil production and carried out at a high heating rate (~ 1000 °C/s or higher), short residence time (< 2s), and moderate temperatures (~ 500 °C) [66,69,70]. Fast pyrolysis is sometimes referred to as flash pyrolysis, particularly at very high heating rates between 1000 – 10,000 °C/s [70–72]. Intermediate pyrolysis which is undertaken at conditions in-between fast and slow pyrolysis yields products that are more evenly distributed between char, liquid, and gas [73,74].

Table 2.2: *Typical product yields(dry weight basis) obtained from wood via different modes of pyrolysis* [67,69].

Type of pyrolysis	Parameters		Products (yield, wt.%)		
	Temperature (°C)	Residence time	Liquid	Char	Gas
Slow	~ 400	Hours to days	30 (70 wt.% water)	35	35
Intermediate	~ 500	10 – 30 s	50 (50 wt.% water)	25	25
Fast	~ 500	< 2 s	75 (25 wt.% water)	12	13

The pyrolysis technique has been used since the dawn of civilization. Its application for the production of char was a major industry in the 1800s, supplying fuel for the industrial revolution until it was replaced by coal [20]. The bio-oil and gas produced can be used for chemical synthesis or in engines and turbines for power generation [19]. The use of bio-oil as refinery feedstock is also being considered [3]. This oil is known to be rich in organic compounds such as carboxylic acids, alcohols, aldehydes, esters, ketones, sugars, phenols, etc.; most of which can be extracted with suitable solvents for further applications [45,75].

In terms of fuel applications, bio-oil contains high moisture content (up to 70 %, Table 2.2) some heavy aromatic compounds, a high O/C ratio (~ 0.5), and high viscosity (~ 120 mm^2/s at 20 °C) which makes it less suitable for direct application in automobile engines [67]. Hence, upgrading of bio-oil is necessary in order that appropriate transportation fuels are obtained. The main routes to transform bio-oil to fuel additives include; hydro-processing, thermal or catalytic cracking, and esterification [76,77].

Pyrolysis can also be performed in the presence of catalysts, bringing about simultaneous pyrolysis of the biomass and upgrading of the resultant bio-oil [67,78]. Zeolite of various forms are the most commonly used catalysts in the catalytic pyrolysis process [67,78–81] though other types including; aluminas and fluid catalytic cracking catalysts [76,81,82] have been also reported.

The upgrading of bio-oil via hydro-treating with catalysts such as Ru/C has been reported to yield a liquid product with high heating value (40 MJ/kg, twice that of the original bio-oil), reduced number of organic acids, aldehydes, ketones, and ethers whereas the amounts of phenolics, aromatics, and alkanes were greatly enhanced [82]. This process is however said to be expensive owing to the need for hydrogen and high pressures (100 – 200 bar) [67,82]. Catalytic cracking of bio-oil, on the other hand, is considered as a cheaper route, and significantly reduces the level of oxygenates in the bio-oil and gives a higher value product than hydro-treating. But it is neither considered a promising alternative due to the high levels of catalyst coking (8 – 25 wt.%) [83], low liquid yield (27 – 44 wt.% compared to 61 wt.%) [84] and low quality of the fuels obtained compared to fossil fuels. Thus far no known process has successfully converted bio-oil to conform to conventional fuel standards.

Nevertheless, Zhang and his fellows [85] lately demonstrated the possibility of producing jet and diesel fuel range hydrocarbons from sawdust via catalytic (HZSM-5) pyrolysis followed by alkylation and hydrogenation. The fuel properties of the two biomass-derived products (i.e. Biofuel-I and Biofuel-II) are compared with commercial jet fuels (Jet A, Jet A1, and JP-8) in Table 2.3. This result (Table 2.3) demonstrates a significant advancement in the quest to produce liquid fuel products of conventional qualities from biomass. Yet, similar to combustion, the moisture content of a suitable biomass feedstock is a maximum of 10 - 40 wt.% [69,86]. Feedstocks with higher moisture content require pre-drying, making the entire pyrolysis process less economical.

Table 2.3: *Properties of sawdust derived biofuels compared with commercial/military jet fuels. Biofuel-I: aromatics biofuel, produced by the catalytic cracking of sawdust over the HZSM-5 catalyst at 500 °C along with the alkylation of the sawdust-derived monomers using the [bmim]Cl–2AlCl$_3$ ionic liquid at 60 °C for 1 hour. Biofuel-II: cyclic alkanes biofuel, produced by the hydrogenation of aromatics over the Pd/AC catalyst at 200 °C for 6 hours. AC = Activated Carbon, u.d. = undetected* [85].

Specification tests	**Commercial/military jet fuels**			**Zhang *et al.*** [85]	
	Jet A	**Jet-A1**	**JP-8**	**Biofuel-I**	**Biofuel-II**
Heat of combustion (MJ/kg)	43.3	43.3	43.0	43.1±1.2	45.9±1.5
Freezing point (^{O}C)	-40	-47	-49	< -70	< -70
Kinetic viscosity @ -20 ^{O}C (mm^2/s)	5.78	4.21	4.10	6.5±0.5	7.2±0.3
Specific gravity @ 15 ^{O}C (g/cm^3)	0.803	0.797	0.799	0.878±0.03	0.828±0.02
Carbon content (wt%)	86.4	86.3	86.2	89.69±2.7	85.72±3.4
Hydrogen content (wt%)	13.5	13.4	13.7	10.26±0.41	14.28±0.86
Total oxygen (wt%)	0.0044	-	-	0.033±0.007	u.d.
Total sulphur (wt%)	<0.3	0.04	0.064	u.d.	u.d.
Average carbon number	11.6	11	10.9	11.5±0.4	11.5±0.7
H/C (mol ratio)	1.91	1.98	1.90	1.37±0.11	1.99±0.10
Average molecular formula	$C_{11.6}H_{22}$	$C_{11}H_{21}$	$C_{10.9}H_{20.9}$	$C_{11.5}H_{15.7}$	$C_{11.5}H_{21.5}$

2.4.2.3 Gasification

Gasification is a form of pyrolysis, which is conducted at higher temperatures, usually > 600 °C [87] in the presence of limited oxygen in order to optimise gas production. The yield of gas is typically ~ 85 wt.% based on dry weight of biomass [69]. This gas, also known as syngas, is usually a mixture of CO, H_2, CH_4, CO_2, and N_2, which could be burnt to produce heat and steam, or used in gas turbines to produce electricity [88]. There are varieties of gasifiers in the market with different sizes and configurations, which feed on a range of fuels, such as wood, charcoal, coconut shells and rice husks [20]. More hydrogen can be produced during gasification by adding steam to the process [89,90], whereas methanol and other synthetic liquid fuels can also be obtained via downstream processes such as methanol synthesis and the Fischer-Tropsch process [89,91]. Gasification of biomass can also be carried out in supercritical and near-supercritical water: 400 – 600 °C and 20 – 40 MPa [87,92–94]. This process is termed hydrothermal gasification (HTG) and H_2 is the principal product gas. The HTG process uses supercritical water both as a reaction media and reactant as illustrated for cellulose in

Scheme 2.1. This novel gasification technique is able to process feedstocks of higher moisture content (~ 40 wt.%) compared to the traditional thermal gasification process which requires feedstocks of < 10 wt.% moisture content [95,96]. Thus, in HTG, the need to dry the starting biomass is normally eliminated, thereby increasing the energy efficiency of the process.

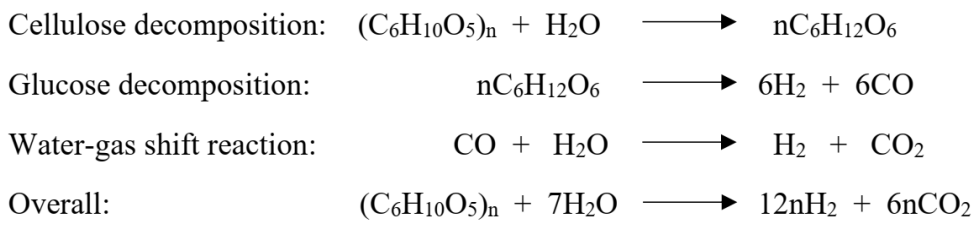

Scheme 2.1: *Simplified reactions that occur during hydrothermal gasification of cellulose and glucose* [97].

The use of catalysts in promoting the rate of gas formation in HTG processes at lower temperatures (350 – 600 °C), for the production of hydrogen from organic materials, has been an area of interest in the past 20 years. The efficiency of different catalysts such as activated carbon, alkaline catalysts, as well as nickel and ruthenium based catalysts, has been verified for hydrothermal gasification of various organic materials [89]. For example, at 550 – 600 °C glucose can be completely gasified with activated carbon or KOH catalyst to yield a gaseous product containing up to 60 mol.% H_2 against a theoretical value of 66.7 mol.% H_2 [97]. Jin *et al.* [98] also investigated the performance of selected homogeneous catalysts [$Ca(OH)_2$, Na_2CO_3, K_2CO_3, NaOH, KOH, LiOH, and $ZnCl_2$], heterogeneous catalysts (Raney-Ni, dolomite, and olivine) and a mixture of Raney-Ni and NaOH in the gasification of peanut shell using supercritical water at 400 °C and 24 - 28 MPa. It was concluded that the mixture of Raney-Ni and NaOH (2:1 weight ratio of Raney-Ni to NaOH) gave the highest hydrogen yield of 54 g/kg of dry feedstock at a residence time of 20 minutes. This shows a 7-fold improvement in hydrogen yield over the non-catalysed process.

2.4.2.4 Liquefaction

Liquefaction is similar to pyrolysis but generally carried out under essentially lower operating temperatures (150 – 420 °C) and moderate to high pressures (1 - 240 bar) [21], with the feed supported as a slurry in a solvent. A reducing gas, usually H_2 or CO, and catalyst are normally added to the process [19]. Under these conditions, the biomass polymers are decomposed into light molecular fragments resulting in a final product which is chiefly liquid (60 – 80 wt.%, dry weight) with minor percentages of gaseous (< 10 wt.%) and solid (~ 20 wt.%) by-products depending on the process conditions as shown in Table 2.4. The liquid fraction which is the product of interest is widely referred to as bio-crude after the evaporation of excess liquefaction solvent and usually contains important chemicals such as alcohols, organic acids, sugars, furanics, and aromatic compounds [99,100]. This liquid fraction may also be separated into oily (bio-oil) and water-soluble fractions with water-soluble fractions richer in sugars and alcohols while bio-oils are richer in aromatic compounds [100,101]. The solid residue (also called bio-char) obtained from the liquefaction process is a carbon-rich material and has potential applications as solid fuel and catalyst [102], whereas the gas stream from liquefaction is normally rich in CO_2, CO, and traces of C_1-C_6 hydrocarbons.

Table 2.4: *Typical product yields (based on biomass dry weight) obtained from the liquefaction of various biomasses under different conditions.*

Biomass type	Solvent	Catalyst	Process conditions*	Product yield (wt.%, dry weight)			Ref
				Solid	Liquid	Gas	
Birchwood sawdust	Water	No catalyst	300 °C, 30 min, 20 bar N_2, B:S = 1:10	33.4	66.4	0.2	[103]**
Birchwood sawdust	Water	Synthetic hydrotalcite (0.5 wt.% of solvent)	300 °C, 30 min, 20 bar N_2, B:S = 1:10	10.6	89.2	0.2	[103]**
Birchwood sawdust	Water	Colemanite (0.5 wt.% of solvent)	300 °C, 30 min, 20 bar N_2, B:S = 1:10	12.1	87.7	0.2	[103]**
Birchwood sawdust	Water	K_2CO_3 (0.5 wt.% of solvent)	300 °C, 30 min, 20 bar N_2, B:S = 1:10	14.1	85.5	0.4	[103]**
Birchwood sawdust	Water	KOH (0.5 wt.% of solvent)	300 °C, 30 min, 20 bar N_2, B:S = 1:10	12.0	87.7	0.3	[103]**
Birchwood sawdust	Water	$FeSO_4$ (0.5 wt.% of solvent)	300 °C, 30 min, 20 bar N_2, B:S = 1:10	21.9	78.0	0.1	[103]**
Birchwood sawdust	Water	MgO (0.5 wt.% of solvent)	300 °C, 30 min, 20 bar N_2, B:S = 1:10	14.2	85.4	0.4	[103]**
Water hyacinth	Water	No catalyst	300 °C, 15 min, 50 rpm, 1 bar N_2 (62 - 90 bar), B:S = 1:6	16.0	80.0	4.0	[104]
Water hyacinth	Water	No catalyst	280 °C, 30 min, 50 rpm, 1 bar N_2 (62 - 90 bar), B:S = 1:6	17.0	76.0	7.0	[104]
Water hyacinth	Water	No catalyst	280 °C, 45 min, 50 rpm, 1 bar N_2 (62 - 90 bar), B:S = 1:6	17.0	76.0	7.0	[104]
Water hyacinth	Water	No catalyst	280 °C, 60 min, 50 rpm, 1 bar N_2 (62 - 90 bar), B:S = 1:6	16.0	76.0	8.0	[104]
Water hyacinth	Water	No catalyst	280 °C, 15 min, 50 rpm, 1 bar N_2 (62 - 90 bar), B:S = 1:3	47.0	44.0	9.0	[104]
Water hyacinth	Water	No catalyst	280 °C, 15 min, 50 rpm, 1 bar N_2 (62 - 90 bar), B:S = 1:12	13.0	81.0	6.0	[104]
Water hyacinth	Water	0.5 N K_2CO_3	280 °C, 15 min, 50 rpm, 1 bar N_2 (62 - 90 bar), B:S = 1:6	19.0	73.0	8.0	[104]

Table 2.4: Continuation…

Biomass type	Solvent	Catalyst	Process conditions*	Product yield (wt.%, dry weight)			Ref
				Solid	Liquid	Gas	
Water hyacinth	Water	1 N K_2CO_3	280 °C, 15 min, 50 rpm, 1 bar N_2 (62 - 90 bar), B:S = 1:6	11.0	82.0	7.0	[104]
Water hyacinth	Water	0.5 N KOH	280 °C, 15 min, 50 rpm, 1 bar N_2 (62 - 90 bar), B:S = 1:6	19.0	75.0	6.0	[104]
Water hyacinth	Water	1 N KOH	280 °C, 15 min, 50 rpm, 1 bar N_2 (62 - 90 bar), B:S = 1:6	11.0	82.0	7.0	[104]
Pine sawdust	Methanol	No catalyst	300 °C, 15 min, 20 bar N_2, B:S = 1:10	58.0	40.3	1.7	[105]**
Pine sawdust	Methanol:water (1:1)	No catalyst	300 °C, 15 min, 20 bar N_2, B:S = 1:10	4.6	89.7	5.7	[105]**
Pine sawdust	Ethanol	No catalyst	300 °C, 15 min, 20 bar N_2, B:S = 1:10	57.0	39.0	4.0	[105]**
Pine sawdust	Ethanol:water (1:1)	No catalyst	300 °C, 15 min, 20 bar N_2, B:S = 1:10	4.5	89.3	6.2	[105]**
Pine sawdust	Water	No catalyst	300 °C, 15 min, 20 bar N_2, B:S = 1:10	30.0	63.2	6.8	[105]**
Pine sawdust	Water:ethanol (3:8 wt:wt)	No catalyst	300 °C, 60 min, 1000 rpm, 1.7 bar N_2 (117 bar), B:S = 2:11	34.0	57.0	9.0	[106]
Pine sawdust	Water:ethanol (3:8 wt:wt)	K_2CO_3 (3.6 wt.% of solvent)	300 °C, 60 min, 1000 rpm, 1.7 bar N_2 (135 bar), B:S = 2:11	19.0	68.0	13.0	[106]
Pine sawdust	Water:ethanol (3:8 wt:wt)	HZSM-5 (3.6 wt.% of solvent)	300 °C, 60 min, 1000 rpm, 1.7 bar N_2 (130 bar), B:S = 2:11	24.0	64.0	12.0	[106]
Pine sawdust	Water:ethanol (3:8 wt:wt)	6%Ni/HZSM-5 (3.6 wt.% of solvent)	300 °C, 60 min, 1000 rpm, 1.7 bar N_2 (133 bar), B:S = 2:11	23.0	62.0	15.0	[106]
Pine sawdust	Water:ethanol (3:8 wt:wt)	12%Ni/HZSM-5 (3.6 wt.% of solvent)	300 °C, 60 min, 1000 rpm, 1.7 bar N_2 (132 bar), B:S = 2:11	23.0	63.0	14.0	[106]

** Pressure is initial pressure (maximum pressure recorded during the reaction in bracket). B:S is the weight ratio of dry biomass-to-solvent.*
*** Mixing rate not reported.*

Liquefaction is considered as one of the promising routes to synthesise diverse platform chemicals from biomass. However, the production of high yields of targeted chemicals remains a major challenge, particularly for lignocellulose feedstocks due to their complex chemical constituent. As noted previously in Section 2.2, the chemical and structural constituent of the three major fragments of lignocellulose (lignin, cellulose, and hemicellulose) are primarily different leading to distinct chemical reactivities during liquefaction. This, therefore, results in the production of numerous chemical products with different yields [99]. It is typical to synthesise 20 or more distinct chemicals from one feedstock during liquefaction [14,105,107]. Figure 2.7 shows potential chemicals and fuels that could be synthesised from lignocellulose's main fragments (cellulose, hemicellulose, and lignin) via liquefaction. These chemicals can be further converted to a variety of other compounds that are useful to the biofuels, polymers, and solvent industries.

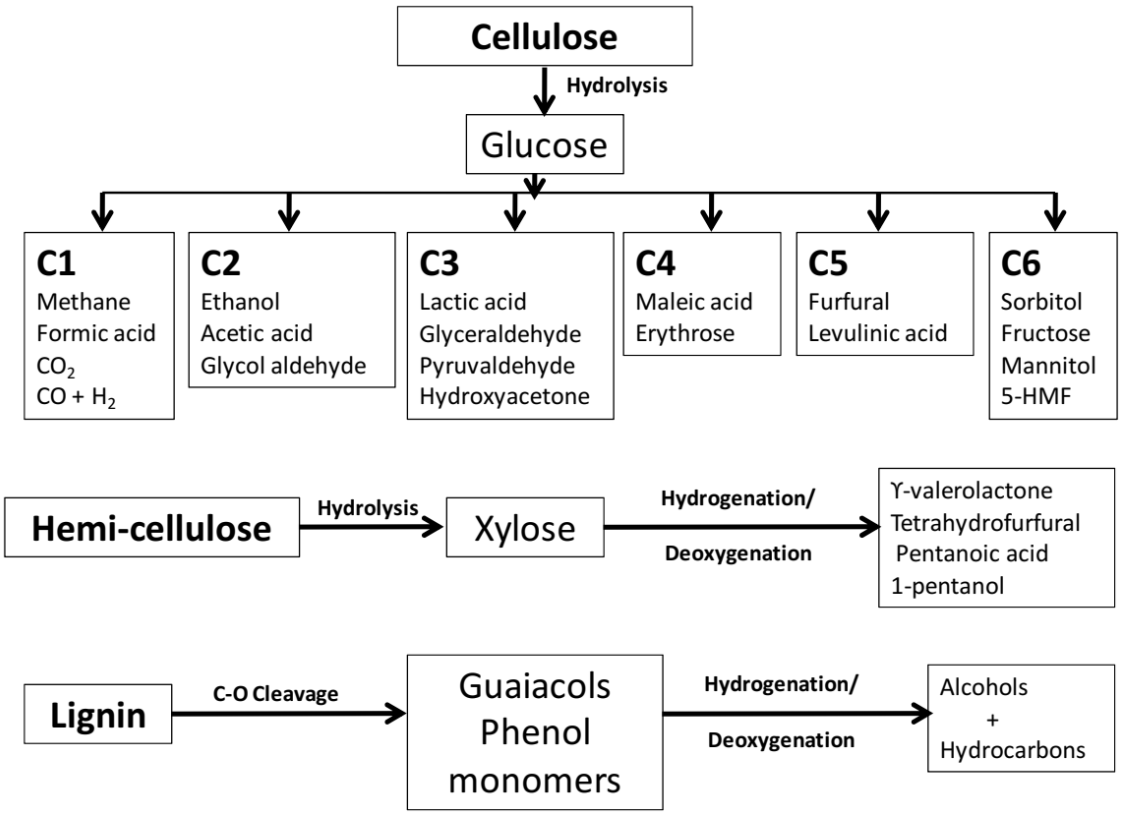

Figure 2.7: *Key chemicals obtained from the decomposition of lignocellulose polymers during liquefaction* [99]. *5-HMF is 5-hydroxymethylfurfural.*

A crucial purpose of liquefaction is to increase the H/C and decrease the O/C ratios of the liquid product relative to that present in the original feedstock to produce a hydrocarbon-like product [108]. To achieve this, hydrogen is assimilated into the process by direct addition or indirectly through the water-gas shift reaction (equation 2.1). Catalysts (commonly homogeneous) are also necessary for depolymerisation, cracking, hydrogenolysis, hydrogenation, and de-oxygenation reactions during the process. Liquefaction is considered as an economically unattractive biomass conversion process owed to the high cost of H_2, CO, and other essential gases for the process [3,21,23]; as well as technical difficulties associated with high-pressure processing [19]. Nonetheless, a few pilot and demonstration plants have been documented: Hydro-Thermal Upgrading (HTU), Catalytic Liquefaction (CatLiq), Thermo-Depolymerization (TDP), and High-Pressure Hydrogenation (DoS) processes [21,100]. A more comprehensive compilation of such hydrothermal liquefaction setups (continuous processes) recently published by Castello *et al.* [109] is presented in Table 2.5.

$$CO + H_2O \longleftrightarrow H_2 + CO_2 \qquad (2.1)$$

A potential route to reduce the cost and technical difficulties associated with high pressure biomass liquefaction is via a milder process called atmospheric liquefaction. This process is carried out at ambient pressure and moderate temperatures of 160 - 240 °C, using high boiling liquids such as polyhydric alcohols as liquefaction solvent. Atmospheric liquefaction of biomass usually leads to the production of a heavy polyol-rich liquid product [110,111] asserted to be suitable for the production of polyurethane foams [111,112]. In 2006, Yu *et al.* [113] attempted to produce polyester from such bio-polyol and concluded that the obtained product could be utilised in making biodegradable garden mulch film. Ethylene glycol, polyethylene glycol [110], glycerol [114,115] and ethylene carbonate [111,116] have been employed as solvents in the atmospheric liquefaction process under the action of acid catalysts. The use of H_2SO_4 [110,116], HC*l*, H_3PO_4 [113], and acidic ionic liquids [117] are reported in the literature; with H_2SO_4 being the most favourable with respect to biomass conversion (up to 99 wt.% reported) [110,113,117]. However, Lu and co-workers [117] claim acidic ionic liquids (AILs) with sulfoalkyl-functionalized imidazolium cations and HSO_4^- anions have the ability to catalyse the liquefaction process to achieve conversions as high as H_2SO_4.

Table 2.5: *Continuous hydrothermal liquefaction (HTL) plants and setups documented in the literature* [109].

Process/Plant	Reactor Concept	Biomass	Throughput (kg/h)	Pressure (bar)	Temp. (°C)	Residence Time (min)	Catalyst
PDU–PERC Albany, *USA*	Tubular/stirred	Wood	230–270	207	330–340	19–100	Na_2CO_3
PDU–LBL Albany, *USA*	Tubular/stirred	Wood	43–360	207	340–345	11.3–465	Na_2CO_3
LBL Berkeley, *USA*	Stirred	Wood	~1	200–230	330–350	~20	-
STORS–EPA, *USA*	Column	Sewage sludge	30	86–148	275–305	90	Na_2CO_3
STORS–Organo Corp., *Japan*	Column	Sewage sludge	240	88–98	290–300	N/A	-
HTU® process Shell, *The Netherlands*	Tubular	Wood	10	180	350	6	-
HTU® process Biofuels B.V., *The Netherlands*	Tubular	Sugar beet pulp, onion pulp	100	180	350	15	-
Pacific Northwest National Laboratories (PNNL), *USA*	Stirred + tubular	Algae Macroalgae Grape pomace Wastewater solids	1.5	200	350	27–50	- - Na_2CO_3 -
University of Sydney, *Australia*	Coils in sandbath	Algae	24–40	200–250	350	15–20	-
University of Illinois, *USA*	Stirred	Swine manure	0.9–2.0	103	305	40–80	-
Iowa State University, *USA*	Tubular	Fungi	3.0–7.5	270	300–400	11–31	-
Chalmers University of Technology, *Sweden*	Fixed bed, with recycle loop	Kraft lignin	1–2	250	350	6–11	ZrO_2, K_2CO_3
Aalborg University, *Denmark*	Tubular	Wood/glycerol Wood	20	300–350	390–420	15	K_2CO_3
Karlsruhe Institute of Technology (KIT), *Germany*	Tubular, with recirculation	Waste biomass	0.29–0.63	250	330–350	5–10	K_2CO_3, ZrO_2
	Tubular, with MeOH gasifier Stirred	Yeast, pomace Algae	0.06–0.61 0.76	200–250 200	330–450 350	1–30 15	K_2CO_3, ZrO_2 -
University of Leeds, *UK*	Coils in sandbath	*Chlorella*	0.6–2.4	185	350	1.4–5.8	-
Aarhus University, *Denmark*	Tubular (bench) Tubular (pilot), with oscillator	Dried digested grains with solubles Wood, sewage sludge, *Spirulina*	0.36–1.44 60	250 220	250–350 350	~20 10	K_2CO_3 KOH, no
Imperial College London, *UK*	Tubular, hexane as co-solvent	Algae	0.03–0.24	180	300–380	0.5–4	-
Bath University, *UK*	Concentric tubular	Wastewater algae	0.18–0.42	160	302–344	17.7–41.8	-

Table 2.5: Continuation…

Process/Plant	Reactor Concept	Biomass	Throughput (kg/h)	Pressure (bar)	Temp. (°C)	Residence Time (min)	Catalyst
University of Twente, *The Netherlands*	Coils in sandbath	*Scenedesmus* sp.	0.06–0.33	150–300	250–350	7–30	-
Cat-HTR™ process Licella, *Australia*	N/A	Pulp/paper, plastics	10,000 t/y [2]	N/A	N/A	N/A	Yes
Hydrofaction™ process Steeper Energy [3], *Denmark-Canada*	Tubular	Wood	20	300–350	390–420	15	K_2CO_3
Green2black™ process Muradel, *Australia*	Tubular	Tires, algae	168	200	360	10	N/A
HTP process Genifuel, *USA*	Stirred + tubular [1]	Sewage sludge	N/A	200	350	45	N/A
W2F process ENI S.p.A., *Italy*	N/A	Organic fraction of municipal solid waste	1–5	100	250–310	60–120	N/A
CatLiq® process SCF Technologies, *Denmark*	Stirred	Wet digested grains with solubles	30	250	350	1–15	ZrO_2
CatLiq® process Altaca Enerji, *Turkey*	N/A	Different wastes and residues	15,000 [2]	250	350	N/A	Yes
TDP process Changing World Technologies, *USA*	N/A	Turkey waste	8500	N/A	200–300 [4]	N/A	-

An advantage of liquefaction over pyrolysis and other thermal processes earlier discussed is its ability to handle feedstocks with high moisture content (> 50 wt.%) without the need for drying [118]. Moreover, the bio-oil (which is the oily component of the liquid product) obtained from liquefaction has lower oxygen content and higher heating value than that from pyrolysis: containing about 10 – 19 wt.% oxygen with a heating value of 30 – 40 MJ/kg [21] compared to approximately 35 wt.% oxygen and 20 – 25 MJ/kg for pyrolysis oil on dry basis [19]. However, lower oil yields of approximately 35 wt.% per feed compared to 80 wt.% for flash pyrolysis and high viscosities are observed [19]. For example, the liquid product from the Lawrence Berkeley Laboratory (LBL) process was said to be similar to bitumen with a viscosity range of 1.1 – 1.2 kg/m^3, while that from the HTU process solidifies at 80 °C [21]. Further examples of typical properties of wood-derived liquefaction oil and fast pyrolysis oil are compared with petroleum-based heavy fuel oil in Table 2.6.

Table 2.6: *Typical properties of wood pyrolysis bio-oil, liquefaction (HTL) bio-oil, and heavy fuel oil* [91].

property	pyrolysis oil	liquefaction oil	heavy fuel oil
moisture content, wt %	15−30	5.1	0.1
pH	2.5		
specific gravity	1.2	1.1	0.94
elemental composition, wt %			
carbon	54−58	73	85
hydrogen	5.5−7.0	8	11
oxygen	35−40	16	1.0
nitrogen	0−0.2		0.3
ash	0−0.2		0.1
higher heating value, MJ/kg	16−19	34	40
viscosity (50°c), cP	40−100	15000 (at 61°C)	180
solids, wt %	0.2−1		1
distillation residue, wt %	up to 50		1

The early research of Appell *et al.* [23] on the conversion of organic waste to oil has been the bedrock of biomass liquefaction processes. Appell and his colleagues discovered that a variety of biomass (agricultural and municipal biomass wastes) could be converted to an oil-like product with gaseous and solid by-products using CO and H_2O in the presence of a suitable catalyst (Na_2CO_3, NH_4OH). In that study, the water-gas shift reaction was the source of hydrogen. The water also served as a solvent and as an excellent medium for hydrolysis of cellulose and other carbohydrates.

According to Chornet and Overend [108] and Behrendt [21], the liquefaction of biomass takes place through a complex sequence of structural and chemical changes as follows:

- solvolysis of biomass into micellar-like structures;
- depolymerisation of hemicellulose, cellulose, and lignin to smaller and soluble molecules;
- thermal and chemical decomposition leading to new molecular rearrangements through dehydration, decarboxylation, C-O and C-C bond ruptures;
- degradation of oxygen-containing functional groups via hydrogenolysis and hydrogenation in the presence of hydrogen.

Chornet and Overend [108] proposed that the extent of the above reactions varies according to the original material, severity of operating conditions and the presence of interacting solvents and catalysts.

Role of solvent in biomass liquefaction

The solvent serves as a vehicle or carrier medium for the entire reaction: supporting the solvolysis, hydration, and other chemical decomposition reactions during biomass liquefaction. This leads to better fragmentation of biomass and dissolution of free radicals [118] from homogeneous catalysts and intermediate products. Such solvents may be aqueous (acidic, alkaline or neutral) or organic. Commonly used solvents are; water, alcohols (e.g. methanol, ethanol) and other high boiling organic solvents (e.g. tetralin, isoquinoline, phenol).

Water is mostly preferred because of its low cost, abundance, and more importantly, acts as a source of hydrogen through the water-gas shift reaction [23]. Liquefaction processes that use water as solvent are popularly termed as hydrothermal liquefaction (HTL); carried out with [119] or without catalyst [103,120]. HTL has been extensively studied under subcritical (160 – 320 °C, ≥ 1 MPa), near-critical (320 – 374 °C, > 10 MPa), and supercritical (> 374 °C, ≥ 22 MPa) conditions [22], Figure 2.8. Biomass conversion in supercritical water mostly favours gas yield at the expense of the liquid product and hence, this process is more appropriately classified as hydrothermal gasification (HTG) as earlier discussed in Section 2.4.2.3.

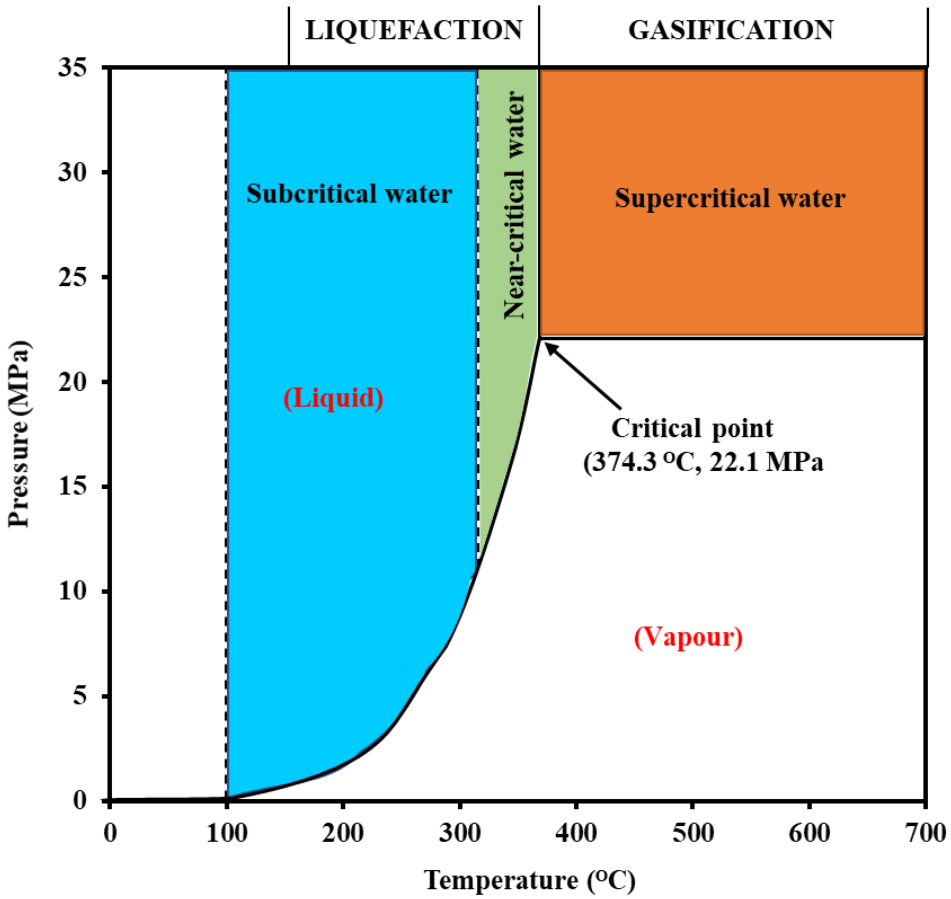

Figure 2.8: *The temperature-pressure phase diagram of water showing typical regions employed for biomass liquefaction and gasification. Adapted from Al-Muntaser* [121].

The use of simple alcohols ($C_1 – C_4$) or alcohol-water mixtures are broadly reported to result in higher biomass conversions over water [26,28]. For instance, > 95 wt.% of eastern white pine sawdust was converted to mainly liquid products using 50 wt.% of cosolvent of either methanol-water or ethanol-water compared to 70 wt.% conversion in just water under the same reaction conditions of 300 °C, 20 bar initial N_2 pressure, 15 min reaction time and biomass:solvent ratio of 1:10 (wt:wt) [105]. Similarly, 82 wt.% conversion of brewer's spent grain was attained using 70 wt.% cosolvent of methanol-water over 72 wt.% conversion in just water at the same reaction conditions of 250 °C, 30 bar initial He pressure, 30 min reaction time and biomass:solvent ratio of 1:10 (wt:wt) [14]. Simple alcohols also have the potential to react with biomass fragments to form products that are more stable. For example, the formation of levulinic acid methyl ester from levulinic acid during the methanol liquefaction of pine saw dust [122]. Aside the solvolysis of lignocellulose fragments, $C_1 – C_3$ alcohols also react with the lipid

(triglycerides and free fatty acids) content of biomass to produce higher-value chemicals such as mono-alkyl esters as illustrated in Schemes 2.2. and 2.3 [14]. Mono-alkyl esters are well known for their fuel applications as biodiesel [49,52].

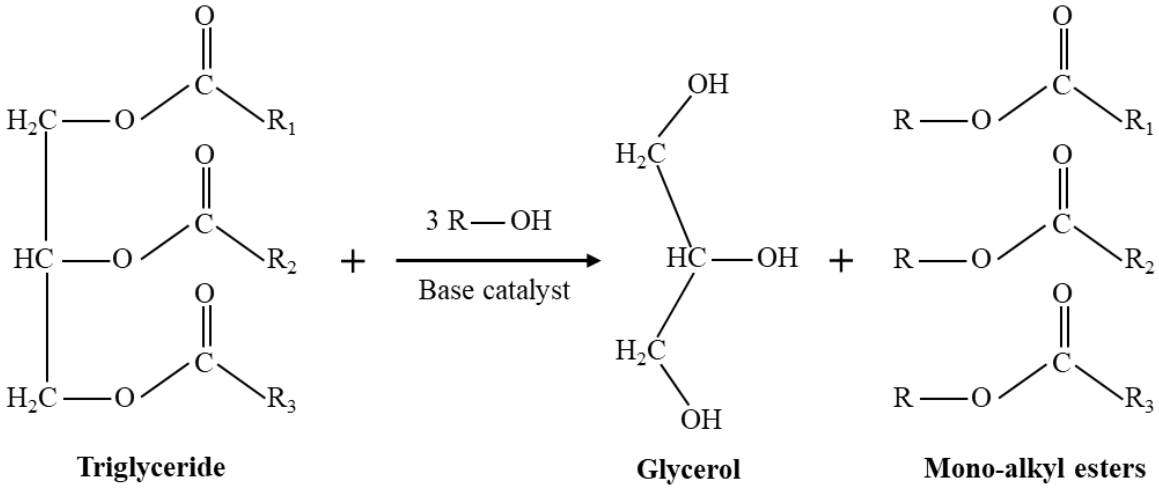

Scheme 2.2: *Transesterification of triglyceride to mono-alkyl esters and glycerol.*

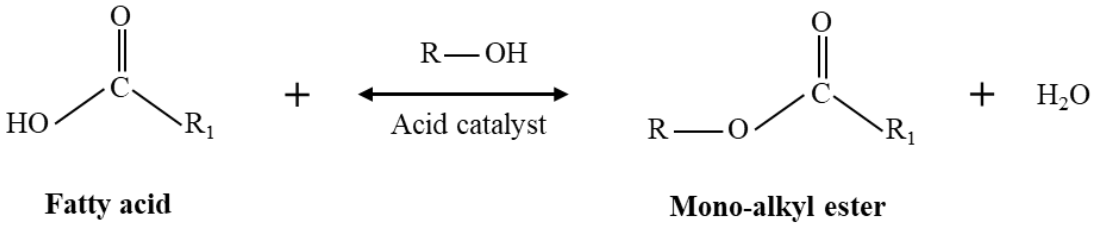

Scheme 2.3: *Esterification of fatty acid to mono-alkyl ester.*

In a separate investigation by Brand *et al.* [26], the liquefaction of red pine sawdust in ethanol was reported to yield bio-crudes (i.e. liquid product after the evaporation of solvent ethanol) with lower average molecular weights (446 – 586 g/mol) compared to products made with water (1173 – 2672 g/mol), signifying the synthesis of smaller molecules in ethanol. This data was obtained at 310 – 400 °C, 50 bar initial N_2 pressure, 30 min reaction time, and biomass:solvent ratio of 6:100 (wt:wt). The findings of Brand *et al.* [26] about the synthesis of smaller molecules in ethanol, however, contradicts those of Nasir [14], where brewer's spent grain liquefaction in various alcohol-water systems (methanol, ethanol, and 2-propanol at 70 wt.% alcohol concentration) rather led to the formation of higher molecular weight compounds when compared to those achieved in a pure water system. A plausible explanation to this inconsistency could be attributed to the

differences in feedstock characteristics or reaction conditions. Though the average molecular weights of the liquid products in Nasir's work [14] were not reported, the GC-MS data on the chemical composition of the products shown in Table 2.7 clearly indicates that the heavier molecules (at retention time beyond 26.5 min) which differentiate the alcohol derived products from the water derived product were largely fatty acids and mono-alkyl esters. Lipids, which include free fatty acids and triglycerides are long-carbon chain (C_4 – C_{55}) molecules and constitute about 10 wt.% of brewer's spent grain on dry weight [123–125]. These lipids and mono-alkyl esters (which are derivatives of the lipids made via esterification or transesterification reactions with simple alcohols, Schemes 2.2. and 2.3) are more soluble in alcohol than water, which could explain their dominance in the alcohol derived samples. On the other hand, it is not too clear whether any of these lipids exist in the red pine sawdust employed by Brand *et al.* [26], however, it is likely that the higher temperatures (310 – 400 °C) employed in that work engenders better C-C bond scission in the alcohol system, whereas such high temperatures rather promote condensation reactions in the water system as reported elsewhere [118]. Thus, simple alcohols may inhibit the tendency of biomass fragments to repolymerise at higher temperatures, as explained by the author [26] and also demonstrated in Table 2.8. The basic properties of the bio-crude oils (i.e. the liquid products after evaporation of solvents) obtained in the ethanol system were said to be more favourable for transportation fuel applications compared to those obtained in the water system.

Table 2.7: *Main chemical compounds identified (via GC-MS) in liquid products obtained from the liquefaction of brewer's spent grain using water and various alcohol-water mixtures as solvents. MeOH = methanol:water, EtOH = ethanol:water, and 2-PrOH = 2-propanol:water, all at alcohol:water ratio of 70:30 (wt:wt). Conditions: 250 °C, 30 bar initial He pressure, 30 min reaction time and biomass:solvent ratio of 1:10 (wt:wt) [14].*

No.	RT (min)	Name	Peak (area %)			
			Water	MeOH	EtOH	2-PrOH
1	6.53	2-(methoxymethyl) furan	-	1.26	-	-
2	7.12	Methyl pyrazine	1.25	2.70	1.86	1.00
3	7.51	Acetoin	2.28	1.31	-	-
4	7.80	1-hydroxy- 2-propanone	2.84	4.26	3.09	1.44
5	8.43	Ethyl ester-2-hydroxy- propanoic acid	-	1.51	1.07	-
6	8.82	2-cyclopentenone	1.36	-	-	-
7	9.03	2-methyl-2-cyclopentenone,	1.06	-	-	-
8	9.26	Acetic acid, hydroxy-, methyl ester	-	1.40	-	-
9	9.65	Propane, 1-(1-methylethoxy)-	-	-	-	1.55
10	10.77	Acetic acid	24.33	5.27	7.16	8.59
12	11.00	1-heptyn-6-one	-	-	-	1.05
13	11.09	Furfural	-	2.93	2.94	-
14	12.85	2,3-Butanediol, [R-(R*,R*)]-	6.08	6.41	2.19	4.33
15	12.96	2-Hydroxy-3-methylsuccinic acid			1.03	
16	13.51	Methyl ester 4-oxo- pentanoic acid	-	2.31	-	-
17	13.76	2,3-Butanediol, [R-(R*,R*)]-	2.46	5.03	1.83	3.07
18	14.02	Hexadecane	-	-	-	6.09
19	14.09	10-methyl- eicosane		-	2.26	
20	14.51	Ethyl ester, 4-oxo- pentanoic acid	-	-	1.72	-
22	14.98	Butyrolactone	1.12	-	-	-
25	18.63	3-methyl-1,2-cyclopentanedione	1.68	1.04	1.36	1.42
26	19.12	2-methoxy-phenol	1.09	-	-	-
27	21.55	4-ethyl-2-methoxy phenol	-	-	1.01	1.16
28	21.73	2-pyrrolidinone	3.75	1.19	1.31	1.66
29	22.69	Butane-2-one, 3-methyl-3-(2-oxopropylamino)-	-	-	1.40	-
30	23.81	Methyl ester hexadecanoic acid	-	2.74	-	-
31	24.07	Isopropyl palmitate	-	-	-	4.54
32	24.33	Ethyl ester hexadecanoic acid	-	-	8.23	-
33	25.07	Glycerol	11.06	3.14	1.77	2.18
34	25.20	4-oxo- pentanoic acid	3.71	-	-	1.01
35	26.03	6-methyl-3-pyridinol	3.67	-	1.46	1.41
36	26.26	2- pyridinone	17.56	7.75	14.54	11.91
37	26.57	9-Hexadecenoic acid	-	-	-	1.64
39	26.84	9-octadecenoic acid ethyl ester	-	-	2.91	-
40	26.94	Methyl ester-8,11- octadecadienoic acid	-	6.17	-	1.52
41	27.08	Isopropyl linoleate	-	-	-	6.05
42	27.36	Ethyl ester-9,12-octadecadienoic acid	-	-	10.87	-
43	27.80	Pidolic acid	-	-	4.48	2.86
44	28.28	Methyl ester-5-oxo-L-prolin	-	4.86	-	-
45	33.01	Octaethylene glycol monododecyl ether	-	4.89	-	-
47	33.14	n-Hexadecanoic acid	-	-	15.21	21.21
48	36.37	Methyl ester-12-hydroxy-9-octadecenoic acid	-	12.06	-	-
53	36.48	Triethylene glycol monododecyl ether	-	-	-	2.65
Total area (%)			84.18	78.21	90.41	88.34

-: Not detected or peak area less than 1% of the total area

Table 2.8: *Average molecular weights of liquid products (bio-crude) obtained from the liquefaction of red pine sawdust using water and ethanol at various temperatures. Conditions: 50 bar initial N_2 pressure, 30 min reaction time, and biomass:solvent ratio of 6:100 (wt:wt)* [26].

Temperature (°C)	**Average molecular weight of bio-crude oil (g/mol)**	
	Water	**Ethanol**
310	1173	586
340	n/a	541
370	n/a	515
400	2672	446

n/a = not available or not determined.

Despite the benefits of simple alcohols highlighted so far, they evaporate very quickly during biomass processing because of their low volatilities, demanding high solvent:feed ratios in the range of 4:1 to 16:1 [26], which could make the process more expensive. Therefore, recent research is focused on the application of higher boiling alcohols such as ethylene glycol and glycerol as alternative solvents for biomass liquefaction. Ethylene glycol [101,126,127] is the most frequently used solvent, particularly in atmospheric liquefaction. It is few times mixed in variable proportions with polyethylene glycol [110] or ethylene carbonate [111,113] for the same process. Ethylene glycol was found to be an active reactant during biomass liquefaction as revealed by proposed reaction mechanisms reported elsewhere [126]. The application of glycerol [30,32,33] in biomass processing is an interesting area which needs further exploration considering the expanding biodiesel industry which results in the production of huge quantities of crude glycerol, approximately 10 wt.% of every quantity of biodiesel produced [128,129]. It has also been claimed in previous investigations [130,131] that glycerol acts as a hydrogen donor solvent under both subcritical and supercritical conditions, hence the ability to successfully apply it in large-scale biomass processing would be economically beneficial in two ways; 1) it could replace the need for the rather expensive gaseous hydrogen and 2) expand the market for crude glycerol which is an undesired by-product from the biodiesel industry.

Other solvents which are products of the biomass liquefaction reaction process (e.g. phenol) have been suggested [21]. Lee and Ohkita [132] claimed to have successfully converted over 90 % of wood in 30 seconds under supercritical conditions of phenol to a liquid product whose combined phenol content is similar to those from conventional liquefaction methods. Acidic solvents are generally believed to hydrolyse polysaccharides at faster rates compared to basic solvents. In summary, a variety of solvents have been tested in literature for the liquefaction of diverse biomass types, yet they are not directly comparable as these studies were carried out in different systems and sometimes under different conditions.

Role of catalyst in biomass liquefaction

Catalysts aid many of the reaction steps that occur during the liquefaction process; acceleration of the water-gas shift reaction (in the hydrothermal process), suppressing char and tar formation while improving yield and quality of liquid product at milder conditions [133–135]. Some reactions (especially at mild conditions like those employed for atmospheric liquefaction) do not progress in the absence of an appropriate catalyst [110,113]. Depolymerisation, cracking, hydrogenolysis, hydrogenation, and de-oxygenation reactions during the liquefaction process have been attributed to the action of catalyst [108].

The role of many homogeneous catalysts including; alkali salts (e.g. carbonates, phosphates), organic acids (e.g. benzenesulfonic acid, methanesulfonic acid), inorganic acids (e.g. sulphuric acid) and hydroxides (e.g. NaOH) have been comprehensively studied for the liquefaction process. Accordingly, alkali catalysts such as Na_2CO_3 [119], K_2CO_3 [103,133] and NaOH [21] are widely reported to possess good activities in biomass conversion besides enhancing the heating value of the obtained liquid product [119]. An experiment conducted by Mun *et al.* [136] on the phenol liquefaction of *Pinus radiate* bark using organic sulfonic acids as catalysts, disclosed high average feed conversions of 97.8 % at a low solvent/feed ratio of 2 as against that of 90.8 % using aqueous sulphuric acid at the same condition. It was concluded that "organic sulfonic acids play an important role in retarding the condensation reaction between phenol and bark components during the acid-catalysed phenol liquefaction process." A general overview of homogeneous catalysts suggests alkali salts (usually, Na_2CO_3 or K_2CO_3) are most suitable for hydrothermal liquefaction [133] whereas, acids (typically H_2SO_4) are

best for atmospheric liquefaction using ethylene glycol [110,113]. Sulphuric acid, however, does not meet the requirements of green chemistry; being highly corrosive and strong oxidant. Hence the need for a greener substitute which has been the motivation of some researchers today.

A potential solution to this problem is the use of acidic ionic liquids (AILs) [117] or heterogeneous catalysts. The high cost of AILs, however, remains a challenge from an economic perspective. The application of heterogeneous catalysts in biomass liquefaction is under critical investigation. Earlier research conducted on wood using Reney-Nickel and Co-Mo catalysts, indicated the formation of lighter liquid compounds in comparison with the non-catalysed process. These catalysts, however, promote higher selectivity towards gas formation and at times relatively poor shift of liquid product [133,137]. In a recent study by Patil and co-workers [28], the heating value of bio-oil produced from wheat straw was boosted from 28 MJ/kg to 30 MJ/kg with the addition of Ru (5 wt.%) on H-beta support catalyst. An enhanced heating value of bio-oil is particularly advantageous for liquid products intended for transportation fuels.

Effect of process parameters on biomass liquefaction

Reaction temperature, solvent-to-biomass ratio, reaction pressure, and residence time, are the main parameters that can be modified during biomass liquefaction. Of these, reaction temperature is widely reported as the most important parameter that significantly influences biomass conversion and product yield [118,138]. It should be stated that meaningful quantitative comparison of experimental results between different research groups has been quite challenging due to differences in reaction conditions and the definitions of product yield. For instance, the definition of biomass conversion and yield of liquid and gaseous products may be based on one of the following; the dry weight of whole biomass, the weight of dry ash-free biomass, the weight of the volatile matter content of the biomass, or the carbon content of the biomass. Nonetheless, few interesting reviews of the impact of varying process parameters are available [21,118,139].

(i) Temperature:

The introduction of heat during liquefaction facilitates bond scission and depolymerisation of biomass and also promotes the solubility of decomposed biomass fragments in the liquefaction solvent [120,140]. Increasing temperature between 160 –

350 °C has been generally reported to result in increasing biomass conversion and yield of liquid product, Figure 2.9. Quantities of hydrocarbons in the liquid product also increase with temperature whereas the amount of oxygenated compounds is reduced as temperature increases [141,142]. Temperatures lower than 157 °C have been reported to yield biomass conversions below 40 wt.% and it is practically impossible to degrade lignocellulosic biomass at temperatures below 120 °C during liquefaction without the assistance of an appropriate catalyst [34,143]. On the other hand, temperatures above 400 °C are noted for excessive gas formation, hence, the recommended range for final temperature for optimum biomass conversion and liquid product yield may vary from 300 to 374 °C depending upon the biomass type. Biomass feedstocks rich in cellulose and hemicellulose usually require lower maximum temperatures 300 – 330 °C whereas feedstocks rich in lignin may require higher temperatures [118].

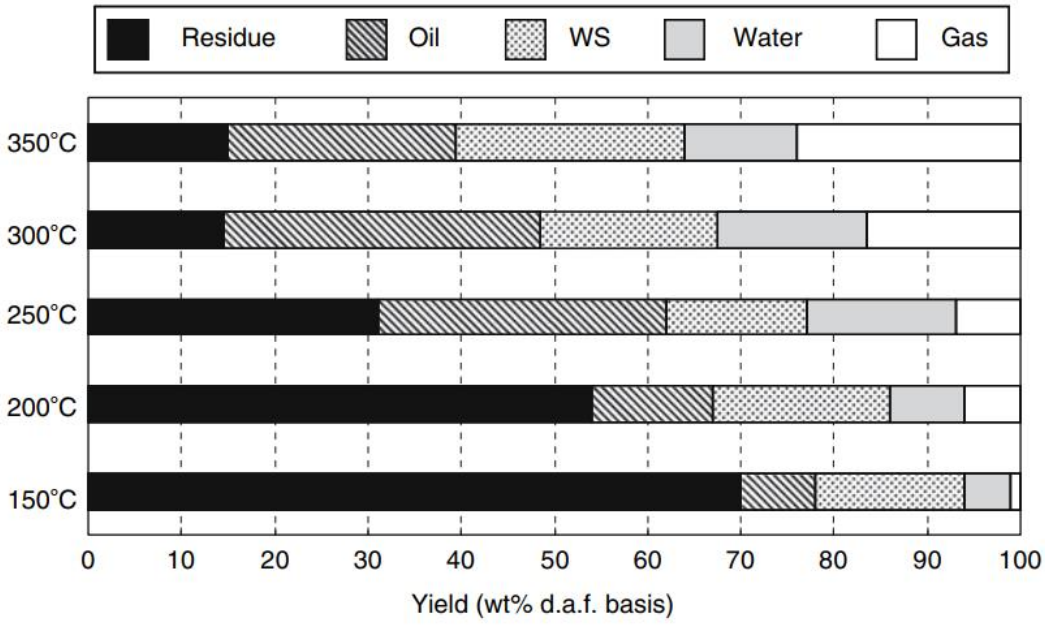

Figure 2.9: *Yield of liquefaction products from eucalyptus as a function of temperature Sugano et al. [143]. Where d.a.f means dry ash-free. Note that the liquid product in this research has been divided into oil, water-soluble product (WS), and water. Reaction conditions: 3 g eucalyptus, 30 g solvent (paper regeneration wastewater), 2 MPa N2 initial pressure, 7 °C /min heating rate, and 0 min hold time at set the temperature.*

(ii) Solvent – to – biomass ratio:

Solvent-to-biomass ratio is another key parameter that affects biomass liquefaction. High amounts of solvents are generally suitable for high biomass conversion and yield of liquid products. Previous investigations [26,105,144] revealed that optimum biomass conversion and yield of liquid products are achieved at solvent-to-biomass mass ratios of

4:1 to 10:1. Ratios less than 4 are usually unfavourable as they are accompanied by mixing challenges resulting in very low biomass conversion and yield of liquid product due to a decrease in heat and mass transfer. According to Brand *et al.* [26], a reduction in ethanol-to-pine wood ratio from 4 to 2.7 resulted in a wet powder which was stuck to the inner walls of the reactor, therefore, pinewood conversion dropped from 85.3 wt.% to 74.2 wt.% whereas biocrude yield dropped from 56.4 wt% to 37.8 wt%. In a similar work by Yin *et al.* [144], on the hydrothermal liquefaction of cattle manure, bio-oil yield declined abruptly from 50 wt.% to < 5 wt.% when the water-to-manure ratio was reduced from 4 to ≤ 2, biomass conversion also dropped from 95 wt.% to 50 – 85 wt.%. Nonetheless, high solvent-to-biomass ratios, particularly > 10 may be less economical since large amounts of solvent demand higher energy inputs and higher cost for waste solvent management [118].

(iii) Pressure and retention time:

Pressure and residence time are considered secondary parameters in terms of their impact on biomass liquefaction. Pressure (beyond ambient pressure) is required to maintain the liquefaction solvent in a single-phase particularly when operating at temperatures above the boiling point of the solvent. Increasing pressure increases solvent density which enhances the diffusion of solvent molecules into the biomass, resulting in improved biomass fragmentation and yield of liquid and gaseous products. Conversely, an excessive increase in local solvent density could also cause a cage effect on biomass C–C bonds resulting in low biomass fragmentation and conversion [118]. Under subcritical and near-critical conditions (≤ 374 °C, ≥ 1 MPa), increasing pressure is generally believed to favour liquid yield via the inhibition of gas formation from liquid products [21]. For instance, Zhang *et al.* [145] reported a sharp increase in corn straw conversion from ~25 wt.% to 69 wt.% with an initial pressure increase from 0 to 4 MPa N_2, and the yield of bio-oil also increased abruptly from 1.2 to 32.5 wt.% during the non-catalytic hydrothermal liquefaction of corn straw at 300 °C and 15 min. A further increase in pressure to 6 MPa was however found to produce a negligible impact on biomass conversion and bio-oil yield. Once supercritical conditions (> 374 °C, ≥ 22 MPa) for liquefaction are achieved, the influence of pressure on the properties of the solvent medium is insignificant; as such, the effect of varying pressure on the yield of liquid product is generally said to be negligible [118,146]. In some supercritical liquefaction studies, increasing pressure was reported to impact negatively on liquid yield, possibly due to excessive gasification. For example, Chan *et al.* [120] observed a 25 % drop in

bio-oil yield from 39 wt.% to 29 wt.% when pressure was increased from 25 MPa to 35 MPa at a reaction temperature of 390 °C, using palm kernel shell and water at a biomass-to-solvent ratio of 1:10, and 1 h reaction time. A similar observation was made for palm mesocarp fibre where bio-oil yield declined from 34 wt.% to 25 wt.% under the same conditions employed for the palm kernel shell. In terms of retention time, optimum biomass conversion, and yield of liquid products are generally reported to occur between 15 – 60 mins. Retention time beyond 60 mins usually results in excessive gas formation at the expense of liquid products whereas retention time less than 15 mins typically results in insufficient biomass conversion [104,105,120].

2.5 Potential applications of sugarcane bagasse and pine needles

2.5.1 Sugarcane bagasse

Sugarcane is the world's top produced agricultural commodity. Its global annual production currently stands at 1.9 billion tonnes [147]. Thus, approximately 250 kg of sugarcane is produced per head globally in a year. 70 % of the world's total sugar is produced from sugarcane [147]. It is also widely used to manufacture ethanol. Sugarcane thrives best in a warm climate and in tropical regions, hence, most of the sugarcane cultivation nations are located in South Asia, South America, and Africa. Figure 2.10 illustrates the top 10 sugarcane producing countries. From Figure 2.10 it is clear that Brazil is the world's leading producer of sugarcane with more than 768 million tonnes of annual production; equivalent to over 40 % of the world's total production [147].

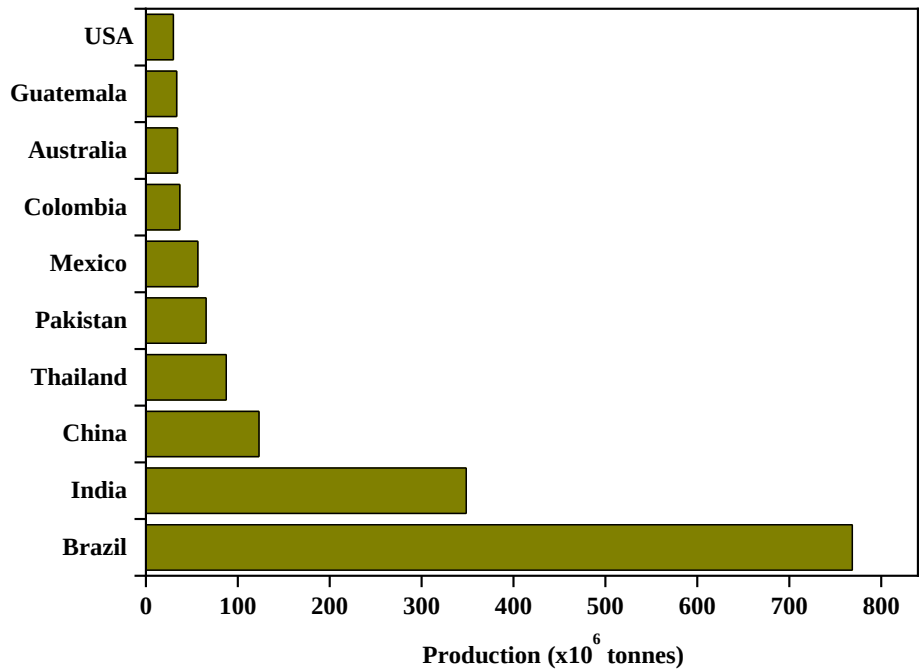

Figure 2.10: *World's top 10 sugarcane producing countries. Data obtained from Atlas Big* [147].

Harvesting and processing of sugarcane generate mainly two types of biomass waste; 1) sugarcane trash and 2) bagasse. Sugarcane trash (Figure 2.11a) is the field residue, e.g. tops and leaves, remaining after harvesting the sugarcane stalk. Bagasse (Figure 2.11b) is the pulpy fibrous by-product of milling which remains after extracting the sugar juice from the stalk. Sugarcane trash is said to represent 15 wt.% of the total above-ground biomass at harvest which is equivalent to about 15 tons per hectare of dry matter [148,149]. Meanwhile, for every 10 tonnes of sugarcane crushed, about 3 tonnes

of wet bagasse is generated. Thus, the amount of bagasse generated is approximately 28 wt.% of the processed sugarcane [150] with up to 50 % weight base moisture content [151].

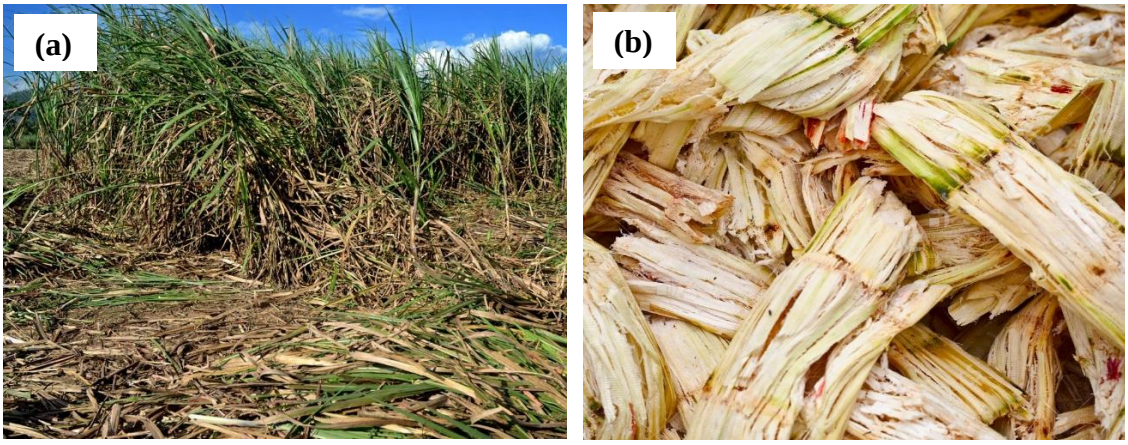

Figure 2.11: *Photographs of (a) sugarcane trash* [152] *and (b) sugarcane bagasse*[153].

Sugarcane trash and bagasse are excellent biomass resources that could be converted into chemicals and other valuable products. They are lignocellulosic materials, typically made up of 30 - 50 % cellulose, 20 - 30 % hemicellulose, and 20 % lignin on a dry weight basis [40]. However, the potential of these residues has largely been ignored by many sugarcane producing countries. Around the world, a portion of the freshly cut green tops is sometimes collected for farm animals, while the majority are burned or left in the fields to decompose [148]. The common practice of burning releases greenhouse gases directly into the atmosphere which poses a threat to the environment.

While sugarcane trash remains underutilised to a great extent, the use of bagasse, on the other hand, is gaining increasing attention these days. Some sugar mills burn bagasse in various systems (e.g. boilers, gasifiers, combine heat and power plants) to generate steam and electricity for internal plant requirements. For example, sugarcane bagasse is the largest renewable source of energy in Brazil today, representing 19.2 % of the Brazilian Energy Matrix in 2010 [151]. Yet, the full potential of sugarcane waste is far from being realised, as much of it is wasted [150]. For instance, Figure 2.12 shows a gradual increase in the gap between bagasse production and its utilisation in Brazil. It could be seen that the bagasse utilisation deficit rose sharply from ~2 million tonnes in 2008 to ~20 million tonnes in 2011 [151]. There is, therefore, the need to develop other routes to the

valorisation of bagasse as well as the trash in contribution to a more circular economy. Moreover, the prevalent thermal technology is however disadvantaged by the need for a feedstock with low moisture content, 15 - 40 wt.% to achieve good quality gaseous fuel and cost benefits [96,154]. Thus, the utilisation of sugarcane waste with high moisture contents up to 70 wt.% [155], as feedstock in these processes requires pre-drying which is energy-intensive.

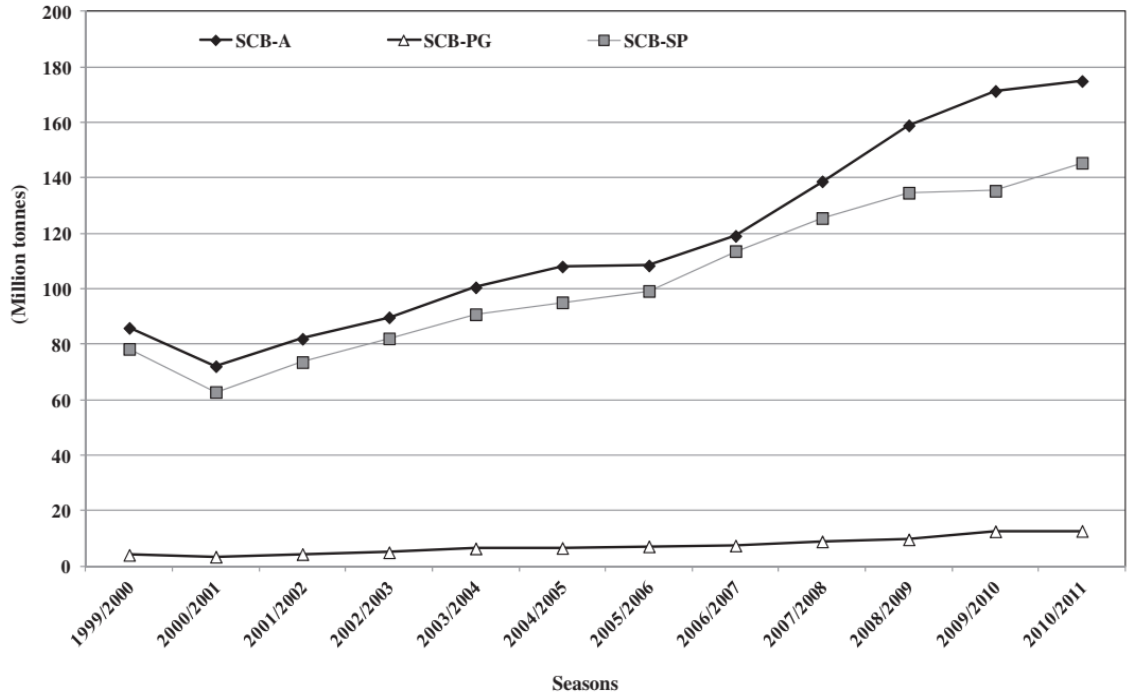

Figure 2.12: *Quantity of sugarcane bagasse available (SCB-A), used for power generation (SCB-PG), and for steam production (SCB-SP) in Brazil from 1999/2000 to 2010/2011* [151].

An alternative/supplementary route to bagasse utilisation that has been of great interest is in the production of bioethanol for fuel applications. This development will not only help reduce the existing gap in sugarcane waste utilisation but also reduce the world's dependence on food resources such as grains and sugars for biofuel production. However, as earlier discussed in Section 2.4.1, the present biochemical technology applied in bioethanol production is complex and less economical, making the price of the resultant ethanol less competitive to fossil-based fuels [60].

Other routes to sugarcane bagasse utilisation currently under laboratory-scale investigation include; the production of activated carbon for various applications, e.g. CO_2 capture [156]; production of valuable chemicals such as xylose, glucose,

arabinose [157,158], lactic acid [158]; organic acids [159,160] and furans [161]. However, most of the chemical production routes are dependent on biochemical techniques where the lignin component of the bagasse is mostly considered as an impurity that needs to be removed prior to the conversion of the poly- and mono- saccharides to these chemicals [158–160]. Activated carbon production, on the other hand, uses pyrolysis where pre-drying of sugarcane bagasse is crucial.

Overall, there exists the prospect of diverse applications of sugarcane waste. Nonetheless, current technologies employed for the conversion of this waste either; 1) require expensive pretreatment steps such as drying or other chemical methods or 2) lack the ability to valorise the entire biomass, particularly the lignin constituent. Hence, the exploration of alternative techniques that could address these issues could make the processing of sugarcane waste (and other agro-residues) more economical and sustainable. A potential technique that could address these issues is liquefaction since it has the ability to convert all three bio-polymers to value-added products and is able to process a wide variety of biomass materials irrespective of their moisture content [14].

2.5.2 Pine needles

The pine family *(Pinaceae*) is made up of many popular conifers like cedars, spruce, pines, and firs, with more than 200 known species [162]. They are very common forest-based plants in the Northern Hemisphere as well as a few parts of the tropics in the Southern Hemisphere [162,163]. They are also the preferred conifers for plantations. For example, pines are estimated to cover 80 % of the tropical forest plantations of Venezuela, 78 % of plantation areas in Chile, 49 % of the plantation areas in Argentina [163]. Pines *(Pinaceae*) are commercially popular for timber [164] wood pulp [163] and turpentine [165]. They are also used for various ornamental purposes, like the Christmas tree during Christmas festivities.

Timber harvesting is one of the potential sources of biomass residues/waste for future bio-refineries. These wastes come in the form of wood stumps, twigs, leaves, etc. [166]. For instance, in 2002, an estimated 178 million metric tonnes of woody residues were generated from the harvest and processing of timber alone in the United States (Figure 2.13). Nearly, 50 % (86 million metric tonnes) of this was unutilised and considered available for recovery [167].

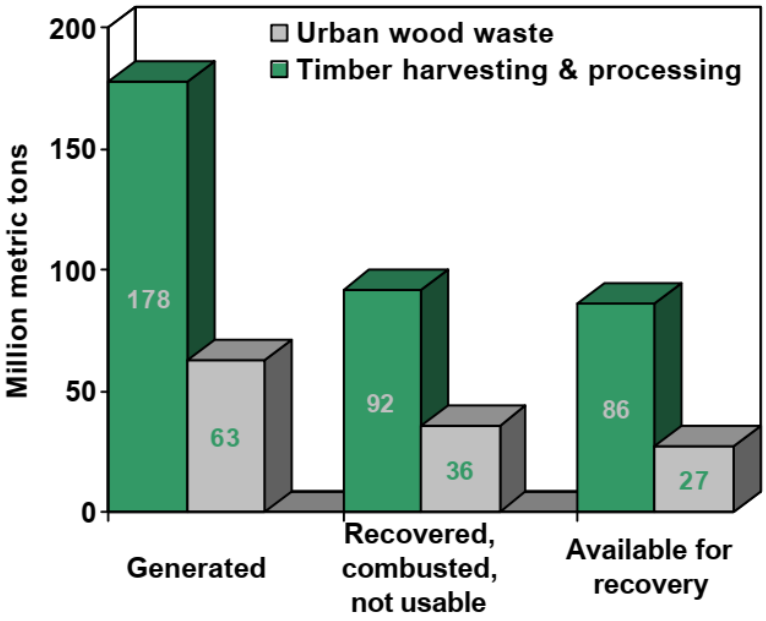

Figure 2.13: *Wood waste generated, recovered, combusted or not usable, and available for recovery in the United States, 2002* [167].

Pine needles are simply, the needle-like leaves of pines *(Pinaceae*) and come in varying lengths between 1.2 – 25 cm depending on the species [168]. Dried, fallen off pine needles are often associated with fires in coniferous forests and hence, air pollution [169,170]. However, these needles are rich in a variety of useful chemicals, *i.e.* lignocellulose, and solvent extractable compounds [171]. The lignocellulose content typically comprises of 60 – 70 % cellulose plus hemicellulose, and approximately 30 - 40 % lignin based on dry weight [39,170,172].

Current commercial applications of pine needles include decorative purposes e.g. basketry [173,174], in beverages and traditional medicines in China [171]. On research-scale, the prospects of making pulp and paper from pine needles were evaluated by Lal *et al.* [39]. It was concluded that the high (> 50 wt.%, dry weight basis) holocellulose content of pine needles makes it a probable feedstock for pulp and paper production, however, its high lignin content (43 wt.%, dry weight) demands high quantity of chemical for bleaching. It was therefore, recommended that pine needles be used for semi- or un-bleached kraft paper. In other studies [172] pine needles were used to enhance the mechanical properties (e.g. yield strength, fracture stress, tensile stress, and ultimate compressive stress) of urea-formaldehyde thermosets. Modified bio-chars from pine needles were also investigated for the successful removal of uranium from aqueous solutions [175]. A recent study by Mahajan *et al.* [176] also demonstrated the potential

of using aqueous pine needles extract for the preservation of cheese. The antimicrobial and antioxidant properties of the extract were attributed to the presence of bioactive phytochemicals, phenolic, and acidic compounds.

Nevertheless, the current applications of pine needles are limited and hence the need to explore other application avenues such as chemical synthesis. It is important that the chosen technique for pine needles valorisation is able to sufficiently convert its high lignin content, approximately 30 – 40 wt.% based on dry weight [39,170,172].

2.6 Conclusion

It could be gathered from the literature survey that agricultural- and forest-based residues/wastes such as sugarcane bagasse and pine needles are potential resources that could be converted to a variety of valuable products, in place of food and fossil-based feedstocks. However, these are generally underexplored, particularly in the area of chemical synthesis.

Sugarcane bagasse and pine needles are rich in lignocellulose, which is a complex mixture of three polymers; cellulose, hemicellulose, and lignin. These polymers are composed of vital C_5 and C_6 monomers which could be exploited for the manufacture of simple and more useful chemicals. Existing pilot-scale processes for the conversion of these materials are mostly complex and expensive owing to feedstock pretreatments. Moreover, these processes are principally biological in nature and effective at the conversion of cellulose and hemicellulose, leaving behind lignin. Thus, there is a need for a technology that can; i) minimise feedstock preparation and ii) effectively valorise all three components of the biomass, to minimise waste generation and make the process more economical.

The liquefaction technique was, therefore, found as the most promising technology for the valorisation of lignocellulosic biomass to platform chemicals and other value-added products. Compared to other techniques, the liquefaction technique can process a wide range of biomass feedstock and moreover possess high thermal efficiencies for conversion of wet feedstocks [91]**;** requiring relatively less energy input and little to no feedstock preparation. This makes it a prospective route for the sustainable synthesis of chemicals from sugarcane bagasse and pine needles.

Chapter 3

Experimental and analytical procedures

CHAPTER 3: EXPERIMENTAL AND ANALYTICAL PROCEDURES

3.1 Introduction

The materials and methods employed in this work are presented in this chapter. Section 3.2 provides details of biomass feedstocks and other materials used in this work followed by sample preparation protocol in Section 3.3. Section 3.4 outlines the procedures followed for the comprehensive characterisation of the biomass materials prior to their application in the reaction studies in Chapters 5 to 7. The biomass feedstocks were analysed for their chemical and thermochemical properties via TGA, FTIR spectroscopy, and a variety of compositional analyses (*i.e.* elemental, proximate, extractives, and bio-polymer compositions). Detailed reaction procedures along with reactor set-ups and product analysis methods are documented in Sections 3.5 and 3.6. Finally, Section 3.7 shows how data reproducibility calculations were established.

3.2 Materials

Two biomass feedstocks (Figure 3.1) ware utilised in this work: i) Pine needles (*Picea abies,* Norway spruce) obtained from The Plant Place, Fen Drayton, UK; and ii) Sugarcane bagasse obtained from a local supplier in Alexandria, Egypt. The choice of pine needles, a forestry waste, and sugarcane bagasse, a typical agricultural waste is to provide a platform to gain insight into the behaviour of lignocellulosic biomass of differing physical and chemical characteristics in chemical synthesis. Table 3.1 outlines the specifications of other materials used as reagents and/or in analytical processes.

Figure 3.1: *Photographs of biomass feedstocks used in this work.*

Table 3.1: *List of chemicals used in this work with their specifications and suppliers.*

Material	Specification	Supplier
Characterisation studies		
2,5-Bis (5-tert-butyl-benzoxazol-2-yl) thiophene (BBOT)	99.8 %	Sigma-Aldrich
Cellulose (Sigmacell)		Sigma-Aldrich
Ethanol	≥ 98.8 %	Sigma-Aldrich
Lignin alkali		Sigma-Aldrich
Potassium bromide	FTIR grade	Alfa Aesar
Sulphuric acid	95 – 98 %	Sigma-Aldrich
Vanadium pentoxide	98.5 %	BDH chemicals
Water	HPLC grade	Alfa Aesar
Air (for TGA)	Zero grade	BOC
Helium gas (for elemental analysis)	> 99.996%	BOC
Nitrogen gas (for TGA)	Oxygen free	BOC
Reaction studies		
Acetone	≥ 99.8 %	Sigma-Aldrich
Ethylene glycol	≥ 99 %	Fisher Scientific
Glycerol	≥ 99 %	Sigma-Aldrich
Sulphuric acid	95 – 98 %	Sigma-Aldrich
Water	Distilled water	Alfa Aesar
Helium gas (for liquefaction & GCMS)	> 99.996%	BOC
For calibrations		
Acetic acid	≥ 99 %	Sigma-Aldrich
Acetone	≥ 99.8 %	Sigma-Aldrich
Ethanol	≥ 99.8 %	Sigma-Aldrich
Furfural	99 %	Sigma-Aldrich
Levulinic acid	98 %	Sigma-Aldrich
Mesityl oxide	90+ %	Alfa Aesar
Methanol	99.8 %	Sigma-Aldrich
Phenol	≥ 99 %	Sigma-Aldrich
Solketal	97 %	Alfa Aesar

3.3 Preparation of biomass materials

Where necessary, the biomass materials were dried, milled and sieved to various particle sizes according to protocols adapted from the American standard for testing materials (ASTM) E871-82 method [177] and the national renewable energy laboratory (NREL) method for the preparation of samples for compositional analysis [178].

For biomass characterisation processes, sugarcane bagasse was reduced to approximately 5 x 10 mm in size and dried at 105 ^{o}C until constant weight (18 - 24 hours), whereas pine needles were dried as received (~1 x 12 mm average) under the same conditions. Detailed drying steps are outlined in Section 3.4.2.1. Both materials were separately milled with a Retsch PM100 planetary ball mill and sieved to various size categories; $\leq$ 200 µm, 200 – 500 µm, 500 – 1000 µm, and ~1000 µm.

An advantage of liquefaction over other techniques is its ability to handle feedstocks with high moisture content since a liquid medium is needed to effectively decompose the solid biomass. However, to establish a common basis of comparison, both pine needles and sugarcane bagasse were dried in an air oven at 105 ^{o}C for 24 h until constant weight prior to their applications in the liquefaction studies. The particle size of dried sugarcane bagasse was reduced to 1 mm, comparable to that of pine needles which were used as received.

Post-reaction residues (bio-char), commercial cellulose and commercial lignin were analysed as obtained without further size reduction unless otherwise stated.

3.4 Characterisation of biomass feedstocks

3.4.1 Thermogravimetric analysis (TGA)

TGA is an analytical technique that continuously measures the mass of a sample while its temperature is altered or maintained over time under a specified atmosphere (vacuum, inert, oxidising or other reactive gases). Changes in the mass of the sample are due to various thermal events such as drying, absorption, vaporisation, oxidation, decomposition, etc. Various information including the purity and thermal stability of the sample can be derived from a simple plot of mass versus time/temperature of the sample

while more detailed information such as the rate of degradation or temperature of maximum weight loss can be obtained from the first derivative of the TGA (DTG). A typical thermogravimetric analyser consists of a precision balance with a ceramic or metal sample pan located inside a furnace with programmable temperature control. Exhaustive information on the principles and applications of thermogravimetry has been provided by Brown [179].

TGA can be applied in diverse ways to study a wide range of solid and liquid materials (e.g. fuels, thermoplastics, and recently for biomass materials [180–182]) following procedures standardised by organisations such as the British Standard (BS), International Organisation for Standardisation (ISO), and the American standard for testing materials (ASTM). In biomass characterisation, TGA is normally used for the study of general thermo-degradation profile [183,184] and proximate analysis [185–187]. Recent attempts were made to quantify the bio-polymer constituents (lignin, hemicellulose, and cellulose) of biomass using the TGA in place of existing traditional wet chemical methods which are otherwise time and material intensive. These attempts, however, achieved little success, due to the overlapping thermal degradation temperatures of the three polymers [181,182,188] as demonstrated in Section 4.3.1.1 (Figure 4.1, Table 4.1 and Table 4.2).

In this research the TGA was used to study the general thermal degradation profile and proximate compositions of sugarcane bagasse and pine needles, using commercial cellulose and lignin as references. The TGA and corresponding DTG of all samples was conducted using a Perkin Elmer TGA 4000 instrument equipped with a Pyris V10.1.0.0412 software suite for data acquisition and processing. Approximately 10 mg of a sample (200 - 500 µm particle size) was used per analysis employing a thermal program (Table 3.2) adapted from the ASTM E1131 – 08 method [189]. Moisture, volatile, fixed carbon, and ash contents of each sample were estimated employing equations 3.1 to 3.4. To establish a common basis of comparison the biomass materials were dried as specified in Section 3.4.2.1 prior to the TG analysis.

Table 3.2: *Thermal program used for TGA and DTG analyses of biomass samples.*

Initial temperature (°C)	Rate (°C/min)	Final temperature (°C)	Hold time (min)	Gas (50 mL/min)
40	-	40	5	N_2
40	20	110	5	N_2
110	20	900	10	N_2
900	-	900	10	Air
900	20	950	10	Air

$$\text{Moisture (wt.\%)} = \frac{\overset{N}{w_{40}} - \overset{N}{w_{110}}}{\overset{N}{w_{40}}} \times 100 \quad (3.1)$$

$$\text{Volatile matter (wt.\%)} = \frac{\overset{N}{w_{110}} - \overset{N}{w_{900}}}{\overset{N}{w_{40}}} \times 100 \quad (3.2)$$

$$\text{Fixed carbon (wt.\%)} = \frac{\overset{N}{w_{900}} - \overset{a}{w_{950}}}{\overset{N}{w_{40}}} \times 100 \quad (3.3)$$

$$\text{Ash (wt.\%)} = \frac{\overset{a}{w_{950}}}{\overset{N}{w_{40}}} \times 100 \quad (3.4)$$

W_{40} is the initial weight of the sample at 40 °C, while W_{110}, W_{900}, and W_{950} are the final weights of the sample at 110 °C, 900 °C, and 950 °C respectively. The gaseous atmosphere under which each weight was measured is represented by the superscripts *"N"* and *"a"* which correspondingly stand for nitrogen and air atmospheres.

3.4.2 Proximate analysis (conventional manual method)

Though the application of TGA in the proximate analysis of biomass materials [185,186] is gaining attention, there is no standardised protocol for this process. This could be a consequence of the enormous variation in the composition and characteristics of biomass materials [10,184,187,190]. Hence, an optimised method for one material might not necessarily be applicable to another. Additionally, most procedures in literature come

with disparities in program temperatures, hold-times, heating rates, and sometimes combustion gases [169,185,187]. Many works in literature applied either of the two methods with very limited literature information on how the chosen TGA protocol compare with the traditional non-instrumental procedures [186,187,191]. It was therefore important that the developed TGA method used in this work is compared with the conventional ASTM manual process. This could serve as a guide for the selection of a method in future works.

The moisture, volatile matter, fixed carbon, and ash contents of the biomass materials were determined manually in line with the ASTM E870 – 82 methods [192] as detailed in Sections 3.4.2.1 to 3.4.2.4.

3.4.2.1 Moisture content

This test covered the determination of total weight (as received) basis of moisture in the feedstock as described in the ASTM E871-82 standard [177]. The sample container (20 cm diameter glass petri dish) was dried at 105 °C for 30 mins in a drying oven with air circulation, cooled in a desiccator and weighed. The container was then loaded with a known weight of pine needles (as received, *i.e.* ~1 x 12 mm average) or sugarcane bagasse (5 x 10 mm particle size) and heated at 105 °C for 16 h in the oven. After 16 h the container with the sample was removed from the oven, cooled to room temperature in the desiccator and weighed immediately. The sample with the container was repeatedly heated at 105 °C for 2 h, cooled and weighed until the difference between the weighings were less than 0.2 % and the final mass recorded. The amount of moisture was determined by applying equation 3.5. It should be noted that the amount of sample is dependent upon the size of the container; as such, the quantity of sample was chosen such that the surface area of each particle in the container prior to drying was exposed to minimise heat transfer limitations.

$$\text{Moisture content (wt.\%)} = \left(\frac{w_i - w_f}{w_i - w_c}\right) \times 100 \qquad (3.5)$$

Where;

w_c = mass of container (g); w_i = initial mass of container and sample before drying (g); and w_f = final mass of container and sample after drying (g)

3.4.2.2 Volatile matter

This test defines the percentage of material liberated, exclusive of moisture vapour upon heating the biomass sample under a rigidly controlled condition based on the ASTM E872-82 standard [193]. The pre-dried sample from Section 3.4.2.1 was milled to 0.5 - 1 mm and dried again at 105 °C until constant weight to get rid of absorbed moisture. A crucible with lid was pre-fired at 950 °C for 30 mins and cooled to room temperature in a desiccator and its weight noted. The crucible was next loaded with 1 g of the dry sample, covered with the lid, weighed and placed in a pre-heated furnace which was maintained at 950 °C. The sample was quickly taken out of the furnace after 7 mins and allowed to cool in a desiccator without disturbing the lid. The final mass of the covered crucible with the sample was then noted once cooled to room temperature and the percentage volatile matter for the sample was calculated as specified in equation 3.6.

$$\text{Volatile matter (wt.\%)} = \left(\frac{w_i - w_f}{w_i - w_c}\right) \times 100 \qquad (3.6)$$

where:

w_c = weight of crucible and lid (g); w_i = initial weight of crucible, lid and sample (g); and w_f = final weight of crucible, lid and sample (g)

3.4.2.3 Ash content

Ash content was estimated as the residue remaining after a moisture-free sample was combusted to 580 °C until constant weight according to the ASTM D1102 – 84 method [194]. Prior to combustion, a crucible with lid was heated at 600 °C in a muffle furnace until constant weight, followed by cooling in a desiccator. For ash content determination, 2 g of a pre-dried sample (Section 3.4.2.1) of 200 - 500 µm particle size was placed in a weighed crucible and heated from room temperature to 580 °C in the muffle furnace. The sample was kept at this temperature for 30 mins, then taken out, cooled in a desiccator and its weight measured. Heating at 580 °C for 30 mins, cooling and weighing were repeated until constant weight to within 0.2 mg was obtained. The crucibles were covered during the cooling and weighing stages to prevent moisture

absorption from the atmosphere. The percentage of ash was determined using equation 3.7.

$$\text{Ash content (wt.\%)} = \left(\frac{w_f}{w_i}\right) \times 100 \qquad (3.7)$$

where:

w_i = mass of oven-dry sample (g); and w_f = mass of ash (g).

3.4.2.4 Fixed carbon

Fixed carbon is a calculated value based on the average percentages of moisture, ash, and volatiles by applying equation 3.8.

$$\text{Fixed carbon (wt.\%)} = [100 - (\%\, moisture + \%\, ash + \%\, volatile\ matter)] \qquad (3.8)$$

3.4.3 Fourier transform infrared spectroscopy (FTIR)

FTIR is a technique used to acquire an infrared spectrum of absorption or transmission of a material (solid, liquid or gas). It is the measurement of the wavelength and intensity of the absorption of infrared light by the sample. The resulting signal at the detector is a spectrum with absorption peaks which correspond to the frequencies of vibrations between the bonds of the atoms making up the material. The spectrum represents a molecular 'fingerprint' of the sample. Because each different material is a unique combination of atoms, no two compounds produce the exact same infrared spectrum [195].

FTIR spectroscopy is therefore utilised for the qualitative analysis (identification) of a wide variety of materials, e.g. inorganic, polymers, etc. [196]. It is also applied in quantitative analysis as the size of the peaks in the spectrum can be directly correlated with the amount of material present. The FTIR spectroscopy comprises of four main sampling techniques: transmission, attenuated total reflection (ATR), diffuse reflectance, and specular reflection. Further information on the principles and applications of FTIR

and IR techniques, in general, is provided by Griffiths & de Haseth [197], Smith [198], and Stuart [196].

In biomass studies, FTIR spectroscopy is often used to explore the chemical structural composition of such materials [199]. It is particularly useful in identifying the presence of the three main bio-polymers (lignin, hemicellulose, and cellulose) in a plant matter. This is normally achieved via the transmission technique where the IR beam passes through the sample [199].

In this work, a Shimadzu IRAffinity-1S FTIR spectrometer was employed for the functional group and general chemical structure analysis of biomass feedstocks and post-reaction residues via transmission. 1 wt.% of samples in KBr (FTIR grade) were made into thin pellets (120 – 150 mg) and scanned 32 times using the Harp-Genzel method within 400 – 4000 cm^{-1} of wavelength at a resolution of 4. The lignocellulose materials were reduced to < 200 µm particle size prior to analysis while the post-reaction residues, commercial cellulose, and lignin were analysed as obtained.

3.4.4 Elemental composition (ultimate) analysis

The elemental (C, H, O, N, S) composition of each sample was determined using a Thermo Scientific FLASH 2000 Organic Elemental Analyzer equipped with a thermal conductivity detector (TCD) and a MAS 200R autosampler. The analyser, which is based on the dynamic combustion of the sample, allows the quantitative determination of carbon, nitrogen, hydrogen, and sulphur in a single run [200].

Approximately 5 mg of a sample mixed with 2.5 – 5.0 mg of vanadium pentoxide catalyst in a tin capsule is introduced into the combustion reactor of the instrument via the Thermo Scientific MAS 200R autosampler. After combustion, the resultant gases are carried by a helium flow through a gas chromatography (GC) column that provides the separation of the combustion gases, and finally, detected by a thermal conductivity detector (TCD). Approximately 5.0 mg 2,5-bis (5-tert-butyl-benzoxazol-2-yl) thiophene (BBOT) was used as a standard in this analysis. Pine needles and sugarcane bagasse were dried and milled to 200 – 500 µm as outlined in Section 3.3 while commercial cellulose and lignin were analysed as supplied. It should be noted that lignin was received with 4 wt.% sulphur

content as confirmed by the results in Figure 4.5. The oxygen composition was estimated by difference using equation (3.9).

$$\text{Oxygen (wt.\%)} = 100 - (\%\ C + \%\ H + \%\ N + \%S + \%\ \text{Ash}\ *) \qquad (3.9)$$

* Residue upon air combustion of samples at 900 - 950 ^{o}C in a Perkin Elmer TGA 4000 system as defined by equation 3.4.

3.4.5 Determination of extractives and bio-polymer constituents

3.4.5.1 Determination of extractives

This procedure covers the determination of non-structural soluble materials in a biomass sample. A two-step exhaustive extraction process using water and ethanol developed by the National Renewable Energy Laboratory (NREL) [201] was followed to quantify the amount of solvent extractable materials in pine needles and sugarcane bagasse. The results are reported as a weight percentage of the dry biomass. The extractives determination was conducted on biomass samples dried at 105 °C for 24 h and milled to 200 – 500 µm particle sizes. The focus of this experiment is to identify what kind of extractable compounds are present in the biomass feedstocks prior to their application in liquefaction studies hence the need to apply the same drying conditions as those used prior to liquefaction. All relevant glassware and thimbles were also dried at 105 °C for 12 – 24 h and cooled in a desiccator prior to the experiment.

For the determination of water-soluble extractives 6 - 8 g of sample was introduced to a tared thimble such that the height of the biomass in the thimble does not exceed the height of the Soxhlet siphon tube (to avoid partial extraction). The thimble with the sample was placed in the Soxhlet apparatus; 190 mL of HPLC grade water was added to a tared 500 mL round bottom flask and connected to the Soxhlet apparatus, condenser, and a heating mantle. The water was heated at 130 °C (by means of a silicon oil heating bath) and refluxed for 20 h, after which the heating was stopped, and the set up left to cool. Once cooled to room temperature, as much water as possible was removed from the Soxhlet extractor and the solids were then washed with 100 mL fresh HPLC grade water and allowed to dry in an oven at 105 °C until constant weight (24 h). These solids are

hereafter referred to as water-extractive-free biomass. The water extract was analysed via GCMS (Section 3.5.4.1) to identify what volatile compounds are present in the biomass.

Note that, for the exhaustive determination of extractives, the wet water-extractive-free biomass with the thimble was left in the Soxhlet ready for the next stage, ethanol extraction. Equation 3.10 was used to calculate the percentage of water extractives in each sample.

$$\text{Water extractives (wt.\%)} = \left(\frac{w_{bm} - w_{wef}}{w_{bm}}\right) \times 100 \qquad (3.10)$$

Where,

w_{bm} = weight of oven-dried biomass, at 105 °C for 24 h (g)

w_{wef} = weight of dried water-extractive-free biomass (g)

For ethanol-soluble extractives, 190 mL of ethanol (≥ 98 %) was added to a tared 500 mL round bottom flask and assembled with the Soxhlet (containing the wet water-extractive-free biomass), condenser, and heating mantle as described above. This was also heated at 130 °C and refluxed for 20 h. Once cooled, the thimble was removed from the extractor and the biomass carefully transferred unto a pre-weighed filter paper. The solids were then washed with 100 mL fresh ethanol and allowed to dry in an oven at 80 °C until constant weight (24 h). These solids are hereafter referred to as extractive-free biomass. FTIR spectroscopy (Section 3.4.3) was used to check for any chemical structural changes in the extractive-free biomass, the results are presented in Section 4.3.3.1 (Figure 4.6)

The ethanol extract was condensed to 30 mL with the aid of a rotary evaporator equipped with a water bath set to 60 °C and a vacuum source. The condensed sample was analysed via GCMS, to have an idea of what extractives are present in the biomass feedstock. The percentage of ethanol extractives was estimated using equation 3.11.

$$\text{Ethanol extractives (wt.\%)} = \left(\frac{w_{bm} - (w_{ef} + w_{we})}{w_{bm}}\right) \times 100 \qquad (3.11)$$

Where,

w_{bm} = weight of oven-dried biomass, at 105 °C for 24 h (g)

w_{ef} = weight of extractives free biomass (g)

w_{we} = weight of water extractives (g)

3.4.5.2 Determination of bio-polymer constituents

This section looks into the determination of acid-insoluble lignin (also known as "Klason lignin") in the biomass samples via a hydrolysis method with 72 wt.% sulphuric acid according to the TAPPI T 222 om-02 method [202]. The difference is reported as the amount of holocellulose (*i.e.* cellulose plus hemicellulose). A solution of 72 wt.% sulphuric acid was made from a 98 % concentrated acid by diluting a 112.65 g of the concentrated acid with 40.65 g of distilled water, which makes enough acid for 4 g of biomass. The acid was cooled to room temperature before applying it in the following procedure.

To determine the amount of Klason lignin, 1 g of extractive-free biomass was mixed with 15 mL of the 72 wt.% sulphuric acid in a beaker. This was stirred frequently at room temperature for 2 h and then diluted to 3 wt.% concentration of sulfuric acid with 560 mL distilled water. The diluted sample was thereafter boiled under reflux for 4 h at 130 °C and allowed to cool and settle overnight. The liquid was decanted, while the solids were washed with hot water at 90 °C until the filtrate turns out neutral when tested with a litmus paper. The solids (Klason lignin) were dried in an oven at 105 °C until constant weight (24 h). The percentage of Klason lignin was reported based on the dry weight of the extractive-free biomass in Table 4.9. The extracted lignin was examined by FTIR spectroscopy (Section 3.4.3), to check if it is free of any structural carbohydrates. The results are presented and discussed in Section 4.3.3.2 (Figure 4.8).

Holocellulose is considered in this work as the amount of dry biomass dissolved by 72 wt.% sulphuric acid. It is normally believed that a portion of the acid-soluble lignin in biomass is dissolved by the sulphuric acid during the Klason lignin extraction process. But, the amount of acid-soluble lignin in softwoods and coniferous biomass such as sugarcane bagasse and pine needles is very minimal, approximately 0.2 - 0.5 wt.% [202]. This amount is considered negligible and hence safe to assume the percentage of dry sugarcane bagasse and pine needles dissolved in 72 wt.% sulphuric acid is holocellulose.

This assumption yielded satisfactory results when compared to those obtained via other methods studied in the literature (Section 4.3.3.2, Table 4.9).

3.5 Reaction studies: Liquefaction procedures and reactors set-up

Biomass liquefaction studies were conducted in two set-ups: i) a reflux set-up at atmospheric pressure (Section 3.5.1), and ii) a Hastelloy C-276 metal autoclave reactor under 30 bar of helium supply pressure (Section 3.5.2). The biomass feedstocks preparation protocols are presented in Section 3.3.

3.5.1 Atmospheric pressure liquefaction

Atmospheric liquefaction was conducted in a 250 mL borosilicate glass flask fitted with a reflux condenser (Figure 3.2), following protocols adapted from literature [111]. This set-up allows a maximum operating temperature of 200 °C, hence all experiments were conducted at temperatures ≤ 190 °C. 20 g of liquefaction solvent with or without catalyst was introduced into the flask and heated to 100 °C. 2 g of the prepared biomass (Section 3.3) was then added to the flask and heated to the desired temperature at which point magnetic stirring was initiated at 300 rpm. An ice-water was used to quench the reaction at the end of the specified reaction time and the resulting products separated by a vacuum filtration process as described in Section 3.5.3.

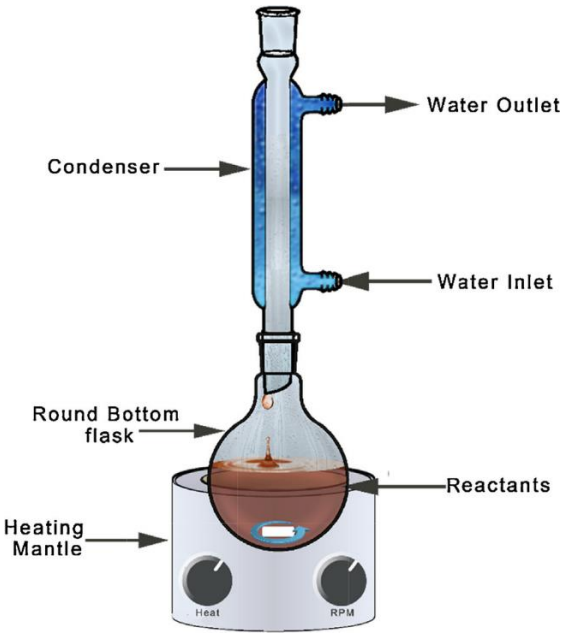

Figure 3.2: *Schematic diagram of a typical reflux set up* [203].

3.5.2 Moderate pressure liquefaction

3.5.2.1 Experimental set-up

A 100 mL capacity autoclave reactor made of Hastelloy C-276 by Parker Autoclave Engineers (Figures 3.3 and 3.4) was used for the moderate-pressure liquefaction studies of the biomass feedstocks. The reaction vessel is equipped with a heating jacket and a stirrer. The stirrer is coupled with a cooling system to prevent excessive heating of the motor. Heating and mixing are measured and controlled via a Parker Autoclave Engineers Universal Reactor Controller (URC). The pressure inside the reactor was measured by means of a McDaniel Controls safety gauge while the internal temperature was measured using a thermocouple connected to the URC.

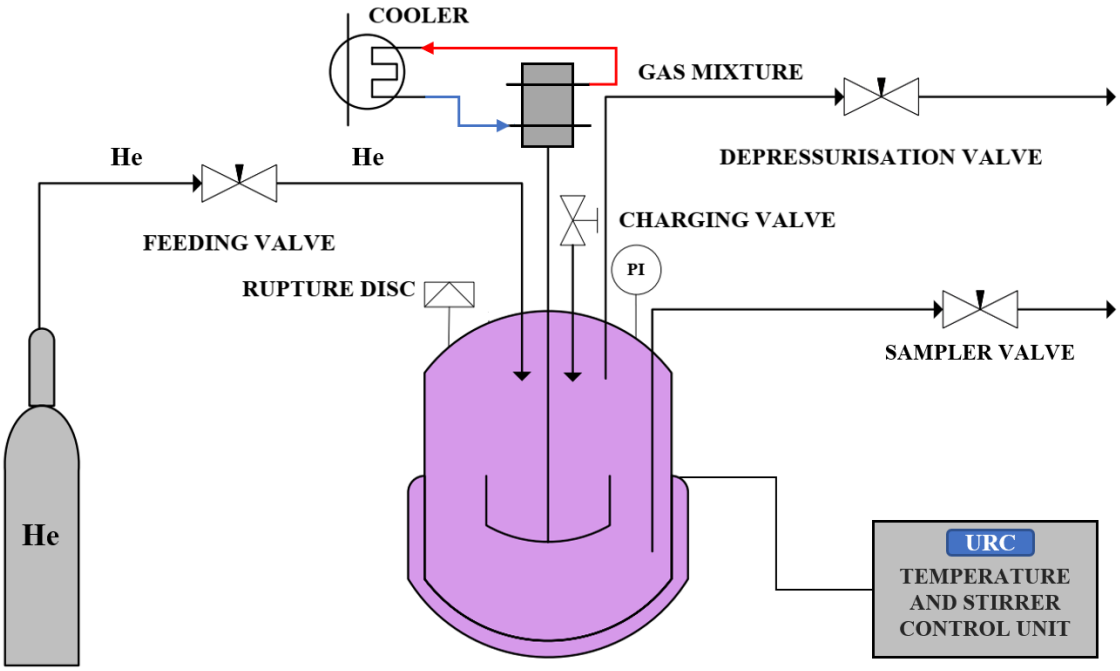

Figure 3.3: *Schematic diagram of the autoclave reactor used for biomass liquefaction. Adapted from Gómez 2017* [204].

3.5.2.2 Experimental procedure

The reaction vessel was charged with 2 g of the prepared biomass feedstock and 20 g of liquefaction solvent with or without catalyst and connected to the reactor head and stirrer assembly. The reactor was then purged three times with helium (30 bar) to remove air and finally loaded with 30 bar of helium for the reaction. This was followed by the

assembly of the heating jacket, and insulators on the reactor to minimise heat loss. The desired temperature, heating and mixing rates were then set via the URC followed by the start-up of heating and the cooling of stirrer motor. Mixing and timing were started immediately, once the set temperature was reached. At the end of the set reaction time, the mixer was stopped, and the reactor was cooled to room temperature in an ice bath. The gaseous phase was released to exhaust, while the liquid product and solid residue mixture were collected for separation (Section 3.5.3) and analysis (Section 3.5.4). Heating and mixing rates were also kept constant at ~15 °C /min, and 300 rpm respectively.

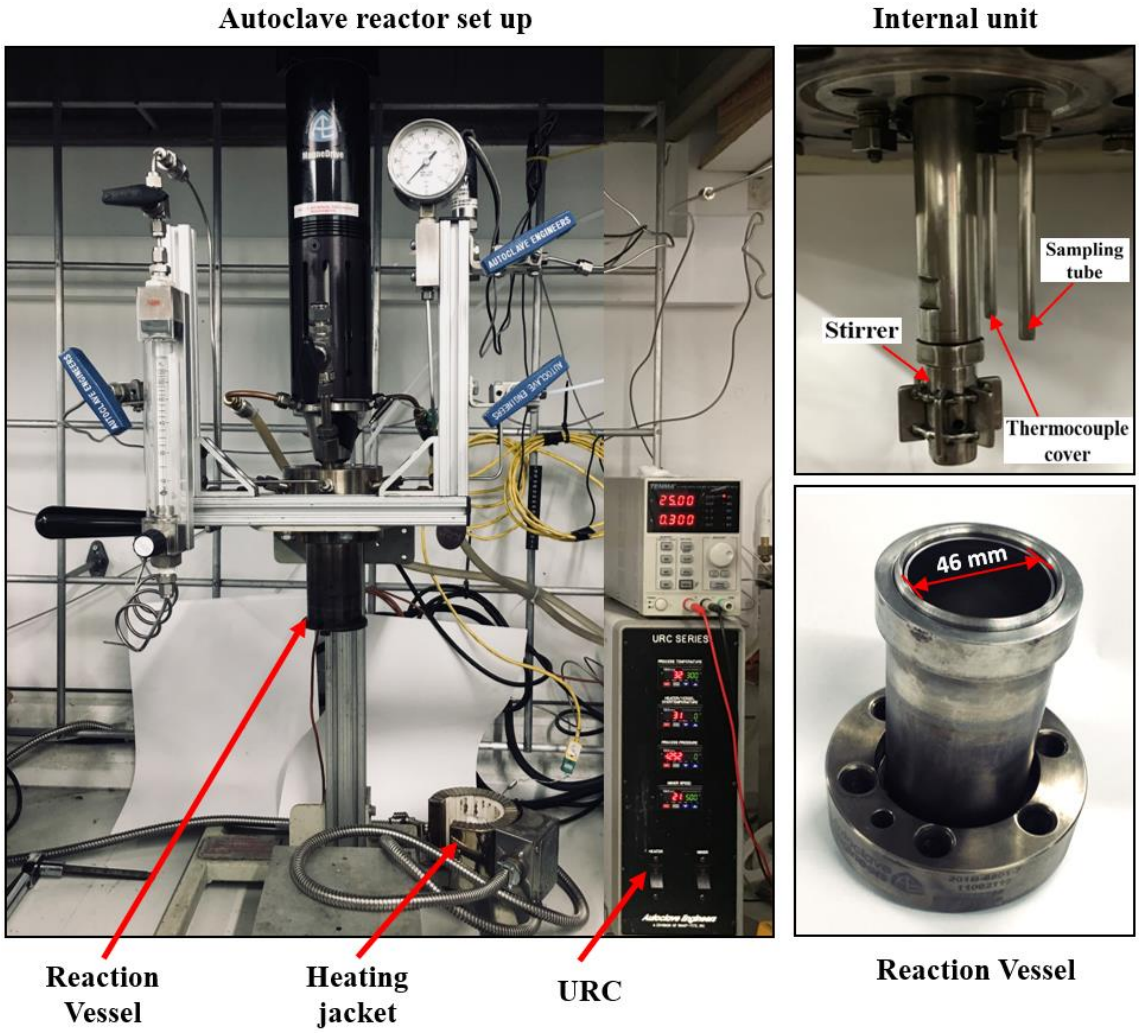

Figure 3.4: *Photographs of the autoclave reactor used for biomass liquefaction highlighting the key components.*

3.5.3 Product (liquid-solid) separation

The fraction of gaseous product from the liquefaction process was considered negligible (Appendix A.1) and hence vented without further analysis. The liquid fraction was, therefore, considered as the main product from all liquefaction experiments, whereas the solid residue (bio-char) was considered as a by-product. In terms of distribution, the yield of liquid product was taken as the weight percentage of dry biomass converted (Section 3.5.7, Equation 3.14), whereas solid yield was taken as the weight percentage of dry biomass unconverted.

Liquid-phase products were separated from the solid residue using a vacuum filtration setup equipped with a Whatman qualitative filter paper, Grade 1. The product from reactions conducted with water as a liquefaction solvent was filtered without the addition of any solvent while all others were filtered with 20 – 60 mL of ethanol or methanol. This was based on a preliminary study conducted to determine the method and solvents suitable for the separation of the post-reaction liquid product from the solid residue. The application of Soxhlet extraction versus vacuum filtration with either acetone or ethanol was studied. In summary, acetone was found to engage in a rapid side reaction with specific reaction products and reactants such as propylene glycol and ethylene glycol in the presence of H_2SO_4 during filtration. Acetone was, therefore considered unsuitable for product separation; as such, ethanol or methanol were used as filtration solvents throughout this work. A brief of this study is documented in Appendix A2. Where required, reactions were conducted in duplicate: one was filtered with methanol and the other with ethanol, to ascertain the full spectrum of products made from the biomass liquefaction process. This also rules out any suspicion of dilution solvent contributing to the formation of identified products. After separation, the filtrate was immediately sent for analysis while the residue was rinsed three times with 20 mL distilled water. The residue was afterward dried at 105 °C for 12 h and its weight determined before characterisation.

3.5.4 Analysis of liquid product (bio-oil)

3.5.4.1 Gas Chromatography-Mass Spectrometry (GCMS)

GCMS is a sequence of two analytical techniques: gas chromatography (GC): separation-followed by mass spectroscopy (MS): detection. The gas chromatogram separates multi-compound samples into individual components so that they reach the MS detector one at a time. This is achieved by a high-resolution fused silica capillary column, or a packed (glass or metal) column housed in a temperature-controlled oven (Figure 3.5). The oven temperature can be controlled to achieve optimum separation. The column contains a solid or non-volatile liquid supported on an inert solid known as the stationary phase.

GC is recommended for materials that can be vaporised without decomposition. The analyte introduced into the injection port is instantly vaporised by high temperature, up to 300 °C and low pressure, 1.3×10^{-5} – 1.3×10^{-2} Pa [205]. The sample is transported through the column by the flow of inert carrier gas, known as the mobile phase (typically nitrogen, helium, and argon). Helium was used in this work. The components of the analyte interact with the stationary phase at varying degrees depending on their affinity for this material as they move along the length of the column; hence dissimilar compounds travel at different velocities and exit the column at distinct retention time. A signal related to the concentration of each compound is produced as they pass through the detector. A plot of this signal as a function of time generates a series of symmetrical peaks in a chromatogram where each peak theoretically represents a unique compound.

Individual compounds may be identified by matching their retention time to the retention time of some standard, while their concentrations may be deduced from the peak area or height when compared against standards of known concentration. A more reliable way of component identification is the use of corresponding mass spectrum data for each compound, *vide infra*.

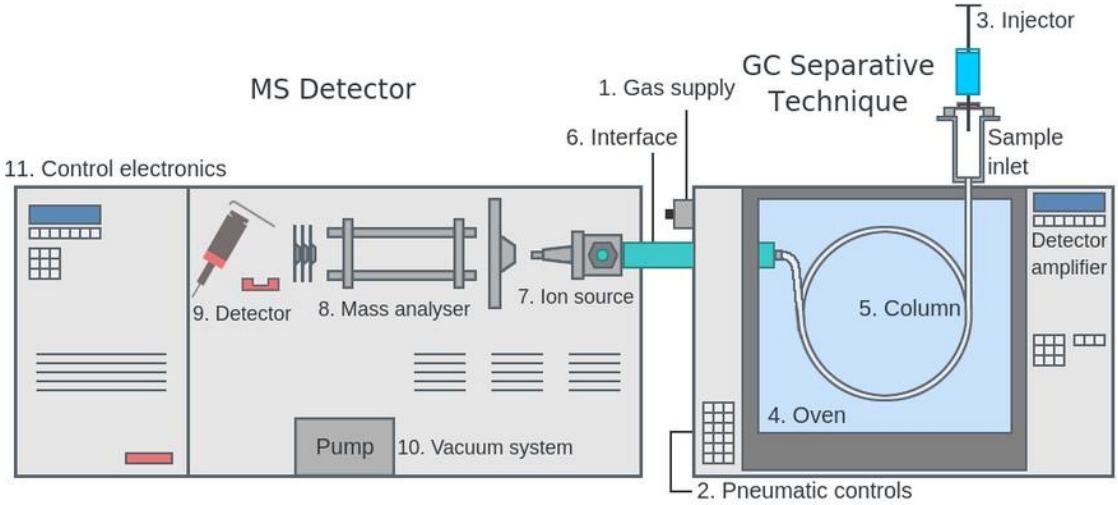

Figure 3.5: *Schematic representation of a gas chromatography-mass spectrometry system* [206].

The mass spectrometer uses an electron impact (EI) or chemical ionisation (CI) technique to ionise volatised compounds (normally neutral) as they elute from the GC for detection purposes [207]. The EI ionisation technique was utilised in this work. In EI, the molecules of the analytes exiting the GC are bombarded with a beam of high energy (70 eV) electrons accelerated from a hot filament. The energised electrons knock off an electron from the organic molecules (M) as depicted in equation 3.12 [208].

$$M + e^- \longrightarrow M^+ + 2e^- \qquad (3.12)$$

The M^+ ion, a cation-radical, is mostly unstable and undergoes a series of fragmentations either by the loss of a neutral molecule or radical. Equation 3.13 illustrates sample decomposition routes of a butyl acetate molecular ion [207]. These ions may further break down into smaller species, where the resultant ions are detected based on their mass-to-charge ratios (m/z). A pattern of fragment ions is obtained from the decomposition process, which is useful in characterising the constituent compounds of the analyte. If these compounds are previously known, they can be identified by comparing their mass spectrum to those available in computer libraries. Further information on the GCMS technique is discussed by Williams and Flemings [207].

$$CH_3COOCH_2CH_2CH_2CH_3.^+ \rightarrow \begin{cases} CH_3\overset{+}{C}=O + C_4H_9O\cdot \\ CH_3COOH + C_4H_8.^+ \end{cases} \qquad (3.13)$$

Analysis procedure

A Shimadzu GCMS-QP2010SE coupled with a mass spectrometer in EI ionisation mode was used for the analysis of the liquid phase products in this work. The GC was equipped with an Agilent HP-Innowax capillary column (length - 30 m; internal diameter - 0.25 mm; film thickness - 0.25 μm, stationary phase - polyethylene glycol) – a polar column suitable for the detection of alcohols, flavours and fragrances, solvents, free organic acids, and essential oils. The products were analysed with the oven temperature program specified in Table 3.3 unless otherwise indicated. Compounds were identified with the assistance of the National Institute of Standards and Technology (NIST) 2011 mass spectra database, version 2.0.

Table 3.3: *GCMS method employed for liquid product analysis.*

Parameter	Specification
Carrier gas	Helium
Injection volume	0.5 - 1 μL
Injection solvent	Methanol or ethanol
Internal standard	1-2 μL per 1500 μL of analyte (sample)
Injector temperature	250 °C
Detector temperature	245 °C
Split ratio	20 - 50
Temperature program	Hold at 40 °C for 5 min, increase to 240 °C at 10 °C/min, hold at 240 °C for 5 min

Prior to analysis each sample was filtered for a second time using a Captiva Premium Syringe Layered Filter of 0.2 μm pore size to ensure the liquids were free from any solid material. Products made using water as liquefaction solvent were analysed as obtained while those produced using ethylene glycol or glycerol were diluted with ethanol or methanol at a sample to solvent ratio of 1:75 – 1:30. Each analyte was mixed with the same and constant amount of an internal standard (*i.e.* propylene glycol or diethylene glycol) prior to analysis. Internal standards were carefully chosen to avoid any chemical interaction with analytes and to be soluble in both analyte and solvent. Propylene glycol was used as an internal standard for liquefied samples produced from water or ethylene glycol systems while diethylene glycol was used for samples produced from glycerol

systems as propylene glycol is a product of glycerol dehydration. The concentration of each product was calculated in grams per litre of liquefaction solvent by calibration with known standards, as explained in Section 3.5.5.

3.5.4.2 High-Performance Liquid Chromatography (HPLC)

In contrast to the GC, HPLC uses a liquid mobile phase to transport the analyte (sample) through the column. HPLC is the best choice for non-volatile and higher molecular weight materials or materials which are likely to degrade when heated [209]. For example, sugars, and large proteins of many thousands of Daltons may be analysed. HPLC can be used to characterise samples over a wide polarity range and is able to analyse ionic samples. Mobile phase components are selected to ensure sample solubility [209].

An HPLC system (Figure 3.6) consists of the column that holds packing material, a pump that moves the mobile phase(s) through the column, and a detector that shows the retention times of the molecules. The pump helps in continuous movement of the mobile phase at a constant flow rate through the system. The sample is introduced into the mobile phase via the injector without the need to stop the flow of mobile phase. As the sample moves through the column, compounds with higher affinity for the stationary phase are retained longer in the column while those with higher affinity for the mobile phase elutes first. Longer columns generally offer better separation of components [210].

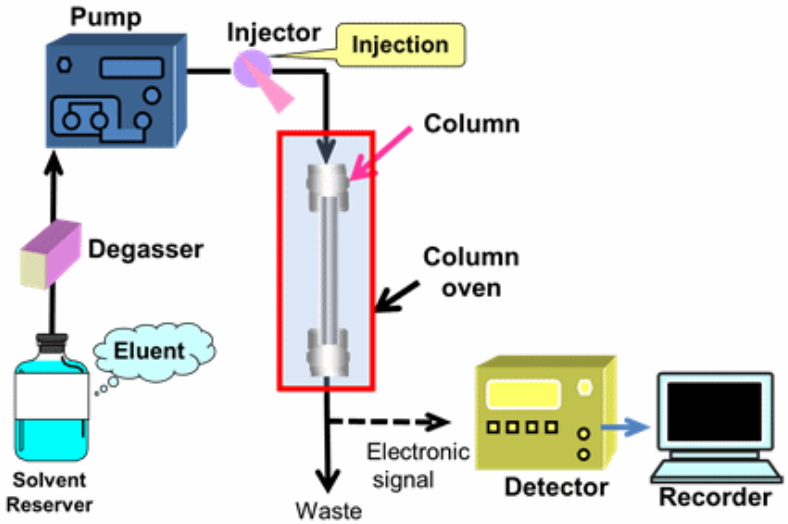

Figure 3.6: *Components of an HPLC system* [210].

There are several detectors for HPLC: UV-visible, florescence, refractive index (RI) detectors, etc. The RI detector, which continuously measures the refractive index of the effluent against a reference was used in this work. The response is proportional to the difference in RI between the reference solvent and compound eluting and its concentration. This response is digitally amplified and sent to a data system where it is recorded as the chromatogram. RI detection is a versatile detection method that can detect almost any sample components that have a different refractive index from the mobile phase. It is the standard detection method commonly employed for sugars analysis [211].

Analysis procedure

In this work, selected liquid products synthesised using water as liquefaction solvent were analysed for sugars using a Waters HPLC system furnished with an Aminex 87H column, and a RI detector for quantification. The Aminex HPX-87H HPLC column is ideal for the analysis of carbohydrates in solution with carboxylic acids, volatile fatty acids, etc. while the RI detector is a standard detection method widely used for analysing sugars. Prior to analysis, the sample was diluted to 1:40 with water; 20 µL of the sample was injected using 5 mM H_2SO_4 as solvent with a flow rate of 0.6 mL/min. The column and detector temperatures were 60 ºC and 30 ºC respectively. The concentration of each product was calculated in grams per litre of liquefaction solvent by calibration with standards of known concentration as explained in Section 3.5.5.

3.5.5 Analyte quantification

The quantification of compounds analysed via GCMS and HPLC methods was achieved by calibration. This involves the analysis of calibration standards (high purity compounds, usually ≥ 99 %) of pre-determined concentrations using the same method used for the analysis of reaction products. For instance, the quantification of phenol via GCMS was conducted as follows.

Five distinct concentrations of phenol (0.2, 0.4, 0.6, 0.8, and 1.0 mg/mL) were made from concentrated phenol (≥ 99 %) using distilled water, after which 1500 µL of each solution was introduced into separate autosampler vials. 1 µL of internal standard (propylene glycol) was dispensed into each of the vials and shaken to homogenize. The samples were

analysed using the method in Table 3.3 with an injection volume of 0.5 µL. An example of the chromatogram and the plot of peak area ratio (*i.e.* ratio of the analyte to internal standard) as a function of concentration are presented in Figures 3.7 and 3.8 respectively.

The concentration, "X" of phenol in a reaction product was subsequently calculated by determining the corresponding concentration of its peak area ratio "Y" from the equation of the calibration line as illustrated in Figure 3.8. Concentrations of chemical compounds obtained in this work were expressed in grams per litre of the liquid product obtained after liquefaction.

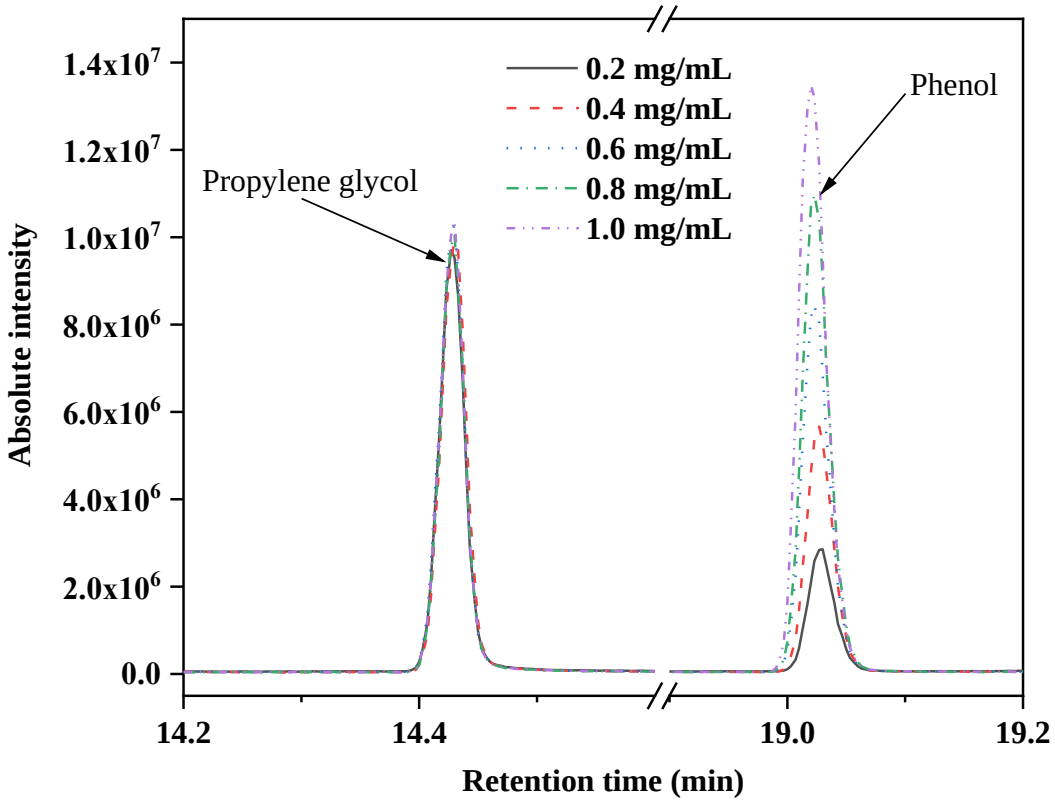

Figure 3.7: *Sample GCMS chromatogram for phenol calibration showing various concentrations of phenol with a fixed amount of propylene glycol (1 µL per 1500 µL of analyte solution) as an internal standard. Injection volume = 0.5 µL.*

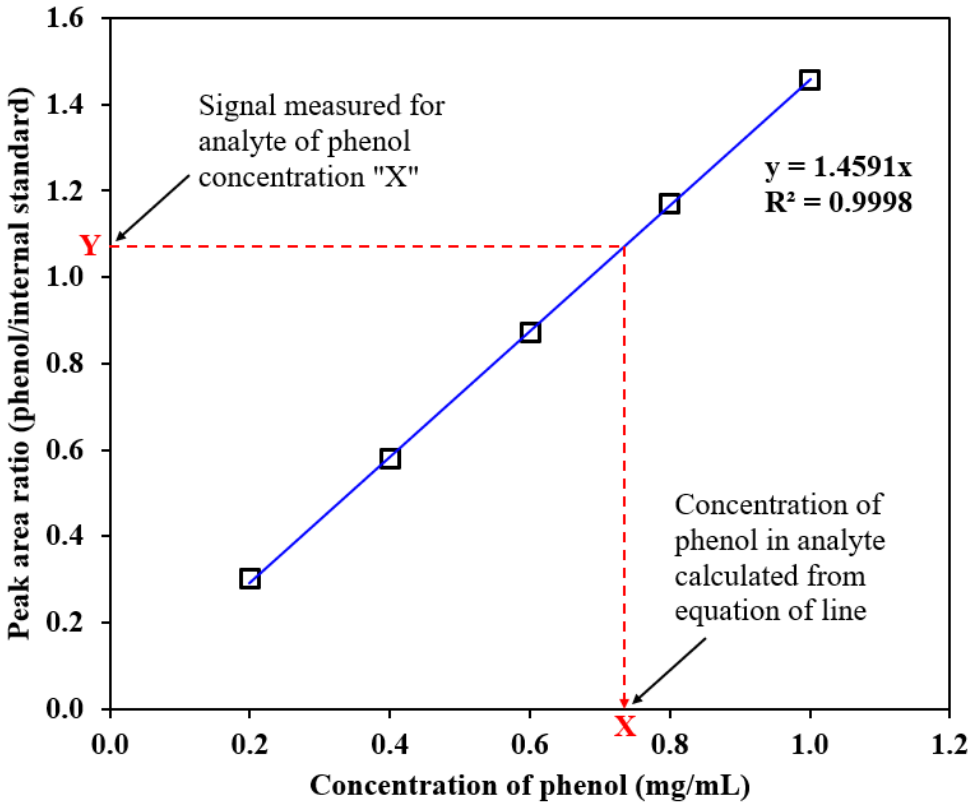

Figure 3.8: *A sample calibration curve (for phenol) via GCMS analysis.*

3.5.6 Analysis of solid residue (bio-char)

The dried bio-chars were analysed using an FTIR spectroscopy. A Shimadzu IRAffinity-1S FTIR spectrometer was employed for the functional group and general chemical structure analysis of the bio-chars via transmission. 1 wt.% of samples in KBr (FTIR grade) were made into thin pellets (120 – 150 mg) and scanned 32 times using the Harp-Genzel method within 400 – 4000 cm^{-1} of wavelength at a resolution of 4. The bio-chars obtained from the reactions were in the form of powders and hence analysed as obtained without further size reduction.

3.5.7 Conversion calculations

In this work, Biomass (BM) conversion is considered as the dry weight of biomass transformed into liquid product. It is calculated based on the weight of biomass introduced into the reactor, using equation 3.14. The conversions of glycerol (G), ethylene glycol (EG) and acetone (A) used as liquefaction solvents were, however, determined via GCMS

analysis using equations 3.15 to 3.17 respectively. Where, initial conc. and final conc. correspond to initial and final concentrations at the start and end of the reaction.

$$\text{BM conversion (wt.\%)} = \frac{\text{mass of dried BM introduced} - \text{mass of dried solid residue}}{\text{mass of BM introduced}} \times 100 \quad (3.14)$$

$$\text{G conversion (wt.\%)} = \frac{\text{initial conc. of G} - \text{final conc. of G}}{\text{initial conc. of G}} \times 100 \quad (3.15)$$

$$\text{EG conversion (wt.\%)} = \frac{\text{initial conc. of EG} - \text{final conc. of EG}}{\text{initial conc. of EG}} \times 100 \quad (3.16)$$

$$\text{A conversion (wt.\%)} = \frac{\text{initial conc. of A} - \text{final conc. of A}}{\text{initial conc. of A}} \times 100 \quad (3.17)$$

3.6 X-ray fluorescence (XRF) spectrometry

XRF spectroscopy is a routine, and relatively non-destructive analytical technique used to determine the chemical (elemental) composition of various materials; solids, powders and liquids. The XRF method hinges on basic principles involving interactions between electron beams and X-rays with samples. XRF analysers determine the chemistry of a material by measuring the fluorescent (or secondary) X-ray emitted from the material when it is excited by a primary X-ray source. Each of the elements present in the sample produces a set of characteristic fluorescent X-rays ("a fingerprint") that is unique for that specific element [212]. XRF spectroscopy is applicable for qualitative and quantitative analysis of the material's composition.

The material is normally irradiated with high energy X-rays from a controlled X-ray tube. When an atom in the sample is struck with an X-ray of enough energy (greater than the atom's K or L shell binding energy), an electron from one of the atom's inner orbital shells is dislodged. The atom regains stability, filling the vacancy left in the inner orbital shell with an electron from one of the atom's higher energy orbital shells. The electron

drops to the lower energy state by releasing a fluorescent X-ray. The energy of this X-ray is equal to the specific difference in energy between two quantum states of the electron. The measurement of this energy is the basis of XRF analysis [212]. Further information on the fundamentals of XRF has been provided by Brouwer [213].

The PANanalytical MagiX Pro X-ray fluorescence spectrometer was employed for the characterisation of the bio-chars and ash used in Chapter 7 of this work. The analysis was externally conducted at the Materials and Engineering Research Institute of Sheffield Hallam University, Sheffield. The samples (0.1 g each) were mixed with cellulose binder (approx. 20 wt.%) and then compacted at 20 tons in a Restch PP40 hydraulic press to form pellets. The pellets were then loaded into the XRF spectrometer so that the XRF spectra could be collected. The instrument uses a rhodium anode for the X-ray source. The emitted X-rays for elements lighter than sodium are too weak to be easily detected by XRF. The cellulose binder is composed of carbon, hydrogen and oxygen so it does not contribute significantly to the XRF spectra produced. XRF data for weight percentage concentration was analysed using the "IQ+" software; the results are given as oxides.

3.7 Reproducibility check

Where necessary, the experiments were conducted at least in triplicate (unless otherwise stated) and the standard deviation (equation 3.18) and experimental errors (equation 3.19) were calculated and used to check the reproducibility of such experimental data. Error bars on graphs were also plotted using the standard deviation to display the variability among replicates. The standard deviation shows the dispersion of individual data about the average. Thus, a low standard deviation signifies less variability while high standard deviation indicates more spread out of data [214].

$$S = \sqrt{\frac{\sum_{i=1}^{n}(X_i - \bar{X})}{n-1}} \tag{3.18}$$

$$\text{E (\%)} = \frac{S}{\bar{X}} \times 100 \tag{3.19}$$

Where,

S is sample standard deviation, X_i is individual measurement; $\bar{X}$ is the sample mean; n is the number of measurements, and E is the percentage reproducibility error.

Chapter 4:

Comprehensive biomass feedstock characterisation

CHAPTER 4: COMPREHENSIVE BIOMASS FEEDSTOCK CHARACTERISATION

4.1 Introduction

As alluded to earlier in Chapter 2 (Section 2.2), biomass materials can vary greatly in composition depending on their type, and source [10,42,184,190]. Hence, it is essential to conduct an adequate analysis of such materials prior to their application in any process to ascertain their suitability for the proposed goal. For example, high fixed carbon content favours the formation of char while high volatile matter content is favourable for the production of liquid and gaseous products [42,190,215]. Environmental and process safety is another important area that cannot be compromised therefore, it is also crucial to evaluate the feedstock in terms of potential technical problems like reactor slagging and environmental pollution from elements such as sulphur and nitrogen [216].

A thorough feedstock characterisation was thus conducted on both pine needles and sugarcane bagasse to determine their physical, chemical and thermal properties prior to their application in the reaction studies in the ensuing chapters. A range of analytical techniques (thermal, spectroscopy, and chromatography), standardised procedures (ASTM and NREL) and adapted protocols from the literature were employed in this study. Section 4.2 gives a summary of the procedures used for the analysis of each parameter, while the results are discussed in Section 4.3.

The thermochemical properties of both feedstocks were first considered in Section 4.3.1. This includes a study of the general thermo-degradation characteristics and proximate composition of the biomasses. Proximate analysis was conducted via a developed TGA method alongside a conventional non-instrumental (manual) method. Both methods are commonly but separately applied, hence the need to compare and know the variation of the outcome between these two methods with respect to the feedstocks under consideration. The results of both methods with respect to pine needles and sugarcane bagasse are compared in Section 4.3.1.2 while detailed interpretations of the proximate composition of the biomass materials are provided in Section 4.3.1.3. Section 4.3.2 explores the structural chemistry and elemental (CHNSO) composition of the feedstocks. Lastly, the non-structural solvent-extractable and structural bio-polymer constituents of the biomass feedstocks are discussed in Section 4.3.3.

All characterisation techniques were applied to dried biomass only (as used for liquefaction experiments) except for proximate analysis under manual method where both dried and wet (as received) were utilised.

4.2 Methods

Procedures for the preparation of biomass feedstocks (pine needles and sugarcane bagasse) prior to any analysis are specified in Section 3.3. Commercial cellulose and lignin, on the other hand, were used as received unless otherwise stated. The thermo-degradation profiles of the biomass materials were studied via TGA using a method adapted from the ASTM E1131 – 08 general technique for compositional analysis of solids and liquids (Section 3.4.1). This was followed by proximate analysis (moisture, volatile matter, ash, and fixed carbon constituents) using the conventional ASTM E870 – 82 non-instrumental methods (Section 3.4.2) and the developed TGA method (Section 3.4.1). FTIR spectroscopy (Section 3.4.3), and elemental analysis (Section 3.4.4) were then used to confirm the lignocellulosic nature of the feedstocks. The elemental analysis is also used to check for levels of any toxic element, particularly sulphur and nitrogen. Section 3.4.5.1 explored the non-structural solvent-soluble component of pine needles and sugarcane bagasse using established NREL methods for the exhaustive determination of extractives in biomass materials. The widely used TAPPI T 222 om-02 method (Section 3.4.5.2) was employed for the quantitative analysis of the lignin content of the biomass materials. Finally, the method used for the estimation of holocellulose constituents (cellulose plus hemicellulose) is explained in Section 3.4.5.2. Where necessary, commercial cellulose and lignin were used as reference materials to facilitate a better understanding of the nature of the biomass feedstocks. Each parameter was determined in triplicate (except where stated) and the mean values reported.

4.3 Results and discussion

4.3.1 Thermochemical characteristics

4.3.1.1 Thermal degradation characteristics

The thermal degradation of commercial cellulose and lignin, as well as 1:1 (wt:wt) mixture of cellulose and lignin, were studied by TGA to understand the decomposition profile of the lignocellulosic biomass feedstocks. The commercial cellulose-lignin mixture was intended to imitate and understand the behaviour of the naturally occurring lignocellulose materials. The results obtained are shown in Figure 4.1 with key highlights in Tables 4.1 and 4.2.

The DTG graphs (Figure 4.1b) show no clear-cut distinction between the degradation temperatures of lignin and cellulose, especially when mixed together. However, the decomposition of cellulose was rapid with major weight loss occurring between 280 – 400 °C. The maximum rate of loss was ~44.5 wt.%/min at 358 °C with no residue at 900 °C prior to combustion. Lignin degradation, on the other hand, was gradual, occurring mainly between 188 - 600 °C with a maximum loss rate of ~4.8 wt.%/min at 325 °C. Such slow thermal decomposition is attributed to the various oxygen functional groups from its structure which have different thermal stabilities, their scission occurring at different temperatures [188]. Lignin was moreover found to possess a high non-oxidisable residue (ash) of ~13.7 wt.% after combustion at 950 °C. Again, the mixture of cellulose and lignin did not indicate any distinct trend for either component but rather exhibited an overlapping intermediate profile between cellulose and lignin as reported elsewhere [182]. Decomposition of the cellulose-lignin mix was within 265 – 420 °C temperature range, recording a moderate loss rate of ~15.8 wt.%/min at 373 °C and a residue of ~5.9 wt.% after combustion at 950 °C. This leftover is the ash content of lignin.

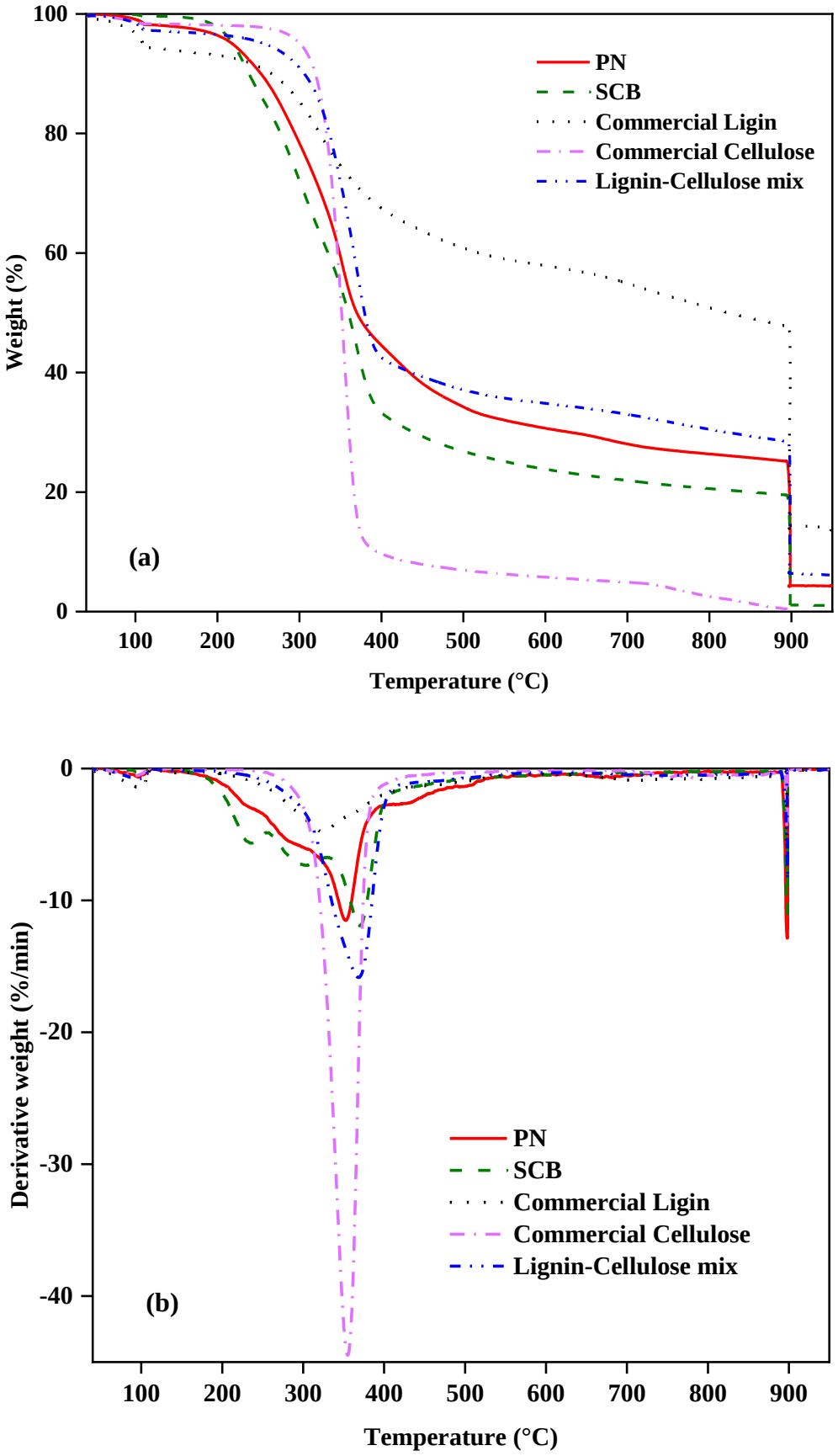

Figure 4.1: *TG (a) and DTG (b) curves at 20 °C/min heating rate for dried pine needles (PN) and sugarcane bagasse (SCB), compared with commercial lignin, commercial cellulose, and a 1:1 (wt:wt) mixture of commercial cellulose and lignin.*

Table 4.1: *Degradation profile of cellulose, lignin, sugarcane bagasse, and pine needles.*

Sample	Decomposition range (°C)	Temp. of max. mass loss (°C)	Max. mass loss rate (wt.%/min)
Cellulose	280 - 400	358	44.5
Lignin	188 - 600	325	4.8
Cellulose-lignin mixture (1:1 wt.)	265 - 420	373	15.8
Pine needles	160 - 600	346	11.5
Sugarcane bagasse	160 - 600	346	16.0

Pine needles and sugarcane bagasse display thermal degradation profiles that are intermediate between pure lignin and cellulose, similar to that of the physical cellulose-lignin mixture (Figure 4.1a). Such similarity is a good indication of the presence of cellulose-lignin polymer mixtures in these feedstocks as shown by the FTIR analysis in Section 4.3.2.1. Both feedstocks comparatively show the same trend of decomposition especially in terms of the range and maximum temperatures of decomposition which was mainly 160 – 600 °C and 346 °C (Figure 4.1b and Table 4.1). The range of degradation also gives a clue to the temperature range within which these materials could undergo effective decomposition when applied in thermal or thermo-chemical reaction processes. The recorded degradation onset temperature of 160 °C is in good agreement with a claim by Demirbas [34] that lignocellulose degradation could not occur below 157 °C. Hence the batch liquefaction reaction studies carried out in the ensuing chapters were limited to a minimum temperature of 160 °C. A more detailed look at Figure 4.1a shows that the decomposition profile of sugarcane bagasse is more comparable with cellulose while that of pine needles is more comparable with lignin; this may be due to the higher cellulose content of bagasse compared to pine needles (Table 4.9). The earlier onset of degradation of both lignocellulose materials is due to the presence of high to moderate volatile compounds, also known as extractives, which were not removed beforehand. This was confirmed by later characterisation steps in this work and discussed in Section 4.3.3 (Figure 4.7).

Slight disparities between pine needles and sugarcane bagasse are nonetheless obvious in the rate of mass loss and residue contents: bagasse recorded a slightly higher maximum loss rate of 16 %/min and 1 wt.% residue while pine needles had a maximum loss of

~11 %/min and ~4 wt.% residue. The higher non-combustible composition and lower mass-loss rate of pine needles compared to bagasse could be attributed to the higher fraction of lignin (the most stable component) in pine needles (28 – 43 %) [39,170,172] compared to that of sugarcane bagasse (20 – 23 %) [217,218]. Further differences are noticeable between the DTG curves of both feedstocks, with pine needles showing several shoulder peaks. The peak at 235 ℃ (also present in bagasse) is due to the loss of extractives as confirmed later in Section 4.3.3.1 (Figure 4.7). Peaks at 286 ^{o}C (pine needles) and 296 °C (for bagasse) might be a result of hemicellulose decomposition which is normally reported to occur within the range of 200 - 350 °C [184,219,220]; a study conducted by Yang *et al*. [221] using pure hemicellulose confirms the degradation range of 220 – 315 °C. The fact that these peaks are found in both extracted and non-extracted biomasses but not found on the thermograms of pure cellulose and lignin further confirms this assertion, Figures 4.1b, 4.7b, and 4.7d. The main decomposition peaks at 346 °C are mostly assigned to cellulose, with temperature ranges of approximately 315 - 400 °C [219,220]. This may, however, include a substantial amount of lignin as confirmed by the DTG curve of the cellulose-lignin mixture in Figure 4.1b. The last shoulder peak at 422 °C of pine needles may be due to an overlying degradation of lignin [182]. Finally, the mass loss at 900 °C, is a result of fixed carbon combustion when nitrogen was replaced with air. At this stage, fixed carbon is decomposed into mainly H_2O and CO_2.

Table 4.2 summarises the deductions made from the thermal degradation study of pine needles and sugarcane bagasse. However, in agreement with the general observation by other researchers [182,219,220], the decomposition of hemicellulose, cellulose, and lignin takes place in relatively close temperature ranges, which partially overlap with no absolute distinction of which thermal feature corresponds to each component.

Table 4.2: *Shoulder peaks from the DTG curves of pine needles and sugarcane bagasse along with assigned components.*

Shoulder peak (°C)		**Assignment**
Pine needles	**Sugarcane bagasse**	
100	100	Moisture
235	235	Extractives
286	296	Hemicellulose
346	346	Cellulose, lignin
422	-	Lignin
900	900	Fixed carbon

4.3.1.2 Proximate analysis methods compared: manual versus TGA

Differences in composition and characteristics of even the same type of biomass material grown in distinct geographical areas are typical [169,185] yet one cannot underestimate the contribution of the variance in analytical methodologies to the inconsistencies in values reported in the literature. Hence, a brief comparative study was conducted on the proximate composition of pine needles and sugarcane bagasse obtained by the developed TGA program and the standard manual methods commonly used in literature to serve as a guide for the selection of either method in future works. The focus of this section is not to develop an optimised TGA method that gives the same proximate analysis results as the manual procedure but rather to investigate the possibility of using sole TGA method for proximate analysis of these feedstocks in the future with confidence. Only a few attempts to compare developed TG proximate analysis methods with conventional manual methods are reported in the literature; these are for municipal solid waste [186], livestock manure [222] and a small number of other types of biomass [187]. However, there is no mention of such a comparison for pine needles and sugarcane bagasse.

A minimum of 9 and 3 replicates of pre-dried samples (as used for reaction studies) were utilised for manual and TG analysis respectively at three different times. Graphical results of the proximate compositions obtained via TGA versus manual methods are presented in Figure 4.2 while the specific values along with the corresponding experimental errors are presented in Appendix B (Tables B1-a and B1-b.) Overall, the standard deviation (bars) and error calculations illustrate very good data reproducibility in both procedures with standard deviations ≤ 0.38 for the TGA method and ≤ 0.83 for the manual method. This shows an improvement over similar work conducted by Cantrell *et al.* [222] on livestock manure where standard deviations as high as 9.97 for TGA and 6.15 for manual (ASTM D3174-04) method were recorded.

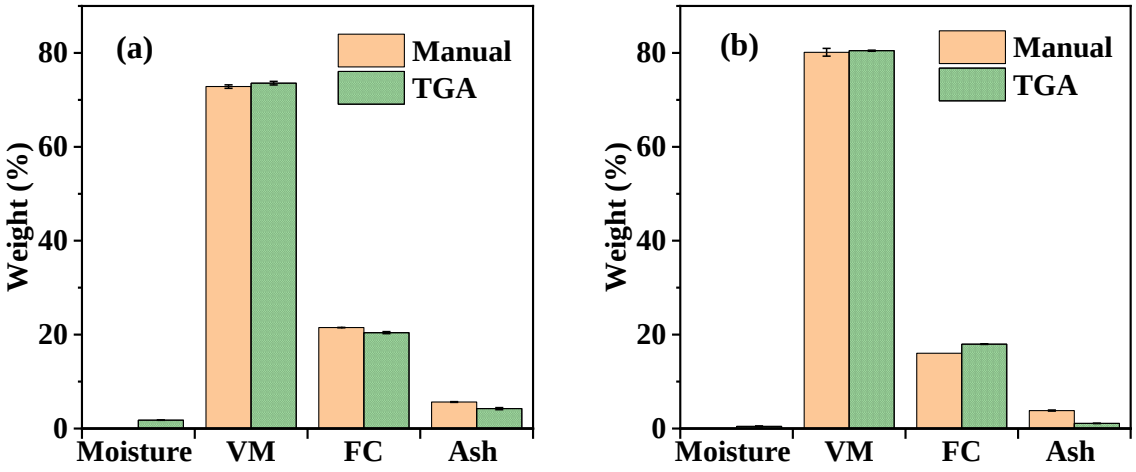

Figure 4.2: *Proximate analysis results for dried (a) pine needles and (b) sugarcane bagasse obtained via non-instrumental (manual) versus TGA methods. Error bars were plotted from the standard deviation of a minimum of three data sets. Fixed carbon was estimated by subtracting the sum of the average volatile matter, ash and moisture from the average dry weight of biomass in the manual method, hence a standard deviation could not be determined. Note: pine needles and bagasse were dried at 105 °C for 24 h in an air oven prior to analysis. VM = volatile matter, FC = fixed carbon.*

Figure 4.2 clearly demonstrates very similar results for volatile matter content irrespective of the method used: approximately 73 wt.% for pine needles and 80 wt.% for sugarcane bagasse. Minor differences could, however, be noticed in the amounts of fixed carbon, ash, and moisture. Less than 2 wt.% moisture content was detected in the biomass samples during the thermogravimetric analysis of the already dried biomass. This could be residual bound water in the sample due to the difference in particle sizes as well as moisture absorbed during the processing (milling and sieving) of biomass prior to thermogravimetric analysis. The milled samples were not oven-dried again after milling for fear of losing low volatiles. The disagreement in moisture content could also be a result of the difference in process temperature between both methods (Tables 4.3a and 4.3b).

Differences in values for fixed carbon are expected since it is an estimated parameter, particularly in the manual method. Thus, the discrepancies in ash and moisture contents as observed in this case results in a discrepancy in fixed carbon content. The maximum difference between techniques occurs in the ash content of sugarcane bagasse where the value obtained by the manual method to that obtained by TGA is approx. 3.5. The higher ash content observed under the manual method could be attributed to the lower

combustion temperature (580 °C for manual against 950 °C for TGA) leading to incomplete combustion of volatile matter and fixed carbon. Absorbed moisture during cooling and weighing of the sample may also be responsible for such observed higher ash content under the manual method though all efforts were made to minimise exposure of the sample to the atmosphere by cooling samples in a desiccator close to the weighing balance. The hypothesis of incomplete combustion was investigated by testing for the presence of C, H, N, and S in the manual ash samples (according to Section 3.4.4). Indeed, a weight reduction of 5.3 and 5.8 percentages were observed for ashes from pine needles and sugarcane bagasse respectively due to the presence of C, and H. Meanwhile, N and S were not detected in either ash.

The standard deviations for volatile content measurements in both methods are relatively high (0.12 – 0.83) compared to those obtained for the other components (0.02 – 0.22). This agrees with findings by Velázquez-Martí *et al.* [191] in a similar study conducted on the various mixtures of wood and leaves of *Euphorbia lancifolia*. Velázquez-Martí *et al.* documented maximum standard deviations of 3.69 and 2.14 for volatile contents measured by TGA and manual methods respectively whereas those for ash contents measurements were respectively 2.91 and 0.18. Apart from the moisture content determination of sugarcane bagasse via TGA, the experimental error calculations rather display a generally higher experimental error margin for ash content over volatile matter in agreement with recent findings by Garcia *et al*. [187] where an average experimental errors of 49.4 % and 5.8 % were reported for ash and volatile matter respectively for 13 biomass materials. Nonetheless, the higher experimental errors could be a consequence of the low ash content of the studied materials. Thus, small numerical differences in replica measurements would result in high experimental errors. The same thing could be said about the moisture content of dried sugarcane bagasse, which recorded the highest experimental error of ~16.6 %. Furthermore, the differences in ash and moisture content for the same material studied under the two methods indicate that variations in proximate compositions reported in the literature for the same type of biomass could not entirely be ascribed to natural differences but also to the disparities in the methods of investigation. Some notable advantages of the TGA method over the manual method include the fact that:

1. It is quick, taking less than 2 hours to obtain the full proximate composition of a feedstock, whereas the manual method takes up to 3 days as established in

Tables 4.3a and 4.3b. However, depending on the size of the furnace, one could do multiple samples in one batch via the manual method while the TGA could only handle a sample at a time.

2. It is safer in terms of physical risk (*i.e.* burns), as one has to handle very hot samples at about 950 °C.
3. The TGA is also more reliable in terms of data reproducibility, while the manual method demands lots of effort and a high level of accuracy to obtain reproducible consistent values.
4. The TGA also minimises the amount of sample needed for the experiment. Thus 5-10 mg for TGA versus ≥ 4000 mg for the manual procedure.

Apart from the minor differences in ash and moisture contents between both methods due to the reasons discussed above, the results obtained from both manual and TGA methods were found to be comparable, and satisfactory when equated to literature figures (Tables 4.4a and 4.4b). Consequently, either method could be applied in the future for the studied feedstocks with attention on ash content. However, a comparative study for a wider range of biomass materials is still vital.

Table 4.3a: *Summary of the manual method (ASTM E870 – 82) used for proximate analysis of the biomass materials.*

	Sample size per analysis, particle size	**Temperature, hold time**	**Total time (heating + hold time)**	**Cooling time**
Moisture	1000 mg min, ≥ 1000 µm	20 - 105 °C @ 10 °C/min, 10 mins	16 - 24 h	4 h
Volatile matter	1000 mg, 500 - 1000 µm	950 °C, 7 min	1.7 h	18 h
Fixed carbon	-	-	-	-
Ash	2000 mg, 200 – 500 µm	20 - 580 °C @ 10 °C/min, 30 min (3x).	2.4 h	17 h
Total per experiment/batch	***3000 mg***		***24.1 – 28.1 h***	***39 h***

Table 4.3b: *Summary of the TGA method used for proximate analysis of the biomass materials.*

	Sample size per analysis, particle size	**Temperature, hold time**	**Total time (heating + hold time)**	**Cooling time**
Moisture	5 - 10 mg, 200 - 500 µm	40 – 110 °C @ 20 °C/min, 10 mins	0.2 h	
Volatile matter	-	110 - 900 °C @ 20 °C/min, 10 mins	0.8 h	
Fixed carbon	-	-	-	
Ash	-	900 - 950 °C @ 20 °C/min, 50 mins	0.4 h	
Total per experiment/batch	***5 - 10 mg***		***1.4 h***	***0.5 h***

Note: Cooling time is time taken to cool the equipment (furnace, oven or TGA) in between experiments or batches.

4.3.1.3 Proximate composition

Figure 4.3 compares the proximate compositions of dried pine needles and sugarcane bagasse to commercial cellulose and lignin, whereas Tables 4.4a and 4.4b show how the proximate compositions of dried and "as received" pine needles and sugarcane bagasse compare with others reported in literature.

Moisture content: Pine needles and sugarcane bagasse respectively possess 12 wt.% and 87 wt.% moisture as received (Tables 4.4a and 4.4b). Biomass materials with > 40 wt.% are best converted via liquefaction to avoid an energy intensive drying process [96]. However, to establish a uniform basis of comparison, both biomasses were dried at 105 °C (Section 3.3) prior to liquefaction. TG analysis of these samples revealed residual moisture compositions of ~1.8 wt.% and ~0.5 wt.% correspondingly at 110 °C (Figure 4.3). This difference was anticipated considering the temperature difference of 5 °C between the two methods. Biomass feedstocks with moisture content above 10 wt.% are normally considered unsuitable for combustion and pyrolysis processes as it reduces the heating value and affects process temperatures as well as decreases the quality of the end products [42,215]. This is however not a problem in liquefaction processes where solvents, especially water is used as liquefaction agents.

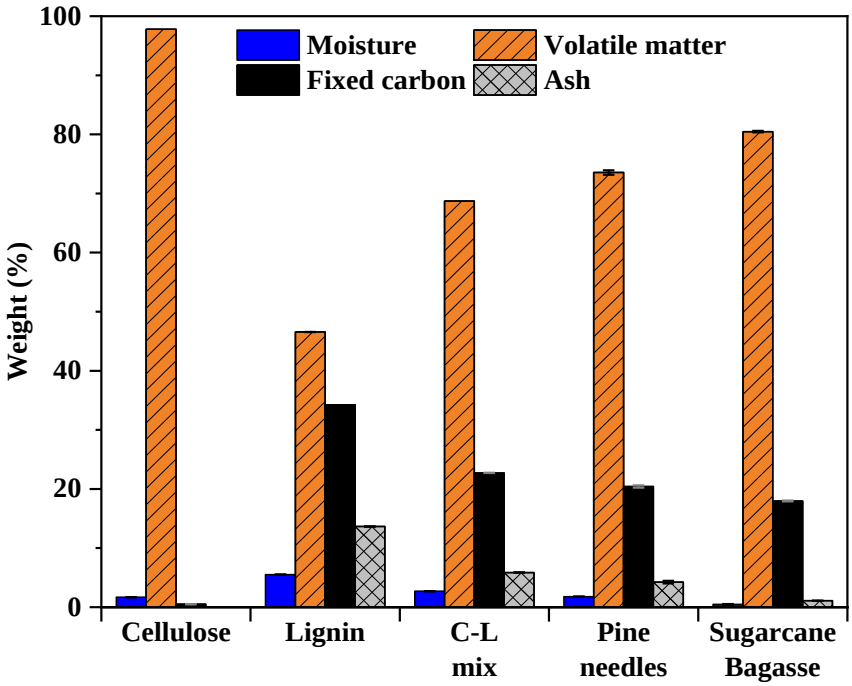

Figure 4.3: *Proximate composition in wt.% (TGA method) of dried pine needles and sugarcane bagasse compared with commercial cellulose, lignin and a 1:1 weight mixture of cellulose and lignin (i.e. C-L mix). Pine needles and bagasse were dried at 105 °C for 24 h in an air oven prior to analysis. Error bars invisible where standard deviations are zero.*

Table 4.4a: *Proximate composition of pine needles compared with others investigated in the literature.*

	As received				**Dry weight basis**		
	This work*	Ref [169]	Ref [169]	Ref [169]	**This work***	Ref [223]	Ref [224]
Moisture	**11.75**	10.20	11.60	21.50			
Volatile matter	**64.28**	73.10	68.40	58.30	**72.83**	74.19	81.90
Fixed carbon	**18.99**	14.60	17.90	17.10	**21.52**	24.07	14.54
Ash	**4.98**	2.10	2.10	3.10	**5.64**	1.74	3.56

** determined via manual method (ASTM E870 – 82).*

Table 4.4b: *Proximate composition of sugarcane bagasse compared with others investigated in the literature.*

	As received			**Dry weight basis**			
	This work*	Ref [225]	Ref [183]	**This work***	Ref [185]	Ref [185]	Ref [225]
Moisture	**86.90**	51.01	13.20				
Volatile matter	**10.50**	40.99	71.00	**80.13**	81.50	71.60	83.66
Fixed carbon	**2.10**	6.44	13.80	**16.04**	13.30	15.80	13.15
Ash	**0.50**	1.57	2.10	**3.83**	5.20	12.60	3.20

** determined via manual method (ASTM E870 – 82).*

Volatile matter and fixed carbon content: Biomass generally possess higher amounts of volatile matter and lower fixed carbon compositions than coal on a dry weight basis [226]. The high volatile matter content of biomass, typically 65 – 85 wt.% [42,226] enhances fuel reactivity [190,215] whereas a high fixed carbon constituent promotes char production [215]; as such, feedstocks with high volatile content are more desirable for thermochemical conversion processes. In this study, both dry pine needles and bagasse contain high volatile matter (73 - 80 wt.%) and low fixed carbon (16 - 22 wt.%) consistent with literature irrespective of the method used, as shown in Tables 4.4a and 4.4b. Such high volatile matter compositions are positive indications that these feedstocks are good for chemical synthesis via thermo-chemical and hence liquefaction processes with potentially high conversions. The higher volatile composition of sugarcane bagasse (80 wt.%) over pine needles (~73 wt.%) could be attributed to its higher content of cellulose. It is clear from Figure 4.3 that pure cellulose contains ~98 wt.% volatile matter, which is about twice the quantity of volatiles in lignin, ~47 wt.%. Pine needles nonetheless under the same condition has almost a quarter more of the amount of fixed carbon in bagasse, which could be related to the higher lignin content of pine needles [227] as established in Section 4.3.3.2 (Table 4.9). The proximate compositions of both feedstocks are much comparable to that of the cellulose-lignin mixture, indicating that these materials are lignocellulosic in nature.

Ash content: Ash is the non-oxidisable, mineral constituent of biomass, composed of various minerals such as potassium and calcium [228]. Ash contents of the real biomasses obtained via TGA are lower than those obtained via the manual method. This is attributable to differences in the program temperatures. Hence, dry bagasse and pine needles recorded 1.1 wt.% and 4.2 wt.% via TGA against 3.8 wt.% and 5.6 wt.% via the manual method in that order. Nevertheless, all these values agree with works done by other researchers (Table 4.5), except the manual ash constituent of pine needles, which is almost a third higher than the ash content observed by Varma and Mondal [224]. High biomass ash content (> 30 wt.% [42]) is normally said to be detrimental, causing operational problems during thermochemical conversion processes, such as slagging in combustion [226]. Nonetheless, the presence of ash in biomass feedstocks could be advantageous in certain processes. For example, a study conducted by Feng and his co-workers [229] on the effects of ash content on the hydrothermal liquefaction of barks concluded that the K and Ca compounds in bark ash catalyse bark conversion into bio-

crude oil. Besides, this thesis (Chapter 7) has demonstrated that the ash content of pine needles is catalytically active during liquefaction; leading to the simultaneous conversion of liquefaction solvent to value-added chemicals.

4.3.2 Structural chemistry and elemental composition

4.3.2.1 Structural chemistry (FTIR analysis)

The FTIR spectra of pine needles, sugarcane bagasse, commercial cellulose, and lignin are presented in Figure 4.4 with detailed band assignments for functional groups shown in Table 4.5.

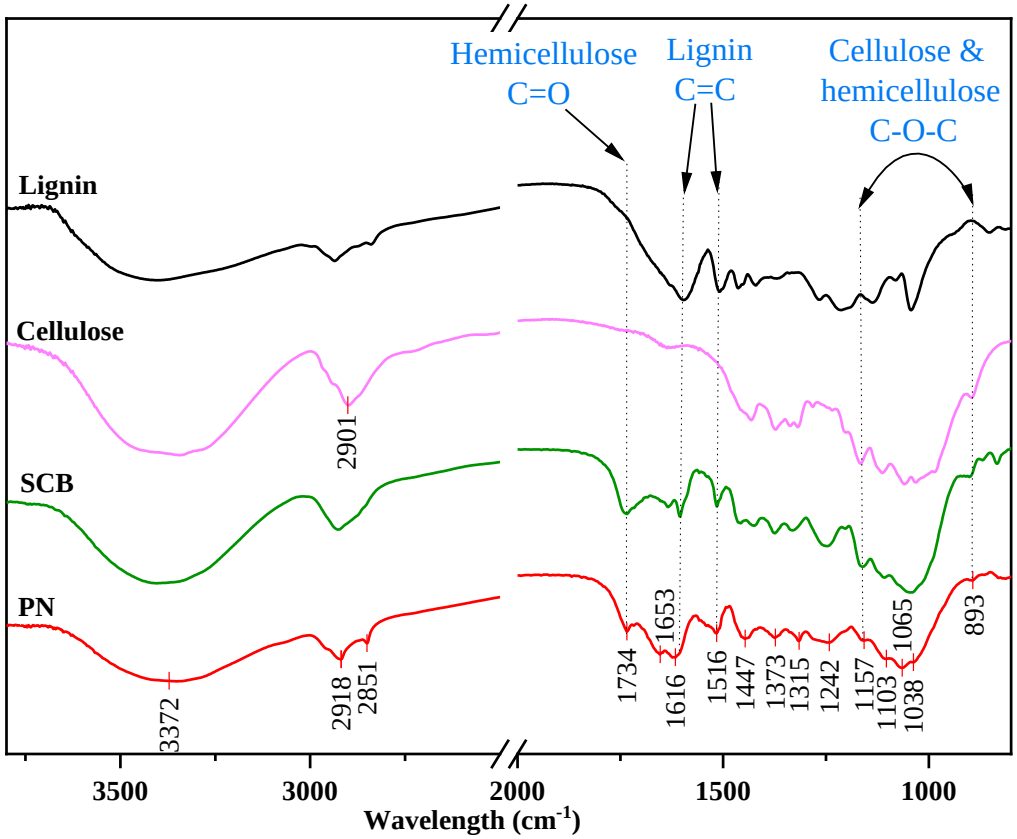

Figure 4.4: *FTIR spectra of dried pine needles and sugarcane bagasse compared with commercial cellulose and lignin. Annotations designate key characteristic bands of hemicellulose, lignin, and cellulose.*

Table 4.5: *Functional groups and equivalent wave numbers from FTIR spectra (Figure 4.4) of pine needles and sugarcane bagasse.*

Wave No. (cm^{-1})	**Assignment**
3372	Broad peak attributed to the stretching of in hydroxyl (O-H) bonds in phenolic and aliphatic groups of lignin (p-coumaryl alcohol, coniferyl alcohol, and sinapyl alcohol) [230–236] as well as the intermolecular O-H stretchings and hydroxyl groups of the sugars units in cellulose and hemicellulose [237–240].
2918; 2851; 2901	C-H vibrations of glucose unit in cellulose. [237–240] C–H stretching in methyl and methylene groups of the side chains of lignin monomeric units [230,232–236]. C-H stretching in aromatic methoxy groups of lignin monomers [230,232,233].
1734	C=O stretching, a characteristic of uronic ester groups of hemicellulose or hemicellulose–lignin complexes (the ester linkage of the carboxylic group of ferulic and p-coumaric acids in hemicelluloses) [235,238,241–243].
1653	H-O-H bending of water [235,238,241].
1616; 1516	C=C vibrations in aromatic skeletons/rings [230,244,245]. Typical characteristic peaks of lignin [240,242,245,246].
1447; 1373	C-H bending in Lignin, cellulose and hemicellulose[233,236,237,246]. 1425 cm^{-1} is also known as the crystallinity band [247].
1315	CH_2 wagging or C-H deformation of cellulose; C–O stretching of syringyl (lignin) derivatives. [234,243,247,248].
1242	Lignin and hemicellulose C–O stretching vibration band [231,247].
1157	C-O-C asymmetric vibration of pyranose ring in cellulose and xylose in hemicellulose[233,234,238,242,249].
1103 - 1038	C-O stretching of the C-O-C in cellulose and hemicellulose [234,235,238,246].
893	C-O-C β-glycosidic linkage between glucose units. Characteristic band of cellulose and hemicellulose [231,237,239,240].

In support of the TGA results, both biomass materials exhibit typical characteristics of lignocellulose as follows: 1734 cm^{-1} corresponds to C=O stretching, a key characteristic of the uronic ester groups of hemicellulose or hemicellulose–lignin complexes (the ester linkage of carboxylic group of ferulic and p-coumaric acids in hemicelluloses) [235,238,241–243]. 1616 cm^{-1} and 1516 cm^{-1} are typically attributed to the C=C vibrations in the aromatic rings of lignin [230,240,242,244–246]. The bands between 1157 – 893 cm^{-1} are usually assigned to C-O and C-O-C vibrations of various cellulose and hemicellulose units. For example, band 893 cm^{-1} is considered a typical characteristic band of cellulose and hemicellulose which represents the C-O-C stretchings of the β-glycosidic linkages between the glucose units [231,237,239,240] whereas, 1157 cm^{-1} is normally assigned to the C-O-C asymmetric vibration of pyranose ring in cellulose and xylose in hemicellulose [233,238,242,249].The O-H (3372 cm^{-1}) and C-H (2851 – 2918 cm^{-1}) peaks for bagasse look more like cellulose while those for pine needles took the form of lignin. This similarly might again be a consequence of the high percentage of lignin in pine needles and vice versa.

4.3.2.2 Elemental composition (CHNSO)

Of importance here are the concentrations of elemental N and S, which are likely to be oxidised to undesirable NOx and SO_2 gases during thermochemical processing of biomass fuels and feedstocks. The S and N contents of the selected lignocelluloses are correspondingly < 0.2 wt.% and <1.5wt.% (Figure 4.5), making these feedstocks safe for thermochemical processes without significant concern about reactor fouling and pollution [42,250].

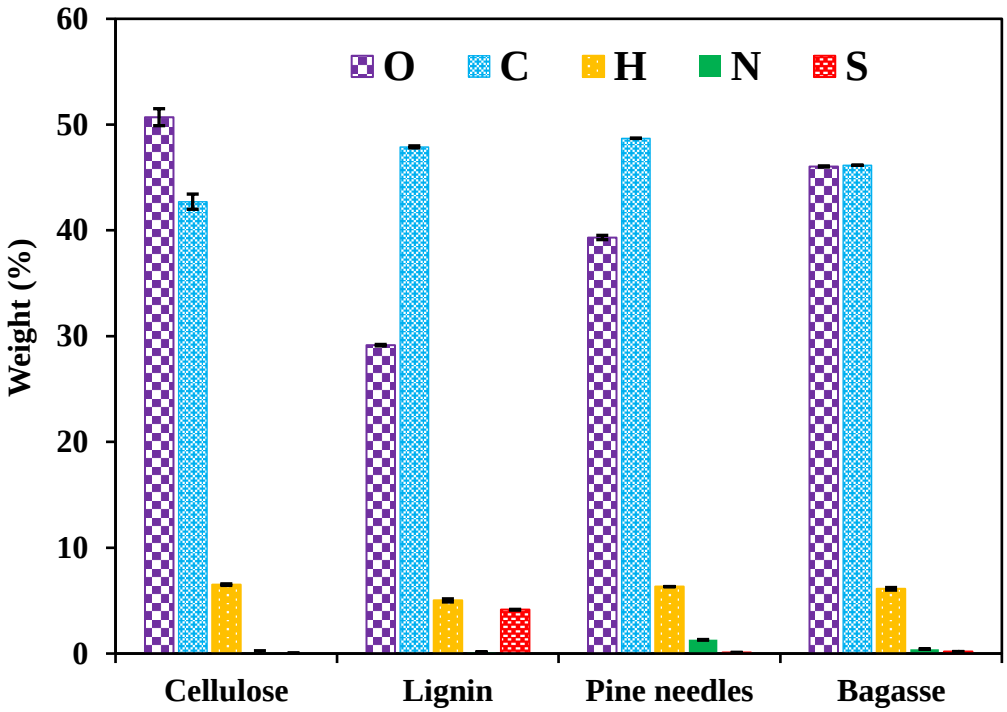

Figure 4.5: *Elemental composition of dried pine needles and bagasse compared with commercial cellulose and lignin. Note: commercial lignin was received with 4 wt.% sulphur content from the supplier.*

The elemental compositions of the chosen biomass wastes could be described as intermediate between pure lignin and cellulose with the composition of bagasse quite similar to cellulose while that of pine needles more like lignin. Specifically, the weight ratio of carbon to oxygen (C/O) for bagasse is ~1, relating to cellulose which is assumed to have an empirical formula of $C_6H_{10}O_5$ (*i.e.* C/O = 0.9) whereas that of pine needles is >1 analogous to lignin, assumed to have an empirical formula of $C_{10.4}H_{12.7}O_{3.4}$ (*i.e.* C/O = 2.3) in the case of softwood lignin [220]. This agrees with the TGA and FTIR data in Figures 4.1 and 4.4 respectively, where the pine needles spectra relate more to lignin and that of sugarcane bagasse is like cellulose. The summary of hemicellulose, cellulose, and lignin contents of pine needles and sugarcane bagasse in Table 4.9 further supports this observation – as the major component of bagasse is cellulose (up to 42 wt.%) [217,218] and that of pine needles is lignin (up to 43 wt.%) [39,170,172]. A literature survey shows that the elemental compositions of both feedstocks largely agree with others documented by other researchers as summarised in Tables 4.6a and 4.6b.

Table 4.6a: *Elemental constituents of dried pine needles compared to others studied in the literature.*

Elements (wt.%)	**This work**	Ref [223]	Ref [169]	Ref [169]	Ref [169]
C	**48.70**	45.81	54.05	53.64	53.36
H	**6.33**	5.38	5.34	5.36	5.91
N	**1.30**	0.98	0.56	0.62	0.61
S	**0.10**	-	0.19	0.20	0.17
O*	**39.33**	46.11	32.58	33.92	31.77
Ash	**4.24****	1.72	2.10	2.10	3.10

** Calculated by difference.*
*** Determined by TGA.*
- Not reported.

Table 4.6b: *Elemental constituents of dried sugarcane bagasse compared to others studied in the literature.*

Elements (wt.%)	**This work**	Ref [223]	Ref [183]	Ref [185]	Ref [185]
C	**46.15**	44.10	51.71	43.79	38.30
H	**6.12**	5.26	5.32	5.96	6.04
N	**0.42**	1.00	0.33	1.69	1.71
S	**0.18**	-	-	-	-
O*	**46.04**	38.54	42.64	43.36	41.35
Ash	**1.09****	11.10	-	5.20	12.60

** Calculated by difference.*
*** Determined by TGA.*
- Not reported.

4.3.3 Extractives and bio-polymer composition

4.3.3.1 Exhaustive extractives constituent

Extractives are the non-structural components of biomass samples that are soluble in water, ethanol or other organic solvents. These extractives are non-chemically bound components of biomass that include sucrose, nitrate/nitrites, protein, ash, chlorophyll, and waxes. These could potentially interfere with the downstream analysis of the biomass sample; particularly the quantification of lignin and structural carbohydrates, hence it is necessary to remove them prior to such analysis. Failure to remove extractable materials may result in, 1) Incorrectly higher amount of lignin due to condensation of unhydrolysed carbohydrates along with acid-insoluble lignin; 2) An error in quantity of structural

carbohydrates. Hydrophobic extractives hinder the penetration of sulfuric acid into the biomass resulting in partial hydrolysis [201].

A two-step thorough extraction process developed by NREL [201] was followed to quantify the amount of water and ethanol extractives in the biomass feedstocks as described in Section 3.4.5.1. Water-soluble materials generally include inorganic materials, non-structural sugars, and nitrogenous material, among others, while ethanol-soluble materials include chlorophyll, waxes, or other minor components. Dry pine needles possess a total of ~34 wt.% extractives: 65 percent water-soluble and 35 percent soluble in ethanol. Sugarcane bagasse, on the other hand, contains ~46 wt.% extractives, of which 66 percent is water-soluble and 34 percent are ethanol-soluble (Table 4.7). The extracts from bagasse and pine needles obtained in this work were analysed via GCMS and the results presented in Tables 4.8a and 4.8b.

Table 4.7: *Percentage of extractives in dried pine needles (Picea abies) and sugarcane bagasse. db = dry biomass.*

	Pine needles	**Sugarcane bagasse**
Water Extractives (wt.% db)	22.00	30.60
Ethanol Extractives (wt.% db)	12.02	15.47
Total	***34.02***	***46.07***

Tables 4.8a and 4.8b, therefore, display the range of volatile compounds identified. Both feedstocks possess a variety of cyclic and straight-chain compounds: carboxylic acids, hexoses, ketones, aldehydes, and aromatics. A total of 13 chemicals were detected in pine needles, of which the water extractives are comprised of C_2 - C_7 compounds while the ethanol extractives are predominantly C_{10} and two C_{12} compounds. Methyl-α-D-mannofuranoside, (~49 %) and 4-hydroxyacetophenone (~27 %) are the major compounds extracted with water from pine needles. The ethanol extractives are largely terpenes as would be expected from a coniferous plant [251]. As such, the main constituent is endo-borneol (~31 %) followed by α-terpineol (~21 %). An identical spectrum of chemicals was extracted from the wood of Scots pine (*Pinus sylvestris*) in the by Salem *et al.* [252] of which borneol was the major constituent (~52 %). Sugarcane bagasse, on the other hand, had a total of 9 C_1 - C_8 extracted compounds: furfural was the only chemical identified in the ethanol extractives while the water extractives are chiefly made up of ~32 % acetic acid and ~19 % 1-hydroxy-2-propanone. The extractable

chemicals found common to both materials are 4-hydroxyacetophenone; acetic acid; and 1-hydroxy-2-propanone.

Table 4.8a: *Chemical composition of extractives from dried pine needles (Picea abies).*

Compound	Common name	No. of Carbon	Area (%)
Water extractives			
Acetic acid	Acetic acid	C_2	7.93
1-hydroxy-2-propanone	Acetol, or Hydroxyacetone	C_3	8.25
4-hydroxyacetophenone	Piceol	C_8	26.83
1,6-anhydro-β-D-glucopyranose	Levoglucosan	C_6	7.60
Methyl-α-D-mannofuranoside	-	C_7	49.39
Ethanol extractives			
Camphor	-	C_{10}	5.52
2,3,3-trimethyl-bicyclo[2.2.1]heptan-2-ol	Camphene hydrate	C_{10}	5.17
Endo-borneol	-	C_{10}	30.58
l-α-terpineol	α-Terpieol	C_{10}	20.56
3-methyl-6-(1-methylethyl)-2-cyclohexen-1-one	Piperitone	C_{10}	11.15
9-methyl-bicyclo[3.3.1]non-2-en-9-ol	-	C_{10}	9.68
Bornyl acetate	-	C_{12}	9.61
9,10-dimethyltricyclo[4.2.1.1(2,5)]decane-9,10-diol	-	C_{12}	7.73

Table 4.8b: *Chemical composition of extractives from dried sugarcane bagasse.*

Compound	Common name	No. of Carbon	Area (%)
Water extractives			
Formic acid	-	C_1	2.15
Acetic acid	-	C_2	31.86
1-hydroxy-2-propanone	Acetol	C_3	19.21
1,2-cyclopentanedione	-	C_5	2.10
dl-glyceraldehyde dimer	Glycerose	C_6	15.25
Catechol	-	C_6	9.73
5-hydroxymethylfurfural	-	C_6	17.45
4-hydroxyacetophenone	Piceol	C_8	2.25
Ethanol extractives			
Furfural	-	C_5	100

The extractive-free biomass samples were examined via TGA and FTIR spectroscopy. The FTIR spectra of the extractive-free biomass samples compared with their non-extracted forms are presented in Figures 4.6, while the TG and DTG results are shown in Figure 4.7. The FTIR spectra did not reveal any chemical structure difference between the non-extracted and extractive-free materials. However, two hypotheses presented earlier, in Section 4.4.1 can now be confirmed via the TG and DTG thermograms:

1) That the earlier onset of degradation of the biomass feedstocks is due to the decomposition of the solvent-extractable compounds. Thus, the T_{onset} for both biomasses increased from 160 °C for non-extracted to 250 °C for extract-free biomass. Indeed, the T_{onset} of the extractive-free biomass is comparable to that of the commercial cellulose-lignin mixture which was 265 °C (Table 4.1).
2) That the first shoulder peak at 235 °C in the non-extracted feedstocks is attributable to the loss of extractives as annotated in Figures 4.7 (b) and (d). The degradation of extractives at a lower temperature is of course due to their higher volatility compared to the other components of the biomasses.

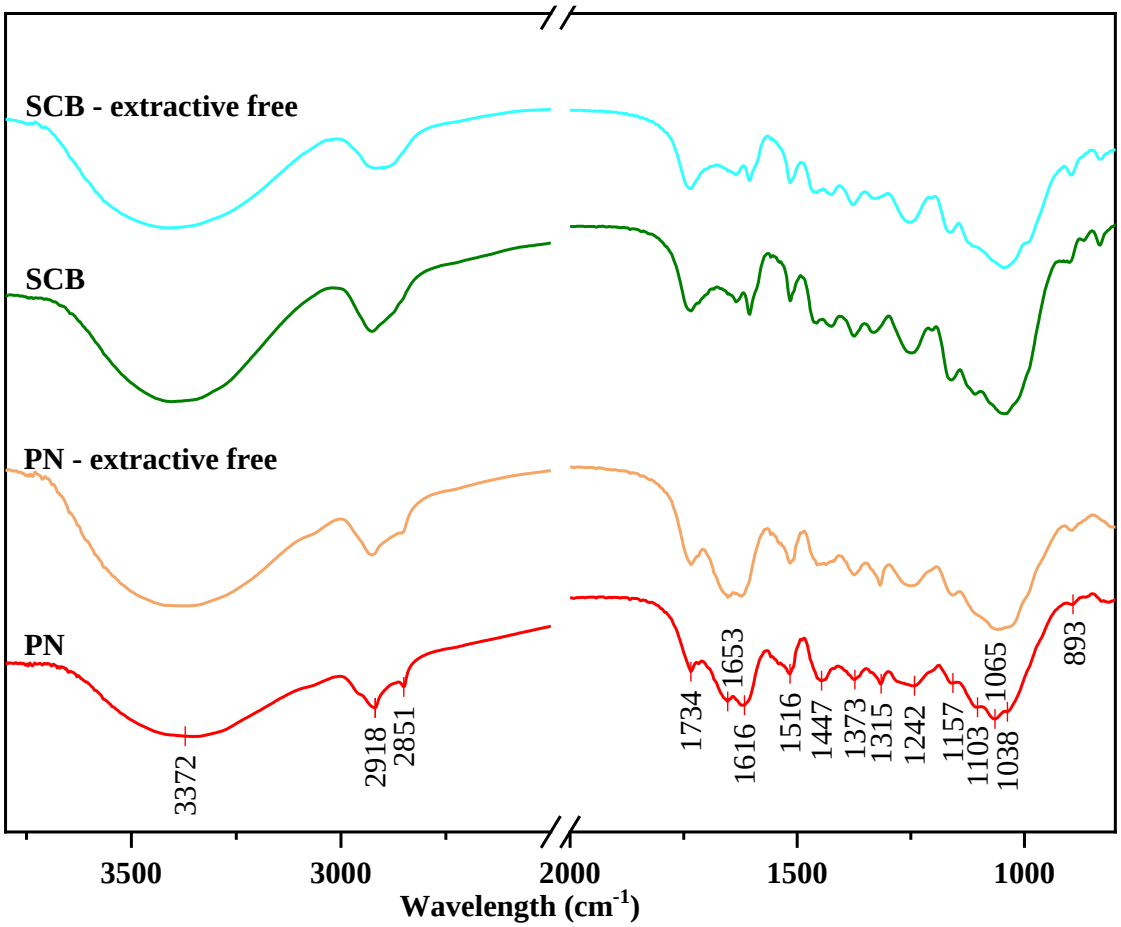

Figure 4.6: *FTIR spectra of extractive-free biomass compared with non-extracted biomass samples. PN = pine needles and SCB = sugarcane bagasse.*

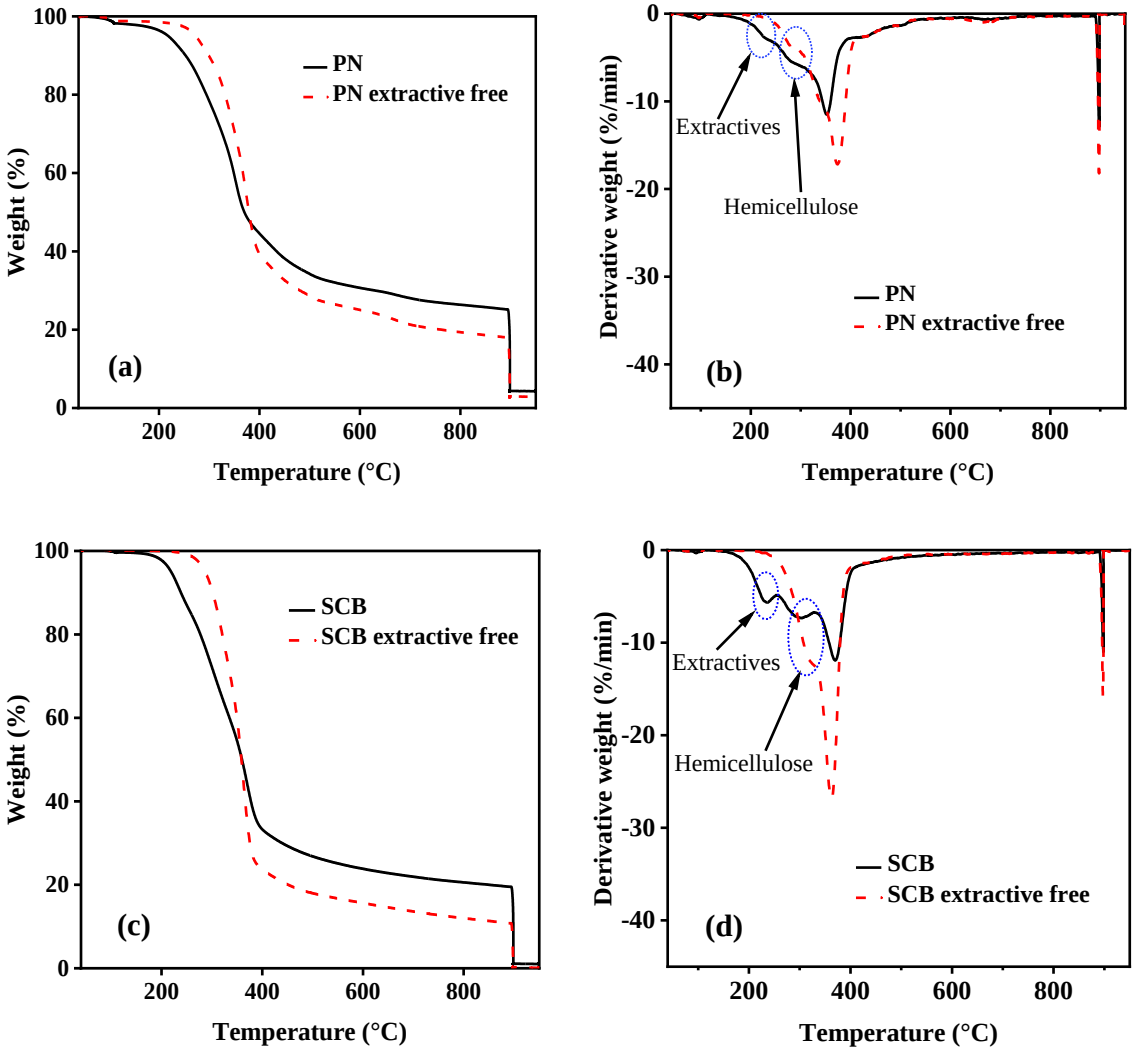

Figure 4.7: *Figures (a) to (d) compares the TG and DTG results of extractive-free versus non-extracted dried biomass samples. PN = pine needles and SCB = sugarcane bagasse.*

In summary, solvent extraction did not in any way affect the chemical structure of the biomass observed via FTIR spectroscopy, however, the temperature at which the biomass begins to degrade during TGA is increased due to the removal of the highly volatile components by the solvents. Most of the extractives, particularly in pine needles are important flavours, ingredients in many cosmetic products and precursors for the manufacture of pharmaceuticals e.g. 4-hydroxyacetophenone, endo-borneol, and *l*-α-terpineol [253]. Thus, a successful industrial-scale process could consider the extraction of these compounds from the feedstock prior to liquefaction. Nonetheless, for the utilisation of bulk/non-extracted biomass, as in this work, the extractives are likely to either remain as components of the final liquid product or converted along with the biopolymers to other products.

4.3.3.2 Bio-polymer constituent

Figure 4.8. compares the FTIR spectra of the extracted lignin from sugarcane bagasse and pine needles with their corresponding extractive-free forms as well as commercial lignin. Inspection of the profile of the extracted lignin from both feedstocks shows greater similarity to commercial lignin than to the original biomass materials. Notably, the fact that the key cellulose and hemicellulose bands in the region between 1157 - 893 cm^{-1} have diminished, indicates a successful lignin extraction process. Clearly, the C-O-C (893 cm^{-1}) β-glycosidic linkage between the glucose units of cellulose and hemicellulose is completely degraded. Moreover, 1157 cm^{-1} which represents the C-O-C asymmetric vibration of pyranose ring in cellulose and xylose in hemicellulose is also diminished. Thus, the sulphuric acid dissolved the carbohydrate components as expected. It is obvious from Figure 4.8 that the characteristic aromatic C=C lignin bands, 1616 cm^{-1}, and 1516 cm^{-1} are now more pronounced signifying enhanced purity of lignin in the extracted form over the extractive-free biomass.

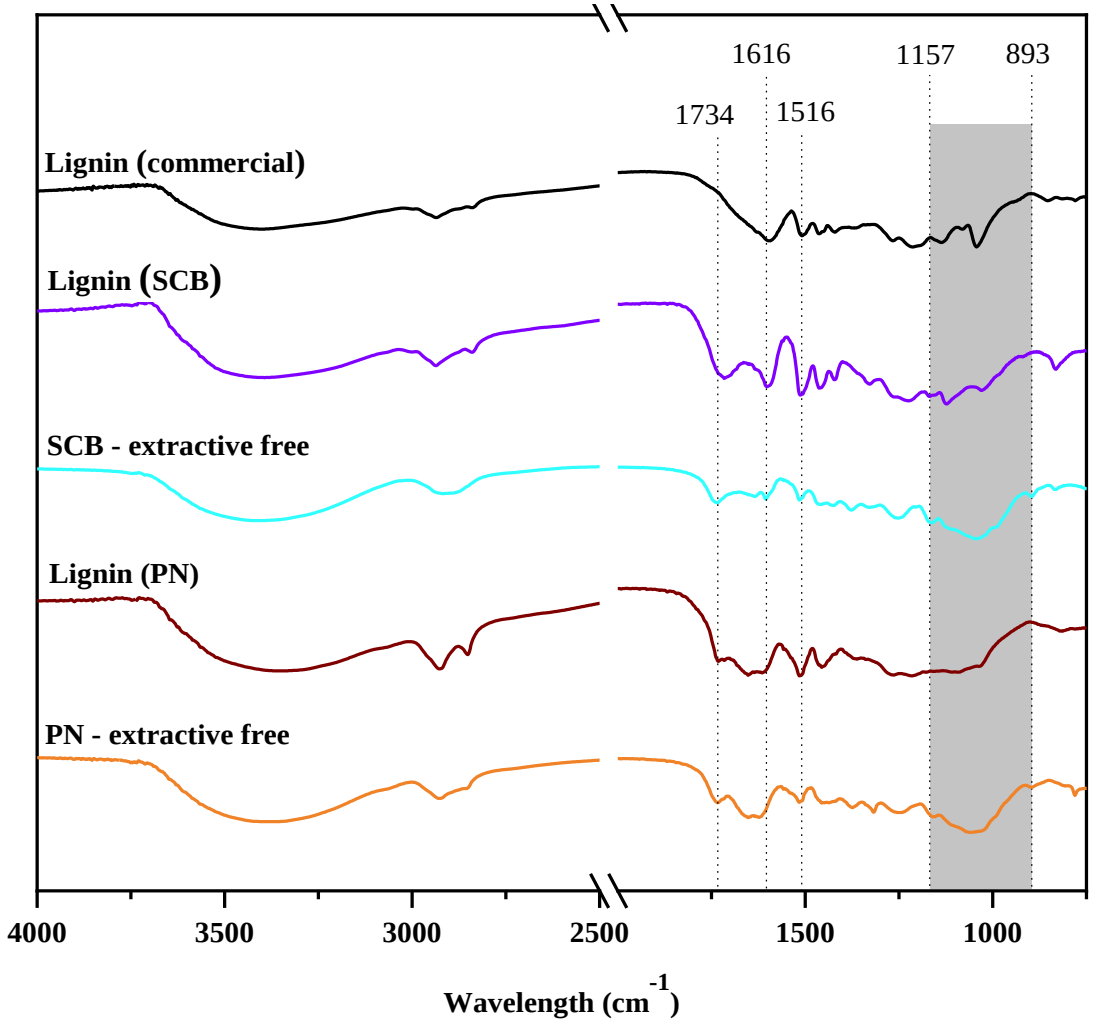

Figure 4.8: *FTIR spectra of extracted lignin compared with extractive-free biomass and commercial lignin. PN = pine needles and SCB = sugarcane bagasse.*

The C=O band around 1734 cm^{-1} in the extracted lignin does, however, show the presence of hemicellulose traces remaining in the extracted lignin, something that should be expected according to literature. According to Carrier *et al.* [181], it is practically impossible to extract lignin in pure form. Therefore, the general postulation that lignin represents the material "insoluble in acid after the hydrolysis of the carbohydrate fraction" is invalid for many biomass samples, particularly herbaceous materials for which proteins can condense with lignin. This they explained is mostly due to incomplete separation of lignin-carbohydrate complexes, as lignin is associated with the carbohydrates via covalent bonds. This claim is also true for the extraction of cellulose and hemicellulose. A critical review of the existing methods for the estimation of cellulose in plant materials have however shown that none gives true cellulose but products containing varying amounts of hemicelluloses including polyuronides [254]. As stated by Sjöström & Alén [255], holocellulose preparation normally involves up to 5 percent loss of carbohydrates, as well as the retention of some small amount of lignin. Thus, no method has yet been found to be 100 % efficient in isolating the bio-polymers into individual pure components [181,254,255].

Nonetheless, the quantitative amounts of lignin and holocellulose obtained for both feedstocks in this work are consistent with those documented in the literature (Table 4.9). For instance, the composition of lignin and holocellulose in pine needles were 32.3 wt.% and 67.7 wt.% respectively which is approx. the same as those recorded by Singha [172], 33.4 wt.% lignin and 67.3 wt.% holocellulose. In the case of sugarcane bagasse, 22.9 wt.% and 77.1 wt.% were recorded for lignin and holocellulose respectively. These values are similar to those obtained by Rezende *et al.* [217], 22.2 wt.% lignin and 59.7 wt.% holocellulose (*i.e.* cellulose plus hemicellulose). The slight difference in holocellulose content could be attributed to the deduction of ash content from the results obtained by Rezende and his colleagues. Generally, pine needles possess a higher proportion of lignin compared to sugarcane bagasse as observed in the literature (Table 4.9).

Table 4.9: *Bio-polymer constituents of extractive-free pine needles and sugarcane bagasse compared with others researched in literature.*

	Pine needles				Sugarcane bagasse		
	This work	[172]	[170]	[39]	**This work**	[217]**	[218]**
Lignin	**32.28**	33.37	27.79	43.24	**22.87**	22.20	20.30
Cellulose	**67.72***	67.29*	64.12*	51.62*	**77.13***	35.20	41.60
Hemicellulose						24.50	25.10

** Holocellulose*

*** The missing percentage was reported as ash.*

4.4 Conclusion

A summary of the composition of pine needles and sugarcane bagasse used as feedstock in this research is provided in Table 4.10. With the aid of FTIR spectroscopy, TGA, proximate and elemental analyses, the nature of the biomass materials was established using commercial cellulose and lignin as reference materials. Sugarcane bagasse was therefore found to be predominantly cellulosic in nature whereas that of pine needles was more ligninic. Proximate analysis conducted on pine needles and sugarcane bagasse revealed high volatile matter contents of > 70 wt.% and > 80 wt.% respectively based on dry weight. The high volatile content is a good indication of probable high biomass conversion during chemicals synthesis, as the chemicals are expected to be predominantly made from the volatile matter component of the biomass. Both biomass materials contain a range of aliphatic and phenolic solvent-extractable compounds. These were mainly C_1 to C_8 compounds with pine needles possessing additional C_{10} to C_{12} terpenes which could be converted to other chemicals along with the main polymer constituent, lignocellulose. The elemental analysis further revealed S and N contents of sugarcane bagasse and pine needles are correspondingly < 0.2 wt.% and < 1.5 wt.% making these feedstocks safe for thermochemical processes without much concern about reactor fouling or environmental pollution.

Thermogravimetric and conventional manual ASTM E870 – 82 methods for proximate composition analysis were compared for pine needles and sugarcane bagasse in this study. Both methods were highly comparable for the determination of volatile matter content while slight discrepancies in ash content were observed potentially due to differences in program temperatures. The thermogravimetric analysis was further useful in establishing

the temperature range needed for the liquefaction of the biomass materials. The TGA results indicate that effective thermal degradation of pine needles and sugarcane bagasse occurs between 160 °C to 600 °C. This information is a vital guide to the selection of a suitable temperature range for the liquefaction studies on pine needles and sugarcane bagasse in the ensuing chapters.

Table 4.10: *Summary of the composition of pine needles (Picea abies) and sugarcane bagasse on a dry weight basis.*

Property	**Pine needles**	**Sugarcane bagasse**
Proximate composition (wt.%) – ASTM E870 – 82		
Volatile matter	72.83 ± 0.37	80.13 ± 0.83
Fixed carbon	21.52	16.04
Ash	5.64 ± 0.07	3.83 ± 0.12
Elemental composition (wt.%) [a]		
C	48.70 ± 0.19	46.15 ± 0.07
H	6.33 ± 0.02	6.12 ± 0.04
N	1.30 ± 0.02	0.42 ± 0.01
S	0.10 ± 0.01	0.18 ± 0.01
O [b]	39.33 ± 0.20	46.04 ± 0.05
Bio-polymer composition (wt.%) [c]		
Lignin	32.28	22.87
Holocellulose	67.72	77.13
Extractives content (wt.%)		
Water extractives	22.00	30.60
Ethanol extractives	12.02	15.47

[a] *Missing percentage is ash content (by TGA).*
[b] *Calculated by difference.*
[c] *Extractive-free basis.*

Chapter 5

Non-catalytic liquefaction

CHAPTER 5: NON-CATALYTIC LIQUEFACTION

5.1 Introduction

Having established the suitability of pine needles and sugarcane bagasse for chemical synthesis in Chapter 4, the aim of this chapter, therefore, is to demonstrate the potential of valorising these waste resources to platform chemicals via a non-catalytic liquefaction process. The liquefaction technique was chosen for this work, owing to its high feedstock versatility, able to process both dry and wet biomass [24]. Nonetheless, for the purposes of comparative studies, both biomass feedstocks were dried to create a common basis of assessment. In this Chapter, pine needles (PN) were used as an exemplar biomass waste with glycerol as a potential green solvent. It was shown earlier in Chapter 4, that effective thermal decomposition of the bulk (non-extracted) pine needles occur between 160 °C to 600 °C, while the lignocellulosic constituents start degrading at 250 °C. The focus of this work is to be able to convert the entire biomass, including the lignocellulosic component to value-added chemicals, therefore, 250 °C was chosen as a suitable starting temperature for all experiments conducted in this Chapter.

One challenge that surfaced in this Chapter, was the ability to identify the biomass-derived products despite the high (> 90 %) biomass conversion achieved. Instead, a high concentration and complex spectrum of glycerol derived compounds were observed. Hence the second part of this chapter was focused on the utilisation of diluted glycerol in an effort to determine the existence of biomass derivatives. The intension is to narrow the distribution of glycerol derived compounds while enhancing the detection of the biomass derivatives. As such, acetone, and water were chosen as cosolvents for the following reasons:

- Most of the glycerol derivatives were glycerol dehydration products, e.g. 1,4-dioxane-2,6-dimethanol. Therefore, water addition is expected to inhibit the formation of these products.
- Acetone is immiscible with glycerol and hence it is anticipated that most of the biomass derivatives would be dissolved in the acetone phase. This would potentially ease their separation from the glycerol phase and therefore enhance their detection via GCMS.
- Furthermore, it has been demonstrated in earlier research [256–258] that the reaction between acetone and glycerol leads to the formation of solketal

(Scheme 5.1), a potential fuel additive which reduces gum formation in gasoline and increases the octane number of gasoline [259]. The formation of solketal is claimed to be a favourable reaction pathway that could yield, as high as 98 % selectivity under specified conditions [260]. As such, this reaction pathway is expected to hinder the formation of other numerous compounds, leading to a reduction in the distribution of glycerol derivatives. Thus, the design of the glycerol-acetone system could serve as a one-pot valorisation process for both biomass and glycerol.

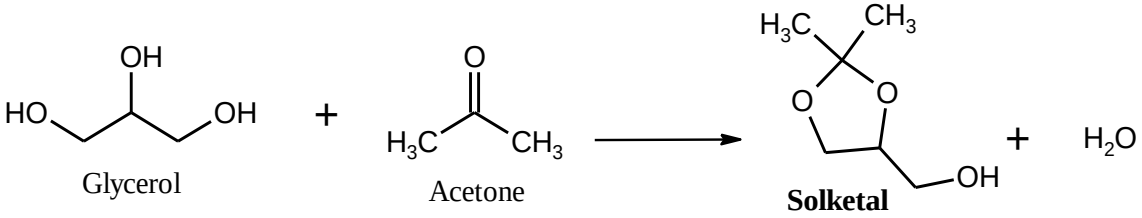

Scheme 5.1: *Ketalisation of glycerol with acetone.*

- Finally, acetone and water have been successfully applied as liquefaction solvents on other biomass types in the past [107], so it is envisaged that the synergistic influence of glycerol and these solvents will boost the conversion of biomass to valuable chemicals. Glycerol and water have been previously applied as cosolvent for biomass liquefaction with outcomes of reduced char formation, and enhanced bio-oil yield with higher fuel quality over hydrothermal liquefaction [30], however, nothing has been reported so far on the application of glycerol and acetone as cosolvent for biomass liquefaction. Therefore, the use of glycerol and acetone as cosolvent in biomass liquefaction is being investigated for the first time in this work.

5.2 Methods

Biomass liquefaction studies were conducted in the Hastelloy C-276 metal autoclave reactor previously described in Section 3.5.2. All reactions were conducted with pine needles in the absence of catalyst, at 250 °C under 30 bar of helium supply pressure. The biomass-solvent ratio was kept at 1:10 (wt:wt), sufficient for homogeneity. 2 g of pine needles with 20 g liquefaction solvent was used in all reactions. The reaction time and mixing rates were kept constant at 1 h and 300 rpm respectively. Pine needles were used

without size reduction. The biomass feedstocks preparation protocols are presented in Section 3.3. An in-depth description of the biomass liquefaction procedure, product separation and analysis, as well as conversion calculations could be found in Sections 3.5.2 to 3.5.7. Figure 5.1, however, provides a summary of the entire process. The following mixtures were employed as liquefaction solvents in the glycerol-cosolvent systems:

- Glycerol:water = 1:0, 1:1, 1:3, 1:6 and 0:1 (mol:mol).
- Glycerol:acetone = 1:0, 1:1, 1:3, 1:6 and 0:1 (mol:mol).

The resultant liquid product was analysed via GCMS and the solid by-product (bio-char) was characterised via FTIR to understand the impact of glycerol on pine needles decomposition. The fraction of gaseous product from the liquefaction process was considered negligible (Appendix A.1) and hence vented without further analysis.

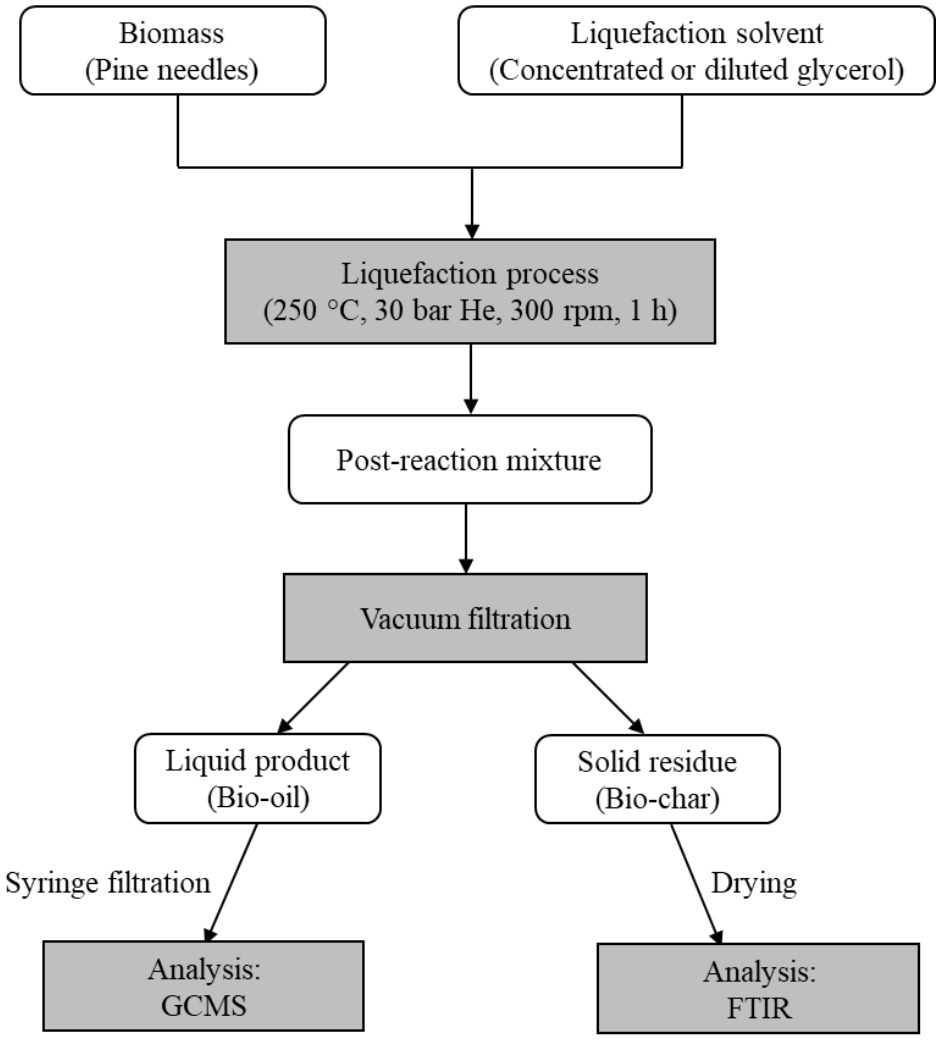

Figure 5.1: *Flow chart for biomass liquefaction studies.*

5.3 Results and discussion

5.3.1 Effect of glycerol on biomass conversion

Pine needles conversion to liquid product for three repeated reactions conducted with concentrated glycerol are presented in Figure 5.2. A very high average biomass conversion of 94 wt.% was achieved in the presence of concentrated glycerol in the non-catalytic liquefaction reaction. The values range between 93 and 94.5 wt.% and are highly reproducible with a standard deviation of ~ 1 %. The decomposition of biomass during liquefaction was studied by conducting an FTIR analysis on the solid residue (bio-char) obtained after the reaction and compared with that of the original feedstock as shown in Figure 5.3. Detailed interpretations of each band were earlier discussed in Chapter 4 (Table 4.5), however, the bands of interest are highlighted on the figure. The FTIR spectra of the resultant bio-char show significant transformation to the original chemical structure of pine needles as illustrated in Figure 5.3. Scission of various characteristic lignin, hemicellulose and cellulose bonds could be observed.

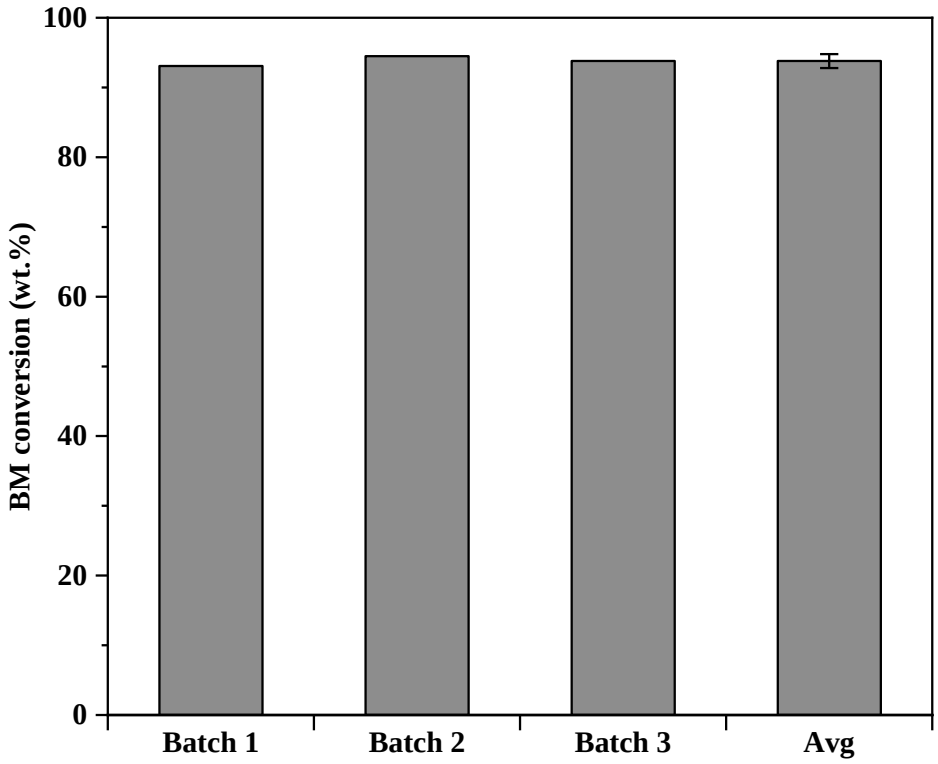

Figure 5.2: *Pine needles conversion in concentrated glycerol. Conditions: 2 g pine needles, 20 g concentrated glycerol, 250 °C, 30 bar He initial pressure, 300 rpm, 1 h.*

For instance, the characteristic aromatic C=C lignin band at 1516 cm^{-1} is completely missing in the bio-char, signifying an extensive lignin decomposition. Also noticeable is an almost total disappearance of the fingerprint C=O stretching of the hemicellulose uronic ester groups at 1734 cm^{-1}. A reduction in the intensity of various bands between 893 and 1159 cm^{-1} attributed to various C-O and C-O-C bonds of cellulose and hemicellulose could be observed. These are all evidence of hemicellulose and cellulose depolymerisation during pine needles liquefaction. Other bands missing in the residue include the 1315 cm^{-1} assigned to the C-H deformation of cellulose or C-O stretching of syringyl (lignin) derivatives, and 1244 cm^{-1} which represents the C-O stretching vibration of various lignin and hemicellulose structures [231,247]. There is also a slight reduction in the intensity of band 3360 cm^{-1}, which is known to represent the hydroxyl groups of the phenolics and sugar units of the lignin and polysaccharide monomer units [238]. The reduction in functional O-H groups in the residue could mean the reduction of sugar and phenolic units in the bio-char as well as the loss of O-H groups to dehydration as part of the liquefaction process. Meanwhile, the presence of the 1616 cm^{-1} (aromatic ring C=C vibrations) and encircled remnant bands between 893 and 1159 cm^{-1} signify the existence of some lignin and carbohydrate fragments in the bio-char.

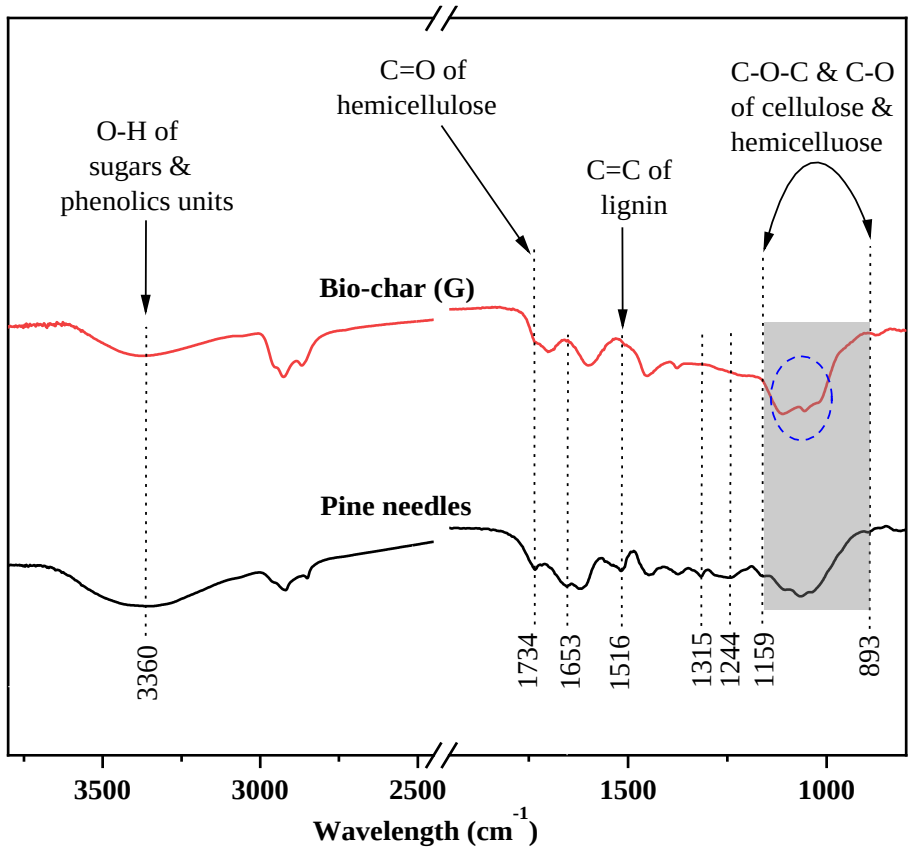

Figure 5.3: *FTIR spectra of bio-char compared with pine needles. Conditions: 2 g pine needles, 20 g concentrated glycerol at 250 °C, 30 bar He initial pressure, 300 rpm, 1 h.*

The significant lignin decomposition supports the claim by Demirbas [34] that glycerol promotes delignification of lignocellulose. The quantity of solid residue in biomass liquefaction processes is normally related to the lignin content [32]. It is widely known that the thermal decomposition of lignin engenders free phenoxyl radicals and that these radicals have a random tendency to form a solid residue through repolymerisation or condensation [32]. However, glycerol is theorised to act as a radical scavenger via hydrogen donation and abstraction reactions [130]. Scheme 5.2 illustrates suggested pathways for various glycerol degradation reactions. Previous studies suggest glycerol, favoured by alkaline conditions, acts as a hydrogen donor, where it undergoes dehydrogenation reactions leading to the formation of dihydroxyacetone [131], or lactic acid [261] as observed in this study (Table 5.1). The donor-hydrogen may then stabilise radicals, reducing or saturating reactive compounds and thereby reducing the amount of char [130]. This possibly explains why a significantly high pine needles conversion was obtained when glycerol was employed as a liquefaction solvent.

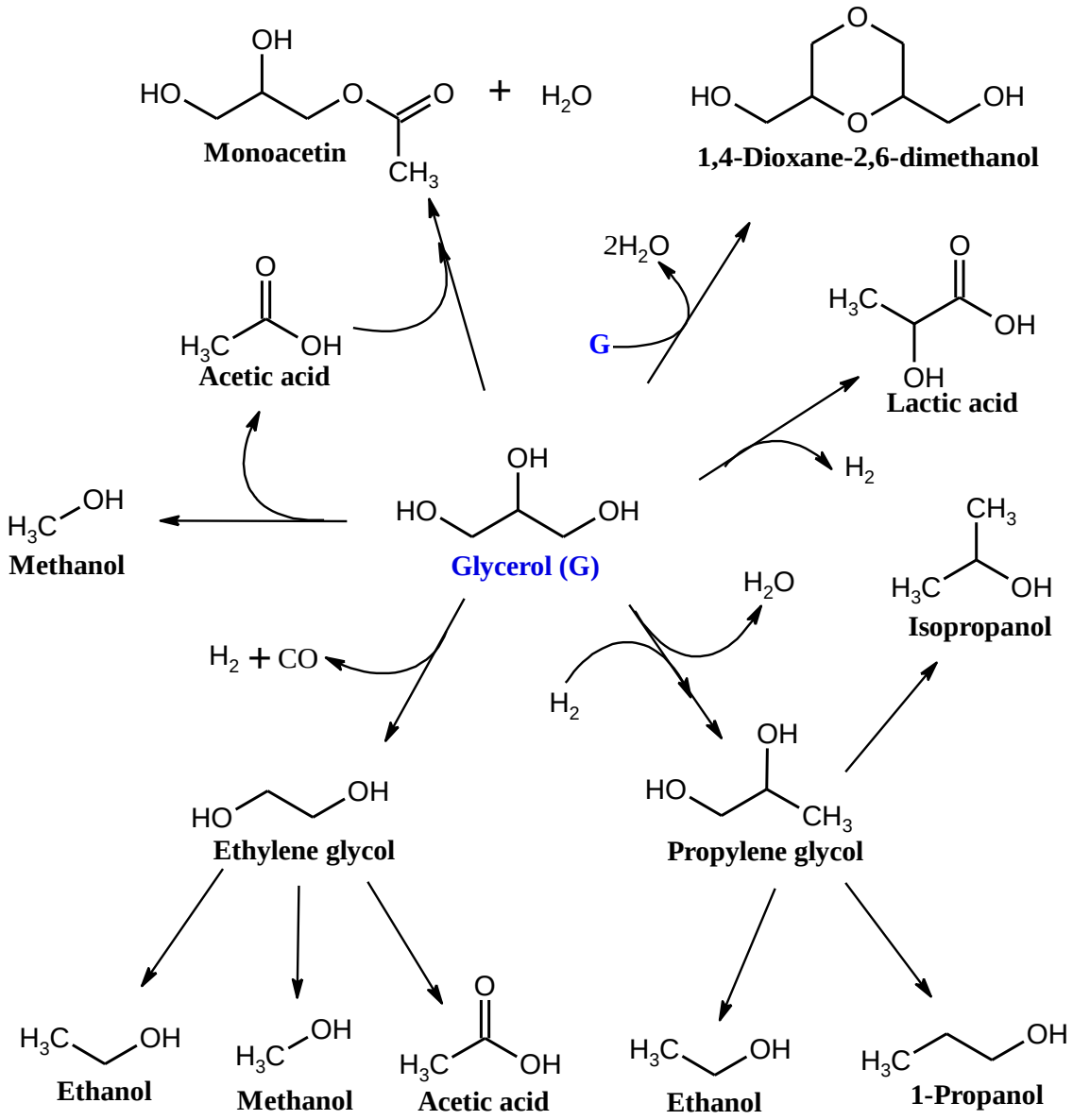

Scheme 5.2: *Proposed pathways for liquid phase glycerol conversion to useful chemicals adapted from Tran & Kannangara* [262].

5.3.2 Composition of liquid product

Prior to pine needles liquefaction, a blank/control experiment (G) consisting of glycerol only was conducted to understand the impact of temperature and pressure on glycerol aside pine needles. The resultant liquid was analysed via GCMS and compared with the liquid product from the glycerol-pine needles reaction (G+PN) as shown in Table 5.1. Hypothetically, this set-up is also useful in understanding the interaction between the biomass and liquefaction solvent towards the synthesis of the compounds identified.

Table 5.1: *Chemical compounds identified (via GCMS) in the liquid product obtained from the liquefaction of pine needles with concentrated glycerol (G+PN) compared with those obtained from glycerol without pine needles (G). Conditions: 2 g pine needles, 20 g concentrated glycerol, 250 °C, 30 bar He initial pressure, 300 rpm, 1 h.*

SN	RT (min)	Name		Peak area (%)	
			Formula	G	G + PN
1	2.24	Methanol	CH_4O	6.3	3.6
2	2.64	Ethanol	C_2H_6O	4.4	4.5
3	4.57	1-propanol	C_3H_8O	4.3	4.1
4	5.08	2-methyl-1,3-dioxolane	$C_4H_8O_2$	1.1	-
5	6.66	2-propen-1-ol	C_3H_6O	3.6	2.2
6	10.07	Acetoin	$C_4H_8O_2$	0.5	-
7	10.35	1-hydroxy-2-propanone	$C_3H_6O_2$	1.1	1.2
8	10.65	Methyl lactate	$C_4H_8O_3$	0.5	-
9	11.39	Diacetone alcohol	$C_6H_{12}O_2$	0.4	-
10	12.63	Acetic acid	$C_2H_4O_2$	2.9	3.6
11	13.47	2,5-hexanedione	$C_6H_{10}O_2$	0.7	-
12	13.83	Propanoic acid	$C_3H_6O_2$	0.6	0.8
13	14.60	Propylene glycol	$C_3H_8O_2$	5.1	11.2
14	15.04	Ethylene glycol	$C_2H_6O_2$	6.1	2.8
15	15.87	2-ethyl-1,3-dioxolane-4-methanol	$C_6H_{12}O_3$	7.8	1.2
16	16.85	1,3-propanediol	$C_3H_8O_2$	1.7	1.5
17	17.10	3-methoxy-1,2-propanediol	$C_4H_{10}O_3$	2.1	3.3
18	17.38	3-ethoxy-1,2-propanediol	$C_5H_{12}O_3$	0.8	1.3
19	18.44	1,2,4-butanetriol	$C_4H_{10}O_3$	0.7	1.1
20	19.37	3-allyloxy-1,2 propanediol	$C_6H_{12}O_3$	1.5	0.5
21	21.23	L-lactic acid	$C_3H_6O_3$	1.6	1.3
22	22.36	Monoacetin	$C_5H_{10}O_4$	3.1	7.8
23	25.11	1,4-dioxane-2,6-dimethanol	$C_6H_{12}O_4$	4.8	20.4
		Total area (%)		***61.6***	***72.3***

It could be seen from Table 5.1, that glycerol without pine needles undergoes a series of reactions such as dehydration, dehydrogenation, and cracking, leading to a range of value-added chemicals as demonstrated in Scheme 5.2. A variety of compounds including simple alcohols (e.g. methanol, ethanol, and propanol), and diols (e.g. propylene glycol, and ethylene glycol) made from glycerol could be seen. About 30 % (by area) of the compounds could not be identified, hence additional analytical techniques would be required for comprehensive studies in the future. A comparative study of the compounds identified in the pine needles liquefaction system (G+PN) with the control experiment (G) shows no significant difference in terms of chemical type. It is therefore not too clear at this stage which chemicals were synthesised from the pine needles. However, the

relative percentage and concentration of certain compounds were altered by the introduction of pine needles. Thus, pine needles could be acting as a catalyst in promoting the yield or selectivity of certain compounds. For instance, the concentrations of selected compounds based on the GCMS peak area shown in Figure 5.4 indicates that the yield of propylene glycol, and 1,4-dioxane-2,6-dimethanol improved by approximately 100 % whereas that of ethylene glycol, and 2-ethyl-1,3-dioxolane-4-methanol experienced reductions of at least a 100 %. Glycerol conversion also slightly increased from 65 wt.% to 70 wt.% in the presence of pine needles.

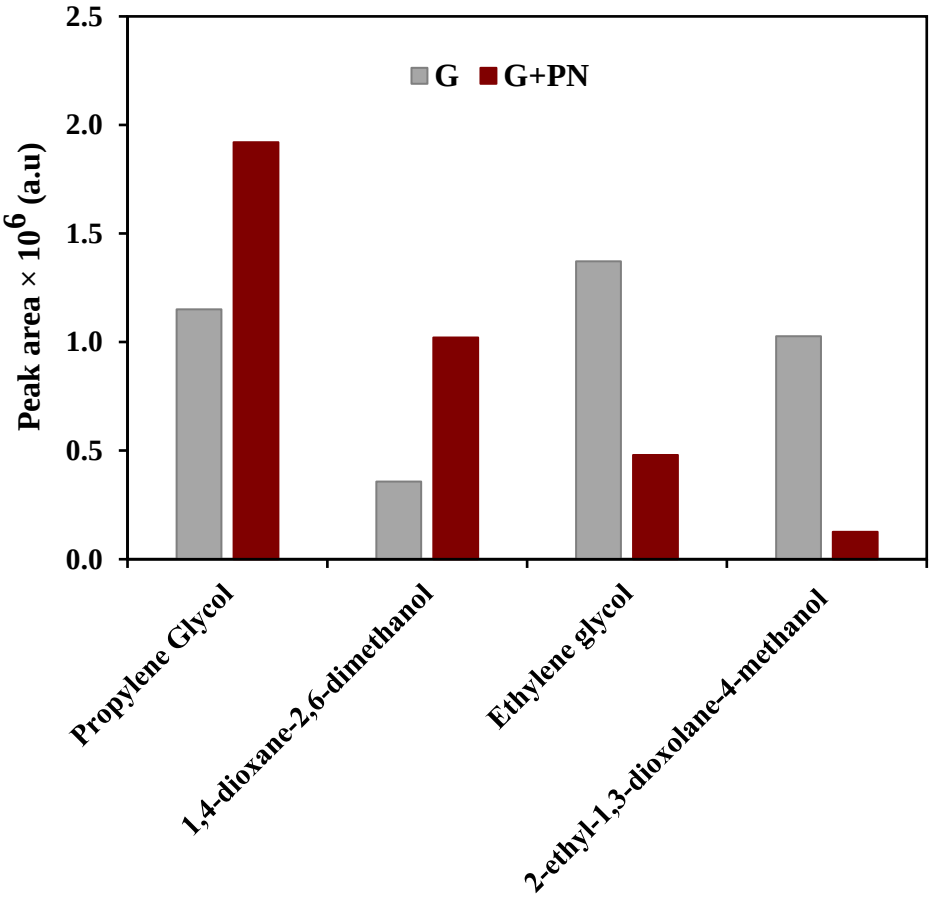

Figure 5.4: *Effect of pine needles on selected compounds in the liquid product obtained from glycerol. Conditions: 2 g pine needles, 20 g solvent, 250 °C, 30 bar He intial pressure, 300 rpm, 1 h. Both samples were diluted to the same concentration and analysed by the same method.*

The catalytic activity of pine needles could emanate from its ash content or other chemical intermediates made from its fragments. In an earlier research by Collett [263] on the application of bio-char as a catalyst for glycerol upgrading, the ash content of bio-char from various biomasses was shown to be catalytically active for the conversion of

glycerol and carbon dioxide to glycerol carbonate and triacetin. The most active catalysts were those with higher ash contents. This activity was attributed to the presence of potassium in the ash. The catalytic potential of pine needles was later considered in Chapter 7 of this thesis.

The high pine needles conversion coupled with the observed transformation to the pine needles' original chemical structure suggests that some biomass derivatives may be present in the liquid phase. As such, the following could explain our inability to discern them;

1) It is possible that similar chemicals were made from both pine needles and glycerol. For example, acetic acid, simple alcohols, acetoin, and lactic acid are potential biomass derivatives as demonstrated in previous research on other biomass materials [14]. Besides, acetic acid was earlier identified as pine needles extractive in Chapter 4 (Table 4.8). Moreover, later studies in Section 5.3.3 on pine needles liquefaction using water and acetone shows the possibility to synthesise acetic acid and simple alcohols from pine needles. In the glycerol system, water made as a by-product of glycerol dehydration (Scheme 5.2) could hydrolyse pine needles into these chemicals. A probable way to trace the precise source of each compound in the mixture is via the use of ^{13}C labelled glycerol, which could be considered in future studies.
2) It could also be that the GCMS technique is not well-suited for the detection of the compounds synthesised from the pine needles in the glycerol system. For instance, glucose, xylose, and other non-volatile compounds are hard to detect via GCMS. Such compounds are best analysed via HPLC and should be considered in future studies.
3) Lastly, GCMS chromatograms from both G and (G+PN) were very complex in distribution, with lots of merging peaks. Hence, it is likely that the biomass-derived products were overshadowed.

While the three possibilities may have competing levels of probability, the latter was investigated in this study. Consequently, two glycerol-cosolvent systems were employed to reduce the concentration and distribution of glycerol derivatives while enhancing the detection of the biomass derivatives. Water and acetone were used as cosolvents as explained earlier in the introduction.

5.3.3 Effect of water and acetone

Prior to the application of the glycerol-cosolvent mixtures, the effect of water and acetone (separately) on biomass decomposition was first checked under the same reaction conditions previously applied in the glycerol system; the results are hereby reported. The percentage weight conversion of pine needles in the individual solvents are presented in Figure 5.5, while the FTIR studies conducted on the bio-chars are shown in Figure 5.6. FTIR analysis was not conducted on the bio-char from the acetone system on a downside and should be considered in future studies to provide better insight into the role of acetone in biomass conversion. Table 5.2 displays the list of compounds identified in the liquid products obtained from the use of water and acetone.

It could be seen from Figure 5.5 that, the use of water and acetone yielded lower biomass conversions when compared to glycerol; 76 wt.% and 44 wt.% conversions were obtained in the presence of water and acetone respectively as against 94 wt.% in the concentrated glycerol system. The lower biomass conversions in water and acetone could be attributed to their less effective lignin degradation, *vide infra*.

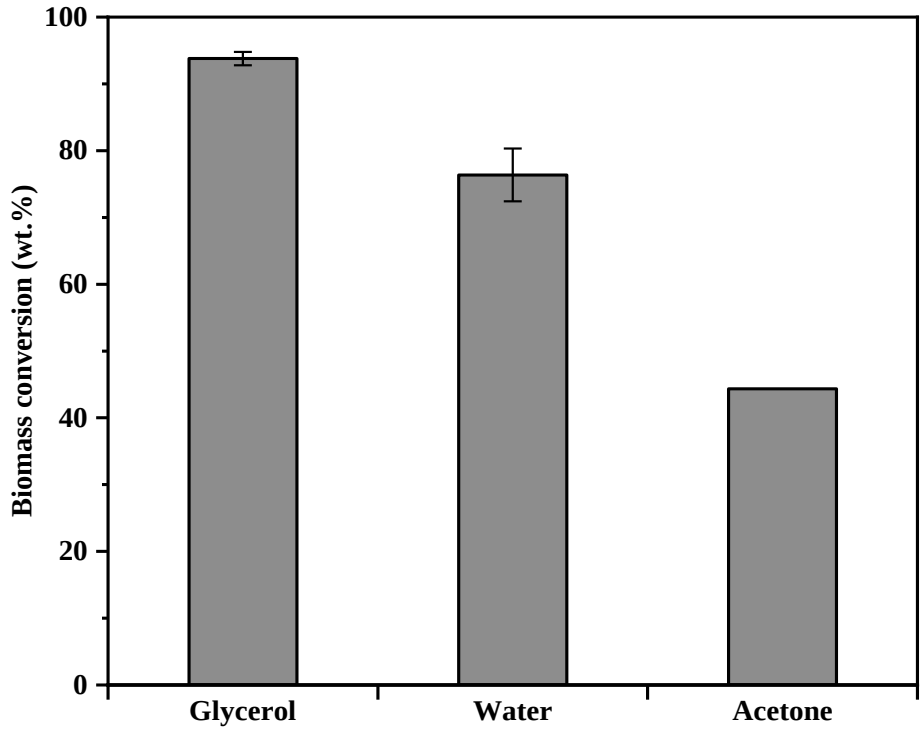

Figure 5.5: *Pine needles conversion in various solvent systems. Conditions: 2 g pine needles, 20 g solvent, 250 °C, 30 bar He initial pressure, 300 rpm, 1 h.*

Comparative studies of the FTIR spectra (Figure 5.6) of bio-chars obtained in the water versus glycerol system illustrates an almost complete degradation of all bands in the characteristic region of cellulose and hemicellulose (*i.e.* 1734 cm^{-1} and between 1159 - 893 cm^{-1}) in the water generated bio-char. These peaks are largely assigned to various C-O bonds vibration in cellulose and hemicellulose [233]. This is a major improvement over the glycerol system where these bands were just reduced in intensity. Nonetheless, in the lignin fingerprint region, the 1516 cm^{-1} band associated with C=C vibrations in aromatic skeletons/rings of lignin monomers [245] is completely degraded in the glycerol derived bio-char but extensively reduced in intensity in the water derived bio-char compared to the original biomass. Therefore, we can understand that cellulose and hemicellulose are better degraded in water whereas lignin is more effectively decomposed by glycerol. Similar research by Liu and Zhang [107] on the effect of acetone, water, and ethanol on pinewood liquefaction also concluded that cellulose is better decomposed in the presence of water. These results also support the previous [32] claim that the amount

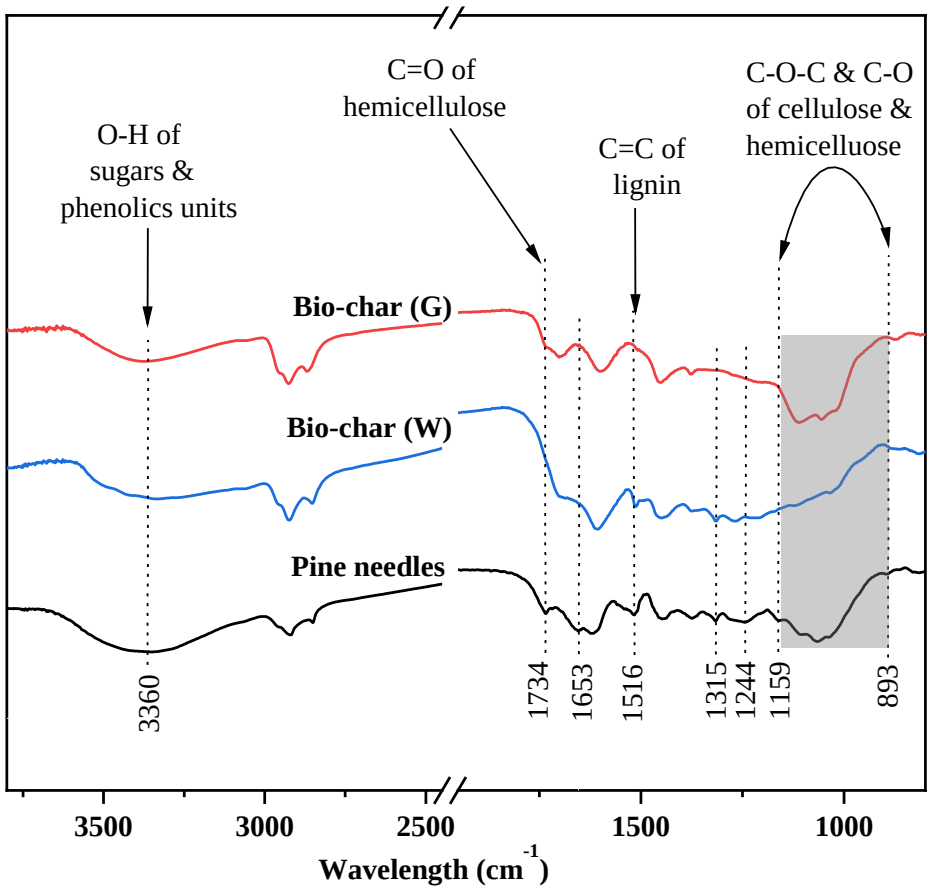

Figure 5.6: *FTIR spectra of bio-chars obtained from pine needles liquefaction using concentrated glycerol (G) and water (W) compared with dried pine needles. Conditions: 2 g pine needles, 20 g solvent at 250 °C, 30 bar He initial pressure, 300 rpm, 1 h.*

of residue obtained during biomass liquefaction is analogous to the lignin content. Thus, the use of lignin scavenging solvents such as glycerol results in significantly high biomass conversion.

Table 5.2 exhibits a variety of biomass-derived products detected via GCMS in the liquid samples; e.g. acetic acid, phenol, and 4-hydroxyacetophenone. Note that, acetone is detected as a biomass derivative during the hydrothermal (with water) liquefaction of pine needles, nonetheless, it is not considered as a product in the acetone system. It is clear from the list of compounds in Table 5.2 that acetic acid could be synthesised from pine needles, as established by earlier works on other biomass feedstocks [14]. Hence, the amount of acetic acid observed earlier (Table 5.1) in the glycerol system is likely to be generated from both pine needles and glycerol. Other dominant products identified in the acetone system are largely acetone derivatives [264,265]; *i.e.* mesityl oxide (47 %), diacetone alcohol (11 %) and isomesityl oxide (9 %) by peak area. Further discussions of the key biomass and solvent derived products are considered along with those obtained from the glycerol-cosolvent systems in the ensuing sections. The ability of acetone and water to decompose pine needles to value-added products discloses the potential for a synergistic effect when combined with glycerol for the same process.

Table 5.2: *Chemical compounds identified (GCMS) in the liquid product obtained from the liquefaction of pine needles with acetone (A) and water (W). Conditions: 2 g pine needles, 20 g solvent, 250 °C, 30 bar He initial pressure, 300 rpm, 1 h.*

SN	RT	Name	Formula	Peak area (%)	
				A+PN	W+PN
1	1.66	Acetone	C_3H_6O	-	9.12
2	2.03	Methanol	CH_4O	2.79	1.49
3	5.50	Isomesityl oxide	$C_6H_{10}O$	9.41	-
4	6.63	Mesityl oxide	$C_6H_{10}O$	47.55	-
5	10.91	Diacetone alcohol	$C_6H_{12}O_2$	10.71	-
6	11.11	2-methyl-2-cyclopenten-1-one	C_6H_8O	-	3.05
7	12.13	Acetic acid	$C_2H_4O_2$	10.31	32.75
8	14.95	2-furanmethanol	$C_5H_6O_2$	3.23	-
9	17.28	2-methoxyphenol	$C_7H_8O_2$	1.34	-
10	17.33	Mequinol	$C_7H_8O_2$	-	6.54
11	18.65	Phenol	C_6H_6O	2.04	29.09
12	19.02	4-ethyl-2-methoxyphenol	$C_9H_{12}O_2$	1.16	-
13	20.55	4-ethylphenol	$C_8H_{10}O$	0.98	-
14	29.51	4-hydroxyacetophenone	$C_9H_{12}O_2$	5.66	9.36
		Total area (%)		***95.18***	***91.40***

5.3.4 Effect of glycerol-cosolvent mixtures

Pine needles liquefaction was conducted using various ratios of glycerol to cosolvent (acetone or water) as outlined in Section 5.2. Control experiments (without pine needles) were also conducted with the various solvents under the same conditions and compared with the pine needles liquefaction reactions. The results are hereby discussed.

Pine needles and glycerol conversions achieved in different solvent systems are presented in Figure 5.7, while sample GCMS chromatograms from the analysis of the resultant liquid products are shown in Figure 5.8. The introduction of cosolvents narrowed the distribution of glycerol derivatives as visible from the corresponding GCMS chromatograms in Figure 5.8. This was however achieved at the expense of biomass conversion, as would be expected. Pine needles conversion declined steadily from 94 wt.% in the presence of concentrated glycerol to 62 wt.% at a dilution factor of 1:6 (glycerol:cosolvent) as seen in Figure 5.7. On the other hand, water reduced glycerol consumption resulting in a decline in conversion from 70 % to ~40 %, while acetone slightly increased glycerol conversion to ~85 %. The former is as a result of the inhibition of glycerol dehydration reactions while the latter is due to the consumption of more glycerol in the side ketalisation reaction to solketal (Scheme 5.1).

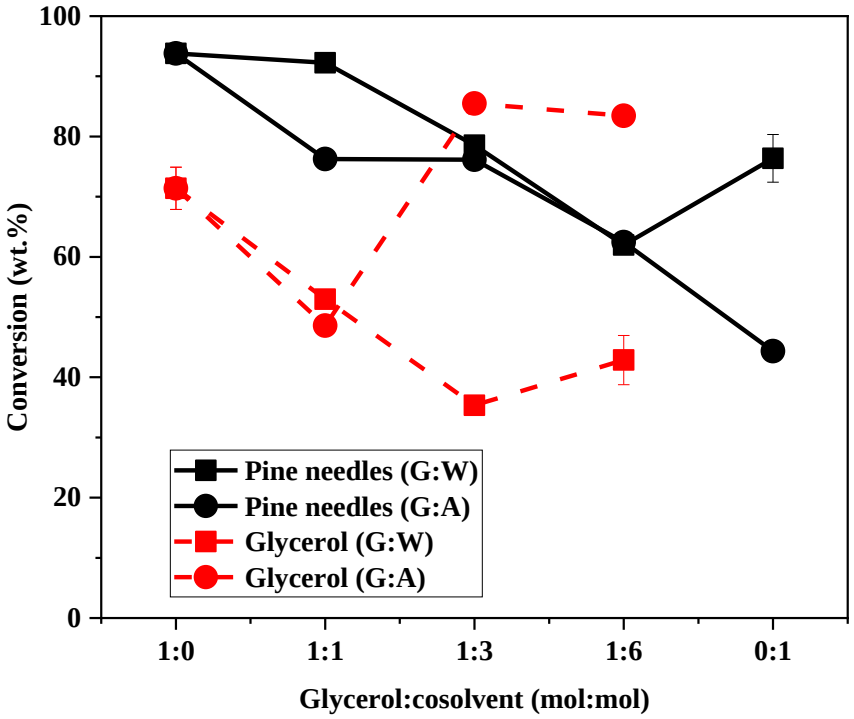

Figure 5.7: *Impact of glycerol-cosolvent mixtures on pine needles (solid lines) and glycerol (dashed lines) conversion. Conditions: 2 g pine needles, 20 g solvent, 250 °C, 30 bar He initial pressure, 300 rpm, 1 h. Shown fits are to guide the eye only.*

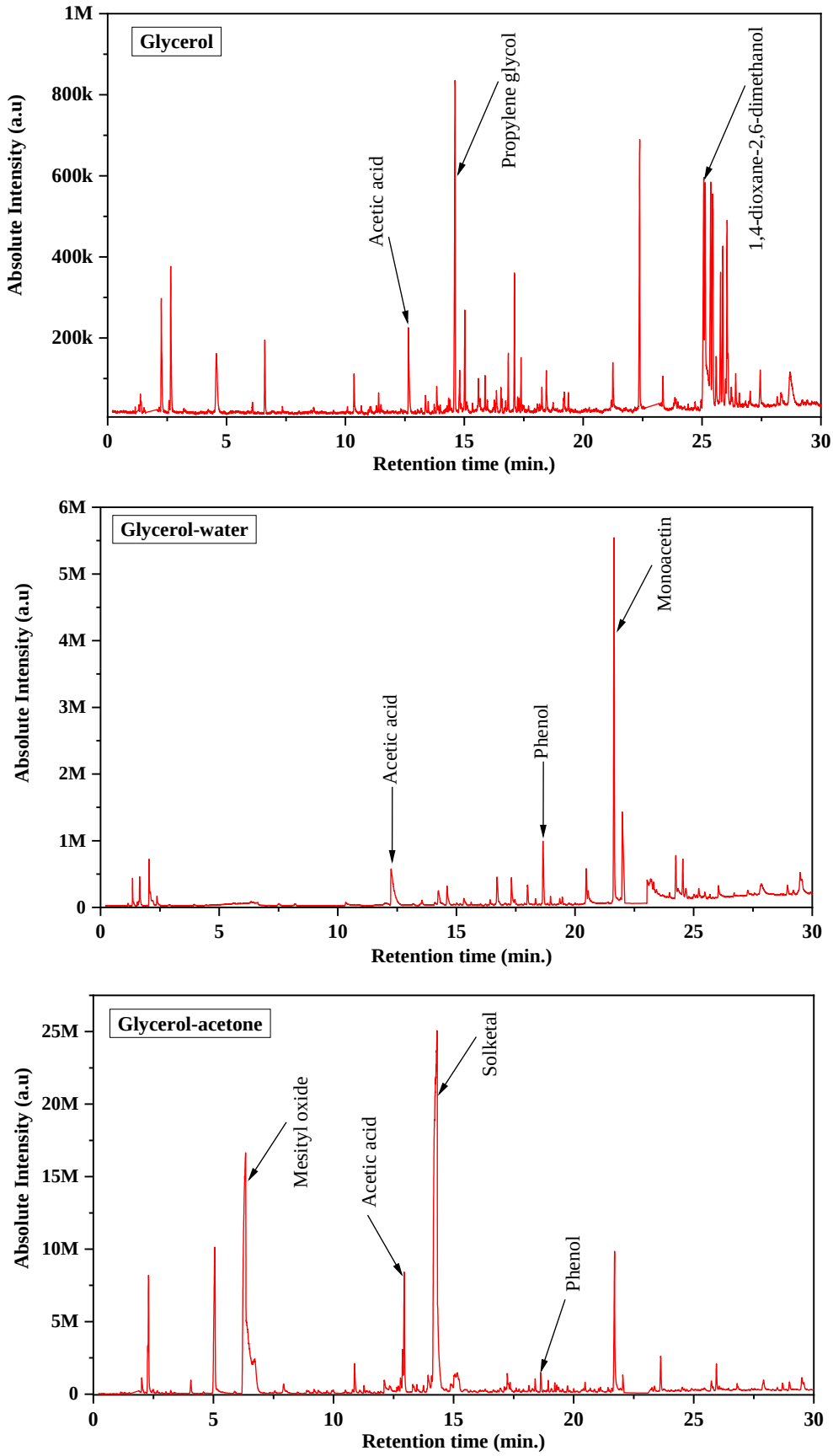

Figure 5.8: *Sample GCMS chromatograms of liquid products obtained from the liquefaction of pine needles using glycerol only versus glycerol-cosolvent mixtures. Conditions: 2 g pine needles, 20 g solvent, 250 °C, 30 bar He initial pressure, 300 rpm, 1 h. Glycerol:cosolvent = 1:3(mol:mol).*

The range of compounds shown in Tables 5.3 and 5.4 illustrate a similar reaction pathway for pine needles in both glycerol-cosolvent systems. Accordingly, similar biomass-derived products could be observed in both systems. The major differences originate from the solvent derivatives as would be expected. In addition to prior knowledge [14,30,130], the distinction of biomass derivatives was largely made by comparing products obtained from the pine needles liquefaction with those obtained from the control experiments. The biomass-derived products are chiefly phenol and other aromatic compounds apart from acetic acid (Tables 5.3 and 5.4). Previous research on the application of glycerol as cosolvent in the hydrothermal liquefaction of aspen wood [130] and rice straw [30] also reported liquid products with significant aromatic species. It is however, not too clear from those studies [30,107,130] if any unique solvent derived compound was observed.

Table 5.3: *Chemical compounds identified (GCMS) in the liquid product obtained from the liquefaction of pine needles with various glycerol-acetone mixtures. Conditions: 2 g pine needles, 20 g solvent, 250 °C, 30 bar He initial pressure, 300 rpm, 1 h. Glycerol:acetone (mol:mol).*

SN	RT (min)	Name	Formula	Peak area (%)		
				1:1	1:3	1:6
1	1.82	2-methylfuran	C_5H_6O	1.1	-	-
2	2.02	Methanol	CH_4O	-	0.4	0.5
3	2.44	Isopropanol	C_3H_8O	11.5	5.0	3.5
4	5.51	Isomesityl oxide	$C_6H_{10}O$	2.2	5.7	6.8
5	6.65	Mesityl oxide	$C_6H_{10}O$	20.1	33.5	32.9
6	8.02	D-limonene	$C_{10}H_{16}$	-	0.4	0.4
7	8.95	Mesitylene	C_9H_{12}	-	0.4	-
8	10.91	Diacetone alcohol	$C_6H_{12}O_2$	-	0.5	1.0
9	12.22	Acetic acid	$C_2H_4O_2$	2.1	0.4	0.7
10	12.45	Glycidol	$C_3H_6O_2$	0.6	-	-
11	13.11	2,5-hexanedione	$C_6H_{10}O_2$	5.1	3.6	3.4
12	14.10	Propylene glycol	$C_3H_8O_2$	0.9	-	-
13	14.25	Solketal	$C_6H_{12}O_3$	44.0	45.3	43.4
14	17.28	2-methoxyphenol	$C_7H_8O_2$	0.6	0.4	0.4
15	18.66	Phenol	C_6H_6O	0.7	0.3	0.6
16	18.97	4-ethyl-2-methoxyphenol	$C_9H_{12}O_2$	0.2	0.2	0.3
17	21.68	Monoacetin	$C_5H_{10}O_4$	10.9	3.8	4.9
		Total area (%)		***100***	***100***	***98.8***

Table 5.4: *Chemical compounds identified (GCMS) in the liquid product obtained from the liquefaction of pine needles with various glycerol-water mixtures. Conditions: 2 g pine needles, 20 g solvent, 250 °C, 30 bar He initial pressure, 300 rpm, 1 h. Glycerol:water (mol:mol).*

SN	RT (min)	Name		Peak area (%)		
				1:1	**1:3**	**1:6**
1	1.35	Acetaldehyde	C_2H_4O	0.6	1.6	2.2
2	1.64	Acetone	C_3H_6O	1.1	2.1	3.3
3	2.04	Methanol	CH_4O	1.7	3.3	3.0
4	2.37	Ethanol	C_2H_6O	1.8	0.9	-
5	3.92	1-Propanol	C_3H_8O	0.6	-	-
6	6.33	2-Propen-1-ol	C_3H_6O	0.5	-	-
7	10.20	1-hydroxy-2-Propanone	$C_3H_6O_2$	1.3	-	-
8	11.70	2-methyl-2-cyclopenten-1-one	C_6H_8O	0.5	-	-
9	12.23	Acetic acid	$C_2H_4O_2$	3.8	12.0	24.6
10	14.10	Propylene glycol	$C_3H_8O_2$	8.6	2.5	-
11	14.53	Ethylene glycol	$C_2H_6O_2$	4.2	2.7	-
12	15.53	2-ethyl-1,3-dioxolane-4-methanol	$C_6H_{12}O_3$	0.9	-	-
13	16.37	1,3-propanediol	$C_3H_8O_2$	0.9	-	-
14	16.66	3-methoxy-1,2-propanediol	$C_4H_{10}O_3$	3.0	3.7	3.0
15	17.30	2-methoxyphenol	$C_7H_8O_2$	0.6	3.1	4.3
16	17.96	1,2,4-butanetriol	$C_4H_{10}O_3$	1.2	2.1	-
17	18.30	Creosol	C_7H_8O	0.3	0.5	-
18	18.64	Phenol	C_6H_6O	1.3	7.0	13.8
19	18.94	4-ethyl-2-methoxyphenol	$C_9H_{12}O_2$	0.2	0.7	-
20	19.33	2-Pyrrolidinone	C_4H_7NO	0.2	0.6	-
21	19.44	3-methylphenol	C_7H_8O	0.2	0.7	-
22	20.50	L-lactic acid	$C_3H_6O_3$	2.2	1.2	-
23	21.65	Monoacetin	$C_5H_{10}O_4$	16.7	30.0	31.0
24	24.67	1,4-dioxane-2,6-dimethanol	$C_6H_{12}O_4$	2.3	1.4	-
25	29.54	4-hydroxyacetophenone	$C_8H_8O_2$	1.1	2.3	10.1
		Total area (%)		***55.9***	***78.4***	***95.3***

Reaction pathways during lignocellulose liquefaction are typically multifaceted, involving among others a combination of C-C bond cleavage, hydrolysis, dehydration and condensation steps as exemplified in Scheme 5.3 [266]. Phenolic compounds (e.g. phenol, creosol and 2-methoxyphenol) are known lignin degradation products, while acetone and acetic acid are known cellulose derivatives [14,266]. Note that, acetone is considered as a product in the glycerol-water system only.

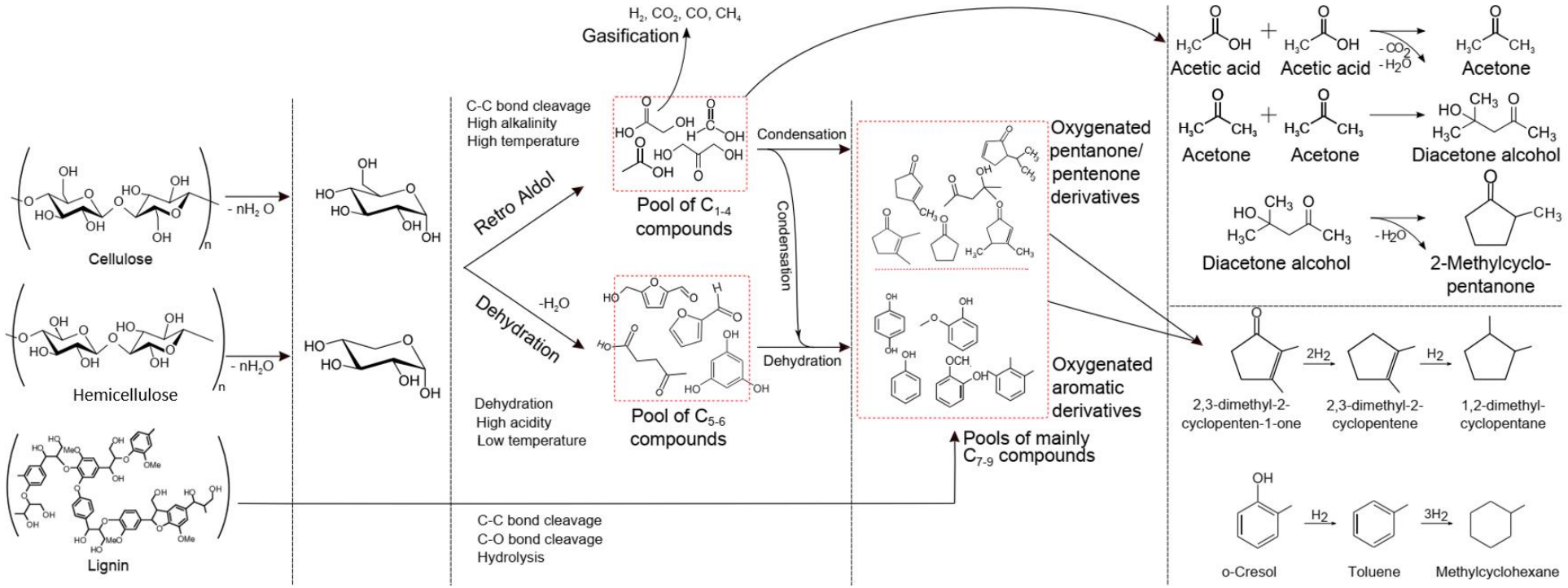

Scheme 5.3: *Exemplar proposed reaction scheme for the formation of valuable chemicals during the liquefaction of lignocellulosic biomass, adapted from Pedersen & Rosendahl* [266].

Advantages of glycerol dilution with water and acetone include;

1) An easier and quicker separation of post-reaction solid-liquid mixtures compared to the concentrated glycerol (i.e. glycerol only) system, also observed by Cao *et al.* [30]. The ease of filtration in the glycerol-water system is as a result of a reduction in viscosity *i.e.* 1500×10^{-3} Pa.s for concentrated glycerol versus 109×10^{-3} Pa.s, 5×10^{-3} Pa.s, and 1×10^{-3} Pa.s for glycerol:water mole ratios of 1:1, 1:3, and 1:6 at 20 °C, and 1 atm. [267,268]. Meanwhile, the ease of separation in the glycerol-acetone system is due to the immiscible property of glycerol with acetone leading to an instantaneous separation of both glycerol and acetone phases once mixing is stopped. The solid residue normally settles with the glycerol phase.
2) Improved selectivity (based on GCMS peak area) of biomass derivatives, particularly in the glycerol-water system. For example, the relative peak area of acetic acid and phenol in the glycerol-water system were ≤ 25 % and ≤ 14 % respectively compared to ≤ 4 % in the concentrated glycerol system.
3) Moreover, the solvent derived products are tailored towards a few compounds with enhanced selectivity. Consequently, solketal (up to 45 %, peak area) was the dominant glycerol derived compound when acetone was used as cosolvent, whereas monoacetin (up to 31 %, peak area) was the major compound found in the glycerol-water system. Solketal is a condensation product of glycerol and acetone as demonstrated in Scheme 5.1, while the condensation of glycerol and acetic acid leads to the formation of monoacetin (Scheme 5.2). It should be highlighted that pine needles could be a potential supplementary source of acetic acid and acetone to the formation of monoacetin and solketal since they (acetic acid and acetone) are well-known biomass-derived products.

   A second dominant by-product, mesityl oxide (up to 31 %, peak area) was observed in the glycerol-acetone system. Mesityl oxide was potentially synthesised from excess acetone via an adol self-condensation reaction [264], Scheme 5.4. It was discovered in the glycerol-acetone system that the introduction of pine needles significantly improved the concentration of mesityl oxide by 2 to 7-fold. This was attributed to a plausible catalytic influence of the bio-char or other pine needles fragments formed in course of the liquefaction reaction. Further investigations into the catalytic potential of pine needles are documented in Chapter 7.

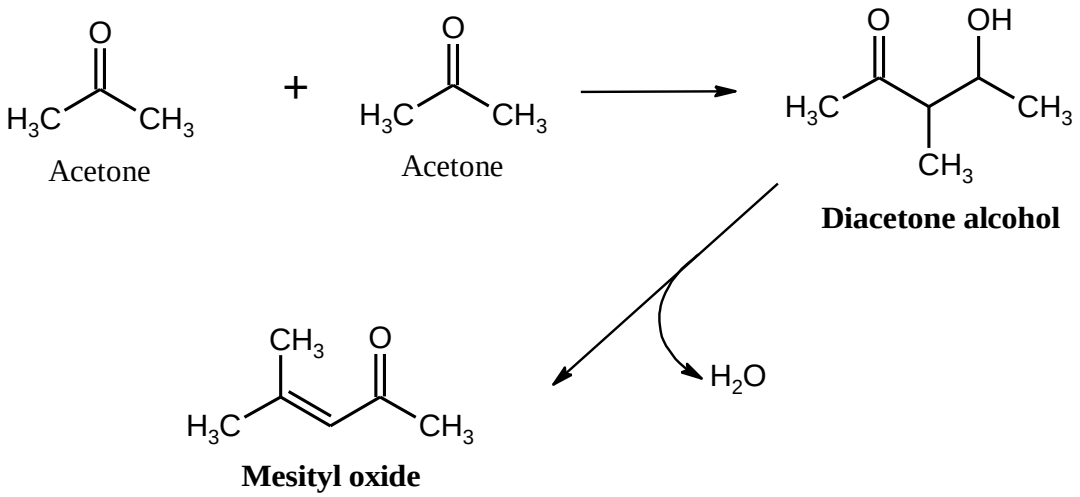

Scheme 5.4: *Simplified reaction scheme for aldol condensation of acetone to mesityl oxide.*

5.3.5 Quantification of targeted products

Considering the wide range of chemicals identified in the liquid products, it was not feasible to determine the yield of each synthesised chemical. Hence the quantification study was targeted at vital dominant species only. The targeted biomass derived chemicals in this chapter were acetic acid and phenol. Solketal and mesityl oxide were the solvent derivatives of interest in the glycerol-acetone system, while monoacetin was the solvent derivative of interest in the glycerol-water system.

Acetic acid is widely employed as a solvent and as a versatile precursor to many other chemicals, e.g. vinyl acetate monomer and various esters. It is also utilised for the manufacture of vinegar. Phenol is an important precursor to a variety of plastics, e.g. nylon and polycarbonates; a precursor to aspirin and other pharmaceuticals; and a widely employed solvent in pharmaceuticals. Solketal is a potential fuel additive that is said to reduce gum formation in and increases octane number of gasoline [259]. Mesityl oxide is a high-value chemical used as a solvent in the manufacture of polyvinyl chloride, polymer resin, and dye [264]. It is also a popular precursor to the production of methyl isobutyl ketone [265]. Monoacetin is used in the manufacture of smokeless powder and dynamite; as a solvent for basic dyes, and in leather tanning.

Current market prices further support the benefits of producing these by-products (solvent derivatives) as part of the biomass valorisation process. For example, the cost per litre of products; solketal is £ 69.20 (97+ %) and mesityl oxide is £ 133.00 (90+ %), are far higher compared to the value of starting materials; acetone costs £ 11.00 (99+ %), and glycerol, £ 22.20 (99+ %). Prices were obtained from the Alfa Aesar website as of December 5th, 2019. Nonetheless, a critical investigation into the economic feasibility of separating and purifying multicomponent products into individual chemical compounds for an end-use would be needed to ensure the sustainability of future biorefineries.

Figures 5.9 to 5.12 compare the concentrations of the selected chemicals obtained in the pine needles liquefaction process with those achieved from the solvents without pine needles (control experiments). By comparing the concentrations of the targeted compounds in the biomass liquefaction systems with those obtained in the absence of pine needles, we can understand that the targeted biomass derivatives were predominantly synthesised from the decomposition of pine needles. Interestingly, the concentration of acetic acid in the glycerol-water control experiments were slightly higher than those observed in the biomass liquefaction systems (Figure 5.9). A possible explanation could be the conversion of acetic acid to other chemicals like monoacetin or other lighter organic compounds in the presence of biomass. For example, acetic acid could lose smaller molecules such as H_2O and CO_2 to form acetone as illustrated in Scheme 5.3.

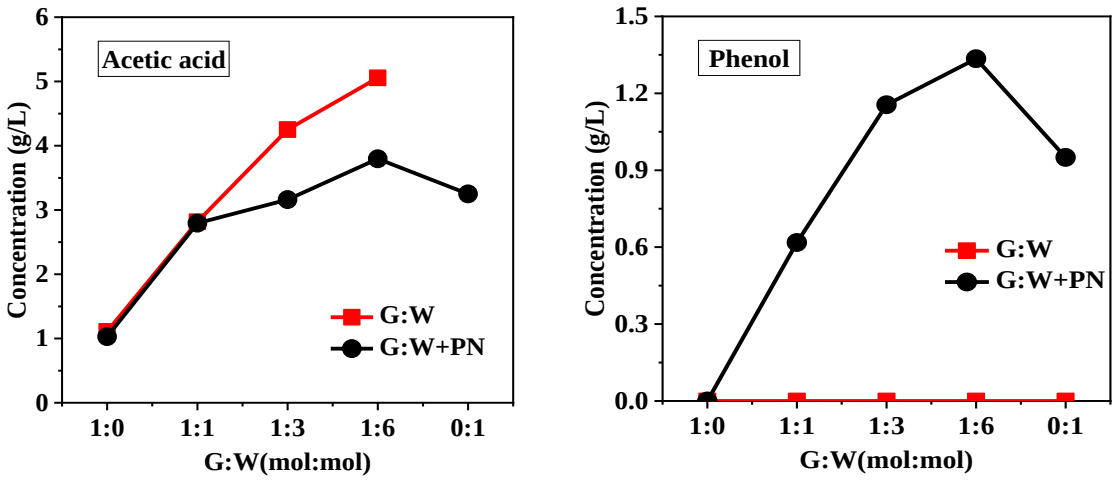

Figure 5.9: *Concentration of acetic acid and phenol in liquid products obtained from the liquefaction of pine needles using various glycerol-water (G:W) concentrations. Conditions: 2 g pine needles (PN), 20 g solvent, 250 °C, 30 bar He initial pressure, 300 rpm, 1 h. Shown fits are to guide the eye only.*

Increasing water content generally resulted in a consistent increase in the concentration of the targeted biomass products; as such, the maximum amounts of acetic acid and phenol recorded in the biomass liquefaction reactions were 3.8 g/L and phenol 1.3 g/L respectively, at G:W (1:6), Figure 5.9.

Conversely, the introduction of acetone suddenly improved the yield of acetic acid and phenol at G:A (1:1) yet, higher concentrations of acetone was not favourable for the formation of these compounds. Precisely, acetic acid concentration improved abruptly from 1 g/L to 5 g/L and phenol from 0 g/L to 1 g/L upon the initial introduction of acetone at G:A (1:1). These values, however, dropped in a similar manner to 1.3 g/L for acetic acid and ~ 0.7 g/L for phenol at G:A (1:3) and G:A (1:6) as noticeable in Figure 5.10. Overall, the present results largely reveal a synergistic influence of glycerol and cosolvent during liquefaction. Clearly, higher yields of phenol and acetic acid are achieved in the cosolvent systems over the individual solvent systems.

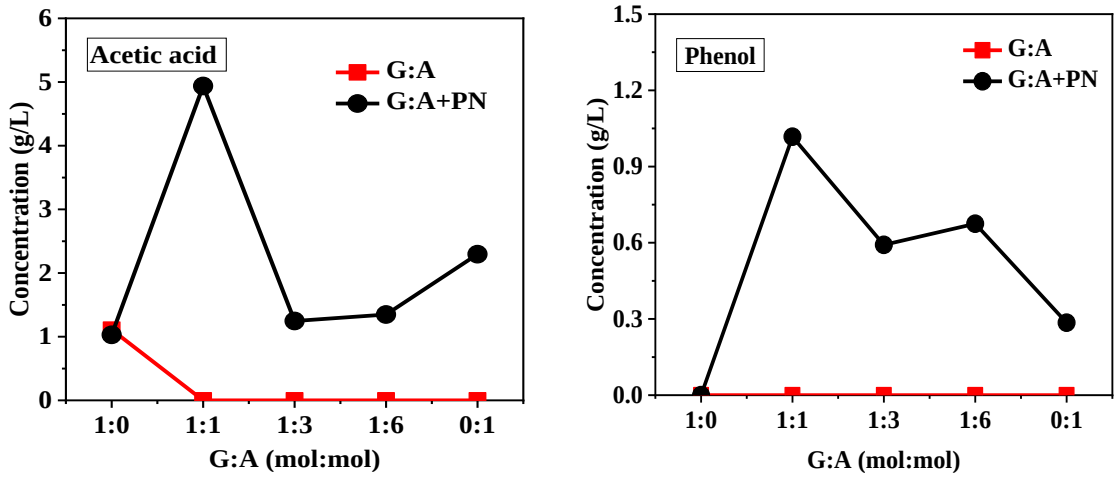

Figure 5.10: *Concentration of acetic acid and phenol in liquid products obtained from the liquefaction of pine needles using various glycerol-acetone (G:A) concentrations. Conditions: 2 g pine needles (PN), 20 g solvent, 250 °C, 30 bar He initial pressure, 300 rpm, 1 h. Shown fits are to guide the eye only.*

Figure 5.11 shows the concentration of monoacetin under various conditions. The addition of water generally improved monoacetin concentration from 3.9 g/L in concentrated glycerol to a maximum of 5.8 g/L at glycerol to water mole ratio of 1:1. This improvement could be ascribed to the availability of more acetic acid (in the presence of water) reacting with glycerol to form more monoacetin. On the other hand, the presence or absence of pine needles had no significant impact on the concentration of monoacetin.

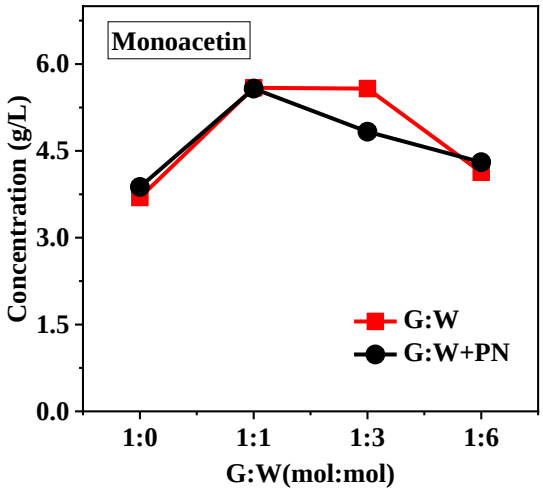

Figure 5.11: *Concentration of monoacetin obtained under various glycerol-water (G:W) concentrations. Conditions: 2 g pine needles (PN), 20 g solvent, 250 °C, 30 bar He initial pressure, 300 rpm, 1 h. Shown fits are to guide the eye only.*

The amount of solketal under various conditions is shown in Figure 5.12 (a). In the absence of pine needles, the concentration of solketal declined progressively from 35 g/L at G:A (1:1) to 18 g/L at G:A(1:6) possibly due to the lower concentration of starting glycerol in that order. The trend is, however, slightly different in the presence of pine needles where the maximum solketal concentration of 39 g/L was recorded at G:A (1:3). Overall, a higher concentration of solketal was achieved in the presence of pine needles as illustrated in Figure 5.12 (a). It is not too clear in this study if the observed trend relates to a potential catalytic activity of the pine needles constituents. However, this observation is consistent with earlier observations made in Section 5.3.2 and 5.3.4, where the concentrations of propylene glycol; 1,4-dioxane-2,6-dimethanol and mesityl oxide were observed to improve in the presence of pine needles. Figure 5.12 (b) illustrates the variations in mesityl oxide concentration with pine needles (10 – 22 g/L) and without pine needles (2-5 g/L).

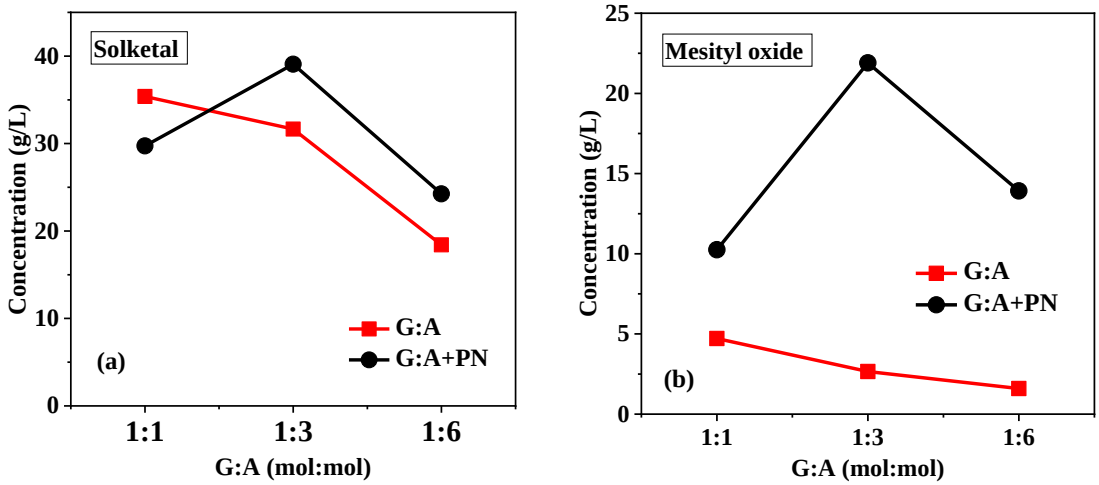

Figure 5.12: *Concentration of solketal and mesityl oxide obtained under various glycerol-acetone (G:A) concentrations. Conditions: 2 g pine needles (PN), 20 g solvent, 250 °C, 30 bar He initial pressure, 300 rpm, 1 h. Shown fits are to guide the eye only.*

The four compounds have a common reaction pathway, which is dehydration/condensation. As such, it is likely that;

1. the by-product water generated from the formation of these four compounds are immediately consumed in the hydrolysis of pine needles, thereby driving forward the dehydration/condensation reaction leading to the synthesis of these chemicals.
2. the pine needle fragments or bio-char produced *in situ* are catalytically active towards the production of these chemicals.

The latter is supported by Collett's work [263] on the application of various bio-chars as catalyst for the synthesis of glycerol carbonate and triacetin. A dehydration/condensation pathway was also established in her work as illustrated in Schemes 5.5 and 5.6.

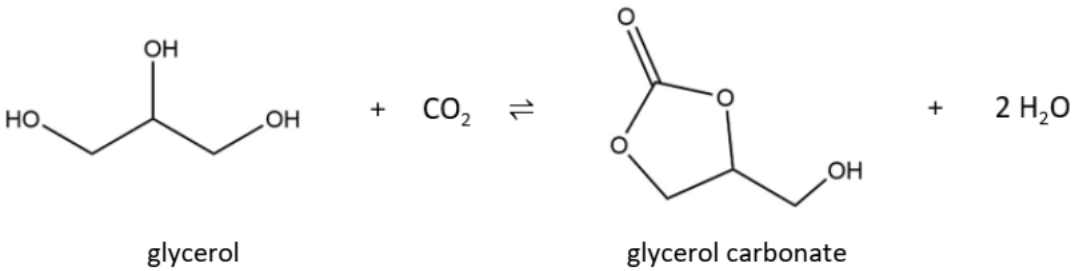

Scheme 5.5: *Reaction for the synthesis of glycerol carbonate from glycerol and carbon dioxide* [263].

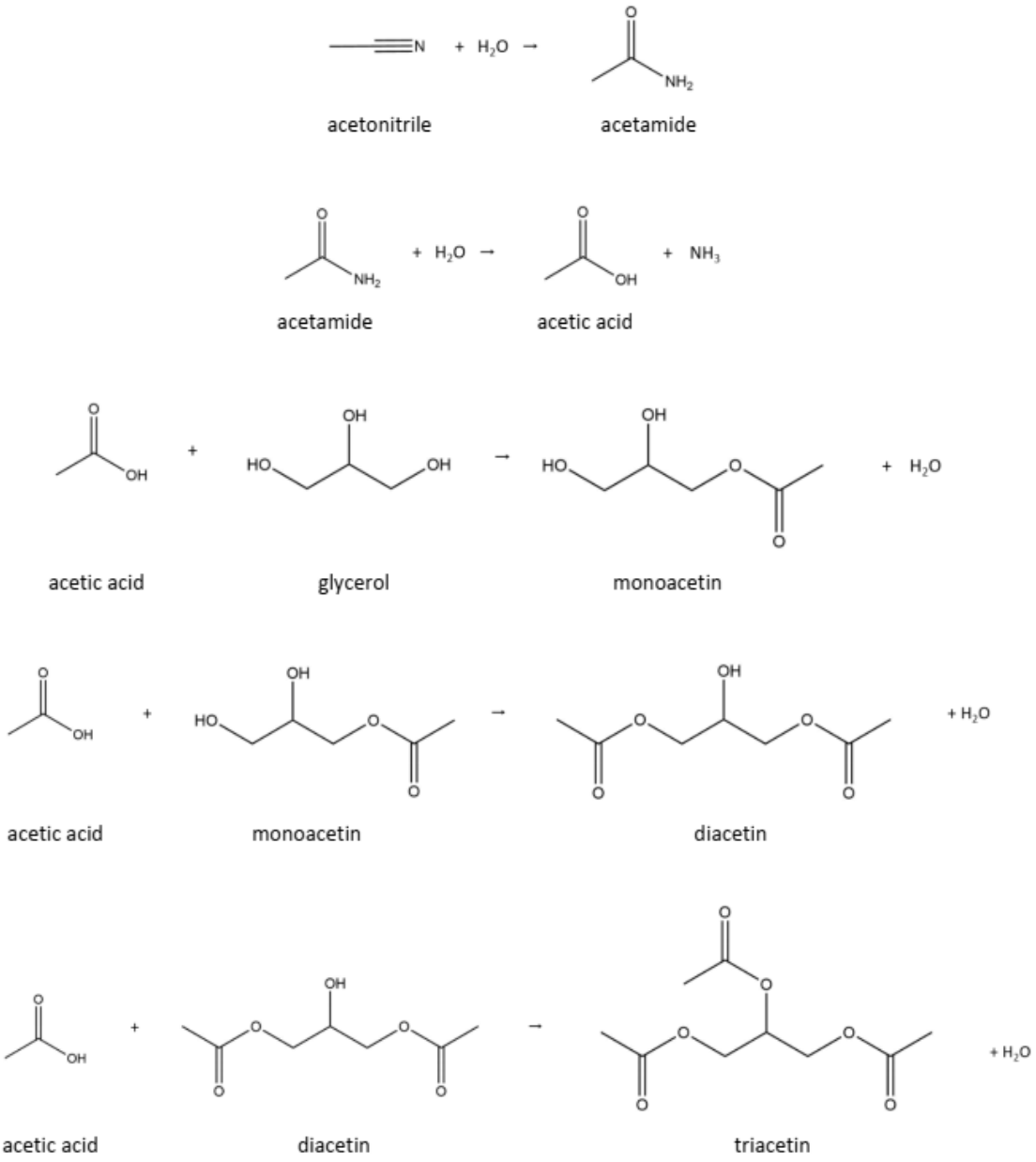

Scheme 5.6: *Proposed pathway to the production of monoacetin from glycerol and acetonitrile* [263].

5.4 Conclusion

This chapter has successfully demonstrated the ability to convert biomass to valuable platform chemicals via a non-catalytic liquefaction process using glycerol, water, acetone, various mixtures of glycerol and acetone, and various mixtures of glycerol and water as green solvents. The application of glycerol-acetone mixtures as liquefaction solvent is investigated for the first time in this study to the best of the authour's knowledge.

The highest biomass conversion of 94 wt.% was achieved in the presence of concentrated glycerol. FTIR analysis of the resultant residues/bio-chars indicates a better decomposition of lignin in the presence of glycerol whereas a better cellulose decomposition was observed in the presence of water.

The application of glycerol-cosolvent as liquefaction solvents generally enhanced the selectivity and yield of targeted biomass derived chemicals. Consequently, the highest concentration of acetic acid (3.8 g/L) and phenol (1.3 g/L) were achieved at a glycerol:water mole ratio of 1:6, whereas in the glycerol:acetone system, the maximum concentration of acetic acid (5 g/L) and phenol (1 g/L) were achieved at a glycerol:acetone ratio of 1:1. The result suggests these products were largely synthesised via the synergistic effect of both solvents on the biomass.

The mixed solvent systems, moreover, served as mediums for the concurrent valorisation of glycerol and biomass, achieving more desired by-products with enhanced selectivity. Solketal (up to 39 g/L) and monoacetin (up to 5.6 g/L) were therefore, the main glycerol derivatives respectively synthesised in the glycerol-acetone, and glycerol-water systems. A second valuable by-product, mesityl oxide (up to 22 g/L) was also made from excess acetone in the glycerol-acetone system. The prospect of producing high-value chemicals from low-value solvents such as glycerol alongside the conversion of biomass waste in a single process may have economic benefits. For example, the number of steps needed to achieve the same results in separate processes could be significantly reduced, potentially making future biorefineries more economical.

Throughout this chapter, the concentration of certain dehydration products was improved upon the introduction of pine needles in various solvent systems. These include mesityl

oxide, propylene glycol; 1,4-dioxane-2,6-dimethanol and solketal. The concentration of mesityl oxide was particularly enhanced by 2 to 7-fold in the glycerol-acetone system. Consequently, it was postulated that biomass or its fragments produced *in situ* are catalytically active towards the dehydration/condensation of glycerol and/or acetone during liquefaction. This hypothesis was investigated further in Chapter 7.

Chapter 6

Catalytic liquefaction and influence of reaction parameters

CHAPTER 6: CATALYTIC LIQUEFACTION AND INFLUENCE OF REACTION PARAMETERS

6.1 Introduction

It was observed in chapter 5 that the utilisation of water as co-liquefaction solvent enhances the selectivity (based on GCMS peak area) of biomass derivatives; acetic acid and phenol, owing to the absence of solvent derivatives. Therefore, this chapter explores further the utilisation of water as a liquefaction solvent under various conditions, using pine needles as exemplar biomass. Specifically, the effect of catalyst (sulphuric acid) and reaction parameters was examined. The results were compared with the performance of ethylene glycol as a solvent under similar conditions. The impact of different biomass; pine needles versus sugarcane bagasse was also investigated.

Sulphuric acid (H_2SO_4) was employed as a homogeneous catalyst in this work owing to its widely reported effectiveness at biomass conversion [110,111,113]. Water at subcritical to near-critical conditions (< 374 °C and < 221 bar) is said [140] to possess excellent properties such as an increase in the solubility of hydrophobic organic compounds like free fatty acids and lignocellulose fragments, which is necessary for the conversion of biomass into valuable platform chemicals. Accordingly, all reactions with water were conducted under 30 bar He initial pressure and at 160 – 300 °C in the autoclave reactor (Section 3.5.2). These parameters resulted in operating/reaction pressures ranging between 60 - 90 bar, thus certifying water remains in a liquid state. The same parameters were employed for the application of ethylene glycol as solvent to ensure a common basis of comparison. Finally, the potential for achieving similar results in a reflux set-up (Section 3.5.1) under milder conditions (atmospheric pressure) using ethylene glycol as liquefaction solvent was investigated.

6.2 Methods

For this work, 2 g of biomass along with 20 g of liquefaction solvent (either water or ethylene glycol) was used. 0.12 g - 0.2 g of H_2SO_4, equivalent to 0.6 - 1 wt.% of liquefaction solvent was employed as catalyst. The atmospheric pressure liquefaction was carried out using ethylene glycol as liquefaction solvent in the reflux set-up described in Section 3.5.1, while the moderate pressure liquefaction was undertaken using water and

ethylene glycol as liquefaction solvents in the autoclave reactor described in Section 3.5.2. A comprehensive explanation of the biomass liquefaction protocols, product separation, and analysis, as well as conversion calculations are documented in Sections 3.5.1 to 3.5.6. Nonetheless, Figure 6.1 provides a summary of the entire process. Selected liquid samples from the water system were subjected to HPLC analysis to determine the existence of non-volatile products such as sugars.

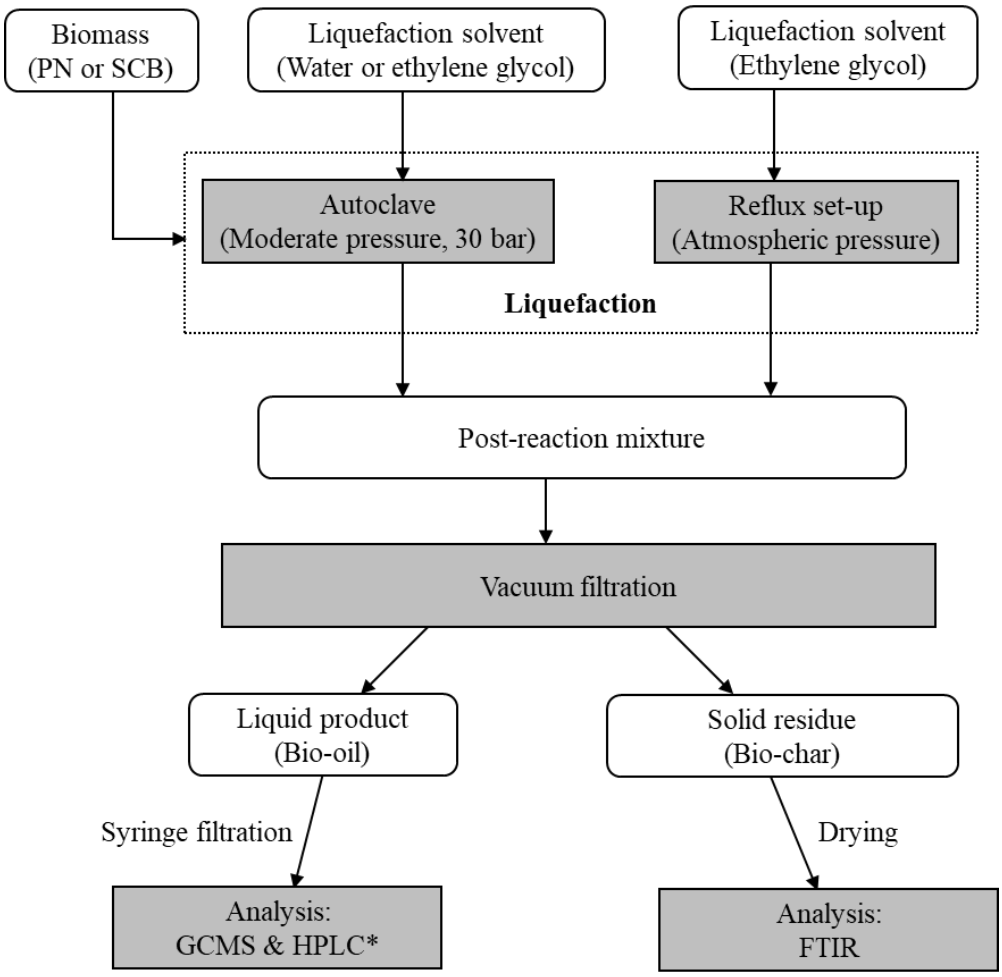

Figure 6.1: *Flow chart for biomass liquefaction studies. *HPLC analysis was conducted on liquid products obtained from the water system only.*

6.3 Results and discussion

6.3.1 Effect of catalyst

Catalysts are generally thought to facilitate many of the reaction steps that occur during the liquefaction process; e.g. cracking, hydrogenation, acceleration of the water-gas shift reaction to the formation of hydrogen and consequently suppressing char formation [133–135]. The application of H_2SO_4 as a catalyst is understood to depolymerise lignocellulose into its monomeric units thereby boosting the extent of reaction [3,110].

A sample distribution of compounds synthesised via the catalytic hydrothermal liquefaction of pine needles in this work is shown in Figure 6.2. Figure 6.3 compares the conversion of pine needles and the quantified results of key chemicals identified in the liquid products. The full distribution of products was later considered in detail in Section 6.3.2.2. Figure 6.4 compares the FTIR spectra of the resultant bio-chars.

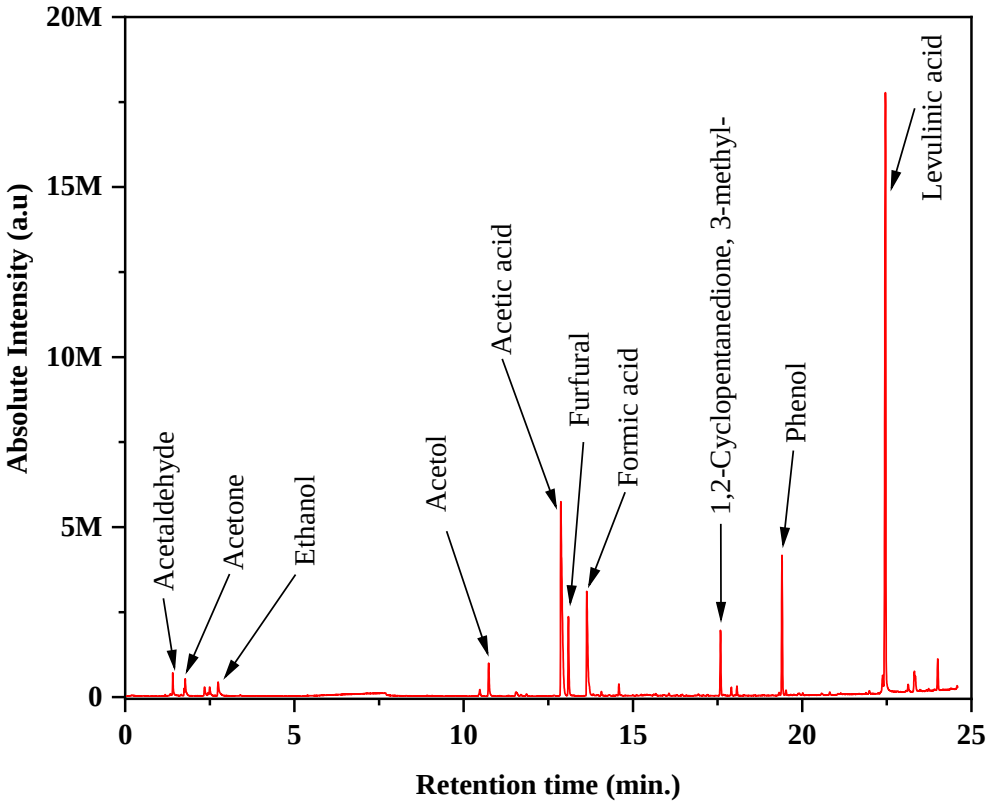

Figure 6.2: *Sample GCMS chromatogram of the liquid product obtained from the catalytic hydrothermal liquefaction of pine needles. Conditions:2 g pine needles, 20 g water, 1 wt.% catalyst, 160 °C, 30 bar He initial pressure, 300 rpm, 1 h.*

Under the same conditions of 250 °C, 30 bar He and 1 h, the addition of 1 wt.% catalyst did not have any significant impact on biomass conversion. As such, 72 wt.% pine needles conversion was achieved in the presence of the catalyst, similar to 76 wt.% in the non-catalytic process (Figure 6.3). The little impact of catalyst on biomass conversion might be due to the low concentration used in this work. The introduction of 1wt.% H_2SO_4 in the liquefaction of bamboo shoot shell by Ye and his co-workers [110] resulted in 45 wt.% conversion (based on biomass dry weight) while this value improved to 99 wt.% when the concentration of H_2SO_4 was increased to ≥ 2 wt.%.

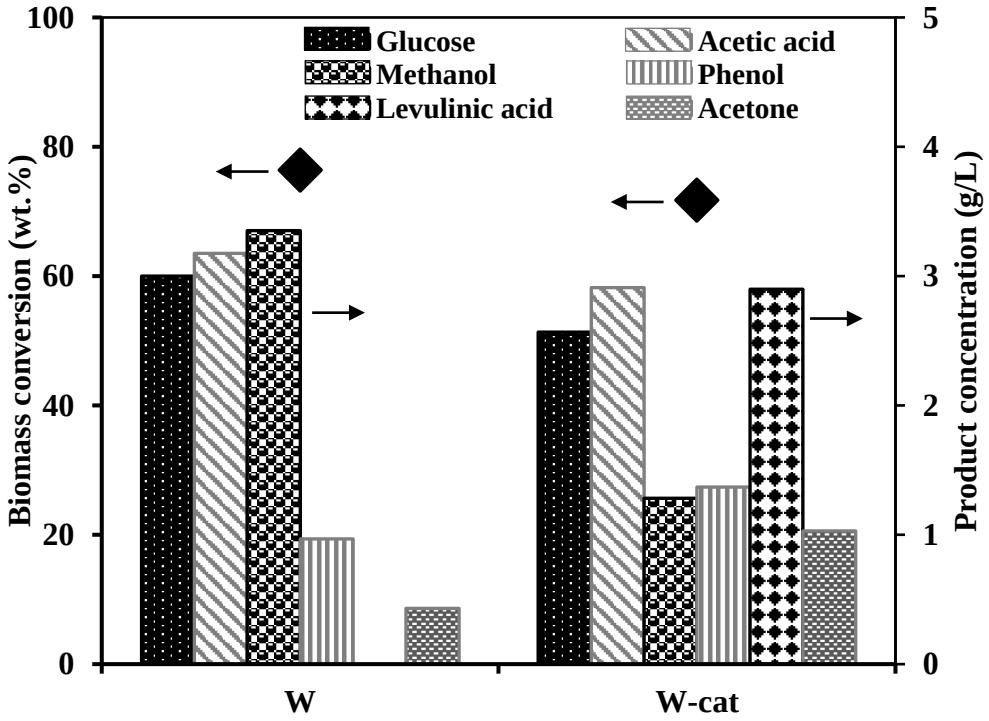

Figure 6.3: *Effect of catalyst on biomass (pine needles) conversion and key compounds identified (GCMS cum HPLC) in the liquid product. 20 g water 1 wt.% catalyst (where applicable) at 250 °C, 30 bar He initial pressure, 300 rpm, 1 h.*

Nevertheless, the composition of the liquid product was altered by the introduction of catalyst. In the absence of catalyst, the most abundant component was methanol, whereas levulinic acid became the most abundant component in the presence of catalyst. Specifically, the concentration of methanol was reduced by almost two-thirds from 3.4 g/L in the absence of a catalyst to 1.3 g/L in the presence of catalyst while 2.9 g/L of levulinic acid was formed. Note that levulinic acid was not detected in the absence of catalyst. The measured pH of water with 1 wt.% H_2SO_4 was ~5, and levulinic acid is a

polysaccharide derived product, normally formed via an acid catalysed hydrolysis process [266]. Therefore, the decrease in pH of the liquefaction solvent from 7 in the absence of catalyst to ~5 in the presence of catalyst potentially facilitated the hydrolysis of polysaccharides to levulinic acid. Thus, the slight drop in glucose concentration from 3.0 g/L (without catalyst) to 2.6 g/L (with catalyst) could be partly ascribed to its consumption in the production of levulinic acid as demonstrated in Scheme 6.1. A more universal proposed route for the conversion of lignocellulosic biomass to other chemicals identified here was earlier illustrated in Chapter 5 (Scheme 5.3). Acetone concentration was doubled from 0.4 g/L to 1 g/L in the presence of catalyst while phenol concentration was also enhanced from 1 g/L to 1.4 g/L. The increase in concentration of acetone and phenol could be the result of better decomposition of biomass fragments under the action of the catalyst.

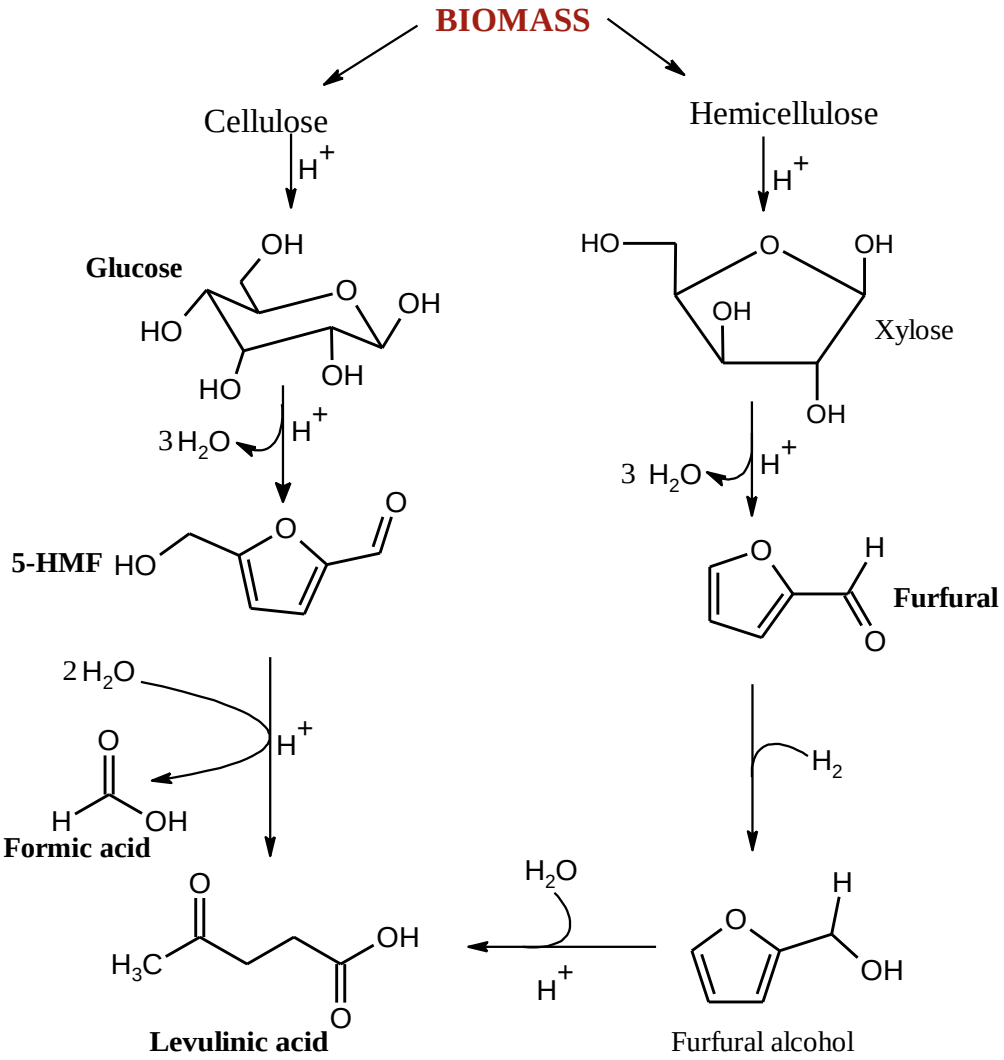

Scheme 6.1: *Proposed reaction pathway to the formation of levulinic acid and other products. Adapted from Liu et al.* [269]. *Detected products in bold.*

The FTIR spectra of the bio-chars (Figure 6.4) display no major difference in terms of lignocellulose structure degradation. Yet, the CH_2 wagging or C-O vibration of lignin (1315 cm^{-1}) which could not degrade in water was completely broken down when the catalyst was added to the process. Of interest in both systems is the complete disappearance of the C-O-C β-glycosidic linkages at 893 cm^{-1} and other cellulose functional groups. The breakage of the C-O-C β-glycosidic linkages and other carbohydrate C-O bonds designate an effective deconstruction of cellulose and hemicellulose into their respective monomeric units; glucose and xylose. This explains the presence of glucose and other carbohydrate derivatives in the liquid fraction. More so, the disintegration of various hemicellulose bonds including 1734 cm^{-1} could be responsible for the existence of acetic acid, furfural, and levulinic acid in the liquid phase products of the water liquefied biomass. Previous works suggest that furfural, acetic acid, levulinic acid, and hydroxymethylfurfural are produced from the breakdown of hexoses and pentoses during thermochemical pretreatments of lignocellulose [126,270,271] as demonstrated in Scheme 6.1.

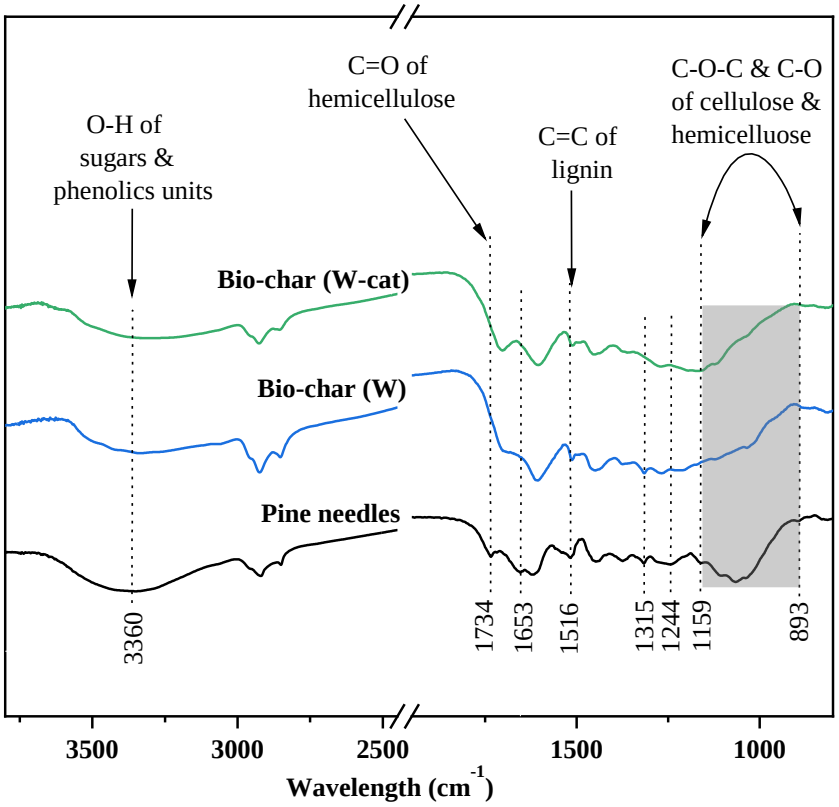

Figure 6.4: *FTIR spectra of bio-chars obtained from pine needles via catalytic (W-cat) vs non-catalytic (W) hydrothermal liquefaction. Conditions: 2 g pine needles, 20 g water, 1 wt.% catalyst (where applicable) at 250 °C, 30 bar He initial pressure, 300 rpm, 1 h.*

6.3.2 Effect of temperature

6.3.2.1 Biomass conversion

An increase in temperature was found to favour biomass conversion during liquefaction. Pine needles conversion increased steadily from 52 wt.% to 72 wt.% when the liquefaction temperature was raised from 160 to 250 °C (Figure 6.5). A further increase in temperature from 250 to 300 °C however, reduced the pine needles conversion slightly to 66 wt.%. Biomass needs to be heated up to promote bond cleavage [140] hence, higher temperatures improve the rate of depolymerisation and cracking of the lignocellulosic components from the biomass matrix structure [120]. Besides, increasing temperature could boost the solvent power of water, thus enhancing the solubility of the decomposed biomass fragments, leading to an increase in biomass conversion.

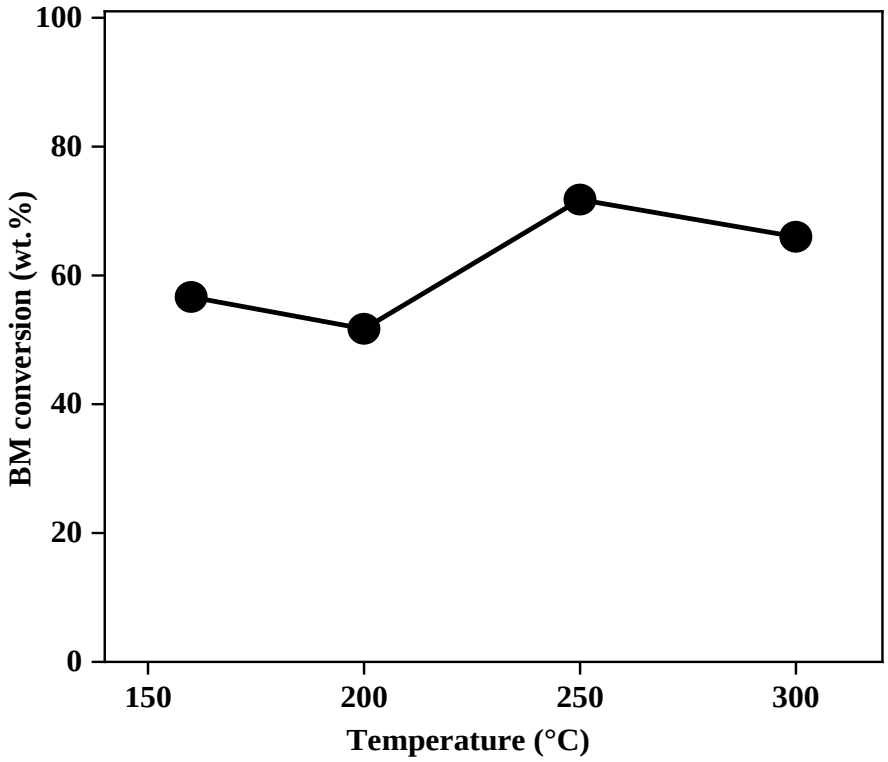

Figure 6.5: *Effect of temperature on pine needles conversion during catalytic hydrothermal liquefaction. Conditions: 2 g pine needles, 20 g water,1 wt.% catalyst, 30 bar He initial pressure, 300 rpm, 1 h. Shown fits are to guide the eye only.*

According to previous investigations [133,140], heated water can act concurrently as a reactant and a catalyst. The presence of water as a reactant leads to hydrolysis reactions and the polymeric structure's degradation for the biomass occurs quickly. Water splits into H^+ and OH^- ions during hydrolysis, with the dissociation increasing rapidly with the increase of temperature [140,269]. For example, the water dissociation constant at 300 °C is about 500 times higher than that at ambient conditions. This results in an increasing rate of both acid and base-catalysed reactions in water, far beyond the natural acceleration [140], leading to a significant increase in the solubility of hydrophobic organic compounds such as free fatty acids. While many biomass compounds such as cellulose and lignin, are not water-soluble at ambient conditions, most are readily solubilised in subcritical or supercritical water [35]. Such biomacromolecules are subjected to a hydrolytic attack, engendering fragmentation and dissolution by water in the near-critical and supercritical regions up to total miscibility leading to an effective biomass decomposition and conversion.

Extensive biomass depolymerisation normally occurs at sufficiently high temperatures, larger than the activation energies for the bond cleavage [118]. This increase both the concentration of free radicals and the probability of repolymerisation of fragmented species. The competition among hydrolysis, fragmentation and repolymerisation reactions defines the role of temperature during liquefaction [118]. Research has disclosed that hydrolysis and repolymerisation occurred simultaneously during liquefaction [272,273]. Depolymerisation of biomass is perceived to be the dominant reaction during the initial stages of liquefaction, where the biomass is decomposed to lighter fragments. These fragments (usually unstable) form new compounds through rearrangements such as condensation, cyclisation, and polymerisation [30]. Repolymerisation is typically active at later stages leading to the formation of char [118]. Thus, the slight drop in biomass conversion at 300 °C could indicate the onset of repolymerisation of fragmented species to char.

6.3.2.2 Product distribution

Table 6.1 displays the full distribution of products at various temperatures. While the effect of temperature on the concentration of the major compounds is considered in Section 6.3.2.3. GCMS analysis of the liquid products obtained from the catalytic hydrothermal liquefaction of pine needles indicates the presence of a variety of organic acids, ketones, alcohols, aldehydes, and phenolics which is consistent with products derived from other biomasses by other researchers [14,134]. Levulinic acid is the dominant product at all temperatures (≤ 45 %) followed by acetic acid (≤ 23 %) and phenol (≤ 17 %), based on peak area. Proposed reaction routes to the synthesis of the identified chemicals (in Table 6.1) from lignocellulosic biomass was earlier shown in Chapter 5 (Scheme 5.3); illustrating pathways for the conversion of cellulose, hemicellulose and lignin towards these chemicals.

Carbohydrates are known to degrade along two main pathways in hot-compressed water; dehydration and retro-aldol condensation. As observed in other studies, the compounds observed in the liquid products, suggest that glucose and xylose follow the dehydration pathway, leading to structures such as furfural and 5-hydroxymethylfurfural (5-HMF) [14,134]. At higher temperatures furfurals undergo decarbonylation losing oxygen and carbon causing a decrease in carbon chain number, or dehydration [266] leading ultimately to the formation of lower molecular weight compounds. According to Pedersen & Rosendahl [266], retro-aldol reactions of sugars are known to produce such short-chained compounds and often found in the water phase, mainly in the form of aldehydes, alcohols, and ketones. These reactions are normally promoted by near-critical or super-critical conditions [274]. Indeed, the liquid product compositions shown in Table 6.1 illustrates this through the sudden disappearance of furfural and 5-HMF and an increase in the formation of simple compounds like acetone, 2-butanone, and acetaldehyde as temperature increases beyond 160 °C. It is also believed that carboxylic acids are also converted to ketones under similar conditions, which could perhaps explain the disappearance of formic acid and appearance of cyclopentenones at temperatures above 200 °C.

Table 6.1: *GCMS identified chemicals in the liquid product obtained from the catalytic hydrothermal liquefaction of pine needles at various temperatures. Conditions: 2 g pine needles, 20 g water, 1 wt.% catalyst, 30 bar He initial pressure, 300 rpm, 1 h.*

	RT* (min)	Name	Formula	Peak area (%)			
				160 (°C)	200 (°C)	250 (°C)	300 (°C)
1	1.41	Acetaldehyde	C_2H_4O	1.0	1.2	2.2	2.0
2	1.66	Propanal	C_3H_6O	-	-	0.4	0.5
3	1.74	2-methylpropanal	C_4H_8O	-	-	1.0	1.0
4	1.77	Acetone	C_3H_6O	1.0	1.6	3.7	4.9
5	2.34	2-butanone	C_4H_8O	0.7	1.4	2.7	3.2
6	2.44	2-methylbutanal	$C_5H_{10}O$	-	-	0.6	0.5
7	2.50	3-methylbutanal	$C_5H_{10}O$	0.6	1.1	2.2	1.6
8	2.75	Ethanol	C_2H_6O	1.4	-	-	1.4
9	10.48	Acetoin	$C_4H_8O_2$	0.5	0.7	0.2	-
10	10.74	1-hydroxy-2-propanone	$C_3H_6O_2$	2.2	2.1	-	-
11	11.51	2-cyclopenten-1-one	C_5H_6O	-	-	1.1	0.9
12	11.65	2-methyl-2-cyclopenten-1-one	C_6H_8O	-	-	2.3	2.2
13	12.87	Acetic acid	$C_2H_4O_2$	21.0	21.9	22.7	21.6
14	13.09	Furfural	$C_5H_4O_2$	4.5	-	-	-
15	13.64	Formic acid	CH_2O_2	9.2	2.1	-	-
16	14.04	Propanoic acid	$C_3H_6O_2$	-	-	0.7	0.7
17	14.59	5-methyl-2-furancarboxaldehyde	$C_6H_6O_2$	0.7	-	-	-
18	17.59	3-methyl-1,2-cyclopentanedione	$C_6H_8O_2$	3.6	3.8	1.4	-
19	17.91	2-methoxyphenol	$C_7H_8O_2$	0.4	1.0	2.8	3.3
20	18.07	Benzyl alcohol	C_7H_8O	0.5	0.4	-	-
21	19.40	Phenol	C_6H_6O	8.0	13.4	17.1	16.6
22	19.91	2-pyrrolidinone	C_4H_7NO	-	-	-	0.7
23	20.17	Cresol	C_7H_8O	-	-	-	0.8
24	21.05	4-ethylphenol	$C_8H_{10}O$	-	-	-	0.5
25	22.46	Levulinic acid	$C_5H_8O_3$	42.6	44.8	33.9	25.3
26	23.13	6-methyl-3-pyridinol	C_6H_7NO	-	-	-	1.0
27	23.31	3-pyridinol	C_5H_5NO	-	-	-	4.1
28	24.01	5-hydroxymethylfurfural	$C_6H_6O_3$	1.8	-	-	-
29	25.61	Catechol	$C_6H_6O_2$	-	-	1.5	3.4
30	29.43	4-hydroxyacetophenone	$C_8H_8O_2$	-	4.6	3.7	3.1
		Total area (%)		***100***	***100***	***100***	***100***

**Note: slight changes in retention time (RT) for the same chemical recorded in previous tables or subsequent tables are due to changes in column length. The tip of the column is normally trimmed occasionally to reduce contamination and ghost peaks from accumulated dirt. This normally results in slight retention time shifts.*

Lignin decomposition, on the other hand, is thought to occur through cleavage reactions or by hydrolysis of ether-bonds forming chiefly oxygenated aromatic derivatives [266], such as phenol and 2-methoxyphenol. These reactions usually progress at temperatures

higher than the cellulose and hemicellulose decomposition reactions. In consequence, the area percentage of phenol, the main lignin derivative in Table 6.1 doubled from 8 % at 160 °C, to 17 % at temperatures beyond 200 °C. This is in agreement with the earlier TGA results in Chapter 4 (Section 4.3.1), which indicates that effective lignin decomposition occurs between 188 to 600 °C. Detailed research conducted by Nasir [14] on the liquefaction of commercial lignin and cellulose also confirmed that the decomposition of lignin to liquid products is favoured by higher reaction temperatures and time compared to cellulose. Under the same conditions of 250 °C and 30 bar He (initial pressure), Nasir reported that the optimum time for the formation of target liquid products was 30 min for cellulose against 120 min for lignin.

6.3.2.3 Concentration of targeted products

Note that glucose was not included in Figure 6.6 because its concentration was not determined in all samples. Nonetheless, the HPLC analysis carried out on samples made at 160 °C and 250 °C contained 1.7 g/L and 2.7 g/L of glucose respectively.

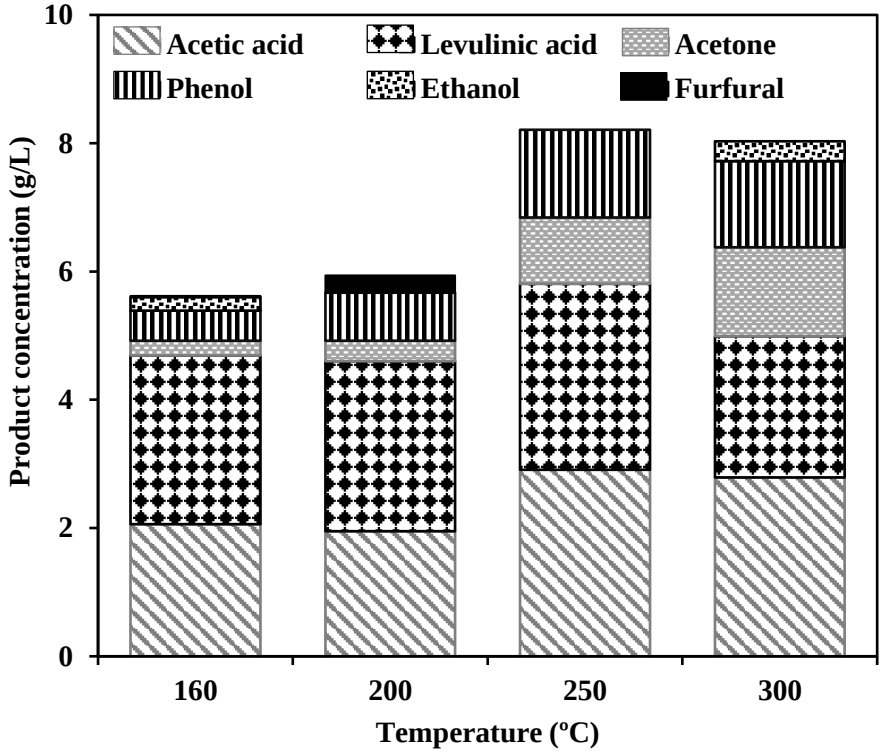

Figure 6.6: *Effect of temperature on biomass conversion and concentration of key GCMS identified compounds in the liquid product obtained via catalytic hydrothermal liquefaction of pine needles. Conditions: 2 g pine needles, 20g water, 1 wt.% catalyst, 30 bar He initial pressure, 300 rpm, 1 h.*

The cumulative concentration of the main GCMS identified species displays a steady increase from 5.62 g/L at 160 °C to 8.21 g/L at 250 °C and remained almost unchanged at 300 °C. Such observation might be a result of better lignocellulose depolymerisation in consequence of the high pressure from the liquefaction solvent at temperatures beyond 200 °C aiding easy decomposition of glycosidic and etheric bonds [34]. As such, the concentrations of almost all products were significantly enhanced at temperatures greater than 200 °C. Specifically, the concentrations of acetone and phenol were doubled to 1.4 g/L each at temperatures > 200 °C. The production of phenol, a known lignin derivative is undoubtedly favoured by higher temperatures, since effective lignin degradation occurs relatively slowly, over a wider temperature range than the cellulose and hemicellulose components of biomass. Acetic acid and levulinic acid, in contrast, are derivatives of cellulosic biomass [275,276] which are sufficiently hydrolysed even at the starting temperature of 160 °C; as such, acetic acid (up to 3 g/L) and levulinic acid (up to 3 g/L) are the dominant products at all temperatures with a combined relative concentration of approximately 70 %, based on Figure 6.6. Levulinic acid is an important precursor to biofuels, biodegradable herbicide and a variety of pharmaceuticals [277].

In summary, 250 °C was found to be the optimum temperature for both biomass conversion and yield of targeted products. At this temperature, pine needles conversion was 72 wt.%, leading to the formation of 3 g/L acetic acid, 3 g/L levulinic acid, 2.7 g/L glucose, 1.4 g/L phenol, and 1 g/L acetone.

6.3.3 Effect of liquefaction solvent (water versus ethylene glycol)

In this section, ethylene glycol (EG) was used as a liquefaction solvent under the same conditions previously studied and the results compared with the water (W) system as discussed *vide infra*.

6.3.3.1 Biomass conversion

Higher biomass conversion is attained in the presence of ethylene glycol over water at all temperatures as illustrated in Figure 6.7. For instance, at the optimum temperature of 250 °C, pine needles conversion recorded in ethylene glycol is 86 wt.% compared to 72 wt.% in water; a difference of 14 wt.%. This improvement could be ascribed to ethylene glycol's higher ability to degrade lignin as explained *vide infra*.

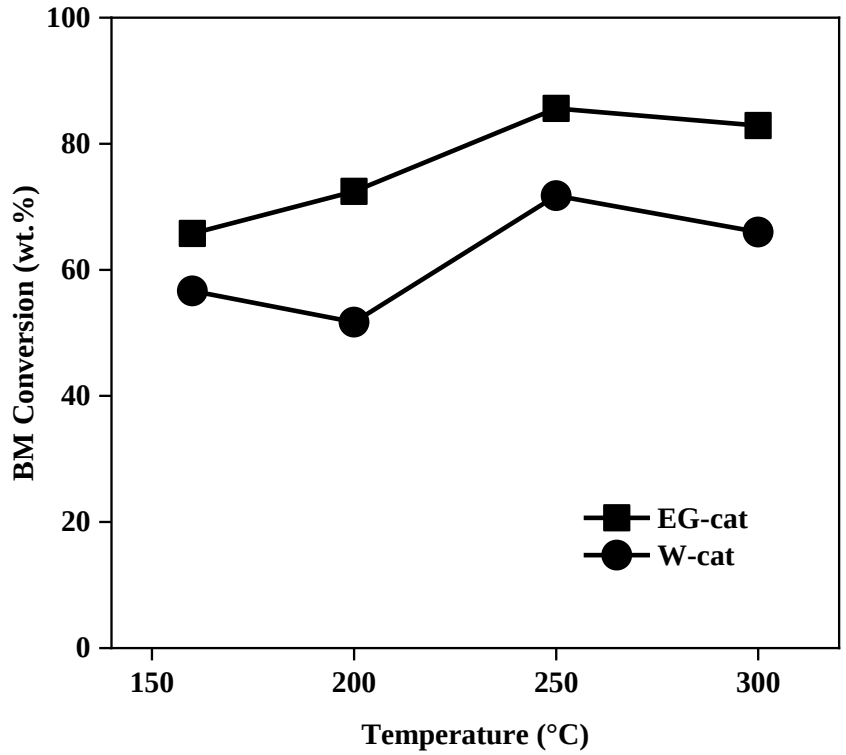

Figure 6.7: *Effect of liquefaction solvent on pine needles conversion. Conditions: 2 g pine needles, 20 g solvent, 1 wt.% catalyst (cat), 30 bar He initial pressure, 300 rpm, 1 h. Shown fits are to guide the eye only.*

Figure 6.8 illustrates the effect of liquefaction solvents on the chemical structure of pine needles. Significant decomposition of all three polymer constituents of lignocellulose is noticeable in the bio-char obtained from the ethylene glycol system. Comparatively, there is a better decomposition of lignin (at 1516 cm^{-1}) in the presence of ethylene glycol over water. Therefore, the liquid product from the ethylene glycol should hypothetically contain higher concentrations of aromatic species. Similarly, the ethylene glycol derived bio-char contains very little to none of the O-H functional group of sugars and phenolic units (3360 cm^{-1}) whereas the water derived bio-char contains a little more of this functional group. Hemicellulose on the other hand, is less effectively degraded in the ethylene glycol as could be seen from the fingerprint band at 1734 cm^{-1}.

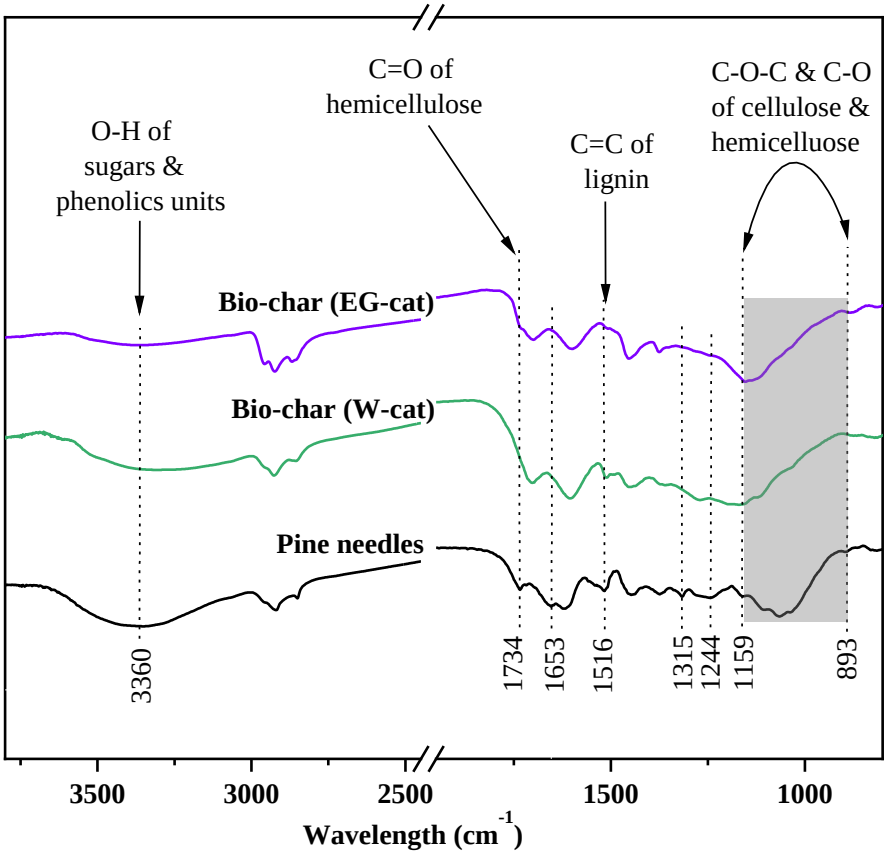

Figure 6.8: *FTIR spectra of bio-chars obtained via catalytic liquefaction of pine needles with water (W-cat) and ethylene glycol (EG-cat). Conditions: 2 g pine needles, 20 g solvent, 1 wt.% catalyst, 250 °C, 30 bar He initial pressure, 300 rpm, 1 h.*

Overall, we can understand that water facilitates a more effective decomposition of hemicellulose and cellulose whereas ethylene glycol facilitates a better decomposition of lignin and cellulose. The higher biomass conversion by ethylene glycol is potentially owed to its ability to deconstruct lignin. As earlier established in Chapter 5, the extent of lignin decomposition during liquefaction directly relates to biomass conversion; as such, solvents with higher lignin deconstruction ability would theoretically yield low post liquefaction residues. The ability of ethylene glycol to deconstruct lignin is much like glycerol; both solvents are polyhydric alcohols with similar properties such as high boiling points. In this work, both solvents were found to participate in similar reaction pathways leading to the generation of water and hydrogen. The donor-hydrogen is believed to stabilise biomass-derived radicals, reduce or saturate reactive compounds and hence reduces the amount of char/residue formed during liquefaction [130]. The reaction pathways to the formation of hydrogen from ethylene glycol are considered in Section 6.3.3.2.

6.3.3.2 Distribution of products

Ethylene glycol as liquefaction solvent

Like glycerol, ethylene glycol was found to participate in a series of side reactions leading to the formation of various value-added chemicals. The full list of compounds identified in a blank/control experiment (without biomass) conducted with ethylene glycol at 250 °C is published in Appendix C (Table C1). Nevertheless, Scheme 6.2 demonstrates proposed reaction routes to the formation of the key compounds identified. The dominant products were glycols which are condensation products of ethylene glycol e.g. diethylene glycol and triethylene glycol, typically promoted in the presence of an acid catalyst. These reactions release water molecules that could aid the hydrolysis of biomass or participate in the water-gas shift reaction with biomass generated CO [278] to form hydrogen for various hydrogenation and hydrogenolysis reactions. Other key routes are the formation of dimethyl acetal, 2-ethoxyethanol and acetic acid which are thought to; involve the transfer of or release hydrogen for the propagation of various biomass liquefaction reactions. The formation of acetic acid from ethylene glycol may contribute to the cumulative concentration of acetic acid obtained via biomass liquefaction.

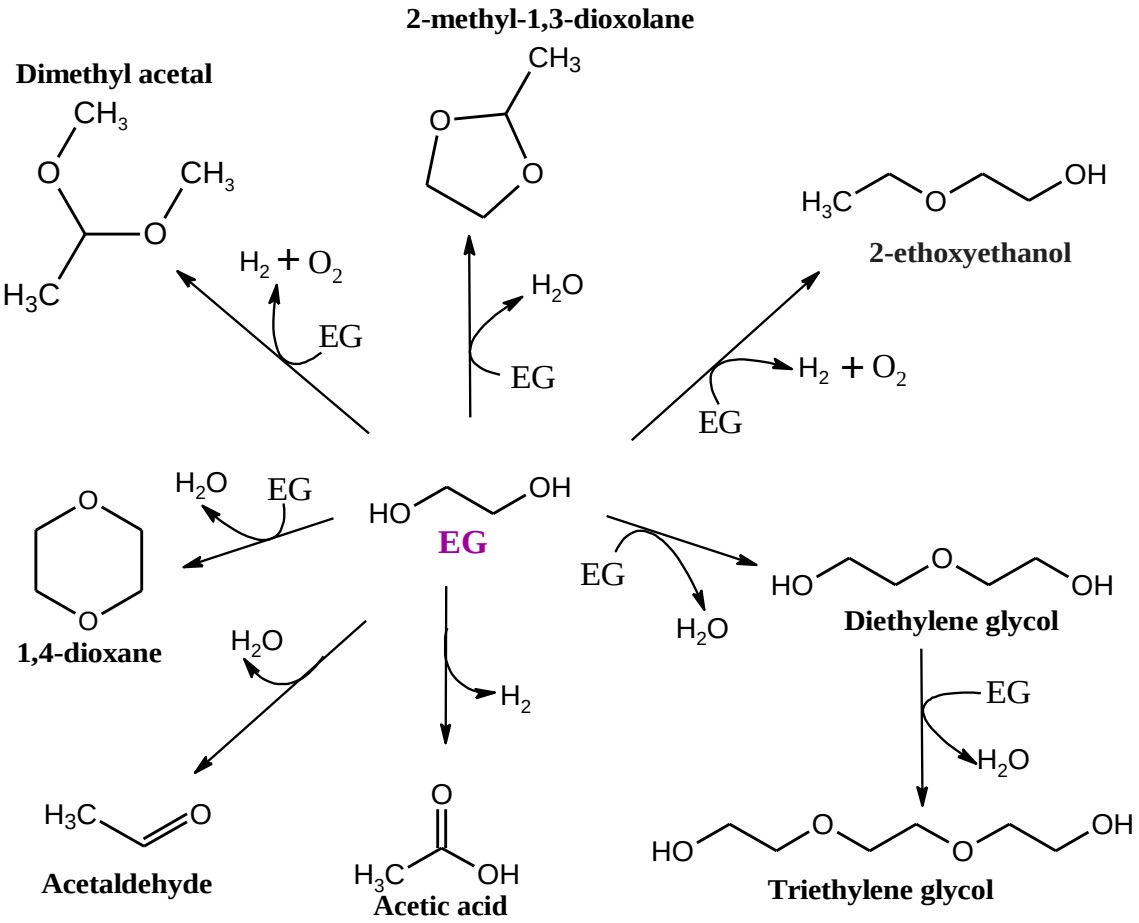

Scheme 6.2: *Plausible routes for the conversion of ethylene glycol to useful chemicals. Conditions: 20 g ethylene glycol, 0.12 g H_2SO_4 as catalyst (1 wt.% catalyst), 30 bar He initial pressure, 300 rpm and 1 h.*

Ethylene glycol versus water

A more comprehensive list of compounds identified at various temperatures in the ethylene glycol system is available in Appendix C (Table C1). However, for this discussion, Table 6.2 documents a sample list of compounds identified in the liquid product obtained via the liquefaction of pine needles with ethylene glycol versus water. Photographs of sample products obtained in the process are captured in Appendix C (Figure C1). Both liquid products are made up of a variety of chemicals including ketones, organic acids, and aromatics with the product from the ethylene glycol (EG) system containing additional glycols and esters. Similar to water, ethylene glycol plays a dual role, as a solvent and reactant during biomass liquefaction. It is perceived to react with biomass fragments and intermediate products to form esters and ketals e.g. ethyl levulinate, ethyl lactate and 2-hydroxyethyl levulinate ethylene ketal (HLEK). It is

understood from past investigations [126,127] that levulinic acid is particularly a favourable biomass intermediate/product that initiates the esterification and ketalisation reaction as demonstrated in Scheme 6.3.

Table 6.2: *Effect of liquefaction solvent on the distribution of compounds identified in the liquid product obtained from the catalytic liquefaction of pine needles. 2 g pine needles, 20 g solvent, 1 wt.% catalyst, 200 °C, 30 bar He initial pressure, 300 rpm, 1 h.*

SN	RT (min)	Name	Formula	Peak area (%)	
				EG	W
1	1.40	Acetaldehyde	C_2H_4O	-	1.2
2	1.67	Dimethyl acetal	$C_4H_{10}O_2$	0.5	-
3	1.78	Acetone	C_3H_6O	-	1.6
4	2.34	2-butanone	C_4H_8O	-	1.4
5	3.00	2-methyl-1,3-dioxolane	$C_4H_8O_2$	2.4	-
6	5.24	1,4-dioxane	$C_4H_8O_2$	1.8	-
7	8.15	2-methoxyethanol	$C_3H_8O_2$	0.2	-
8	9.03	2-ethoxyethanol	$C_4H_{10}O_2$	0.1	-
9	10.28	Acetoin	$C_4H_8O_2$	-	0.7
10	12.82	Acetic acid	$C_2H_4O_2$	0.1	21.9
11	16.02	Ethyl lactate	$C_5H_{10}O_3$	0.2	-
12	18.80	2-(2-hydroxyethoxy)ethyl acetate	$C_6H_{12}O_4$	0.6	-
13	19.07	Diethylene glycol	$C_4H_{10}O_3$	60.1	-
14	19.38	Phenol	C_6H_6O	0.1	13.4
15	19.50	2-[2-(2-ethoxyethoxy)ethoxy]ethanol	$C_8H_{18}O_4$	0.2	-
16	22.38	Levulinic acid	$C_5H_8O_3$	0.1	44.8
17	22.45	Triethylene glycol	$C_6H_{14}O_4$	22.6	-
18	24.18	2-hydroxyethyl levulinate ethylene ketal	$C_9H_{16}O_5$	0.5	-
19	25.68	Tetraethylene glycol	$C_8H_{18}O_5$	4.4	-
20	29.32	4-hydroxyacetophenone	$C_8H_8O_2$	0.3	4.6
		Total area (%)		***94***	***90***

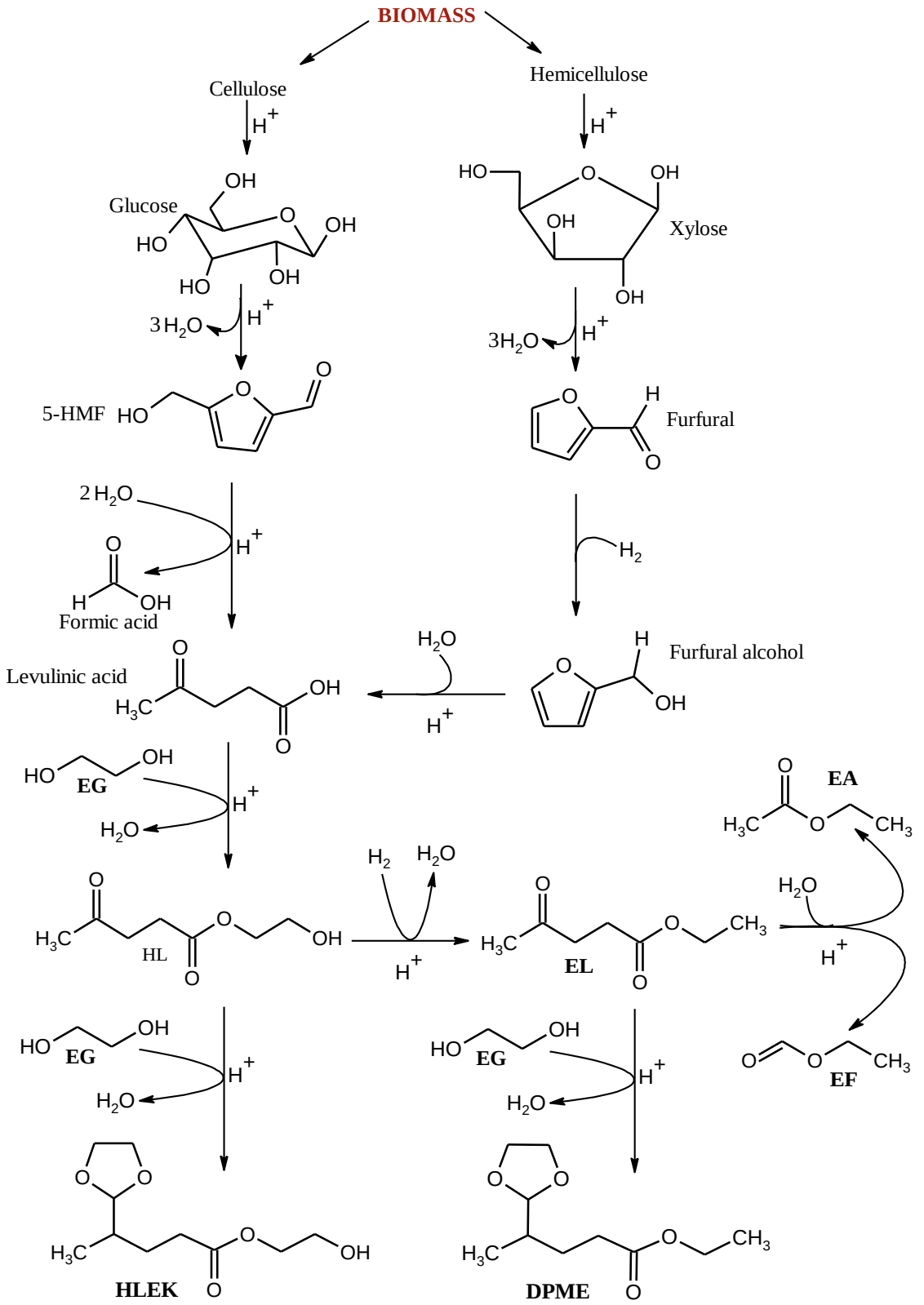

Scheme 6.3: *Proposed reaction pathways for the formation of various esters and ketals via acid catalysed liquefaction of biomass with ethylene glycol, adapted from Amarasekara and Wiredu* [126]. *Note: HL is 2-hydroxyethyl levulinate; ethyl levulinate (EL); 2-hydroxyethyl levulinate ethylene ketal (HLEK); ethyl 3-(2-methyl-1,3-dioxolan-2-yl)propanoate (DPME); ethyl formate (EF); and ethyl acetate (EA).*

Thus, the reaction pathway in both solvents is essentially the same at the beginning where the lignocellulose is somehow fragmented. The cellulose and hemicellulose components of the biomass are then hydrolysed into their respective key monomers; glucose, and xylose [279,280]. Glucose and xylose then undergo a sequence of acid catalysed dehydration and rehydration reactions to form levulinic acid, and other polysaccharide derivatives [126,127,279,280]. Levulinic acid is largely stable in water, whereas in the ethylene glycol system, it is subsequently esterified by ethylene glycol to form an intermediate ester, 2-hydroxyethyl levulinate [126,281]. This intermediate compound then participates in two parallel paths of reactions; 1) an acid ketalisation reaction with ethylene glycol at the carbonyl functional group to form HLEK [126,127,281]. 2) a hydrogenolysis cum dehydration reaction to ethyl levulinate. Similarly, ethyl levulinate in one route reacts with a molecule of ethylene glycol at the carbonyl group to produce ethyl 3-(2-methyl-1,3-dioxolan-2-yl)propanoate (DPME) while in another route undergoes a hydration cum decomposition reaction to form ethyl formate and ethyl acetate. Lignin, on the other hand, is decomposed into various aromatic compounds, mainly phenol.

The ethylene glycol derived product is largely dominated by the glycols; diethylene glycol, and triethylene glycol. Though these by-products may enhance the value of the entire process, the water system is potentially more advantageous with respect to the selectivity of targeted biomass-derived chemicals. For instance, levulinic acid represents a dominant 45 % of the total peak area of compounds in the water derived product whereas, in the ethylene glycol system, it is only 0.1 %. As such, separation and purification of these targeted products for end-use in the ethylene glycol system might be more challenging and less economical compared to the water system.

6.3.3.3 Concentration of targeted product

The concentration of all major products in the ethylene glycol system could not be determined in this work on a downside. However, the concentration of the top four GCMS identified biomass derivatives in the water system; acetic acid, levulinic acid, acetone, and phenol, were compared with those obtained in the ethylene glycol system as shown in Figure, 6.9. Though the cumulative relative peak area of these four compounds in the ethylene glycol system (up to 15 %) is much lower compared to the water system (up to 80 %), the actual concentration displays a different trend. Apart from levulinic acid, the concentration of acetic acid, acetone, and phenol were generally higher in the presence of ethylene glycol, particularly at 250 °C and 300 °C. For instance, the highest concentration

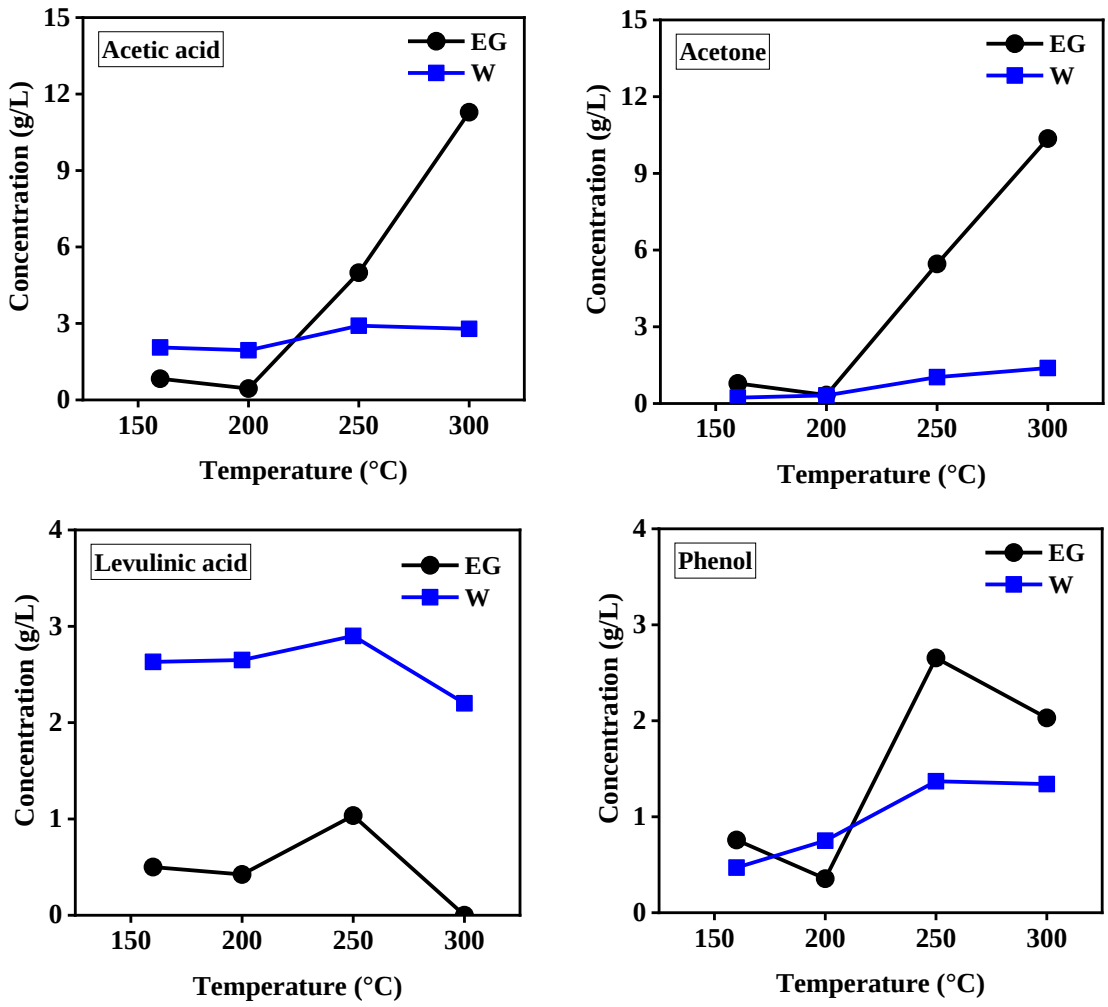

Figure 6.9: *Effect of liquefaction solvent; water (W) and ethylene glycol (EG) on the concentration of acetic acid, acetone, levulinic acid, and phenol at various temperatures. Conditions: 2 g pine needles, 20 g solvent, 1 wt.% catalyst, 30 bar He initial pressure, 300 rpm, 1 h. Shown fits are to guide the eye only.*

of acetic acid (11.2 g/L) and acetone (10.4 g/L) in the ethylene glycol system were 4 to 7 times higher than those obtained in the water system (*i.e.* 2.9 g/L for acetic acid and 1.4 g/L for acetone) at 300 °C. The highest phenol concentration was achieved at 250 °C in the ethylene glycol system is (2.7 g/L) twice that attained in the water system (1.4 g/L). In contrast, the concentration of levulinic acid in the ethylene glycol system (≤ 1.0 g/L) was 3 times lesser than that observed in the water system (≤ 3 g/L) 250 °C. This could be ascribed to the consumption of levulinic acid in the formation of various esters and ketals such as HLEK.

In summary, the choice of liquefaction solvent plays a significant role in biomass conversion as well as the distribution and concentration of the resultant products.

6.3.4 Effect of pressure

The prospect of converting biomass to value-added chemicals at atmospheric pressure was exploited in this section. Ethylene glycol was used as solvent throughout this section because it gave higher biomass conversion, besides, water cannot be heated beyond 100 °C at ambient pressure. The results were compared with those attained under 30 bar of helium (initial pressure) to ascertain the influence of pressure.

6.3.4.1 Biomass and ethylene glycol conversion

Figure 6.10 compares pine needles and ethylene glycol conversions obtained at 160 °C under atmospheric pressure (~1 bar) with those obtained previously under 30 bar He (supply pressure). Pine needles conversion increased from 65 wt.% at 30 bar to 81 wt.% at atmospheric pressure, ethylene glycol conversion, however, remained unaffected at approx. 80 wt. % by pressure variation. This supports an earlier report by Hao *et al.* [127] that ethylene glycol converts glucose in an open atmospheric pressure reaction, rather than a high-pressure one. The decline in biomass conversion at elevated pressure could be explained by a potential solvent cage effect. The degradation of biomass depends upon the breakage of C-C linkages. However, an increase in pressure sometimes results in an increase in local solvent density which causes a cage effect for these bonds. This cage effect inhibits C–C bonds breakage, which ends up in low fragmentations, and therefore low biomass conversion [118].

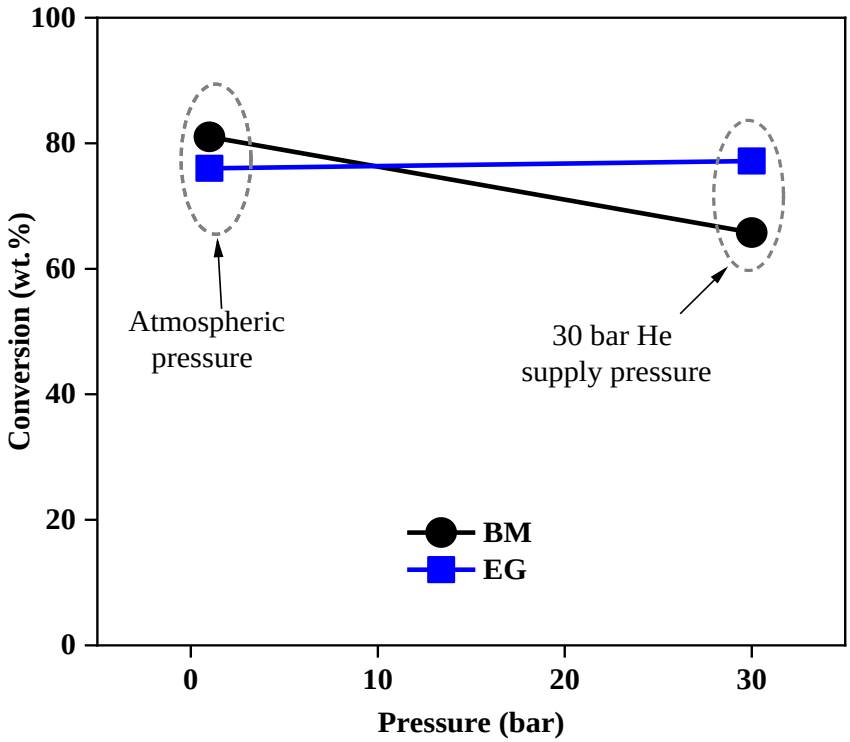

Figure 6.10: *Effect of pressure on pine needles (BM) and ethylene glycol (EG) conversion. Conditions: 2 g pine needles, 20 g ethylene glycol, 1 wt.% catalyst, 160 °C, 300 rpm, 1 h. Shown fits are to guide the eye only.*

6.3.4.2 Product distribution

Under atmospheric pressure, esters are the main chemicals synthesised from biomass apart from the solvent derived glycols as depicted by the sample GCMS chromatogram in Figure 6.11. They include; ethyl formate, ethyl acetate, ethyl levulinate, DPME, and HLEK. Thus the reaction pathway under atmospheric condition is more defined and less complex compared to the pressurised system; narrowing the distribution of products. Earlier in Table 6.2, we observed a wider range of products including ketones, organic acids, phenolics, esters, and glycols in the pressurised system whereas only esters and glycols are observed here in the atmospheric pressure system. Nonetheless, the absence of phenolic compounds in the atmospheric liquefaction system could signify an ineffective lignin valorisation process.

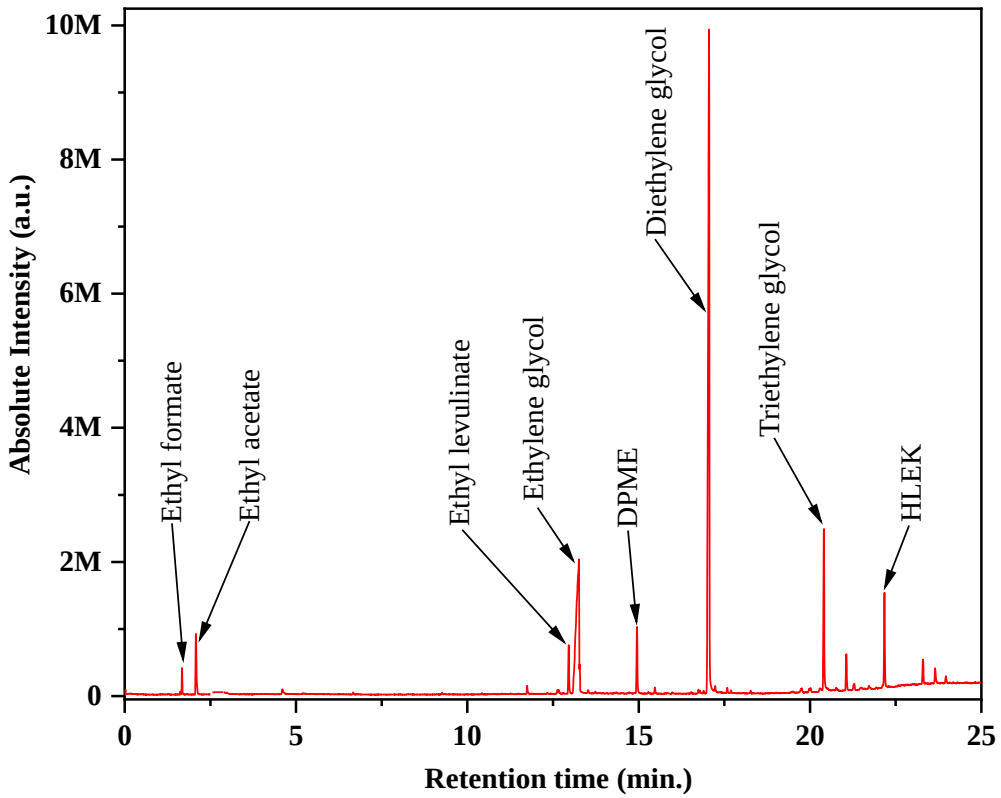

Figure 6.11: *Sample GCMS chromatogram of liquid product obtained via atmospheric liquefaction of biomass.* Conditions: *2 g sugarcane bagasse, 20 g ethylene glycol, 0.6 wt.% catalyst, 160 °C, 300 rpm, 1 h. Note: ethylene glycol represents the left-over reactant.*

6.3.5 Role of different biomass

Biomass type did not play any significant role on the type of compounds synthesised in this study. Under the same conditions of 160 °C, 300 rpm, 1 h, sugarcane bagasse conversion was ~90 wt.% while that of pine needles was ~80 wt.% (Figure 6.12). In terms of biomass-derived chemicals, both feedstocks demonstrate the formation of similar compounds. These are mainly esters, comprising of HLEK, DPME, ethyl levulinate, ethyl formate, and ethyl acetate. All five compounds were detected in the liquefied product of sugarcane bagasse whereas only three of these; HLEK, ethyl formate, and ethyl acetate were found in that of pine needles (Figure 6.13). A thorough quantitative analysis was not conducted on these products, however, HLEK stands out as the main product from both biomass feedstocks (Figure 6.13). Levulinic acid ketals and esters have lately gained attention as polymer additives and biodegradable surfactants [282–284]. Ethyl levulinate, is a popular food flavour [285] and a potential fuel additive [286], for the enhancement of cold flow properties [287]. Common applications of ethyl acetate are; cosmetics and solvent, whereas ethyl formate is also known for its use as solvent and food flavour.

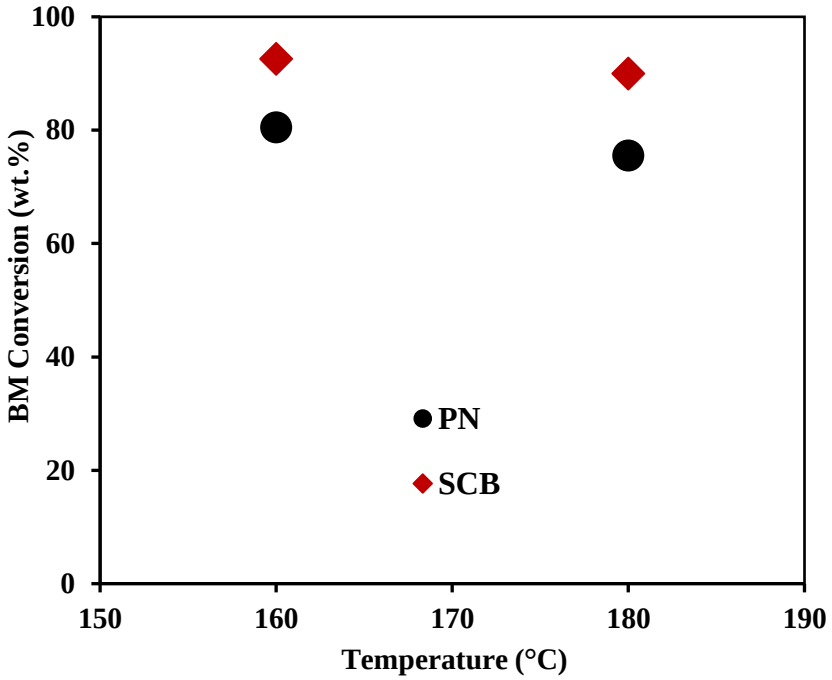

Figure 6.12: *Sugarcane bagasse (SCB) versus pine needles (PN) conversion. Conditions:2 g biomass, 20 g ethylene glycol, 1wt.% catalyst, 300 rpm, atmospheric pressure, 1 h.*

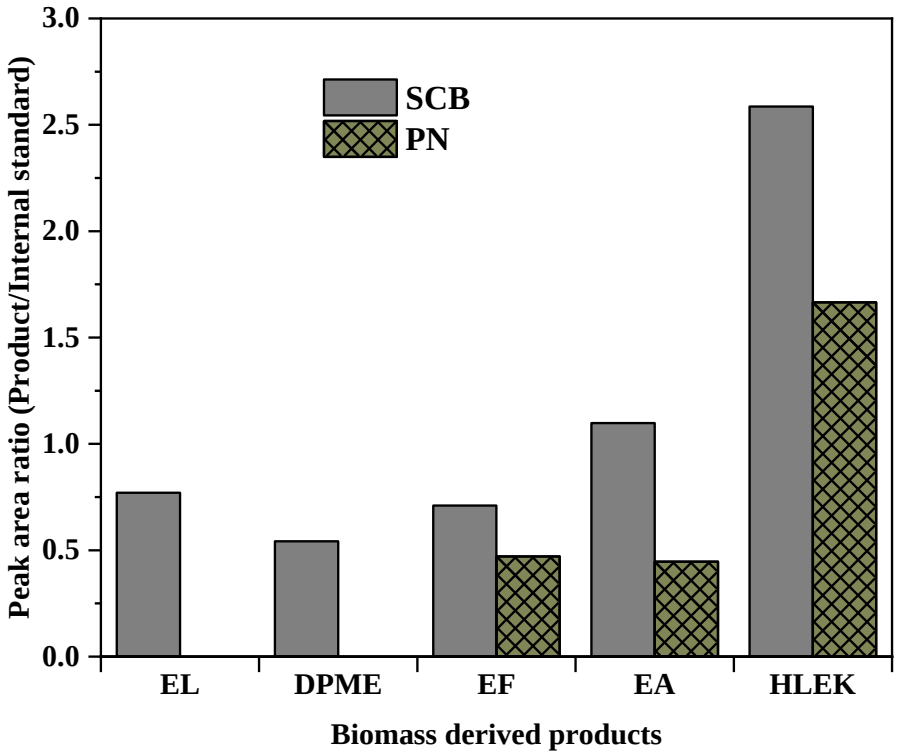

Figure 6.13: *Comparison of biomass derived products from the atmospheric liquefaction of sugarcane bagasse (SCB), and pine needles (PN). Conditions:2 g biomass, 20 g ethylene glycol, 160 °C, 300 rpm, 1 h. 0.6 wt.% and 1 wt.% catalyst were used for SCB, and PN respectively.*

6.4 Conclusion

The catalytic liquefaction of biomass was investigated in this chapter using water and ethylene glycol as liquefaction solvents. Precisely focusing on the influence of catalyst (H_2SO_4), reaction parameters (temperature and pressure), liquefaction solvent, and biomass type (pine needles versus sugarcane bagasse) on biomass conversion and product distribution.

In this work, the application of H_2SO_4 as catalyst (1wt.% of liquefaction solvent) was found to promote the formation of levulinic acid, a major biomass-derived product in the hydrothermal liquefaction process (at 160 – 250 °C), which was not otherwise observed. The introduction of catalyst however, did not play any significant role in biomass conversion. Instead, temperature variation was found to play a key role in both biomass conversion and product distribution. An increase in temperature from 160 – 300 °C largely resulted in an improved biomass conversion as well as an increase in the yield of aromatic and some light organic compounds. For instance, pine needles conversion in ethylene glycol (catalytic) increased from 65 wt.% at 160 °C to ~ 86 wt.% at 250 – 300 °C. Overall, 250 °C was the optimum temperature for both biomass conversion and yield of targeted products for all solvents, at 30 bar. Under these conditions, pine needles conversion via catalytic hydrothermal liquefaction was 72 wt.%, leading to the formation of 3 g/L acetic acid, 3 g/L levulinic acid, 2.7 g/L glucose, 1.4 g/L phenol, and 1 g/L acetone.

Under elevated pressure of 30 bar, both solvents (water and ethylene glycol) were found to facilitate the degradation of the three constituents of the lignocellulose matrix to the synthesis of a variety of organic compounds. However, ethylene glycol was observed to be more effective at lignin decomposition than water resulting in higher biomass conversion across all studied conditions; as such, the highest pine needles conversion of 86 wt.% was recorded at 250 °C in the ethylene glycol system, higher than the 72 wt.% achieved in the presence of water. In this thesis, ethylene glycol is perceived to work in a similar fashion as glycerol; releasing water and hydrogen for various biomass hydrolysis and hydrogenation/hydrogenolysis steps through various side dehydration/condensation and decomposition routes. Water is also a known hydrogen donor solvent via the water-gas shift reaction.

It was understood that the application of water and ethylene glycol in biomass liquefaction follow the same reaction pathway at the beginning but slightly distinct at later stages. Both systems generally commence with the fragmentation of the biomass lignocellulose matrix into monomeric units such as monosaccharides and aromatic monomers. This is followed by a sequence of dehydration and rehydration of the monosaccharides into a range of organic acids and ketones. These products are observed to be largely stable in the water system whereas in the ethylene glycol system, keto acids such as levulinic acid undergo an esterification and ketalisation processes to form various esters and ketals. Levulinic acid, acetic acid, and phenol were therefore found as dominant chemicals in the water system while additional compounds such as ethyl lactate, 2-hydroxyethyl levulinate ethylene ketal were among the key biomass-derived products identified in the ethylene glycol system. The use of ethylene glycol moreover leads to the production of additional valuable by-products such as diethylene glycol; 1,4-dioxane; and triethylene glycol via a side self-condensation and dehydration reactions. In terms of targeted biomass-derived products, the highest concentration of acetic acid (11.2 g/L), acetone (10.4 g/L) and phenol (2.7 g/L) was attained in the ethylene glycol system while the highest concentration of levulinic acid (3 g/L) was observed in the water system.

Biomass reaction pathways under atmospheric pressure were more defined and directed towards the formation of esters and ketals whereas, the products from the pressurised system contained a wider range of chemicals. The products identified in the atmospheric pressure process were mainly cellulose and hemicellulose derivatives. Finally, comparative liquefaction studies (under atmospheric pressure) conducted on sugarcane bagasse and pine needles demonstrate the synthesis of similar chemicals. Indicating the prospect to successfully apply other biomass types in this process; be it agricultural- or forest-based.

In summary, this chapter has demonstrated that almost every parameter whether solvent, catalyst, temperature or pressure has an influence on biomass conversion but more predominantly, product distribution. Hence the choice of solvent or parameters should be informed by the products of interest. For example, acid catalysed hydrothermal liquefaction at elevated pressure would be recommended for levulinic acid synthesis while the application of ethylene glycol at atmospheric pressure might be considered for the production of esters.

Chapter 7

Potential role of biomass as a heterogeneous catalyst

CHAPTER 7: POTENTIAL ROLE OF BIOMASS AS A HETEROGENEOUS CATALYST

7.1 Introduction

Earlier in Chapter 5, it was discovered that the introduction of pine needles into a glycerol system greatly improved the concentration of various solvent derived products during liquefaction. It was, therefore, postulated that biomass (pine needles) is catalytically active during liquefaction; promoting a simultaneous conversion of liquefaction solvents to platform chemicals. These products were mainly dehydration products synthesised from glycerol and/or acetone. Among other chemicals, the concentration of mesityl oxide was enhanced by up to 7-fold. Mesityl oxide (MO) is a typical adol self-condensation product of acetone [264].

Consequently, the focus of this chapter is to investigate the potential role of biomass (pine needles) and bio-char formed *in situ* as heterogeneous catalysts in the conversion of liquefaction solvents to value-added chemicals during biomass liquefaction. The role of pine needles as catalyst was first investigated in various glycerol-acetone systems. The results indicated that MO was the most favoured compound; as such, the second part of work in this chapter was focused on the application of pine needles and externally prepared bio-char (which resemble the material generated *in situ*) as catalyst in the conversion of acetone to mesityl oxide. It was perceived that the ash content of the bio-char plays a role in its activity as suggested in previous research [263]. Therefore, to appreciate the influence of ash, two other bio-chars; rice husk bio-char and softwood bio-char of varying ash content (earlier studied [263] by our research group) and ash made from pine needles were exploited in addition to the pine needles bio-char.

For clarification, bio-char is the dark carbonaceous residue obtained after the thermal or thermochemical processing of biomass. The standard/conventional method of producing bio-char is via pyrolysis, though, it is also obtained as by-product of biomass liquefaction or gasification. Bio-char is chiefly composed of fixed carbon with variable percentages (0 – 43 wt.%) of ash depending on the biomass type and process used in obtaining it [263]. Ash is simply, the mineral or non-oxidizable component of biomass as earlier discussed in Chapter 3 (Section 3.4.2.3) and Chapter 4 (Section 4.3.1.3).

7.2 Methods

Pine needles bio-char (PNB) was produced via a pyrolysis process at 950 °C, as described in Section 3.4.2.2. A furnace combustion process described in Section 3.4.2.3 was employed to produce pine needles ash (PNA). Rice husk bio-char (RHB) and softwood bio-char (SWB) were obtained from the UK Biochar Research Centre at the University of Edinburgh. RHB and SWB were made by pyrolysis at 550 °C in a Stage III unit, described by Buss *et al.* [288]. Ash was used as obtained whereas the particle size of bio-chars was reduced to < 200 µm (comparable to ash). Pine needles were utilised both as a whole (~1 x 12 mm average) and milled (< 200 µm). The ratios of glycerol:acetone were 1:1, 1:3, and 1:6 (mol:mol). These reactions are the same as were conducted earlier in Chapter 5. All additional reactions were conducted under the same conditions as described in Chapter 5; using the autoclave reactor (Section 3.5.2) under 30 bar of helium, at 250 °C, 1 h, and 300 rpm. 1 – 2 g of catalyst was used per 20 g of reactant (solvent).

Figure 7.1 illustrates a summary of the experimental process. An exhaustive description of biomass feedstocks preparation, reaction procedure, product separation and analysis, as well as conversion calculations are discussed in Sections 3.3, and 3.5.2 to 3.5.7. An X-ray fluorescence spectrometer discussed in Section 3.6 was used to determine the mineral (non-organic) elemental composition of the bio-chars and ash. MO selectivity was determined using equation 7.1.

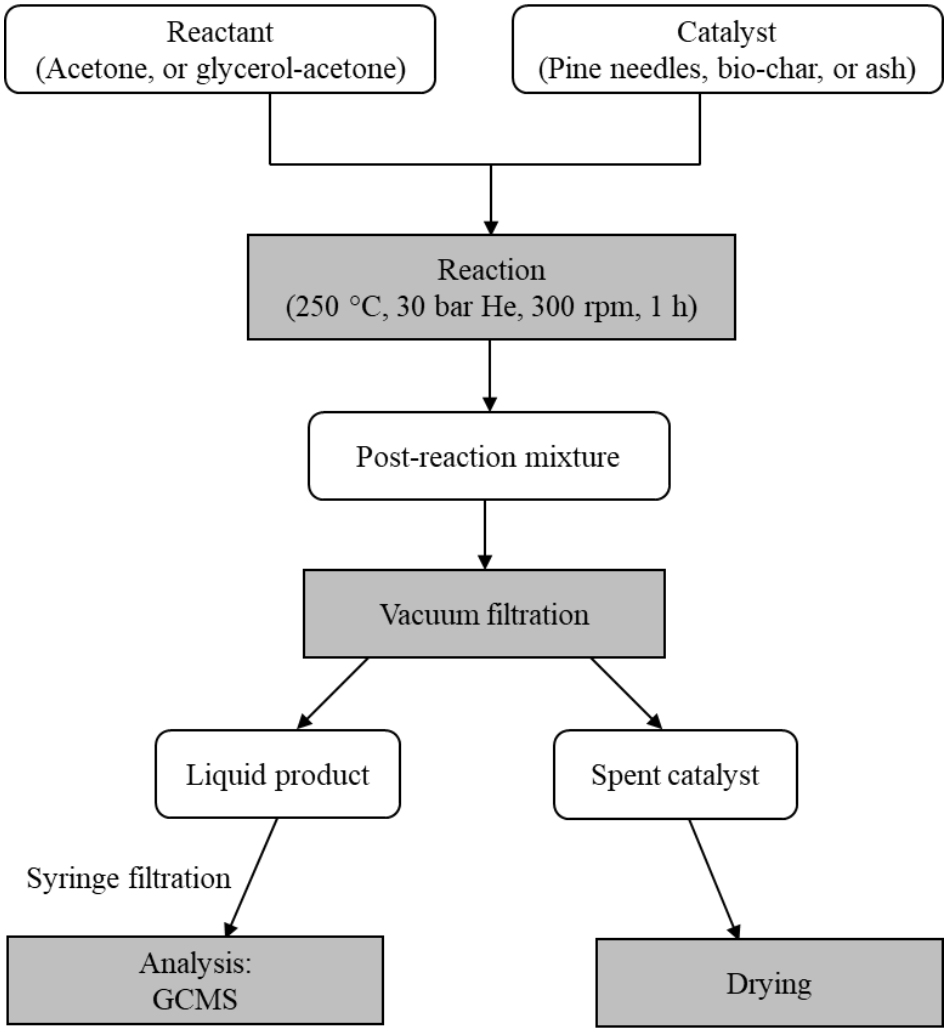

Figure 7.1: *Flow chart for studies on the potential application of biomass, bio-char, and ash as heterogeneous catalysts.*

$$\text{Selectivity of MO (\%)} = \frac{\text{moles of MO formed}}{\text{moles of acetone consumed}} \times 100 \qquad (7.1)$$

7.3 Results and discussion

7.3.1 Catalytic effect of pine needles (PN)

Figure 7.2 shows three key products; isopropanol, mesityl oxide (MO), and solketal obtained from reactions conducted in the glycerol-acetone systems with and without pine needles. Relatively, there is a general improvement in the concentration of all three products upon the introduction of pine needles. Under the same conditions, the rise in concentrations of solketal and isopropanol caused by pine needles (PN) addition is comparatively small, whereas the amount of MO does increase substantially in reactions where pine needles were present. For instance, at G:A (1:3), the amount of solketal increased slightly from 32 g/L (without PN) to 39 g/L (with PN), isopropanol rose from 5 g/L (without PN) to 8 g/L (with PN) while the concentration of MO, increased by 7-fold from 3 g/L (without PN) to 22 g/L (with PN). Thus, a component of pine needles could be catalytically active for the conversion of excess acetone to MO.

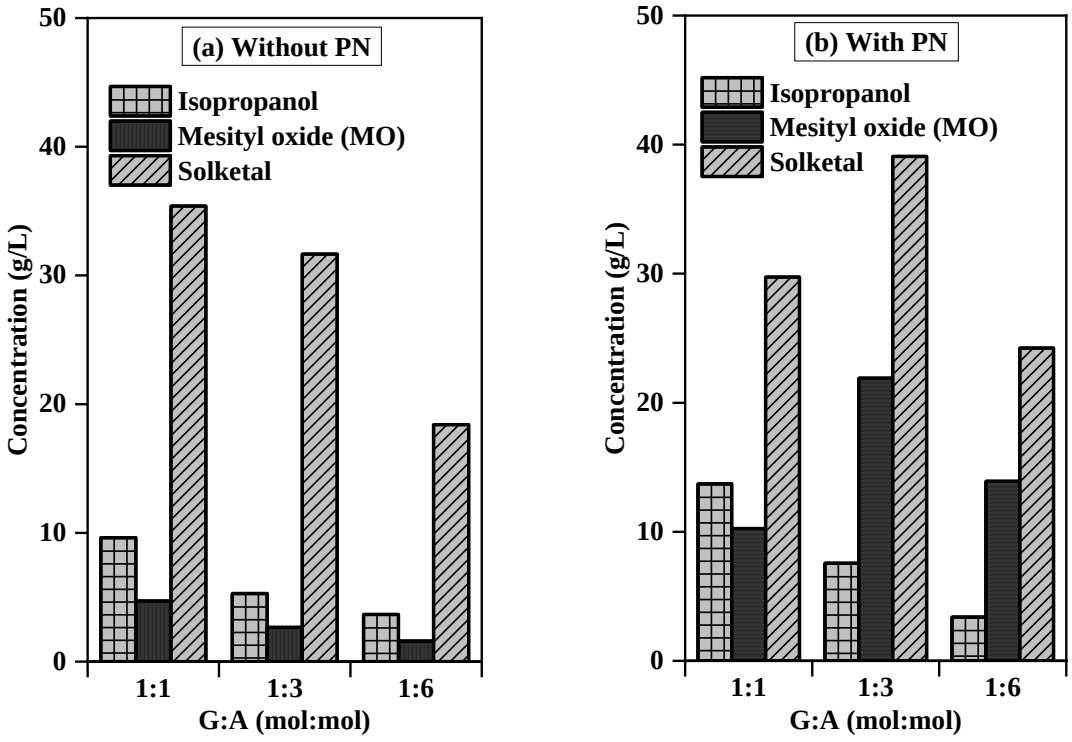

Figure 7.2: *Effect of pine needles as catalyst on the concentration of key products obtained from the liquefaction of pine needles with various mixtures of glycerol (G) and acetone (A). Conditions: 2 g pine needles, 20 g solvent, 250 °C, 30 bar He initial pressure, 300 rpm, 1 h.*

From previous research, basic catalysts such as calcium carbide [264] and Mg-Al layered double hydroxides [289,290] are more effective for the adol self-condensation of acetone. Consequently, it was perceived in this study that, the ash content of the biomass or bio-char generated in course of the liquefaction could be responsible for the observed increase in the yield of MO. Ash from plant sources is known to be alkaline in nature, consisting of carbonates or oxides of metals such as potassium, calcium, silicon, and phosphorus [228,291,292]. Bio-char and ash from plant sources have been successfully applied as catalyst in various reactions including, biodiesel synthesis [292], glycerol upgrading [263], tar reforming and biomass hydrolysis [293]. However, nothing is reported on their application in acetone conversion or MO synthesis. Therefore, two standard bio-chars of various ash content made from different biomass sources (i.e. softwood bio-char, and rice husk bio-char), as well as bio-char and ash made externally from pine needles were explored for their catalytic activity on the synthesis of MO from acetone in Section 7.3.2.

Prior to the application of the bio-chars and ash, the influence of glycerol on MO synthesis was briefly investigated. Two control (blank) experiments were therefore undertaken using acetone only with and without pine needles and the results compared with the glycerol-acetone system as shown in Figure 7.3. Without any pine needles and glycerol,

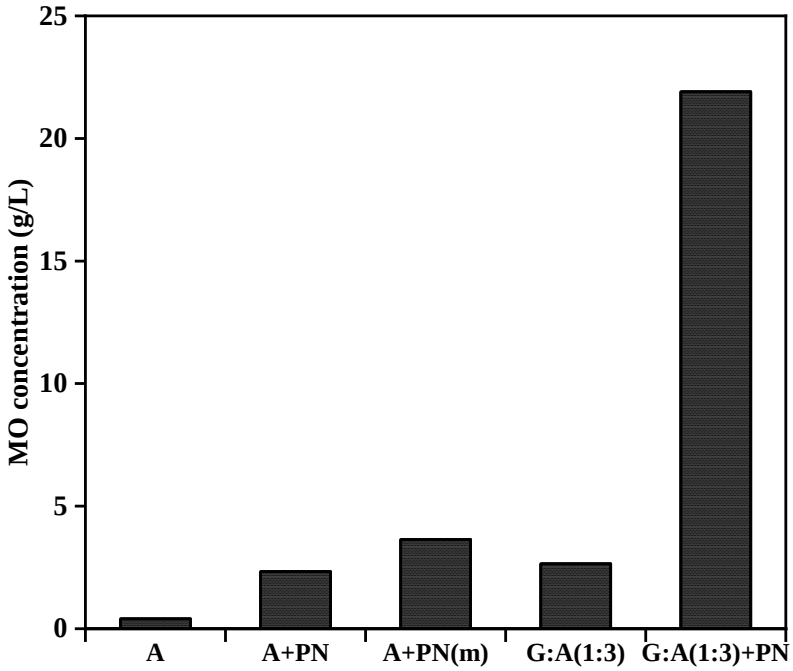

Figure 7.3: *Effect of pine needles (PN) and glycerol (G) on mesityl oxide concentration. Conditions: 2 g PN*, 20 g solvent, 250 °C, 30 bar He initial pressure, 300 rpm, 1h. *Where applicable. PN is whole pine needles, PN-m is milled pine needles, < 200 µm).*

the quantity of MO synthesised from acetone was 0.4 g/L (A). The addition of whole pine needles (PN) and milled pine needles (PN-m) slightly improved MO concentration to 2.3 g/L and 3.6 g/L respectively as seen in Figure 7.3. The addition of glycerol to acetone also resulted in a minor increase in MO concentration to 2.7 g/L. Nonetheless, these improvements are insignificant when likened to the 22 g/L achieved by the combined effect of pine needles and glycerol, "PN+G:A(1:3)". Pictures (Figure 7.4) of the residue obtained from these reactions illustrate virtually no transformation to the physical structure of the pine needles when reacted with acetone, picture (a). Pictures (c) and (d) however designate a more effective breakdown of pine needles in the presence of glycerol, leading to the formation of char.

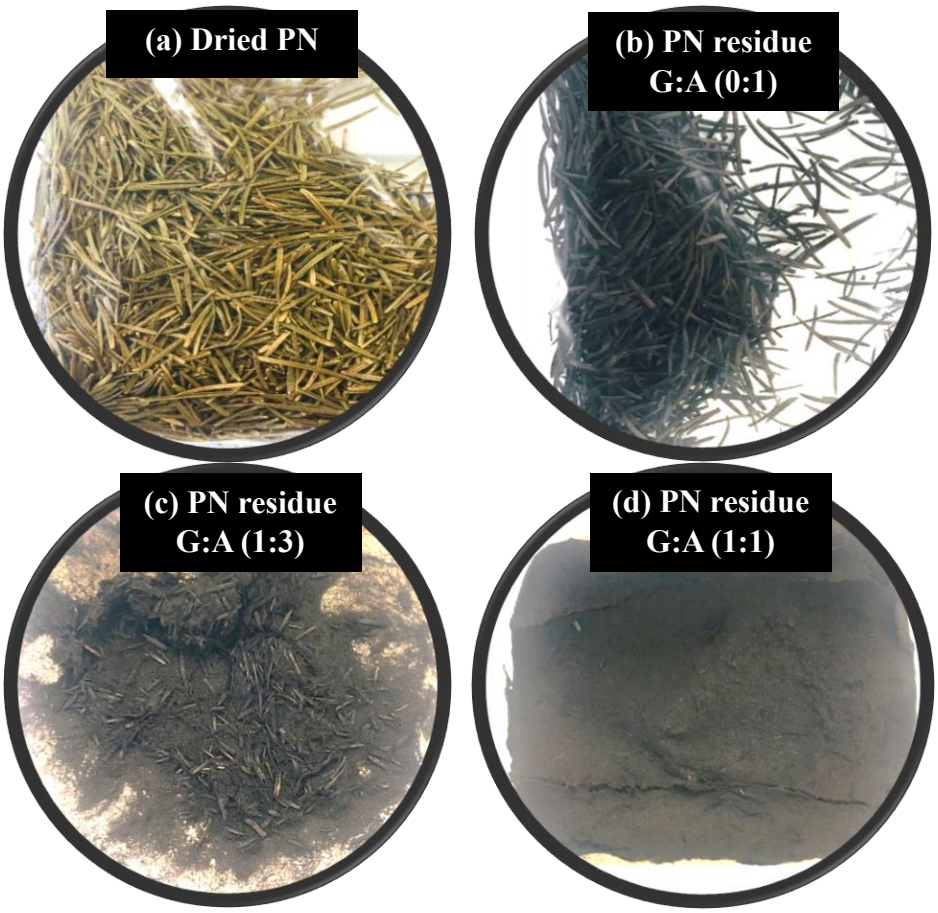

Figure 7.4: *Pictures of dried pine needles compared with residues obtained from the liquefaction of pine needles with various solvents. Conditions: 2 g pine needles (PN), 20 g solvent, 250 °C, 30 bar He initial pressure, 300 rpm, 1 h.*

Since particle size reduction of pine needles had a negligible impact on MO concentration, we can understand that;

1. the formation of biomass degradation products via the liquefaction effect of glycerol could be responsible for the observed catalytic activity. A recent review by Collett and McGregor [294] demonstrated that the *in situ* formation of carbonaceous deposits on heterogeneous catalysts could act as active sites, e.g. in alkane dehydrogenation reactions. Hence, the potential of bio-char (a typical carbonaceous material) acting as a catalyst in this liquefaction system stands tall. Section 7.3.2 therefore, explores the catalytic potential of bio-chars and ash on mesityl oxide synthesis from acetone.
2. a change in pH of the reaction mixture from the degradation of pine needles could also catalyse this reaction. This second claim could, however, not be ascertained in this work, as the pH of the reaction mixture was not monitored.

7.3.2 Catalytic effect of bio-chars and ash

It should be restated that the focus of this section is to find out the component of pine needles enhancing the concentration of mesityl oxide (MO), not to improve on the conversion of acetone or yield of MO. Hence, the bio-chars and ash were used without any modification, apart from particle size reduction. Pore size characterisation or other surface and structural functionality studies have not been undertaken on these bio-chars and hence comparisons are made based on the assumption that all active species are available for this reaction. This may quite deviate from reality.

The percentage of ash content and elemental (oxide) compositions of the bio-chars and ash are documented in Table 7.1. It was not possible to determine the elemental oxide compositions as a percentage of the total weight of the material; as such, each component was reported as a percentage of the total weight of oxides present in the materials. Pine needles ash (PNA) and pine needles bio-char (PNB) consist mostly of silicon, potassium, calcium, and phosphorus. Rice husk bio-char (RHB) consists mostly of silicon and softwood bio-char (SWB) consists mostly of potassium and calcium.

Table 7.1: *Ash content and mineral composition of bio-chars and ash used as catalyst in mesityl oxide synthesis studies. Softwood bio-char (SWB), rice husk bio-char (RHB), pine needles bio-char (PNB), and pine needles ash (PNA).*

		SWB	**RHB**	**PNB**	**PNA**
[a] ***Ash content (wt.% of bio-char, dry basis)***					
		0 [b]	42.9 [b]	26.2	100
[c] ***Non-organic elemental composition (wt.% of total oxides, dry basis)***					
Element	**Compound**				
Na	Na_2O	-	-	4.8	1.0
Mg	MgO	3.9	1.1	3.8	4.7
Al	Al_2O_3	-	-	-	0.8
Si	SiO2	4.7	89.2	12.2	24.0
P	P_2O_5	4.6	1.4	10.9	11.8
S	SO_3	3.3	0.3	3.1	3.8
Cl	Cl	-	0.7	1.3	0.4
K	K_2O	29.3	5.3	27.6	28.3
Ca	CaO	38.8	0.9	32.1	23.2
Ti	TiO_2	-	0.2	-	-
Mn	MnO	6.1	0.4	2.5	1.4
Fe	Fe_2O_3	5.9	0.5	0.7	0.2
Cu	CuO	3.4	-	0.4	-
Zn	ZnO	-	-	0.2	0.2
Sr	SrO	-	-	0.1	0.1
Ag	Ag_2O	-	-	0.4	-
Ba	BaO	-	-	-	0.2
Total elements		***100***	***100***	***100***	***100***

[a] *Determined by TGA*
[b] *As reported in a previous study by Collett* [263]
[c] *Determined by XRF*
- Not detected

For this study, glycerol was taken out of the system to clearly appreciate the impact of the catalysts on MO synthesis from acetone. The results are presented in Figures 7.5 and 7.6. The introduction of bio-char or ash significantly improved MO concentration as could be seen from Figure 7.5. The pine needles bio-char (PNB) almost doubled MO concentration to 5 g/L from 2.8 g/L in the presence of milled pine needles (PN-m), whereas the addition of pine needles ash (PNA) resulted in the highest concentration of (15.8 g/L), this represents an almost 6-fold increase over the concentration in the presence of PN-m. Among the three bio-chars, the trend of MO concentration increase was SWB (3 g/L) followed by RHB (4 g/L) and PNB (5 g/L). Overall, the highest acetone conversion (14 %) and MO concentration (15.8 g/L) were attained in the presence of PNA. Nonetheless, bio-chars with higher ash content did not necessarily result in a higher

acetone conversion or MO yield. This narrows down the cause of catalytic activity to a particular mineral component of the catalysts. For instance, potassium was reported as the most active component of various bio-chars and ashes including RHB, responsible for the conversion of glycerol and carbon dioxide to triacetin and glycerol carbonate in Collett's work [263]. In that work, potassium in bio-char and ash was hypothesised to possess dehydrating capabilities. In this work, all four materials used as catalyst possess considerable amounts of potassium oxide, up to 29 wt.% relative to other minerals. Therefore, the dehydrating potential of potassium could still explain the observed improvement in MO concentration in the presence of the bio-chars and ash. On the other hand, previous research shows that alkaline catalysts are most suitable for the adol self-condensation of acetone [264]. Therefore, the catalytic influence of the ash and bio-chars could originate from the overall basic properties of these materials.

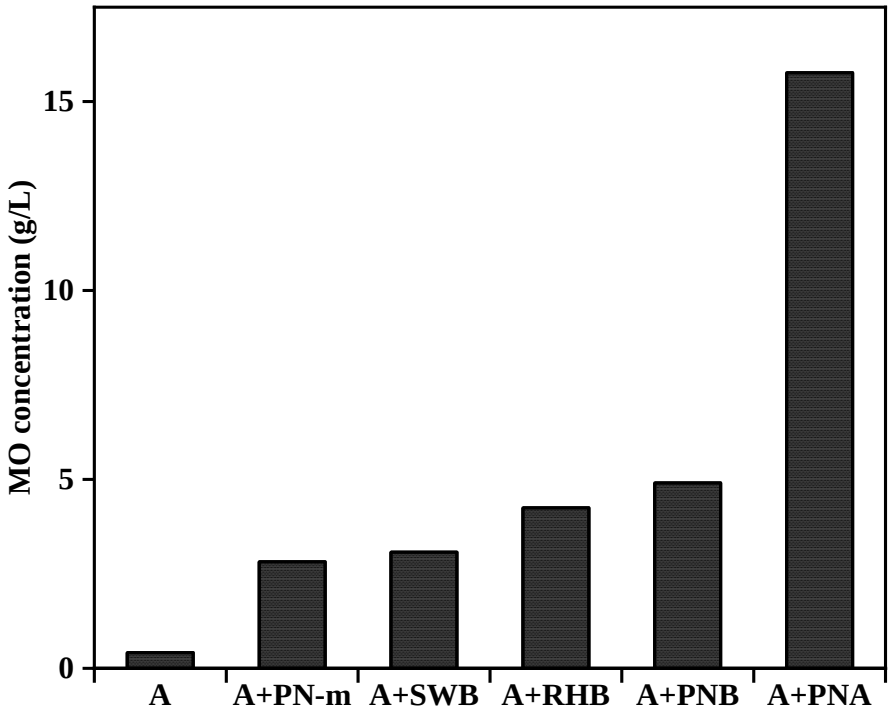

Figure 7.5: *Effect of various bio-chars and ash as catalyst on mesityl oxide concentration (g/L). Conditions: 20 g acetone, 1 g catalyst, 250 °C, 30 bar He initial pressure, 300 rpm, 1 h.*

It could be noticed in Figure 7.6 that the selectivity of MO to a certain degree increases with ash content of the bio-chars; RHB with the highest ash content of 43 wt.% resulted in a MO selectivity of 8 % which is an 8-fold improvement over the non-catalytic process.

The overall highest MO selectivity of 13.5 % was attained in the presence of PNA. These selectivity figures are rather low considering that, the proportion of MO compared to other products was approx. 70 % based on GCMS peak area, the remnants were primarily diacetone alcohol and isomesityl oxide (Table D1, Appendix D). A possible explanation could be the formation of gaseous products, which were not considered in this work. Thus, the analysis of the post-reaction gaseous component should be considered in future studies.

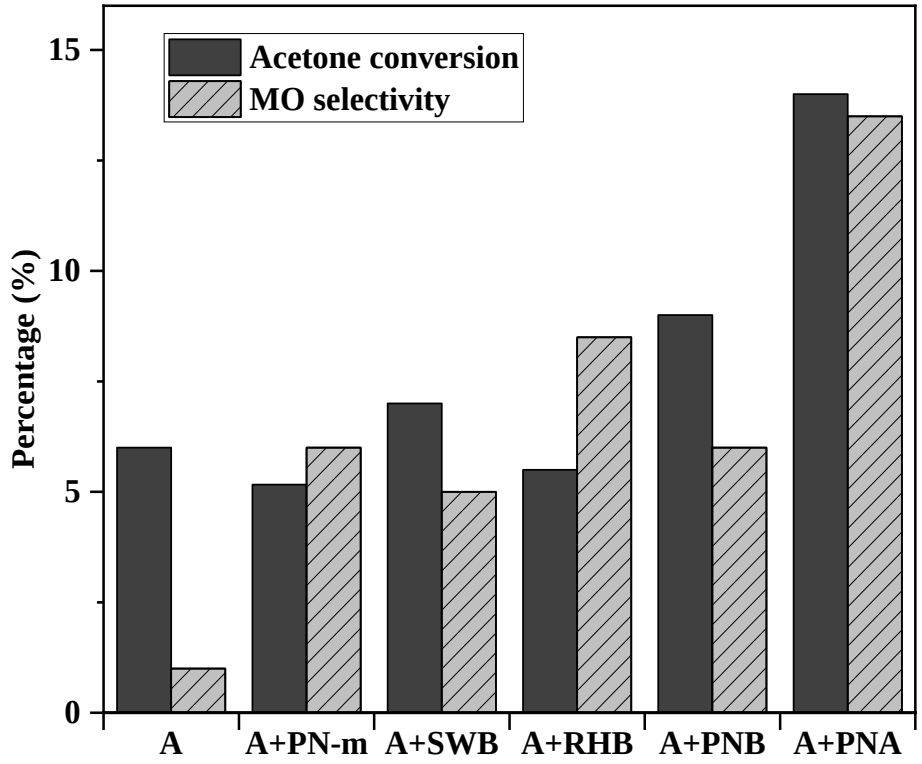

Figure 7.6: *Effect of pine needles, bio-chars, and ash as catalyst on mesityl oxide selectivity and acetone conversion. Conditions: 20 g acetone, 1 g catalyst, 250 °C, 30 bar He initial pressure, 300 rpm, 1 h.*

While it is obvious that ash content plays a significant role in the yield of MO, it is also possible that carbon contributes to this, as observed previously [263]. For example, 3 g/L of MO was recorded in the presence of SWB which had negligible ash content, this is a significant improvement in MO concentration over the non-catalytic process (0.4 g/L). Thus, the catalytic influence of bio-char could be a combined effect of the carbon and mineral components.

In summary, we can understand that in the biomass liquefaction system, the decomposition of biomass by glycerol and acetone exposes the carbon and ash content of the biomass (in the form of bio-char) which facilitates the side adol condensation of excess acetone to mesityl oxide. This scenario is important considering the development of future sustainable biorefineries. Specifically, the potential to reduce complex and series of industrial processes into a one-pot process is achievable. A typical case study is demonstrated in this work where biomass waste is converted into valuable chemicals along-side the conversion of low-value liquefaction solvents to value-added products.

7.4 Conclusion

In this chapter, the *in situ* formation of bio-char during biomass liquefaction was discovered to be catalytically active towards the synthesis of MO from excess acetone in the glycerol-acetone system. Further exploration of unmodified, externally prepared bio-chars of varying ash content (which represents the material generated *in situ*) suggests that the catalytic activity of the bio-char is a combination of its carbon and mineral (ash) constituents with the mineral constituents playing a more significant role.

The application of bio-char and ash in the synthesis of mesityl oxide (MO) has been demonstrated for the first time in this work, which provides the foundation for further research. A maximum of 14 % acetone conversion and 13.5 % MO selectivity was achieved in the presence of ash prepared from pine needles. While these figures may be relatively low compared to other chemical-based catalysts, the application of catalysts from renewable and environmentally friendly sources is vital for future research in light of the development of a sustainable industry.

Chapter 8

Conclusions and suggestions for future work

CHAPTER 8: CONCLUSIONS AND SUGGESTIONS FOR FUTURE WORK

8.1 Introduction

This research sought to explore waste from biomass-derived sources to produce high-value products that could serve as feedstock to the chemical and fuel industries. In light of this, two biomass materials: i) Pine needles (*Picea abies*, Norway spruce) obtained from The Plant Place, Fen Drayton, UK; and ii) Sugarcane bagasse obtained from a local supplier in Alexandria, Egypt were experimented. Specifically, the impact of three selected low-cost solvents; glycerol, water, and ethylene glycol on biomass conversion and resultant products during liquefaction were investigated. The following objectives were therefore established to accomplish the set goal:

1. To understand the chemical composition, as well as the physical, chemical and thermal characteristics of sugarcane bagasse and pine needles via various characterisation techniques.
2. To explore the range of chemicals that could be synthesised from the liquefaction of lignocellulosic biomass in various solvent systems (water, glycerol and ethylene glycol) using pine needles as an exemplary feedstock.
3. To advance our understanding of the role of various solvents (water, glycerol and ethylene glycol) in biomass liquefaction processes under similar reaction conditions.
4. To design a novel route to the one-pot simultaneous valorisation of biomass and glycerol.
5. To investigate the effect of sulphuric acid as a homogeneous catalyst and the effect of process parameters (temperature, and pressure) on biomass conversion and product yield.
6. To evaluate the effect of biomass type (pine needles versus sugarcane bagasse) on biomass conversion and the chemical composition of the resultant liquid product.
7. To investigate the potential role of biomass and bio-char formed *in situ* as a heterogeneous catalyst during liquefaction.

This chapter, therefore, highlights the key findings of the experimental works carried out in each chapter in Section 8.2 and provides some suggestions for future research in Section 8.3.

8.2 Conclusion

Feedstock characterisation

As an important step to determine the suitability of the selected feedstocks for chemical synthesis, a thorough feedstock characterisation was conducted on pine needles and sugarcane bagasse via various analytical techniques. Both biomasses were found to possess high volatile matter contents (> 70 wt.%) which make them suitable feedstocks for chemicals synthesis with potential high conversion. Besides elemental sulphur and nitrogen contents of both biomasses were below 0.2 wt.% and 1.5 wt.% respectively, making these feedstocks safe for thermochemical processes without much concern about reactor fouling or environmental pollution.

Biomass liquefaction and the potential role of biomass as a heterogeneous catalyst

This research has demonstrated the potential to convert lignocellulosic biomass waste into liquid products containing a variety of organic acids, alcohols, phenolics, sugars and esters under various conditions. The composition of the liquid product was largely affected by the type of liquefaction solvent and process conditions. For instance, 1) the compositions of liquid products at moderate pressure (30 bar) were generally made up of organic acids, alcohols, and aromatics. While these compounds were largely stable in water, organic acids such as levulinic acid were converted to esters and ketals in the ethylene glycol system. 2) a wider range of chemicals were observed in the ethylene glycol and glycerol systems over water owing to the formation of additional compounds from the side decomposition or condensation reactions of excess solvent in these systems.

The application of catalyst largely promoted the synthesis of levulinic acid whereas an increase in temperature enhanced biomass conversion and the concentration of most biomass derivatives. At the optimum temperature of 250 °C, the highest biomass conversion achieved in glycerol (without catalyst) was 94 wt.%, followed by ethylene glycol (86 wt.%, with catalyst) and water (72-76 wt.%, with or without catalyst). The

higher biomass conversion obtained in the presence of ethylene glycol and glycerol was attributed to their higher ability to decompose lignin. Though water achieved a relatively lower biomass conversion and, in some cases, lower concentration of targeted biomass derivatives, the selectivity (based on GCMS peak area) of the biomass derived compounds were much higher in the water system due to the absence of competing solvent derivatives.

All three solvents were perceived as indirect sources of hydrogen via various hydrogen transfer reactions or through the water-gas shift reaction. Liquefaction is considered as an economically unattractive biomass conversion process owed to the high cost of H_2 and other essential gases for the process [3,21,23]. Hence, the potential to replace the high-cost hydrogen gas with these cheap solvents may offer economic benefits.

Finally, it was revealed in this work for the first time that the *in situ* formation of bio-char during biomass liquefaction possesses catalytic capabilities for the co-valorisation of liquefaction solvents to value-added chemicals. This catalytic activity was attributed to the mineral (ash) constituent of the bio-char. These findings provide the foundation for the design of a concurrent one-pot biomass valorisation and liquefaction solvent upgrading processes, as demonstrated in Chapters 5 and 7.

8.3 Suggestions for future work

Potential role of biomass as a heterogeneous catalyst

While the current work has been successful at establishing the plausible *in situ* catalytic effects of biomass and its constituents during liquefaction, this basically serves as a foundation for future research. Particularly, the design of simultaneous one-pot biomass valorisation and liquefaction solvent upgrading processes taking advantage of the *in situ* catalytic activity of biomass could be considered. Moreover, the application of biomass, bio-char and ash in mesityl oxide synthesis or other condensation/dehydration reactions could be further explored.

In this work, externally prepared representative materials were employed, however, future studies could investigate the performance of bio-char made via the liquefaction process compared with the externally prepared materials. The performance of

heterogeneous catalysts is normally underpinned by various factors such as pore size, structure and other surface functionalities, hence a more thorough characterisation of the biomass materials might be necessary to comprehensively explain their performance in any reaction. Comprehensive information on bio-char and other carbonaceous catalysts characterisation techniques are discussed in the literature [263,294]. It might be more useful to conduct the same experiments with demineralised materials to facilitate a better understanding of their catalytic activity with respect to the role of ash. Methods of bio-char and ash demineralisation are discussed elsewhere [229,263].

Product analysis

HPLC analysis conducted on selected liquid products made via hydrothermal liquefaction revealed the presence of valuable non-volatile chemicals such as glucose. The same was however not carried out for products obtained in the ethylene glycol and glycerol systems, hence it was not too clear if these samples contained any of such products. Thus, for effective evaluation of each solvent on product yield, it is essential to analyse all samples with the same technique to clearly understand the full composition of each product made in different systems. The use of HPLC together with GCMS would be beneficial to ascertain a more comprehensive chemical composition of the liquid products. Moreover, the quantification of major solvent derived products made in the ethylene glycol system could be considered in future studies to ensure an equal basis of judgement between the glycerol and ethylene glycol system.

Process economics - product separation/purification

Though the simultaneous conversion of liquefaction solvents and biomass may be economical in terms of reducing the number of reaction steps, the cost of separating multi-component products for final use would have to be critically examined against the cost of multiple reaction steps in light of future large-scale processes.

REFERENCES

[1] Allen M R, Dube O P, Solecki W, Aragón-Durand F, Cramer W, Humphreys S, Kainuma M, Kala J, Mahowald N, Mulugetta Y, Perez R, Wairiu M and Zickfeld K 2018 *Framing and Context. In: Global Warming of 1.5°C. An IPCC Special Report on the impacts of global warming of 1.5 °C above pre-industrial levels and related global greenhouse gas emission pathways, in the context of strengthening the global response to ...* ed V Masson-Delmotte, P Zhai, H-O Pörtner, D Roberts, J Skea, P R Shukla, A Pirani, W Moufouma-Okia, C Péan, R Pidcock, S Connors, J B R Matthews, Y Chen, X Zhou, M I Gomis, E Lonnoy, T Maycock, M Tignor and T Waterfield (Available at: <https://www.ipcc.ch/site/assets/uploads/sites/2/2019/05/SR15_Chapter1_Low_Res.pdf>)

[2] Zhang C 2019 Lignocellulosic Ethanol: Technology and Economics *Alcohol Fuels - Current Technologies and Future Prospect* (IntechOpen) pp 1–21

[3] Alonso D M, Bond J Q and Dumesic J A 2010 Catalytic conversion of biomass to biofuels *Green Chem.* 12 1493

[4] UNCTAD 2014 The global biofuels market: Energy security, trade and development. Policy Brief No. 30. UNCTAD/PRESS/PB/2014/3 (No.30) 1–3

[5] Kaewphan N and Gheewala S H 2013 Greenhouse gas evaluation and market opportunity of bioplastic bags from Cassava in Thailand *J. Sustain. Energy Environ.* 4 15–9

[6] Noe R 2017 This Cassava-Based Plastic Bag Alternative is Biodegradable, Even Edible *Retrieved from <https//www.core77.com/posts/68988/This-Cassava-Based-Plastic-Bag-Alternative-is-Biodegradable-Even-Edible> [Accessed 16.01.2019]*

[7] Mergner R, Janssen R, Rutz D, de Bari I, Sissot F, Chiaramonti D, Giovannini A, Pescarolo S and Nistri R 2013 *Lignocellulosic Ethanol Process and Demonstration* (WIP Renewable Energies, Munich, Germany)

[8] Valk M 2014 *Availability and cost of agricultural residues for bioenergy generation: International literature review and a case study for South Africa* (Masters Thesis, Universiteit Utrecht, The Netherlands)

[9] Hoornweg D and Bhada-tata P 2012 What a waste: A global review of solid waste management. *World Bank, Urban Dev. Ser. Knowl. Pap.* 98

[10] Vassilev S V., Baxter D, Andersen L K, Vassileva C G and Morgan T J 2012 An overview of the organic and inorganic phase composition of biomass *Fuel* 94 1–33

[11] Lee H V., Hamid S B A and Zain S K 2014 Conversion of lignocellulosic biomass to nanocellulose: Structure and chemical process *Sci. World J.* 2014 1–22

[12] Talebnia F, Karakashev D and Angelidaki I 2010 Production of bioethanol from wheat straw: An overview on pretreatment, hydrolysis and fermentation *Bioresour. Technol.* 101 4744–53

[13] Cardona C A, Quintero J A and Paz I C 2010 Production of bioethanol from sugarcane bagasse: Status and perspectives *Bioresour. Technol.* 101 4754–66

[14] Nasir N A 2019 *Hydrothermal Liquefaction of Lignocellulosic Biomass* (Ph.D. Thesis. The University of Sheffield, UK)

[15] Wagner J L, Le C D, Ting V P and Chuck C J 2017 Design and operation of an inexpensive, laboratory-scale, continuous hydrothermal liquefaction reactor for the conversion of microalgae produced during wastewater treatment *Fuel Process. Technol.* 165 102–11

[16] Raikova S, Le C D, Beacham T A, Jenkins R W, Allen M J and Chuck C J 2017 Towards a marine biorefinery through the hydrothermal liquefaction of macroalgae native to the United Kingdom *Biomass and Bioenergy* 107 244–53

[17] Refaat A A 2010 Archive of SID Different techniques for the production of biodiesel from waste vegetable oil *Int. J. Environ. Sci. Tech* 7 183–213

[18] Jenkins R W, Stageman N E, Fortune C M and Chuck C J 2014 Effect of the type of bean, processing, and geographical location on the biodiesel produced from waste coffee grounds *Energy and Fuels* 28 1166–74

[19] Bridgwater A V. 1994 Catalysis in thermal biomass conversion *Appl. Catal. A, Gen.* 116 5–47

[20] Demirbaş A 2001 Biomass resource facilities and biomass conversion processing for fuels and chemicals *Energy Convers. Manag.* 42 1357–78

[21] Behrendt F, Neubauer Y, Oevermann M, Wilmes B and Zobel N 2008 Direct liquefaction of biomass *Chem. Eng. Technol.* 31 667–77

[22] Peterson A A, Vogel F, Lachance R P, Fröling M, Antal, Jr. M J and Tester J W 2008 Thermochemical biofuel production in hydrothermal media: A review of sub- and supercritical water technologies *Energy Environ. Sci.* 1 32

[23] Appell H R, Fu Y C, Friedman S, Yavorsky P M and Wender I 1971 Converting Organic Wastes to Oil: A Replenishable Energy Source *U.S. Bur. Mines*

[24] Gollakota A R K, Kishore N and Gu S 2018 A review on hydrothermal co-liquefaction of biomass *Appl. Energy* 81 926–45

[25] Qu Y, Wei X and Zhong C 2003 Experimental study on the direct liquefaction of Cunninghamia lanceolata in water *Energy* 28 597–606

[26] Brand S, Susanti R F, Kim S K, Lee H shik, Kim J and Sang B I 2013 Supercritical ethanol as an enhanced medium for lignocellulosic biomass liquefaction: Influence of physical process parameters *Energy* 59 173–82

[27] Guo Y, Yeh T, Song W, Xu D and Wang S 2015 A review of bio-oil production from hydrothermal liquefaction of algae *Renew. Sustain. Energy Rev.* 48 776–90

[28] Patil P T, Armbruster U and Martin A 2014 Hydrothermal liquefaction of wheat straw in hot compressed water and subcritical water-alcohol mixtures *J. Supercrit. Fluids* 93 121–9

[29] Li C, Zhao X, Wang A, Huber G W and Zhang T 2015 Catalytic Transformation of Lignin for the Production of Chemicals and Fuels *Chem. Rev.* 115 11559–624

[30] Cao L, Zhang C, Hao S, Luo G, Zhang S and Chen J 2016 Effect of glycerol as co-solvent on yields of bio-oil from rice straw through hydrothermal liquefaction *Bioresour. Technol.* 220 471–8

[31] Zheng Z, Pan H, Huang Y, Chung Y H, Zhang X and Feng H 2011 Rapid liquefaction of wood in polyhydric alcohols under microwave heating and its liquefied products for preparation of rigid polyurethane foam *Open Mater. Sci. J.* 5 1–8

[32] Demirbaş A 2000 Mechanisms of liquefaction and pyrolysis reactions of biomass *Energy Convers. Manag.* 41 633–46

[33] Pedersen T H, Grigoras I F, Hoffmann J, Toor S S, Daraban I M, Jensen C U, Iversen S B, Madsen R B, Glasius M, Arturi K R, Nielsen R P, Søgaard E G and Rosendahl L A 2016 Continuous hydrothermal co-liquefaction of aspen wood and glycerol with water phase recirculation *Appl. Energy* 162 1034–41

[34] Demirbas A 2008 Liquefaction of biomass using glycerol *Energy Sources, Part A Recover. Util. Environ. Eff.* 30 1120–6

[35] Razali N A, Conte M and McGregor J 2019 The role of impurities in the La2O3 catalysed carboxylation of crude glycerol *Catal. Letters* 149 1403–14

[36] Katryniok B, Paul S, Bellière-Baca V, Rey P and Dumeignil F 2010 Glycerol dehydration to acrolein in the context of new uses of glycerol *Green Chem.* 12 2079

[37] Possato L G, Chaves T F, Cassinelli W H, Pulcinelli S H, Santilli C V and Martins L 2017 The multiple benefits of glycerol conversion to acrolein and acrylic acid catalyzed by vanadium oxides supported on micro-mesoporous MFI zeolites *Catal. Today* 289 20–8

[38] Possato L G, Cassinelli W H, Garetto T, Pulcinelli S H, Santilli C V. and Martins L 2015 One-step glycerol oxidehydration to acrylic acid on multifunctional zeolite catalysts *Appl. Catal. A Gen.* 492 243–51

[39] Lal P S, Sharma A and Bist V 2013 Pine Needle - An Evaluation of Pulp and Paper Making Potential *J. For. Prod. Ind.* 2 42–7

[40] Bizzo W A, Lenço P C, Carvalho D J and Veiga J P S 2014 The generation of residual biomass during the production of bio-ethanol from sugarcane, its characterization and its use in energy production *Renew. Sustain. Energy Rev.* 29 589–603

[41] McKendry P 2002 Energy production from biomass (part 2): Conversion technologies *Bioresour. Technol.* 83 47–54

[42] García R, Pizarro C, Lavín A G and Bueno J L 2012 Characterization of Spanish biomass wastes for energy use *Bioresour. Technol.* 103 249–58

[43] Pérez J, Muñoz-Dorado J, De La Rubia T and Martínez J 2002 Biodegradation and biological treatments of cellulose, hemicellulose and lignin: An overview *Int. Microbiol.* 5 53–63

[44] Ramos L P 2003 The chemistry involved in the steam treatment of lignocellulosic materials *Quim. Nova* 26 863–71

[45] Mohan D, Pittman C U and Steele P H 2006 Pyrolysis of wood/biomass for bio-oil: A critical review *Energy and Fuels* 20 848–89

[46] Renewable Fuels Association 2020 Annual Fuel Ethanol Production *Retrieved from <https//ethanolrfa.org/statistics/annual-ethanol-production>*

[47] Tiseo I 2020 Global biodiesel production by country 2019 *Retrieved from <https//www.statista.com/statistics/271472/biodiesel-production-in-selected-countries/#~text=The%20United%20States%20and%20Brazil,gallons%20of%20biodiesel%20by%202025.>*

[48] Balat M, Balat H and Oz C 2008 Progress in bioethanol processing *Prog. Energy Combust. Sci.* 34 551–73

[49] Meher L C, Vidya Sagar D and Naik S N 2006 Technical aspects of biodiesel production by transesterification - A review *Renew. Sustain. Energy Rev.* 10 248–68

[50] Marchetti J M, Miguel V U and Errazu A F 2007 Possible methods for biodiesel production *Renew. Sustain. Energy Rev.* 11 1300–11

[51] Lotero E, Liu Y, Lopez D E, Suwannakarn K, Bruce D A and Goodwin J G 2005 Synthesis of biodiesel via acid catalysis *Ind. Eng. Chem. Res.* 44 5353–63

[52] Hill J, Nelson E, Tilman D, Polasky S and Tiffany D 2006 Environmental, economic, and energetic costs and benefits of biodiesel and ethanol biofuels. *Proc. Natl. Acad. Sci. U. S. A.* 103 11206–10

[53] Kim S and Dale B E 2004 Global potential bioethanol production from wasted crops and crop residues *Biomass and Bioenergy* 26 361–75

[54] Ballesteros M, Oliva J M, Negro M J, Manzanares P and Ballesteros I 2004 Ethanol from lignocellulosic materials by a simultaneous saccharification and fermentation process (SFS) with Kluyveromyces marxianus CECT 10875 *Process Biochem.* 39 1843–8

[55] Zhang Y, Dubé M A, McLean D D and Kates M 2003 Biodiesel production from waste cooking oil: 1. Process design and technological assessment *Bioresour. Technol.* 89 1–16

[56] Kimble M, Pasdeloup M-V and Spencer C 2008 Sustainable Bioenergy Development in UEMOA Member Countries *United Nations Found. Press Cent.* 152

[57] EurObserv'ER Report 2014 *The state of renewable energies in Europe* (EurObserv'ER, pp.45)

[58] Weiland P 2010 Biogas production: Current state and perspectives *Appl. Microbiol. Biotechnol.* 85 849–60

[59] Sánchez Ó J and Cardona C A 2008 Trends in biotechnological production of fuel ethanol from different feedstocks *Bioresour. Technol.* 99 5270–95

[60] Rosales-Calderon O and Arantes V 2019 A review on commercial-scale high-value products that can be produced alongside cellulosic ethanol *Biotechnol. Biofuels* 12

[61] Mcaloon A, Taylor F, Yee W, Ibsen K and Wooley R 2000 *Determining the Cost of Producing Ethanol from Corn Starch and Lignocellulosic Feedstocks* (No. NREL/TP-580-28893. National Renewable Energy Lab., Golden, CO (US))

[62] Hossain S, Theodoropoulos C and Yousuf A 2019 Techno-economic evaluation of heat integrated second generation bioethanol and furfural coproduction Techno-economic evaluation of heat integrated second generation bioethanol and furfural coproduction *Biochem. Eng. J.* 144 89–103

[63] Sefidari H, Razmjoo N and Strand M 2014 An experimental study of combustion and emissions of two types of woody biomass in a 12-MW reciprocating-grate boiler *Fuel* 135 120–9

[64] Bindig R, Butt S, Hartmann I, Matthes M and Thiel C 2012 Application of Heterogeneous Catalysis in Small-Scale Biomass Combustion Systems *Catalysts* 2 223–43

[65] Ragland K. W. D J A and A J B 1991 Properties of wood for combustion analysis *Bio-resource Technol. J.* Vol. 37 161–8

[66] Park J, Lee Y, Ryu C and Park Y K 2014 Slow pyrolysis of rice straw: Analysis of products properties, carbon and energy yields *Bioresour. Technol.* 155 63–70

[67] Bulushev D A and Ross J R H 2011 Catalysis for conversion of biomass to fuels via pyrolysis and gasification: A review *Catal. Today* 171 1–13

[68] Demirbaş A and Arin G 2002 An overview of biomass pyrolysis *Energy Sources* 24 471–82

[69] Bridgwater A V. 2012 Review of fast pyrolysis of biomass and product upgrading *Biomass and Bioenergy* 38 68–94

[70] Kan T, Strezov V and Evans T J 2016 Lignocellulosic biomass pyrolysis: A review of product properties and effects of pyrolysis parameters *Renew. Sustain. Energy Rev.* 57 1126–40

[71] Uddin M N, Techato K, Taweekun J, Rahman M M, Rasul M G, Mahlia T M I and Ashrafur S M 2018 An overview of recent developments in biomass pyrolysis technologies *Energies* 11

[72] Mante, Ofei D; Agblevor F A 2011 Catalytic conversion of biomass to biofuels *Biomass Conv. Bioref.* 1 203–15

[73] Yang Y, Brammer J G, Mahmood A S N and Hornung A 2014 Intermediate pyrolysis of biomass energy pellets for producing sustainable liquid, gaseous and solid fuels *Bioresour. Technol.* 169 794–9

[74] Hornung A, Apfelbacher A and Sagi S 2011 Intermediate pyrolysis: A sustainable biomass-to-energy concept-biothermal valorisation of biomass (BtVB) process *J. Sci. Ind. Res. (India).* 70 664–7

[75] Luo Z, Wang S, Liao Y, Zhou J, Gu Y and Cen K 2004 Research on biomass fast pyrolysis for liquid fuel *Biomass and Bioenergy* 26 455–62

[76] Zhang X, Wang T, Ma L, Zhang Q and Jiang T 2013 Hydrotreatment of bio-oil over Ni-based catalyst *Bioresour. Technol.* 127 306–11

[77] Elliott D C 2007 Historical developments in hydroprocessing bio-oils *Energy and Fuels* 21 1792–815

[78] Williams P T and Nugranad N 2000 Comparison of products from the pyrolysis and catalytic pyrolysis of rice husks *Energy* 25 493–513

[79] Luo X, Hu S, Zhang X and Li Y 2013 Thermochemical conversion of crude glycerol to biopolyols for the production of polyurethane foams *Bioresour. Technol.* 139 323–9

[80] Aho A, Kumar N, Eranen K, Salmi T, Hupa M and Murzin D Y 2008 Catalytic pyrolysis of woody biomass in a fluidized bed reactor: Influence of the zeolite structure *Fuel* 87 2493–501

[81] Samolada M C, Papafotica a. and Vasalos I a. 2000 Catalyst Evaluation for Catalytic Biomass Pyrolysis *Energy & Fuels* 14 1161–7

[82] Wildschut J, Mahfud F H, Venderbosch R H and Heeres H J 2009 Hydrotreatment of Fast Pyrolysis Oil Using Heterogeneous Noble-Metal Catalysts *Ind. Eng. Chem. Res.* 48 10324–34

[83] Zhang Q, Chang J, Wang T and Xu Y 2007 Review of biomass pyrolysis oil properties and upgrading research *Energy Convers. Manag.* 48 87–92

[84] Nguyen T S, Lefferts L, Saisankargupta K B and Seshan K 2015 Catalytic Conversion of Biomass Pyrolysis Vapours over Sodium-Based Catalyst: A Study on the State of Sodium on the Catalyst *ChemCatChem* 7 1833–40

[85] Zhang Y, Bi P, Wang J, Jiang P, Wu X, Xue H, Liu J, Zhou X and Li Q 2015 Production of jet and diesel biofuels from renewable lignocellulosic biomass *Appl. Energy* 150 128–37

[86] Akhtar J and Saidina Amin N 2012 A review on operating parameters for optimum liquid oil yield in biomass pyrolysis *Renew. Sustain. Energy Rev.* 16 5101–9

[87] Modell M 1985 *Gasification and Liquefaction of Forest Products in Supercritical Water. In: Overend R.P., Milne T.A., Mudge L.K. (eds) Fundamentals of Thermochemical Biomass Conversion* (Elsevier Applied Science Publishers Ltd, England)

[88] Hayashi J I, Kudo S, Kim H S, Norinaga K, Matsuoka K and Hosokai S 2014 Low-temperature gasification of biomass and lignite: Consideration of key thermochemical phenomena, rearrangement of reactions, and reactor configuration *Energy and Fuels* 28 4–21

[89] Azadi P and Farnood R 2011 Review of heterogeneous catalysts for sub- and supercritical water gasification of biomass and wastes *Int. J. Hydrogen Energy* 36 9529–41

[90] Blanco P H, Wu C, Onwudili J A, Dupont V and Williams P T 2014 Catalytic Pyrolysis/Gasification of Refuse Derived Fuel for Hydrogen Production and Tar Reduction: Influence of Nickel to Citric Acid Ratio Using Ni/SiO2 Catalysts *Waste and Biomass Valorization* 5 625–36

[91] Huber G W, Iborra S and Corma A 2006 Synthesis of transportation fuels from biomass: Chemistry, catalysts, and engineering *Chem. Rev.* 106 4044–98

[92] Matsumura Y, Minowa T, Potic B, Kersten S R A, Prins W, Van Swaaij W P M, Van De Beld B, Elliott D C, Neuenschwander G G, Kruse A and Antal M J 2005 Biomass gasification in near- and super-critical water: Status and prospects *Biomass and Bioenergy* 29 269–92

[93] Luterbacher J S, Froling M, Vogel F, Marechal F and Tester J W 2009 Hydrothermal gasification of waste biomass: Process design and life cycle asessment *Environ. Sci. Technol.* 43 1578–83

[94] Madenoğlu T G, Sağlam M, Yüksel M and Ballice L 2013 Simultaneous effect of temperature and pressure on catalytic hydrothermal gasification of glucose *J. Supercrit. Fluids* 73 151–60

[95] Liu C F and Sun R C 2010 *in "Cereal straw as resources for sustainable biomaterials and biofuels: Chemistry, extraction, lignins, hemicellulose, and cellulose"* (Elsevier, UK)

[96] Sansaniwal S K, Rosen M A and Tyagi S K 2017 Global challenges in the sustainable development of biomass gasification: An overview *Renew. Sustain. Energy Rev.* 80 23–43

[97] Fang Z, Minowa T, Fang C, Smith, R L, Inomata H and Kozinski J A 2008 Catalytic hydrothermal gasification of cellulose and glucose *Int. J. Hydrogen Energy* 33 981–90

[98] Jin H, Lu Y, Guo L, Zhang X and Pei A 2014 Hydrogen production by supercritical water gasification of biomass with homogeneous and heterogeneous catalyst *Adv. Condens. Matter Phys.* 2014 e160565

[99] Kohli K, Prajapati R and Sharma B K 2019 Bio-based chemicals from renewable biomass for integrated biorefineries *Energies* 12

[100] Toor S S, Rosendahl L, Nielsen M P, Glasius M, Rudolf A and Iversen S B 2012 Continuous production of bio-oil by catalytic liquefaction from wet distiller's grain with solubles (WDGS) from bio-ethanol production *Biomass and Bioenergy* 36 327–32

[101] Zhang T, Zhou Y, Liu D and Petrus L 2007 Qualitative analysis of products formed during the acid catalyzed liquefaction of bagasse in ethylene glycol *Bioresour. Technol.* 98 1454–9

[102] Atiqah Nasir N, Davies G and McGregor J 2020 Tailoring product characteristics in the carbonisation of brewers' spent grain through solvent selection *Food Bioprod. Process.* 120 41–7

[103] Nazari L, Yuan Z, Souzanchi S, Ray M B and Xu C 2015 Hydrothermal liquefaction of woody biomass in hot-compressed water: Catalyst screening and comprehensive characterization of bio-crude oils *Fuel* 162 74–83

[104] Singh R, Balagurumurthy B, Prakash A and Bhaskar T 2015 Catalytic hydrothermal liquefaction of water hyacinth *Bioresour. Technol.* 178 157–65

[105] Cheng S, DCruz I, Wang M, Leitch M and Xu C 2010 Highly efficient liquefaction of woody biomass in hot-compressed alcohol-water co-solvents *Energy and Fuels* 24 4659–67

[106] Cheng S, Wei L, Alsowij M, Corbin F, Boakye E, Gu Z and Raynie D 2017 Catalytic hydrothermal liquefaction (HTL) of biomass for bio-crude production using Ni/HZSM-5 catalysts *AIMS Environ. Sci.* 4 417–30

[107] Liu Z and Zhang F S 2008 Effects of various solvents on the liquefaction of biomass to produce fuels and chemical feedstocks *Energy Convers. Manag.* 49 3498–504

[108] Chornet E and Overend R P 1985 Biomass Liquefaction : An Overview. In: Overend R.P., Milne T.A., Mudge L.K. (eds) Fundamentals of Thermochemical Biomass Conversion. *Springer, Dordr.* 967–1002

[109] Castello D, Pedersen T H and Rosendahl L A 2018 Continuous hydrothermal liquefaction of biomass: A critical review *Energies* 11

[110] Ye L, Zhang J, Zhao J and Tu S 2014 Liquefaction of bamboo shoot shell for the production of polyols *Bioresour. Technol.* 153 147–53

[111] Yu F, Le Z, Chen P, Liu Y, Lin X and Ruan R 2008 Atmospheric pressure liquefaction of dried distillers grains (DDG) and making polyurethane foams from liquefied DDG *Appl. Biochem. Biotechnol.* 148 235–43

[112] Abdel Hakim A A, Nassar M, Emam A and Sultan M 2011 Preparation and characterization of rigid polyurethane foam prepared from sugar-cane bagasse polyol *Mater. Chem. Phys.* 129 301–7

[113] Yu F, Liu Y, Pan X, Lin X, Liu C, Chen P and Ruan R 2006 Liquefaction of corn stover and preparation of polyester from the liquefied polyol *Appl. Biochem. Biotechnol.* 130 574–85

[114] Hu S and Li Y 2014 Two-step sequential liquefaction of lignocellulosic biomass by crude glycerol for the production of polyols and polyurethane foams *Bioresour. Technol.* 161 410–5

[115] Hu S, Wan C and Li Y 2012 Production and characterization of biopolyols and polyurethane foams from crude glycerol based liquefaction of soybean straw *Bioresour. Technol.* 103 227–33

[116] Yamada T and Ono H 1999 Rapid liquefaction of lignocellulosic waste by using ethylene carbonate *Bioresour. Technol.* 70 61–7

[117] Lu Z, Fan L, Wu Z, Zhang H, Liao Y, Zheng D and Wang S 2015 Efficient liquefaction of woody biomass in polyhydric alcohol with acidic ionic liquid as a green catalyst *Biomass and Bioenergy* 81 154–61

[118] Akhtar J and Amin N A S 2011 A review on process conditions for optimum bio-oil yield in hydrothermal liquefaction of biomass *Renew. Sustain. Energy Rev.* 15 1615–24

[119] Midgett J S, Stevens B E, Dassey A J, Spivey J J and Theegala C S 2012 Assessing feedstocks and catalysts for production of bio-oils from hydrothermal liquefaction *Waste and Biomass Valorization* 3 259–68

[120] Chan Y H, Yusup S, Quitain A T, Tan R R, Sasaki M, Lam H L and Uemura Y 2015 Effect of process parameters on hydrothermal liquefaction of oil palm biomass for bio-oil production and its life cycle assessment *Energy Convers. Manag.* 104 180–8

[121] Al-Muntaser A A, Varfolomeev M A, Suwaid M A, Yuan C, Chemodanov A E, Feoktistov D A, Rakhmatullin I Z, Abbas M, Domínguez-Álvarez E, Akhmadiyarov A A, Klochkov V V. and Amerkhanov M I 2020 Hydrothermal upgrading of heavy oil in the presence of water at sub-critical, near-critical and supercritical conditions *J. Pet. Sci. Eng.* 184

[122] Xu J, Jiang J, Hse C Y and Shupe T F 2013 Effect of methanol on the liquefaction reaction of biomass in hot compressed water under microwave energy *Energy and Fuels* 27 4791–5

[123] Mussatto S I, Dragone G and Roberto I C 2006 Brewers' spent grain: Generation, characteristics and potential applications *J. Cereal Sci.* 43 1–14

[124] del Río J C, Prinsen P and Gutiérrez A 2013 Chemical composition of lipids in brewer's spent grain: A promising source of valuable phytochemicals *J. Cereal Sci.* 58 248–54

[125] Fărcaş A C, Socaci S A, Dulf F V., Tofană M, Mudura E and Diaconeasa Z 2015 Volatile profile, fatty acids composition and total phenolics content of brewers' spent grain by-product with potential use in the development of new functional foods *J. Cereal Sci.* 64 34–42

[126] Amarasekara A S and Wiredu B 2015 Acidic ionic liquid catalyzed liquefaction of cellulose in ethylene glycol; Identification of a new cellulose derived cyclopentenone derivative *Ind. Eng. Chem. Res.* 54 824–31

[127] Hao W, Tang X, Zeng X, Sun Y, Liu S and Lin L 2015 Catalytic Conversion of Glucose to Levulinate Ester Derivative in Ethylene Glycol *bioresources.com* 10 4191–203

[128] Vicente G, Martínez M and Aracil J 2004 Integrated biodiesel production: A comparison of different homogeneous catalysts systems *Bioresour. Technol.* 92 297–305

[129] Johnson D T and Taconi K A 2007 The Glycerin Glut: Options for the Value-Added Conversion of Crude Glycerol Resulting from Biodiesel Production *Wiley Intersci.* 338–48

[130] Pedersen T H, Jasiunas L, Casamassima L, Singh S, Jensen T and Rosendahl L A 2015 Synergetic hydrothermal co-liquefaction of crude glycerol and aspen wood *Energy Convers. Manag.* 106 886–91

[131] Wolfson A, Dlugy C, Shotland Y and Tavor D 2009 Glycerol as solvent and hydrogen donor in transfer hydrogenation-dehydrogenation reactions *Tetrahedron Lett.* 50 5951–3

[132] Lee S H and Ohkita T 2003 Rapid wood liquefaction by supercritical phenol *Wood Sci. Technol.* 37 29–38

[133] Toor S S, Rosendahl L and Rudolf A 2011 Hydrothermal liquefaction of biomass: A review of subcritical water technologies *Energy* 36 2328–42

[134] Zhu Z, Rosendahl L, Toor S S, Yu D and Chen G 2015 Hydrothermal liquefaction of barley straw to bio-crude oil: Effects of reaction temperature and aqueous phase recirculation *Appl. Energy* 137 183–92

[135] Mazaheri H, Lee K T, Bhatia S and Mohamed A R 2010 Subcritical water liquefaction of oil palm fruit press fiber for the production of bio-oil: Effect of catalysts *Bioresour. Technol.* 101 745–51

[136] Mun S P, Gilmour I A and Jordan P J 2006 Effect of Organic Sulfonic Acids as Catalysts during Phenol Liquefaction of Pinus radiata Bark *J. Ind. Eng. Chem.* 12 720–6

[137] Araya P E, Droguett S E, Neuburg H J and Badilla-Ohlbaum R 1986 Catalytic wood liquefaction using a hydrogen donor solvent. *Can. J. Chem. Eng.* 64 775–80

[138] Jindal M K and Jha M K 2015 Effect of process conditions on hydrothermal liquefaction of biomass *IJCBS Res. Pap.* 2

[139] Zhang S, Yang X, Zhang H, Chu C, Zheng K, Ju M and Liu L 2019 Liquefaction of Biomass and Upgrading of Bio-Oil: A Review *molecules*

[140] Isa K M, Abdullah T A T and Ali U F M 2018 Hydrogen donor solvents in liquefaction of biomass: A review *Renew. Sustain. Energy Rev.* 81 1259–68

[141] Ren R, Han X, Zhang H, Lin H, Zhao J, Zheng Y and Wang H 2018 High yield bio-oil production by hydrothermal liquefaction of a hydrocarbon-rich microalgae and biocrude upgrading *Carbon Resour. Convers.* 1 153–9

[142] de Caprariis B, De Filippis P, Petrullo A and Scarsella M 2017 Hydrothermal liquefaction of biomass: Influence of temperature and biomass composition on the bio-oil production *Fuel* 208 618–25

[143] Sugano M, Takagi H, Hirano K and Mashimo K 2008 Hydrothermal liquefaction of plantation biomass with two kinds of wastewater from paper industry *J. Mater. Sci.* 43 2476–86

[144] Yin S, Dolan R, Harris M and Tan Z 2010 Subcritical hydrothermal liquefaction of cattle manure to bio-oil: Effects of conversion parameters on bio-oil yield and characterization of bio-oil *Bioresour. Technol.* 101 3657–64

[145] Zhang S, Zhou S, Yang X, Xi W, Zheng K, Chu C, Ju M and Liu L 2020 Effect of operating parameters on hydrothermal liquefaction of corn straw and its life cycle assessment *Environ. Sci. Pollut. Res.* 27 6362–74

[146] Zhang S, Yang X, Zhang H, Chu C, Zheng K, Ju M and Liu L 2019 Liquefaction of biomass and upgrading of bio-oil: A review *Molecules* 24 1–30

[147] Atlas Big 2018 World sugarcane production map *Retrived from Atlas Big <https//www.atlasbig.com/en-us/countries-sugarcane-production> Accessed [01.12.2019]*

[148] Zafar S 2019 Biomass Resources from Sugar Industry *BioEnergy Consult*

[149] Smithers J 2014 Review of sugarcane trash recovery systems for energy cogeneration in South Africa *Renew. Sustain. Energy Rev.* 32 915–25

[150] Dantas G A, Legey L F L and Mazzone A 2013 Energy from sugarcane bagasse in Brazil: An assessment of the productivity and cost of different technological routes *Renew. Sustain. Energy Rev.* 21 356–64

[151] Hofsetz K and Silva M A 2012 Brazilian sugarcane bagasse: Energy and non-energy consumption *Biomass and Bioenergy* 46 564–73

[152] The Jakarta Post 2017 Two stages enterprises to convert sugarcane waste into fertilizers *Retrieved from <https//www.thejakartapost.com/news/2017/06/05/two-state-enterprises-to-convert-sugarcane-waste-into-fertilizers.html> [Accessed 01.12.2019]*

[153] FeaturePics (n.d.) Sugarcane bagasse *Retrieved from <https//www.featurepics.com/online/Sugarcane-Bagasse-2326768.aspx%0D> [Accessed 01.12.2019]*

[154] Eke J, Onwudili J A and Bridgwater A V. 2019 Influence of Moisture Contents on the Fast Pyrolysis of Trommel Fines in a Bubbling Fluidized Bed Reactor *Waste and Biomass Valorization* 0 0

[155] Mthembu L D 2015 *Production of levulinic acid from sugarcane bagasse* (Masters Thesis. Durban University of Technology Durban, South Africa)

[156] Guo Y, Tan C, Sun J, Li W, Zhang J and Zhao C 2020 Porous activated carbons derived from waste sugarcane bagasse for CO2 adsorption *Chem. Eng. J.* 381

[157] Lavarack B P, Griffin G J and Rodman D 2002 The acid hydrolysis of sugarcane bagasse hemicellulose to produce xylose, arabinose, glucose and other products *Biomass and Bioenergy* 23 367–80

[158] Laopaiboon P, Thani A, Leelavatcharamas V and Laopaiboon L 2010 Acid hydrolysis of sugarcane bagasse for lactic acid production *Bioresour. Technol.* 101 1036–43

[159] Soares L A, Braga J K, Motteran F, Sakamoto I K, Monteiro P A S, Seleghim P and Varesche M B A 2018 Bioconversion of Sugarcane Bagasse into Value-Added Products by Bioaugmentation of Endogenous Cellulolytic and Fermentative Communities *Waste and Biomass Valorization* 10 1899–912

[160] Sindhu R, Gnansounou E, Binod P and Pandey A 2016 Bioconversion of sugarcane crop residue for value added products – An overview *Renew. Energy* 98 203–15

[161] Gomes G R, Rampon D S and Ramos L P 2018 Production of furan compounds from sugarcane bagasse using a catalytic system containing ZnCl2/HCl or AlCl3/HCl in a biphasic system *J. Braz. Chem. Soc.* 29 1115–22

[162] Anon Pinaceae. (n.d.). In Wikipedia *Retrieved from <https//en.wikipedia.org/wiki/Pinaceae#cite_note-2> [Accessed 10.07.2019]*

[163] Area M C and Popa V 2014 *Wood Fibres for Papermaking* (Smithers Rapra Technology Ltd. Shawbury, UK)

[164] Ranta-Maunus A, Denzler J K and Stapel P 2011 *Strength of European timber. Part 2. Properties of spruce and pine tested in Gradewood project*

[165] Masten S and Haneke K E 2002 Turpentine (Turpentine Oil, Wood Turpentine, Sulfate Turpentine) *NTP (National Toxicol. Program)* 1–88

[166] Sari D R and Ariyanto 2018 The potential of woody waste biomass from the logging activity at the natural forest of Berau District, East Kalimantan *IOP Conf. Ser. Earth Environ. Sci. 144 012061*

[167] Mckeever D B 2004 Inventories of woody residues and solid waste wood available for recovery in the united states, 2002 *USDA For. Serv. For. Prod. Lab. Madison, Wisconsin USA*

[168] Prim Pines (n.d.) The pine needle *Retrieved from <https//www.primpines.com/pineneedle.html> [Accessed 11.06.19]*

[169] Dhaundiyal A and Gangwar J 2015 Kinetics of the thermal decomposition of pine needles *ACTA Univ. SAPIENTIAE Agric. Environ.* 7 5–22

[170] Ghosh M K and Ghosh U K 2011 Utilization of Pine needles as bed material in solid state fermentation for production of Lactic acid by Lactobacillus strains *BioResources* 6 1556–75

[171] Zeng W C, Jia L R, Zhang Y, Cen J Q, Chen X, Gao H, Feng S and Huang Y N 2011 Antibrowning and Antimicrobial Activities of the Water-Soluble Extract from Pine Needles of Cedrus deodara *J. Food Sci.* 76 318–23

[172] Singha A S and Thakur V K 2009 Study of mechanical properties of urea-formaldehyde thermosets reinforced by pine needle powder *bioresources* 4 292–308

[173] Millikin L L 1920 *Pine Needle Basketry* (J. L. Hammett Company, Cambridge Massachusetts, USA)

[174] Mallow J M and (n.d.) Prim Pines Gallery *Prim pines. Retrieved from <https//www.primpines.com/gallery.html> [Accessed 11.06.19]*

[175] Philippou K, Anastopoulos I, Dosche C and Pashalidis I 2019 Synthesis and characterization of a novel Fe3O4-loaded oxidized biochar from pine needles and its application for uranium removal. Kinetic, thermodynamic, and mechanistic analysis *J. Environ. Manage.* 252

[176] Mahajan D, Bhat Z F and Kumar S 2016 Pine needles (Cedrus deodara (Roxb.) Loud.) extract as a novel preservative in cheese *Food Packag. Shelf Life* 7 20–5

[177] ASTM E-82 2014 Standard Test Method for Moisture Analysis of Particulate Wood Fuels 1 *ASTM Int.* 82 2

[178] Hames B, Ruiz R, Scarlata C, Sluiter A, Sluiter J and Templeton D 2008 Preparation of Samples for Compositional Analysis Laboratory Analytical Procedure *Natl. Renew. Energy Lab.* 1–9

[179] Brown M E 2001 *Introduction to thermal analysis: techniques and applications. Vol. 1.* (Kluwer Academic Publishers, The Netherlands)

[180] Cai J, Wang Y, Zhou L and Huang Q 2007 Thermogravimetric analysis and kinetics of coal / plastic blends during co-pyrolysis in nitrogen atmosphere *Fuel Process. Technol.* 89

[181] Carrier M, Loppinet-Serani A, Denux D, Lasnier J M, Ham-Pichavant F, Cansell F and Aymonier C 2011 Thermogravimetric analysis as a new method to determine the lignocellulosic composition of biomass *Biomass and Bioenergy* 35 298–307

[182] Sebio-Puñal T, Naya S, López-Beceiro J, Tarrío-Saavedra J and Artiaga R 2012 Thermogravimetric analysis of wood, holocellulose, and lignin from five wood species *J. Therm. Anal. Calorim.* 109 1163–7

[183] Lee Y, Park J, Gang K S, Ryu C and Yang W 2013 Production and Characterization of Biochar from Various Biomass Materials by Slow Pyrolysis *Food Fertil. Technol. Cent.* 1–11

[184] Singh Y D, Mahanta P and Bora U 2017 Comprehensive characterization of lignocellulosic biomass through proximate, ultimate and compositional analysis for bioenergy production *Renew. Energy* 103 490–500

[185] Munir S, Daood S S, Nimmo W, Cunliffe A M and Gibbs B M 2009 Thermal analysis and devolatilization kinetics of cotton stalk, sugar cane bagasse and shea meal under nitrogen and air atmospheres *Bioresour. Technol.* 100 1413–8

[186] Agrawal R 2009 Compositional Analysis of Solid Waste and Refuse Derived Fuels by Thermogravimetry *Compos. Anal. by Thermogravim.* 259-259–13

[187] García R, Pizarro C, Lavín A G and Bueno J L 2013 Biomass proximate analysis using thermogravimetry *Bioresour. Technol.* 139 1–4

[188] Brebu M and Vasile C 2010 Thermal degradation of lignin- a review *Cellul. Chem. Technol.* 44 353–63

[189] ASTM E1131 − 08 2015 Standard Test Method for Compositional Analysis by Thermogravimetry 1 *ASTM Int.* 08 6

[190] Vassilev S V., Vassileva C G and Vassilev V S 2015 Advantages and disadvantages of composition and properties of biomass in comparison with coal: An overview *Fuel* 158 330–50

[191] Velázquez-Martí B, Gaibor-Chávez J, Niño-Ruiz Z and Cortés-Rojas E 2018 Development of biomass fast proximate analysis by thermogravimetric scale *Renew. Energy* 126 954–9

[192] ASTM Standard E870 −82 2013 Standard Test Methods for Analysis of Wood Fuels *ASTM Int.* 1–2

[193] ASTM E − 82 2013 Standard Test Method for Volatile Matter in the Analysis of Particulate Wood Fuels *ASTM Int.* 1–3

[194] ASTM D1102-84 2013 Standard Test Method for Ash in Wood *ASTM Int.* 1–2

[195] Thermo Nicolet Corporation 2001 *Introduction to Fourier Transform Infrared Spectrometry*

[196] Stuart B H 2004 *Infrared Spectroscopy: Fundamentals and Applications* (John Wiley & Sons Ltd, West Sussex, England)

[197] Griffiths P R and de Haseth J A 2007 *Fourier transform infrared spectrometry* (John Wiley & Sons, Inc., Hoboken, New Jersey, USA)

[198] Smith B C 2011 *Fundamentals of Fourier transform infrared spectrometry* (Taylor and Francis Group, LLC, USA)

[199] Allison G A 2012 Application of Fourier Transform Mid-Infrared Spectroscopy (FTIR) for Research into Biomass Feed-Stocks *Fourier Transform. - New Anal. Approaches FTIR Strateg.*

[200] Krotz L and Giazzi G 2014 Thermo Scientific FLASH 2000 CHNS Analyzer : Stability , Linearity , Repeatability and Accuracy *Thermo Fish. Sci. Inc.*

[201] Sluiter A, Ruiz R, Scarlata C, J. Sluiter and Templeton D 2008 *Determination of Extractives in Biomass: Laboratory Analytical Procedure (LAP). Technical Report NREL/TP-510-42619*

[202] Technical Association of Pulp and Paper Industry 2006 Acid-insoluble Lignin in Wood and Pulp (T222 Om-02) *TAPPI Stand.* 1–7

[203] Aditha S K, Kurdekar A D, Chunduri L A A, Patnaik S and Kamisetti V 2016 Aqueous based reflux method for green synthesis of nanostructures: Application in CZTS synthesis *MethodsX* 3 35–42

[204] Gómez L Q 2017 *Hydrothermal conversion of CO2 into higher hydrocarbons and oxygenates.* (Ph.D. Thesis. The University of Sheffield, UK)

[205] Patel I (n.d.) Gas Chromatography / Mass Spectrometry *Retrieved from <http//ishigirl.tripod.com/pchem/gc_ms.html> [Accessed 16.07.2019]*

[206] Diagram.alimb.us (n.d.) Gc Ms Block Diagram *Retrieved from <https//diagram.alimb.us/50-gc-ms-block-diagram-gk8x/gc-ms-block-diagram-lcms-block-diagram-pcr-diagram-elsavadorla-2/> [Accesssed 16.07.2019]*

[207] Williams D H and Fleming I 1995 *Spectroscopic Methods in Organic Chemistry* (McGraw-Hil, New York, USA)

[208] Pavia D L, Lampman G M, Kriz G S and Vyvyan J R 2009 *Introduction to spectroscopy, 4th edition* (Cengage Learning, USA)

[209] Chromacademy (n.d.) The theory of HPLC: Introduction *Crawford Sci.*

[210] Showa Denko America Inc. 2019 HPLC 101 *Retrieved from <https//www.shodexhplc.com/lessons/lesson-1-introduction-to-hplc/> [Accessed 01.05.2019]*

[211] Shimadzu (n.d.) Methods for Separating Sugars *Retrieved from <https//www.shimadzu.com/an/hplc/support/lib/lctalk/50/50intro.html> [Accessed 16.08.2018]*

[212] ThermoFischer Scientific XRF Technology *Retrieved from <https//www.thermofisher.com/uk/en/home/industrial/spectroscopy-elemental-isotope-analysis/spectroscopy-elemental-isotope-analysis-learning-center/elemental-analysis-information/xrf-technology.html> [Accessed 16.10.2019]*

[213] Brouwer P 2010 *Theory of XRF: Getting acquainted with the principles* (PANalytical BV, The Netherlands)

[214] Barde P and Barde M 2012 What to use to express the variability of data: Standard deviation or standard error of mean? *Perspect. Clin. Res.* 3 113

[215] Joshua J A, Ahiekpor J C and Kuyea A 2016 Nigerian Hardwood (Nesogordonia papaverifera) Sawdust Characterization: Proximate Analysis, Cellulose and Lignin Contents *Lignocellulose* 5 50–8

[216] Stahl R, Henrich E, Gehrmann H J, Vodegel S and Koch M 2004 Definition of a standard biomass *RENEW – Renew. fuels Adv. power trains* SES6-CT-20 1–14

[217] Rezende C A, De Lima M, Maziero P, Deazevedo E, Garcia W and Polikarpov I 2011 Chemical and morphological characterization of sugarcane bagasse submitted to a delignification process for enhanced enzymatic digestibility *Biotechnol. Biofuels* 4 54

[218] Kim M and Day D F 2011 Composition of sugar cane, energy cane, and sweet sorghum suitable for ethanol production at Louisiana sugar mills *J. Ind. Microbiol. Biotechnol.* 38 803–7

[219] Di Blasi C 2008 Modeling chemical and physical processes of wood and biomass pyrolysis *Prog. Energy Combust. Sci.* 34 47–90

[220] Burhenne L, Messmer J, Aicher T and Laborie M P 2013 The effect of the biomass components lignin, cellulose and hemicellulose on TGA and fixed bed pyrolysis *J. Anal. Appl. Pyrolysis* 101 177–84

[221] Yang H, Yan R, Chen H, Lee D H and Zheng C 2007 Characteristics of hemicellulose, cellulose and lignin pyrolysis *Fuel* 86 1781–8

[222] Cantrell K B, Martin J H and Ro K S 2011 Application of Thermogravimetric Analysis for the Proximate Analysis of Livestock Wastes *J. ASTM Int.* 7 102583

[223] Safi M J, Mishra I M and Prasad B 2004 Global degradation kinetics of pine needles in air *Thermochim. Acta* 412 155–62

[224] Varma A K and Mondal P 2016 Physicochemical characterization and kinetic study of pine needle for pyrolysis process *J. Therm. Anal. Calorim.* 124 487–97

[225] Channiwala S A and Parikh P P 2002 A unified correlation for estimating HHV of solid, liquid and gaseous fuels *Fuel* 81 1051–63

[226] McKendry P 2002 Energy production from biomass (part 1): overview of biomass *Bioresour. Technol* 83 37–46

[227] Marsoem S N and Irawati D 2016 Basic properties of Acacia mangium and Acacia auriculiformis as a heating fuel *AIP Conf. Proc.* 1755

[228] Monti A, Di Virgilio N and Venturi G 2008 Mineral composition and ash content of six major energy crops *Biomass and Bioenergy* 32 216–23

[229] Feng S, Yuan Z, Leitch M and Xu C C 2014 Hydrothermal liquefaction of barks into bio-crude - Effects of species and ash content/composition *Fuel* 116 214–20

[230] Boeriu C G, Bravo D, Gosselink R J A and Van Dam J E G 2004 Characterisation of structure-dependent functional properties of lignin with infrared spectroscopy *Ind. Crops Prod.* 20 205–18

[231] Yang J, Lu X, Liu X, Xu J, Zhou Q and Zhang S 2017 Rapid and productive extraction of high purity cellulose material via selective depolymerization of the lignin-carbohydrate complex at mild conditions *Green Chem.* 19 2234–43

[232] Tan S S Y, MacFarlane D R, Upfal J, Edye L A, Doherty W O S, Patti A F, Pringle J M and Scott J L 2009 Extraction of lignin from lignocellulose at atmospheric pressure using alkylbenzenesulfonate ionic liquid *Green Chem.* 11 339

[233] Xu F, Yu J, Tesso T, Dowell F and Wang D 2013 Qualitative and quantitative analysis of lignocellulosic biomass using infrared techniques: A mini-review *Appl. Energy* 104 801–9

[234] Hurtubise F G and KrÄSSIG H 1960 Classification of Fine Structural Characteristics in Cellulose by Infrared Spectroscopy Use of Potassium Bromide Pellet Technique *Anal. Chem.* 32 177–81

[235] Su Y, Du R, Guo H, Cao M, Wu Q, Su R, Qi W and He Z 2015 Fractional pretreatment of lignocellulose by alkaline hydrogen peroxide: Characterization of its major components *Food Bioprod. Process.* 94 322–30

[236] Shen X-J, Wang B, Pan-li H, Wen J-L and Sun R-C 2016 Understanding the structural changes and depolymerization of Eucalyptus lignin under mild conditions in aqueous AlCl3 *RSC Adv.* 6 45315–25

[237] Rojas J, Lopez A, Guisao S and Ortiz C 2011 Evaluation of several microcrystalline celluloses obtained from agricultural by-products *J. Adv. Pharm. Technol. Res.* 2 144

[238] Sofla M R K, Brown R J, Tsuzuki T and Rainey T J 2016 A comparison of cellulose nanocrystals and cellulose nanofibres extracted from bagasse using acid and ball milling methods *Adv. Nat. Sci. Nanosci. Nanotechnol.* 7

[239] Abderrahim B, Abderrahman E, Mohamed A, Fatima T, Abdesselam T and Krim O 2015 Kinetic Thermal Degradation of Cellulose, Polybutylene Succinate and a Green Composite: Comparative Study *World J. Environ. Eng. Vol. 3, 2015, Pages 95-110* 3 95–110

[240] Long J, Li X, Guo B, Wang F, Yu Y and Wang L 2012 Simultaneous delignification and selective catalytic transformation of agricultural lignocellulose in cooperative ionic liquid pairs *Green Chem.* 14 1935

[241] Liew F K, Hamdan S, Rahman M R, Rusop M, Lai J C H, Hossen M F and Rahman M M 2015 Synthesis and characterization of cellulose from green bamboo by chemical treatment with mechanical process *J. Chem.* 2015

[242] Luo Y, Fan J, Budarin V L, Hu C and Clark J H 2017 Microwave-assisted hydrothermal selective dissolution and utilisation of hemicellulose in Phyllostachys heterocycla cv. pubescens *Green Chem.* 19 4889–99

[243] Santoni I, Callone E, Sandak A, Sandak J and Dirè S 2015 Solid state NMR and IR characterization of wood polymer structure in relation to tree provenance *Carbohydr. Polym.* 117 710–21

[244] Tian J, Fu S and Lucia L A 2015 Ionic Liquid-Based Molecular Oxygen Oxidation of Eucalyptus Kraft Lignin to Obtain a Suite of Monomeric Aromatic By-Products *J. Wood Chem. Technol.* 35 280–90

[245] Lu Y, Sun Q, Yang D, She X, Yao X, Zhu G, Liu Y, Zhao H and Li J 2012 Fabrication of mesoporous lignocellulose aerogels from wood via cyclic liquid nitrogen freezing–thawing in ionic liquid solution *J. Mater. Chem.* 22 13548

[246] Oliva M, Manzanares P, Ballesteros I, Chamorro M Á, Felicia S, Ballesteros M and Moreno A D 2017 A Sequential Steam Explosion and Reactive Extrusion Pretreatment for Lignocellulosic Biomass Conversion within a Fermentation-Based Biorefinery Perspective *Fermentation* 3 15

[247] Phinichka N and Kaenthong S 2016 Regenerated cellulose from high alpha cellulose pulp of steam-exploded sugarcane bagasse *J. Mater. Res. Technol.* 1–11

[248] Sills D L and Gossett J M 2012 Using FTIR to predict saccharification from enzymatic hydrolysis of alkali-pretreated biomasses *Biotechnol. Bioeng.* 109 353–62

[249] Zhang P Y, Wampler J L, Bhunia A K, Burkholder K M, Patterson J A and Whistler R L 2004 Effects of arabinoxylans on activation of murine macrophages and growth performance of broiler chicks *Cereal Chem.* 81 511–4

[250] Ramirez J A, Brown R J and Rainey T J 2015 A review of hydrothermal liquefaction bio-crude properties and prospects for upgrading to transportation fuels *Energies* 8 6765–94

[251] Breitmaier E 2006 *Terpenes Flavors, Fragrances, Pharmaca, Pheromones* (WILEY-VCH)

[252] Salem M Z M, Zeidler A, Böhm M, Mohamed M E and Ali H M 2015 GC/MS Analysis of Oil Extractives from Wood and Bark of Pinus sylvestris, Abies alba, Picea abies, and Larix decidua *BioResources* 10 7725–37

[253] Yao S S, Guo W F, Lu Y and Jiang Y X 2005 Flavor characteristics of lapsang souchong and smoked lapsang souchong, a special chinese black tea with pine smoking process *J. Agric. Food Chem.* 53 8688–93

[254] Chattopadhyay H and Sarkar P B 1946 A new method for the estimation of cellulose *Proc Natl Inst Sci India 12(1)23–46* VOL. XII

[255] Sjöström E and Alén R 2013 *Analytical methods in wood chemistry, pulping, and papermaking* (Springer Science & Business Media)

[256] Gonçalves M, Rodrigues R, Galhardo T S and Carvalho W A 2016 Highly selective acetalization of glycerol with acetone to solketal over acidic carbon-based catalysts from biodiesel waste *Fuel* 181 46–54

[257] Vicente G, Melero J A, Morales G, Paniagua M and Martín E 2010 Acetalisation of bio-glycerol with acetone to produce solketal over sulfonic mesostructured silicas *Green Chem.* 12 899–907

[258] Manjunathan P, Maradur S P, Halgeri A B and Shanbhag G V. 2015 Room temperature synthesis of solketal from acetalization of glycerol with acetone: Effect of crystallite size and the role of acidity of beta zeolite *J. Mol. Catal. A Chem.* 396 47–54

[259] Mota C J A, Da Silva C X A, Rosenbach N, Costa J and Da Silva F 2010 Glycerin derivatives as fuel additives: The addition of glycerol/acetone ketal (solketal) in gasolines *Energy and Fuels* 24 2733–6

[260] Priya S S, Selvakannan P R, Chary K V R, Kantam M L and Bhargava S K 2017 Solvent-free microwave-assisted synthesis of solketal from glycerol using transition metal ions promoted mordenite solid acid catalysts *Mol. Catal.* 434 184–93

[261] Pastor-Pérez L, Merlo A, Buitrago-Sierra R, Casella M and Sepúlveda-Escribano A 2015 Bimetallic PtSn/C catalysts obtained via SOMC/M for glycerol steam reforming *J. Colloid Interface Sci.* 459 160–6

[262] Tran N H and Kannangara G S K 2013 Conversion of glycerol to hydrogen rich gas *Chem. Soc. Rev.* 42 9454–79

[263] Collett C H 2018 *Improving the sustainability of heterogeneous catalysis through understanding the role of carbon* (Ph.D. Thesis, The University of Sheffield, UK)

[264] Xu X, Meng H, Lu Y and Li C 2018 Aldol condensation of refluxing acetone on CaC2 achieves efficient coproduction of diacetone alcohol, mesityl oxide and isophorone *RSC Adv.* 8 30610–5

[265] Thotla S, Agarwal V and Mahajani S M 2007 Simultaneous production of diacetone alcohol and mesityl oxide from acetone using reactive distillation *Chem. Eng. Sci.* 62 5567–74

[266] Pedersen T H and Rosendahl L A 2015 Production of fuel range oxygenates by supercritical hydrothermal liquefaction of lignocellulosic model systems *Biomass and Bioenergy* 83 206–15

[267] Poling B E, Thomson G H, Friend D G, Rowley R L and Wilding W V 2008 *Perry's Chemical Engineers' Handbook: Section 2 Physical and Chemical Data* (New York: McGraw-Hill)

[268] Glycerine Producers' Association 1963 Physical Properties of Glycerine and Its Solutions *Glycerine Prod. Assoc.*

[269] Liu H M, Li M F, Yang S and Sun R C 2013 Understanding the mechanism of cypress liquefaction in hot-compressed water through characterization of solid residues *Energies* 6 1590–603

[270] Caspeta L, Castillo T and Nielsen J 2015 Modifying Yeast Tolerance to Inhibitory Conditions of Ethanol Production Processes *Front. Bioeng. Biotechnol.* 3 1–15

[271] Palmqvist E and Hahn-Hägerdal B 2000 Fermentation of lignocellulosic hydrolysates. II: Inhibitors and mechanisms of inhibition *Bioresour. Technol.* 74 25–33

[272] Gai C, Li Y, Peng N, Fan A and Liu Z 2015 Co-liquefaction of microalgae and lignocellulosic biomass in subcritical water *Bioresour. Technol.* 185 240–5

[273] Tran K Q 2016 Fast hydrothermal liquefaction for production of chemicals and biofuels from wet biomass – The need to develop a plug-flow reactor *Bioresour. Technol.* 213 327–32

[274] Sasaki M, Furukawa M, Minami K, Adschiri T and Arai K 2002 Kinetics and mechanism of cellobiose hydrolysis and retro-aldol condensation in subcritical and supercritical water *Ind. Eng. Chem. Res.* 41 6642–9

[275] Grilc M, Likozar B and Levec J 2014 Hydrodeoxygenation and hydrocracking of solvolysed lignocellulosic biomass by oxide, reduced and sulphide form of NiMo, Ni, Mo and Pd catalysts *Appl. Catal. B Environ.* 150–151 275–87

[276] Huo Z, Fang Y, Yao G, Zeng X, Ren D and Jin F 2015 Improved two-step hydrothermal process for acetic acid production from carbohydrate biomass *J. Energy Chem.* 24 207–12

[277] Werpy T and Petersen G 2004 *Top Value Added Chemicals From Biomass Volume I: Results of Screening for Potential Candidates from Sugars and Synthesis Gas* ((No. DOE/GO-102004-1992). National Renewable Energy Lab., Golden, CO (US))

[278] Yan X, Ma J, Wang W, Zhao Y and Zhou J 2018 The effect of different catalysts and process parameters on the chemical content of bio-oils from hydrothermal liquefaction of sugarcane bagasse *BioResources* 13 997–1018

[279] Putro J N, Soetaredjo F E, Lin S Y, Ju Y H and Ismadji S 2016 Pretreatment and conversion of lignocellulose biomass into valuable chemicals *RSC Adv.* 6 46834–52

[280] Tiong Y W, Yap C L, Gan S and Yap W S P 2018 Conversion of Biomass and Its Derivatives to Levulinic Acid and Levulinate Esters via Ionic Liquids *Ind. Eng. Chem. Res.* 57 4749–66

[281] Bulat J A and Liu H J 1976 A practical synthesis of cis-jasmone from levnliinic acid *Can. J. Chem. Eng.* 5 4–6

[282] Mullen B D, Badarinarayana V, Santos-Martinez M and Selifonov S 2010 Catalytic selectivity of ketalization versus transesterification *Top. Catal.* 53 1235–40

[283] Freitas F A, Domenico L, Lachter E R, Galletti R A M, Antonetti C, Thamires B C and Nascimento R S V. 2016 Heterogeneous catalysis for the ketalisation of ethyl levulinate with 1,2-dodecanediol: Opening the way to a new class of bio-degradable surfactants *Catal. Commun.* 84–7

[284] Amarasekara A S and Animashaun M A 2016 Acid Catalyzed Competitive Esterification and Ketalization of Levulinic Acid with 1,2 and 1,3-Diols: The Effect of Heterogeneous and Homogeneous Catalysts *Catal. Letters* 146 1819–24

[285] Burdock G A 2010 *Fenaroli's handbook of flavor ingredients.* (CRC Press, Taylor & Francis Group, LLC, New York)

[286] Luan Q, Liu L jun, Gong S, Lu J, Wang X and Lv D 2018 Clean and efficient conversion of renewable levulinic acid to levulinate esters catalyzed by an organic-salt of H4SiW12O40 *Process Saf. Environ. Prot.* 117 341–9

[287] Joshi H, Moser B R, Toler J, Smith W F and Walker T 2011 Ethyl levulinate: A potential bio-based diluent for biodiesel which improves cold flow properties *Biomass and Bioenergy* 35 3262–6

[288] Buss W, Graham M C, MacKinnon G and Mašek O 2016 Strategies for producing biochars with minimum PAH contamination *J. Anal. Appl. Pyrolysis* 119 24–30

[289] Celaya-Sanfiz A, Morales-Vega N, De Marco M, Iruretagoyena D, Mokhtar M, Bawaked S M, Basahel S N, Al-Thabaiti S A, Alyoubi A O and Shaffer M S P 2015 Self-condensation of acetone over Mg-Al layered double hydroxide supported on multi-walled carbon nanotube catalysts *J. Mol. Catal. A Chem.* 398 50–7

[290] Álvarez M G, Frey A M, Bitter J H, Segarra A M, de Jong K P and Medina F 2013 On the role of the activation procedure of supported hydrotalcites for base catalyzed reactions: Glycerol to glycerol carbonate and self-condensation of acetone *Appl. Catal. B Environ.* 134–135 231–7

[291] Demeyer A, Voundi Nkana J C and Verloo M G 2001 Characteristics of wood ash and influence on soil properties and nutrient uptake: An overview *Bioresour. Technol.* 77 287–95

[292] Basumatary S, Nath B and Kalita P 2018 Application of agro-waste derived materials as heterogeneous base catalysts for biodiesel synthesis *J. Renew. Sustain. Energy* 10

[293] Xiong X, Yu I K M, Cao L, Tsang D C W, Zhang S and Ok Y S 2017 A review of biochar-based catalysts for chemical synthesis, biofuel production, and pollution control *Bioresour. Technol.* 246 254–70

[294] Collett C H and McGregor J 2016 Things go better with coke: The beneficial role of carbonaceous deposits in heterogeneous catalysis *Catal. Sci. Technol.* 6 363–78

[295] Gadamsetti S, Rajan N P, Rao G S and Chary K V R 2015 Acetalization of glycerol with acetone to bio fuel additives over supported molybdenum phosphate catalysts *J. Mol. Catal. A Chem.* 410 49–57

[296] Ramazanov D N, Dzhumbe A, Nekhaev A I, Samoilov V O, Maximov A L and Egorova E V 2015 Reaction between Glycerol and Acetone in the Presence of Ethylene Glycol *Pet. Chem.* 55 140–5

APPENDIX A

A.1 Mass balances of preliminary liquefaction experiments

The purpose of Table A1 is to display the distribution of solids, liquid, and gaseous products obtained from the liquefaction of sugarcane bagasse and pine needles under various conditions. It can be seen from Table A1 that a minor quantity of liquefaction solvent is lost to gas as well, therefore, the percentage of gas in this work was estimated based on the total mass of biomass and liquefaction solvent introduced. It is assumed in this work that no catalyst was lost to gas. The results demonstrate that the total amount of gas from both biomass and solvent was insignificant (less than 2 wt.%); as such, the gas phase was neglected in subsequent liquefaction experiments conducted in Chapters 5 - 7. Although the preliminary experiment did not investigate gas yield for the entire spectrum of reaction parameters employed in Chapters 5 - 7 (i.e. 160 – 300 °C and 1 – 30 bar), previous research [103,105,122] conducted on various biomass feedstocks under similar conditions (i.e. 180 - 350 °C and 20 bar) reported gas yields between 0.1 – 5 wt.% (based on dry biomass weight), which were considered negligible.

Table A1: *Mass balances of preliminary liquefaction experiments of sugarcane bagasse and pine needles. Liquefaction solvent: ethylene glycol, catalyst:H_2SO_4.*

Biomass type	Process conditions	Catalyst (wt.% of solvent)	INPUT		OUTPUT			
			Biomass (g)	Solvent (g)	Solids * (g)	Liquid (g)	Gas ** (g)	Gas (wt.% of biomass + solvent)
Blank/control experiments								
-	160 °C, 1 h, 1 bar, 300 rpm	-	-	20.00	0.00	19.95	0.05	0.25
-	160 °C, 1 h, 1 bar, 300 rpm	0.6 wt.%	-	20.00	0.00	19.68	0.32	1.60
Biomass liquefaction experiments								
Sugarcane bagasse	160 °C, 1 h, 1 bar, 300 rpm	-	2.00	20.00	1.46	20.18	0.36	1.64
Sugarcane bagasse	160 °C, 1 h, 1 bar, 300 rpm	0.6 wt.%	2.00	20.00	0.19	21.54	0.26	1.19
Pine needles	160 °C, 1 h, 1 bar, 300 rpm	0.6 wt.%	2.00	20.00	0.95	20.74	0.31	1.41
Pine needles	160 °C, 1 h, 1 bar, 300 rpm	1 wt.%	2.00	20.00	0.39	21.51	0.10	0.45
Pine needles	160 °C, 1.5 h, 1 bar, 300 rpm	1 wt.%	2.00	20.00	0.40	21.43	0.17	0.77
Pine needles	160 °C, 2 h, 1 bar, 300 rpm	1 wt.%	2.00	20.00	0.48	21.27	0.25	1.14
Pine needles	170 °C, 1 h, 1 bar, 300 rpm	1 wt.%	2.00	20.00	0.49	21.26	0.25	1.14
Pine needles	170 °C, 1.5 h, 1 bar, 300 rpm	1 wt.%	2.00	20.00	0.45	21.24	0.31	1.41

- not applied
** dry weight*
*** by difference*

A.2 Suitability of solvent and method for product (liquid-solid) separation

A.2.1 Methods

To identify a suitable solvent and method for product separation, four batches of biomass liquefaction experiments (A, B, C, and D) and two control experiments (I and II) were conducted under the same conditions on sugarcane bagasse, details of each process input are specified in Table A2. The product of each reaction was separated using a different combination of method with solvent: Soxhlet or vacuum filtration with either acetone or ethanol as outlined in Table A2. The findings are discussed in Section A.2.2.

Table A2: *Process input and methods of product separation for various batches of liquefied biomass (sugarcane bagasse). Conditions:2 g BM, 20 g EG, 0.12 g H_2SO_4 as catalyst at 160 °C, atmospheric pressure, 300 rpm, 1 h.*

Reactions (batch)	Process input (materials)	Product separation process
Biomass liquefaction experiments		
A	BM + EG + catalyst	Filtration + Ethanol, at room temperature
B	”	Filtration + Acetone, at room temperature
C	”	Soxhlet + Ethanol, 108 °C, 5 h
D	”	Soxhlet + Acetone, at 80 °C, 5 h
Control experiments		
I	EG only	--
II	EG + catalyst	--

A.2.2 Results and discussion

The method of product separation did not affect biomass conversion which was approximately 90 wt.% as evident in Figure A1. Ethylene glycol conversion was however, largely affected by the solvent type. Overall, the filtration of the post-reaction mixture with ethanol stands out as the most suitable in the options studied owing to the following reasons:

1. Ethanol did not have any undesired impact on the separation process, whereas acetone was found to needlessly engage in an acetalisation side reaction with ethylene glycol and propylene glycol (internal standard) in the presence of the catalyst (H_2SO_4) to produce 1,2dioxolane,2,2-dimethyl-, and 1,3dioxolane,2,2,4-trimethyl- respectively

as demonstrated in Schemes A1 and A2. This resulted in falsely higher conversion figures for ethylene glycol (Figure A1). Ethylene glycol conversion, therefore, increased by 35 % when acetone was employed for product filtration compared to ethanol. This claim was confirmed by the results of GCMS analysis of the controlled reactions, I and II. The samples I and II was divided into two halves each, one half of each sample was diluted with acetone and the other with ethanol just before analysis. The resulting total ion chromatogram is shown in Figure A2 while the calculated ethylene glycol conversion is plotted in Figure A1. In the absence of H_2SO_4, ethylene glycol remained 100 % unreacted (batch I), even when mixed with acetone. However, the presence of H_2SO_4 promoted the observed acetalisation of ethylene glycol and propylene glycol. The acetalisation reaction is so quick that it proceeded immediately acetone was added to the product mixture of reaction II just prior to analyses (Figure A2). Note the drastic decrease in peak heights of ethylene glycol and propylene glycol (internal standard), as well as the appearance of dioxolane derivatives when acetone was used as sample diluent. In fact, recent research has demonstrated that the acetalisation of polyols could progress at temperatures below 40 °C in the presence of an acid catalyst with conversions as high as 90 % within 5 min. [295,296].

2. As one would expect, comparatively less volume of ethanol to acetone is lost through evaporation: typically, 12 % of ethanol against ~28 % of acetone as documented in Table A3.

3. Though some level of precaution is needed to obtain a particle-free extract (product) while using vacuum filtration, this process takes less time (*i.e.* ~ 0.5 h versus 5 h) and consumes less energy compared to the Soxhlet extraction. Figure A1 further, indicates comparatively lower consumption of ethylene glycol with the use of filtration over Soxhlet. For example, ethylene glycol conversion increased slightly from 58 % for filtered products to 64 % for Soxhlet extracted products when ethanol was used as a solvent for separation. Such an increase (6 %) in ethylene glycol consumption could be lost to the self-condensation reaction of ethylene glycol at elevated temperatures (see Section 6.3.3.2 of Chapter 6).

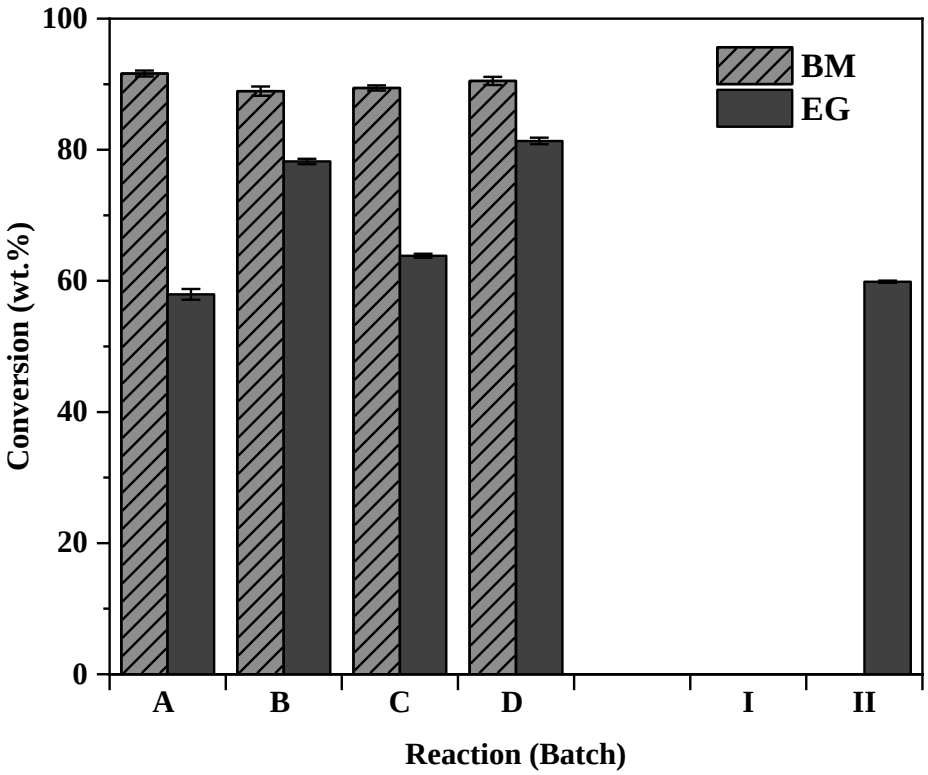

Figure A1: *Effect of solvent used for product separation on biomass and ethylene glycol conversion for different batches of reaction. Conditions:2 g BM (sugarcane bagasse), 20 g EG, and 0.12 g H_2SO_4 as catalyst at 160 °C, 30 bar He, 300 rpm, 1 h.*

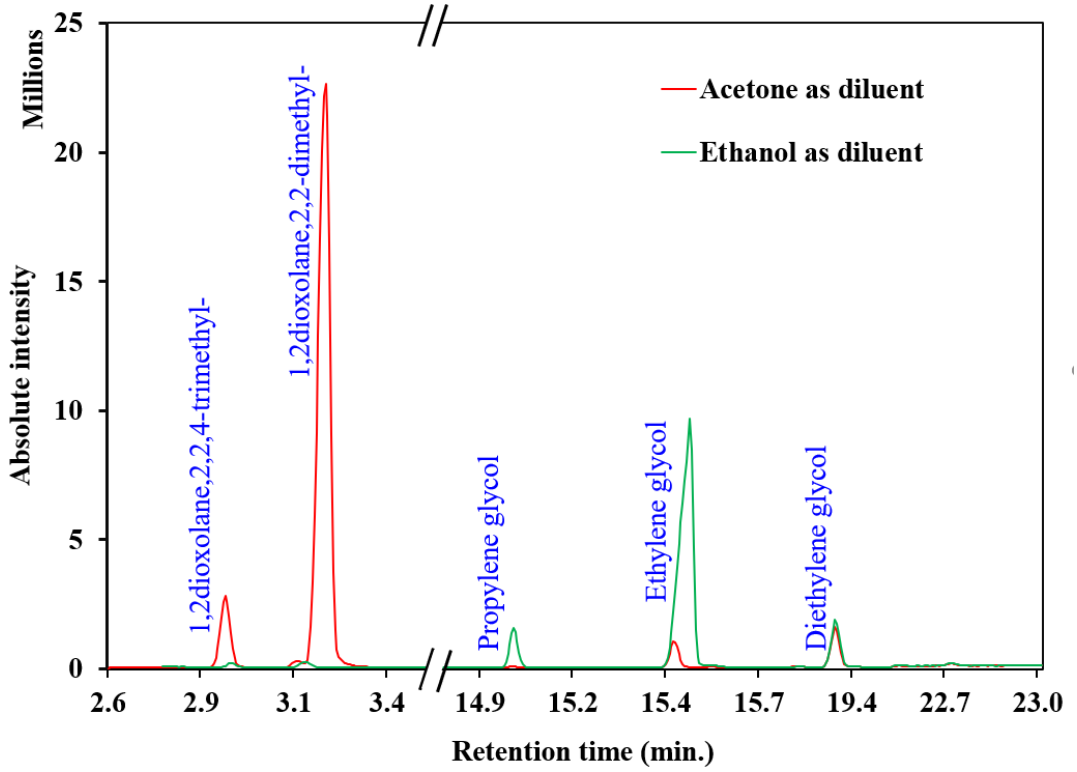

Figure A2: *GCMS chromatogram for control experiment "II" using two separate solvents; acetone, and ethanol for product dilution. Note the peak heights of ethylene glycol and propylene glycol in both cases, as well as the appearance of dioxolane derivatives when acetone was used.*

Table A3: *Amount of solvent used versus amount recovered during product separation.*

Batch	Volume of solvent used (ml)	Volume of solvent recovered (ml)	Percentage of solvent lost (%)
A	60	53 ± 0.68	12
B	60	43 ± 1.18	28
C	180	158 ± 1.10	12
D	180	136 ± 2.43	24

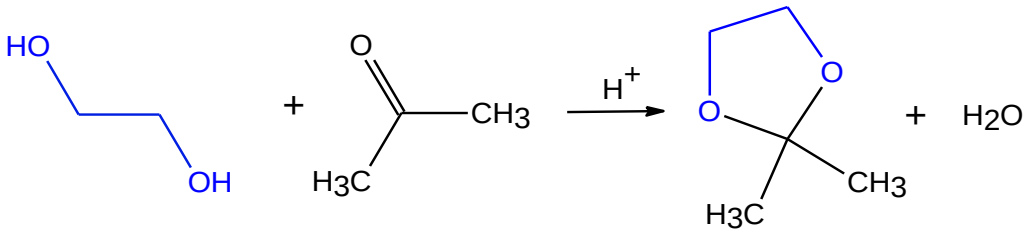

Scheme A1: *Reaction of ethylene glycol with acetone to form 1,2dioxolane,2,2-dimethyl-, and water.*

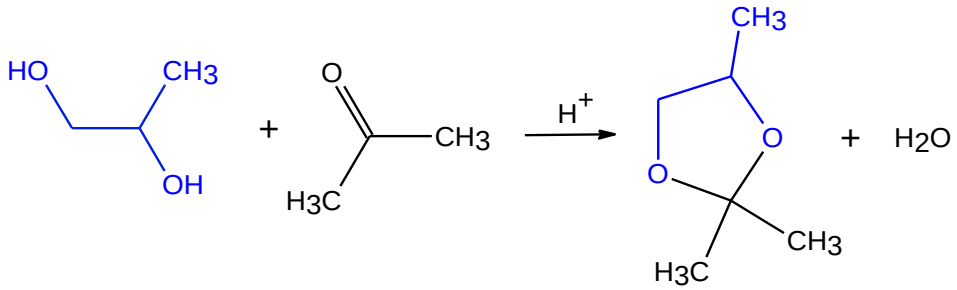

Scheme A2: *Reaction of propylene glycol with acetone to form 1,3dioxolane,2,2,4-trimethyl- and water.*

APPENDIX B

B.1 Supplementary information on proximate composition of pine needles and sugarcane bagasse (Chapter 4)

Table B1-a: *Proximate composition of pine needles obtained via manual versus TGA methods with the corresponding standard deviations and experimental errors. Values reported as the mean ± standard deviation in weight %.*

Component (wt.%)	Manual	E (%)	TGA	E (%)
Moisture	-		1.79 ± 0.03	1.57
Volatile matter	72.83 ± 0.37	0.51	73.55 ± 0.38	0.52
Fixed carbon	21.52	-	20.42 ± 0.21	1.02
Ash	5.64 ± 0.07	1.27	4.24 ± 0.22	5.10

Table B1-b: *Proximate composition of sugarcane bagasse obtained via manual versus TGA methods with the corresponding standard deviations and experimental errors. Values reported as the mean ± standard deviation in weight %.*

Component (wt.%)	Manual	E (%)	TGA	E (%)
Moisture	-		0.47 ± 0.08	16.58
Volatile matter	80.13 ± 0.83	1.04	80.47 ± 0.12	0.15
Fixed carbon	16.04	-	17.97 ± 0.07	0.37
Ash	3.83 ± 0.12	3.17	1.09 ± 0.02	1.44

APPENDIX C

C.1 Supplementary information for Chapter 6

Table C1: *GCMS identified compounds in liquid products obtained from the liquefaction of pine needles using ethylene glycol as solvent. Reaction conditions: 2 g pine needles, 20 g ethylene glycol, 0.12 g H_2SO_4 as catalyst (1 wt.% catalyst), 30 bar He initial pressure, 300 rpm and 1 h. Control is a blank experiment without pine needles (only ethylene glycol and 1 wt.% catalyst at 250 °C.*

SN	RT (min)	Name	Formula	Peak area (%)				
				Control	160 (°C)	200 (°C)	250 (°C)	300 (°C)
1	1.40	Acetaldehyde	C_2H_4O	1.7	0.7	-	1.3	1.2
2	1.66	Furan	C_4H_4O	-	-	-	-	0.2
3	1.67	Dimethyl acetal	$C_4H_{10}O_2$	8.4	-	0.5	-	-
4	1.78	Acetone	C_3H_6O	-	0.1	-	0.3	0.3
5	2.21	Ethyl acetate	$C_4H_8O_2$	-	-	-	-	0.2
6	2.34	2-butanone	C_4H_8O	-	-	-	-	0.4
7	2.89	Ethanol	C_2H_6O	0.4	0.4	-	2.4	-
8	3.00	2-methyl-1,3-dioxolane	$C_4H_8O_2$	4.8	2.4	2.4	2.4	-
9	3.54	2-pentanone	$C_5H_{10}O$	-	-	-	-	0.3
10	5.24	1,4-dioxane	$C_4H_8O_2$	18.8	3.5	1.8	6.0	6.3
11	7.58	1-Butanol	$C_4H_{10}O$	-	-	-	-	0.3
12	8.15	2-methoxyethanol	$C_3H_8O_2$	-	0.4	0.2	0.8	1.2
13	9.03	2-ethoxyethanol	$C_4H_{10}O_2$	0.8	0.3	0.1	0.9	1.4
14	10.28	Acetoin	$C_4H_8O_2$	-	-	-	-	0.1
15	12.82	Acetic acid	$C_2H_4O_2$	0.4	0.2	0.1	0.5	0.7
16	15.04	2-(2-ethoxyethoxy)ethanol,	$C_6H_{14}O_3$	0.9	-	-	-	0.6
17	16.02	Ethyl lactate	$C_5H_{10}O_3$	-	0.2	0.2	0.6	0.5
18	16.96	N-methoxymethyl-N-methylacetamide	$C_5H_{11}NO_2$	-	-	-	0.3	0.2
19	17.18	2-isopropoxyethyl propionate	$C_8H_{16}O_3$	-	-	-	0.3	0.6
20	18.80	2-(2-hydroxyethoxy)ethyl acetate	$C_6H_{12}O_4$	0.4	0.9	0.6	1.5	1.4
21	19.07	Diethylene glycol	$C_4H_{10}O_3$	20.5	60.0	60.1	43.5	46.4
22	19.38	Phenol	C_6H_6O	-	0.3	0.1	0.5	0.2
23	19.50	2-[2-(2-ethoxyethoxy)ethoxy]ethanol	$C_8H_{18}O_4$	0.7	-	0.2	-	0.3
24	20.99	Phenol, 4-ethyl-	$C_8H_{10}O$	-	0.1	-	0.3	0.4
25	21.28	2-(methoxymethoxy)propanoic acid	$C_5H_{10}O_4$	-	-	-	0.8	0.6
26	22.03	2-hydroxypropanamide	$C_3H_7NO_2$	-	-	-	1.5	0.7
27	22.38	Levulinic acid	$C_5H_8O_3$		0.2	0.1	0.2	
28	22.45	Triethylene glycol	$C_6H_{14}O_4$	18.7	18.4	22.6	18.2	22.6
29	24.18	2-hydroxyethyl levulinate ethylene ketal	$C_9H_{16}O_5$		0.1	0.5		
30	24.71	Dimethyl diglycolcarbonate	$C_8H_{14}O_7$	-	-	-	0.9	0.2
31	25.68	Tetraethylene glycol	$C_8H_{18}O_5$	13.7	6.6	4.4	9.9	7.3
32	26.21	3-methoxy-1,2-propanediol	$C_4H_{10}O_3$	-	-	-	1.5	1.2
33	29.32	4-hydroxyacetophenone	$C_8H_8O_2$	-	-	0.3	-	-
34	31.36	Pentaethylene glycol	$C_{10}H_{22}O_6$	7.7	1.8	0.9	2.7	3.0
		Total area (%)		***98***	***97***	***95***	***97***	***99***

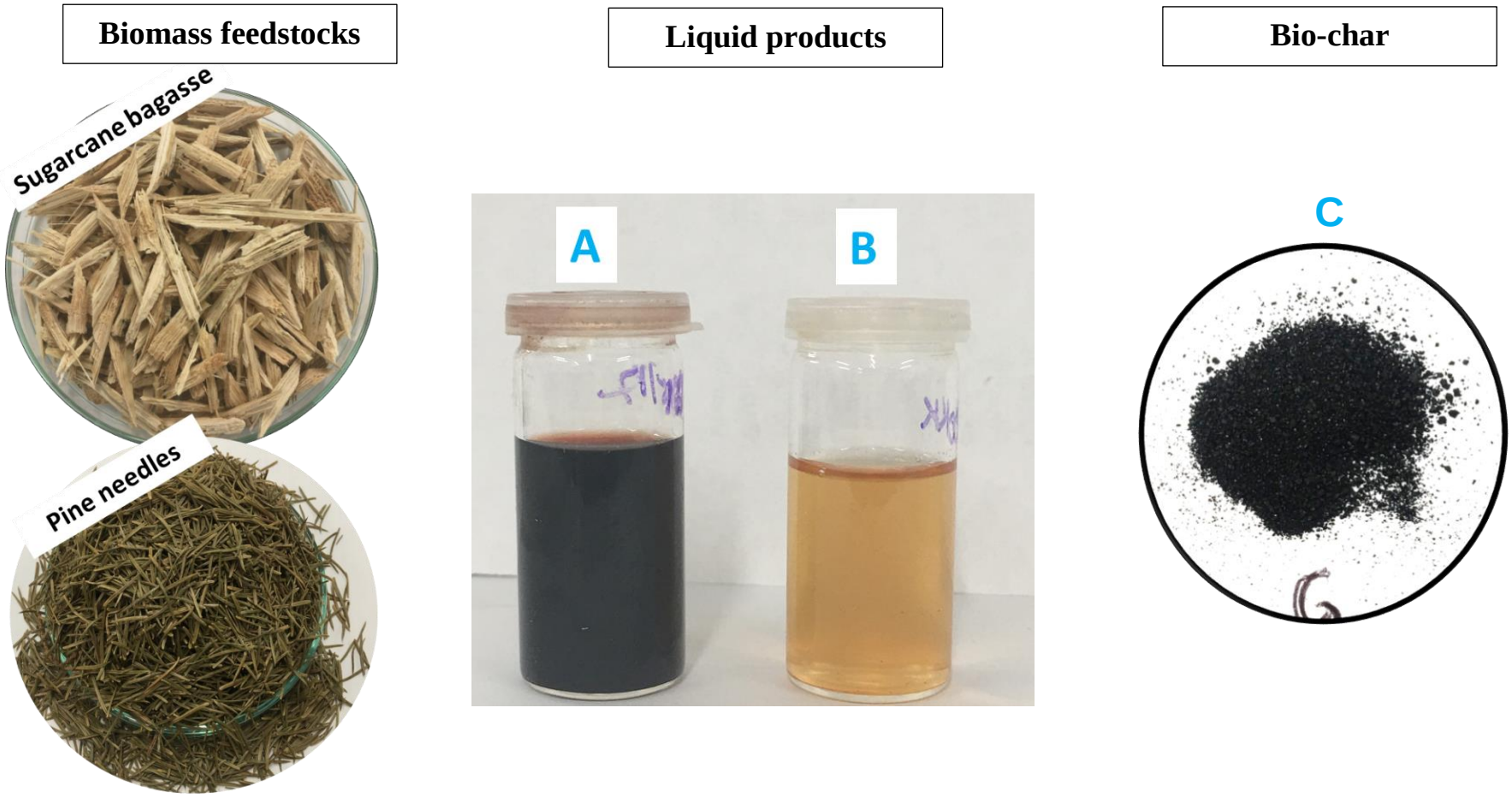

Figure C1: *Photographs of biomass feedstocks and samples of liquid products from pine needles liquefaction using (A) ethylene glycol and (B) water as liquefaction solvent. Picture C is a sample bio-char obtained from the liquefaction process.*

APPENDIX D

D.1 Supplementary information for Chapter 7

Table D1: *Key products identified (GCMS) in the liquid product obtained from the self-condensation of acetone (A) using various catalysts. Softwood bio-char (SWB), rice husk bio-char (RHB), pine needles bio-char (PNB), and pine needles ash (PNA).*

Product	**Peak area (%)**				
	A	**A+SWB**	**A+RHB**	**A+PNB**	**A+PNA**
Mesityl oxide	66.8	65.7	66.1	72.2	71.9
Isomesityl oxide	1.6	13.5	14.1	12.0	9.4
Diacetone alcohol	31.6	20.0	19.0	15.1	8.3
Total	***100.0***	***99.2***	***99.2***	***99.3***	***89.6***

APPENDIX E

E.1 Selected media publications

E.1.1 Your Christmas tree could help save the planet (BBC News)

Available at: https://www.bbc.co.uk/news/science-environment-46647790

Home | UK | World | Business | Election 2019 | Tech | Science | Health

Science & Environment

Your Christmas tree could help save the planet

By Mark Kinver
Environment reporter, BBC News

27 December 2018

Your unwanted Christmas tree could be processed to produce important chemicals and cut emissions, say researchers.

Pine needles could provide feedstock to create new products, such as sweeteners and paint, as well as cut emissions.

Currently, an estimated seven million trees each year end up in landfill.

A study from the University of Sheffield suggests the process would also result in zero waste, therefore easing pressure on our waste services.

Growth of recycled trees

"By now we all know about the problem of greenhouse gas emissions, and the need to reduce carbon emissions," explained Cynthia Kartey, a PhD student at the university's Department of Chemical and Biological Engineer

"I see biomass waste as a potential alternative source of feedstock for the chemical industry, for example," she told BBC News.

For example, some of the substances found in pine needles are an active ingredient in perfume.

Despite recent attention on the problems caused by the global proliferation of plastic, the popularity of artificial Christmas trees continue to grow.

However, an estimated eight million "natural" Christmas trees are still bought in the UK each year.

Alas, the vast majority - about seven million of them - end up in landfill after 12th Night.

Seasonal and circular economy

However, by identifying the value from the trees in the form of the potential feedstock for the chemical industry would make it economically sensible to send them to biorefineries, says Miss Kartey.

This could also lead to a reduction in the UK's carbon footprint as it would cut our dependency on imported plastic trees and a reduction in the amount of tree biomass ending up in landfill, she explained.

Colleague Dr James McGregor added: "The use of biomass - material derived from plants - to produce fuel and chemicals currently manufactured from fossil resources will play a key role in the future global economy.

"If we can utilise materials that would otherwise go to waste in such process, thereby recycling them, then there are further benefits."

Share this story About sharing

Science & Environment

E.1.2 New recycling process could help your Christmas tree lead a surprising second life (The Conversation)

Available at: https://theconversation.com/new-recycling-process-could-help-your-christmas-tree-lead-a-surprising-second-life-107984

THE CONVERSATION

Academic rigour, journalistic flair

Green Christmas. Happy Hirtzel/Shutterstock

New recycling process could help your Christmas tree lead a surprising second life

December 28, 2018 9.44am GMT

Author

Cynthia Kartey

PhD Researcher in Chemical Engi

University of Sheffield

It wouldn't be Christmas without a tree, but which is more sustainable – a real tree or a plastic one?

You might expect anything plastic to be the least environmentally friendly option. It's true that manufacturing plastic trees consumes a lot of energy, and so does shipping them, to the UK from where they're commonly manufactured in China, for example. Although you can use a plastic tree for many years, most aren't recyclable and ultimately still end up in landfill.

However, real trees aren't necessarily the greener option. The UK uses as many as 8m natural Christmas trees during the festive period each year and sadly, about 7m of these are discarded. The other million are mainly used as compost, though many people avoid this based on the assumption that the low pH of pine needles (between 3.2 and 3.8) will make the soil acidic.

Christmas trees such as the Norway spruce and Nordman fir have hundreds of thousands of pine needles which take a long time to decompose compared to other tree leaves. When they rot, they emit huge quantities of greenhouse gases. According to The Carbon Trust, the carbon footprint of a 2m-tall real Christmas tree is equivalent to 16kg of CO_2 if it ends up in landfill. That's 100,000 tonnes of greenhouse gases from the 7m trees that end up languishing in landfills every year.

Pine needles take a long time to rot, releasing methane and carbon dioxide as they do. Kroshanosha/Shutterstock

A tree is for life, not just for Christmas

A better solution would be to reuse the pine needles and the trees. My research at the University of Sheffield has been investigating whether there are useful products that we can get from pine needles and how to produce these.

Like most plant biomass, 85% of a pine needle is a structurally complex polymer known as lignocellulose, which is rich in carbohydrate and aromatic compounds. The structural rigidity of lignocellulose makes it unattractive and useless in most industrial processes because of the high energy intensity needed to break it down.

My research is focused on how the complex structure of this polymer can be broken down into simple industrial chemical feedstocks of high value and low molecular weight, such as sugars, organic acids and phenolics – chemicals which are important raw materials in industrial manufacturing.

By a process called liquefaction which uses moderate temperatures and environmentally-friendly solvents like glycerol or water, the pine needles are converted into a liquid with a solid byproduct called bio-char. The warm solvent helps to break down the complex chemical structure of pine needles into smaller chemical molecules, which make up the liquid.

The reaction vessel for the liquefaction process. Cynthia Kartey, Author provided

This liquid product typically results in glucose, acetic acid and phenol. Glucose is used in the production of sweeteners for food, acetic acid in making paint, adhesives and even vinegar, and phenol in the manufacture of medicines.

None of the products from this process are wasted – even the bio-char can be used as a catalyst for other chemical reactions.

The tree doesn't need to be fresh either, as the process applied in this work can effectively handle both dry and wet biomass, eliminating the need for an expensive drying process. This is a key advantage of the liquefaction technique over traditional technologies such as combustion and gasification, whose efficiency depends on the moisture content of the biomass.

This method also works well with other forms of biomass waste and can be used for any species of pine. An industry built on this process could convert much of the available biomass waste from food crops and forestry management into vital products.

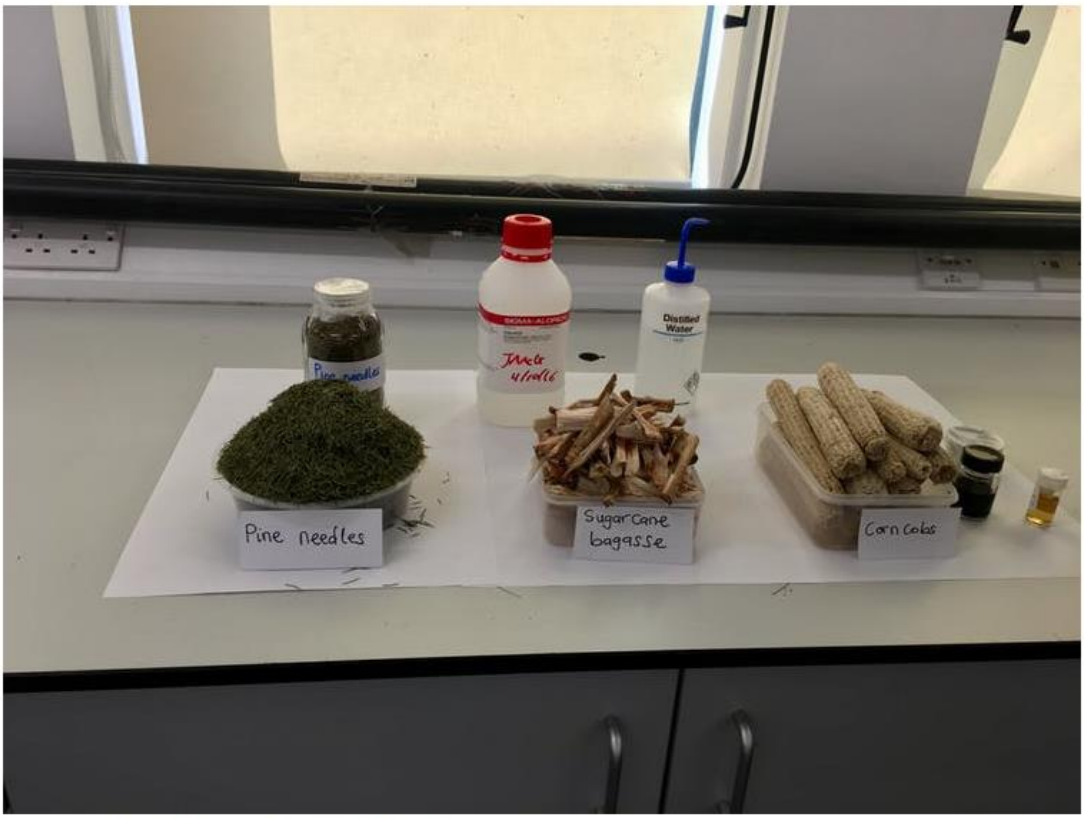

A selection of biomass waste which can be saved from landfill. Cynthia Kartey, Author provided

Aside from converting biomass waste into precious materials, this process adds value to otherwise less useful solvents such as crude glycerol – an unwanted byproduct from the biodiesel manufacturing industry. Using glycerol increases how much of the biomass waste can be converted to liquid product compared to the commonly used water process, known as hydrothermal liquefaction. More than 90% of pine needle mass is converted in the presence of glycerol compared to only 60% with water.

The benefits of this research are huge. It can help reduce carbon emissions by decreasing dependence on imported artificial Christmas trees and limiting the amount of biomass sent to landfill. If commercially feasible, this could make industrial processes more sustainable by creating new products from something that was previously considered waste. Long after the festive period is over we could continue using this method to recycle forest and agricultural waste on a much larger scale, bringing greater benefits throughout the year.